University of Southampton

A LIGAND OF PEROXISOME-PROLIFERATOR-ACTIVATED RECEPTOR γ (PPARγ), HAS POTENTIAL IN THE TREATMENT OF NEUROBLASTOMA

Helen Anne Rodway
BSc (Hons.)

A thesis submitted for the degree of
DOCTOR OF PHILOSOPHY

Department of Biochemistry
Faculty of Science

March, 2002

UNIVERSITY OF SOUTHAMPTON

ABSTRACT

FACULTY OF SCIENCE

BIOCHEMISTRY

Doctor of Philosophy

A Ligand of Peroxisome-Proliferator-Activated Receptor γ (PPARγ), has Potential in the Treatment of Neuroblastoma

By Helen Anne Rodway

Neuroblastoma is the most common solid childhood tumour and has a high mortality rate. Neuroblastoma affects very young children and is usually diagnosed post-metastasis, when more than resection of the primary tumour is required to treat the disease. Other treatments include chemotherapy and radiotherapy, which have many side effects and a more effective, less toxic treatment is sought. A small percentage of neuroblastomas can spontaneously regress without treatment and this has lead to research into using agents such as retinoic acid to mimic this phenomenon. Retinoic acid acts through retinoic acid receptors and can effectively inhibit the growth of neuroblastoma cell lines *in vitro*, however clinical trials have shown that it is less effective against metastatic disease *in vivo*. Therefore, agents which activate another transcription factor, the peroxisome proliferator-activated receptor (PPAR), have been investigated to establish their efficacy at inhibiting neuroblastoma cell growth and their potential as treatments for neuroblastoma. Two human neuroblastoma cell lines, IMR-32 and Kelly, were used as these represent neuroblastoma with poor prognosis. There are three isoforms of PPARs, α, β and γ and activation of PPARγ has been shown to inhibit the growth of many cancer cell types. PPARs α, β and γ are activated by fatty acids and PPARγ is also activated by the fatty acid metabolite, 15-deoxy$\Delta^{12,14}$-prostaglandin J_2 ($15dPGJ_2$). Fatty acids marginally inhibited IMR-32 cell growth and altered the membrane phospholipids of the cells. Fatty acids activated PPAR-induced transcription, but this did not relate to their cellular effects as docosahexaenoic acid, which had the greatest effect on the cells, activated PPARs almost the least. $15dPGJ_2$ inhibited the growth of IMR-32 and Kelly cell lines, but was more effective than fatty acids. $15dPGJ_2$ induced IMR-32 cells to arrest at G_2/M phase of the cell cycle, coinciding with nuclear translocation of p53 and down-regulation of PAX3. Subsequently, the cells died by a process, which required *de novo* protein synthesis, but did not exhibit features of classical apoptosis. IMR-32 cells treated with $15dPGJ_2$ underwent autophagic cell death. This involved the formation of autophagic vesicles, which can target cellular components such as mitochondria for destruction and resulted in cell death. Decoy oligonucleotides to PPARs prevented $15dPGJ_2$ from inhibiting IMR-32 cell growth and showed that $15dPGJ_2$ acts specifically through PPARs. Sphingosine-1-phosphate (S1P) can be removed from foetal calf serum by delipidation. Culturing IMR-32 cells under delipidated conditions altered the cellular effects of PPAR ligands. Both $15dPGJ_2$ and fatty acids effectively inhibited the growth of IMR-32 cells and induced apoptosis. S1P activates mitogen-activated protein kinases (MAPKs), which can down-regulate PPARγ activity. Therefore under delipidated conditions, a higher level of activation of PPARγ may result in IMR-32 cells undergoing apoptosis instead of autophagy. This suggests that PPARγ ligands such as $15dPGJ_2$ have therapeutic potential in the treatment of cancers including neuroblastoma. PPARγ ligands may also be more effective in combination with inhibitors of MAPKs or S1P, as removal of S1P from the culture medium affects the response of neuroblastoma cells to PPARγ ligands.

Acknowledgements

Where to start....? I guess I should start by thanking all of the people who have directly helped with the completion of the lab work for my thesis. Firstly I should thank the De Bonville Family and the Wessex Cancer Trust for funding the project. I would like to thank my long-suffering supervisor, Dr. Karen Lillycrop, who provided help, ideas and input, if only I could read her writing!!! I also want to thank in no particular order Dr. Tony Postle, Dr. Alan Hunt and Dr. Jan Kohler for their advice and endless help throughout the 3 years. A note of thanks should also go to Dr. Anton Page of the Southampton General Hospital Electron Microscopy Unit for his assistance with my defining result (!) and to Dr. Bob Broadbridge who kindly made the caspase 3 substrate.

I would also like to thank my fellow inmates – especially Róisín, my partner in crime - I miss our Wednesday night movie "fests" and the butterscotch angel delight! I'd also like to mention Hazel and Debbie – fellow "Angels". More shout-outs to past and present members of the Lillycrop, Barton and DOC groups and Coffee Club (R.I.P.), especially Robert for adding that danger level to my first year in Bolditz. On the social front, mentions should be made of those people I managed to drag to the pub and fellow wine-tasters (you know who you are). Finally Conrad and his spare room deserve special thanks for saving me from living in a cardboard box on the Common.

Last, but most importantly, I would like to thank my family, who wholeheartedly supported me throughout my undergraduate and postgraduate degrees with encouragement, love (and money!) Special thanks to Mum and Dad and to Alison, David and George – you're brilliant – I couldn't have done it without you. Also to my grandparents, especially Grandad who added a bit of drama whilst I was slogging through the end of my writing. Finally, to Neil, well I did it - my "magnificent octopus" finally has all of its legs and the coffee table will no longer be wobbly! Thanks for your all your support, encouragement, optimism and patience (I have tested it well) - I couldn't have done it without you either. You're a star!

October 24 - November 22

SCORPIO

You've embarked on an adventure and already you're wondering if it was a wise move. It could end up costing you a lot of money, taking up a lot of your time or stretching your already limited emotional resources. Ought you perhaps turn back and attempt something less ambitious? Perhaps. But you don't want to. What you want is to be told that if you persevere, things will come right. Indeed they will, eventually. All you are missing is a realistic time scale of expectation. You want to see immediate change but you are going to have to settle for a slow one. That's fine as long as you convince yourself that it's worth making a few temporary sacrifices.....

My stars for the day from the Sunday Times sometime early in my first year and they seem to sum up my Ph.D. throughout.

Table of Contents

List of Abbreviations

8(S)-HETE	8(S)-Hydroxyeicosatetraenoic Acid
9-*cis* RA	9-*cis* Retinoic Acid
15dPGJ$_2$	15-deoxy$\Delta^{12,14}$-Prostglandin J_2
AA	Arachidonic Acid
ACTR	Activator of the Thyroid and Retinoic Acid Receptor
ADD-1	Adipocyte Determination and Differentiation Factor
AIB1	Amplified in Breast Cancer 1
ANOVA	Analysis of variance
ARA70	Androgen Receptor Co-Activator
ATP	Adenosine Triphosphate
azPC	Azelaoyl Phosphatidylcholine
BADGE	Bisphenol A Diglycidyl Ether
BCA	Bicuichoninic Acid
BDU	Bromodeoxyuridine
BSA	Bovine Serum Albumin
CAD	Caspase Activated DNAase
CAT	Chloramphenicol Acetyl Transferase
CBP/p300	CREB Binding Protein
C/EBP	CAAT Enhancer Binding Protein
CH	Cycloheximide
CMV	Human Cytomegalovirus
COX-1	Cyclo-oxygenase Type 1
COX-2	Cyclo-oxygenase Type 2
CREB	CAMP Responsive Element Binding Protein
Δ^{12}-PGJ$_2$	9-deoxy$\Delta^{9,12}$-13,14-dihydro-Prostaglandin D_2
Da	Dalton
dATP	Deoxyadenosine Triphosphate
DBD	DNA Binding Domain
dCTP	Deoxycytidine Triphosphate
DEPC	Diethyl Pyrocarbonate

DFF	DNA Fragmentation Factor
dGTP	Deoxyguanosine Triphosphate
DHA	Docosahexaenoic Acid
DMEM	Dulbecco's Modified Eagle's Medium
DMSO	Dimethyl Sulphoxide
dNTP	Deoxynucleoside Triphosphate
DTT	Dithiothreitol
dTTP	Deoxythymidine Triphosphate
EDTA	Ethylenediaminetetraacetic Acid
eIF2	Elongation Initiation Factor 2
ER	Endoplasmic Reticulum
ERK-1	Extracellular Signal Regulated Kinase-1
ERK-2	Extracellular Signal Regulated Kinase-2
ES Cells	Embryonic Stem Cells
ESI MS	Electrospray Ionisation Mass Spectrometry
FAAR	Fatty Acid Activated Receptor
FCS	Foetal Calf Serum
FKHR	Forkhead Transcription Factor
γ-LA/gLA	Gamma Linolenic Acid/Gamma Linolenic Acid (graphs only)
G418	Geneticin® Disulphate Salt
GRIP1/NcoA2	Glucocorticoid Receptor Interacting Protein/Nuclear Co-Activator 2
HBS	Hepes Buffered Saline
HBSS	Hank's Balanced Salt Solution
HEPES	*N*-(2-Hydroxyethyl)Piperazine-*N*'-(2-Ethanesulphonic Acid)
HIV-1	Human Immunodeficiency Virus-1
HMG-CoA	3-Hydroxy-3-Methylglutaryl Coenzyme A
HRP	Horseradish Peroxidase
HSR	Homogeneously Staining Region
HUVECs	Human Umbilical Vein Endothelial Cells
ICAD	Inhibitor of Caspase Activated DNAase
IκB	Inhibitor of NFκB

IKK	IκB Kinase
IL-2	Interleukin-2
IL-8	Interleukin-8
JAK2/STAT5b	Janus kinase 2/Signal Transducer and Activator of Transcription 5b
JNK	c-Jun N-terminal kinase
LB	Lennox L Broth Medium
LBD	Ligand Binding Domain
LPL	Lipoprotein Lipase
KCl	Potassium Chloride
kDa	Kilo Dalton
KH_2PO_4	Potassium Dihydrogen Phosphate
LDL	Low-Density Lipoprotein
LPA	Oleoyl-Lysophosphatidic Acid
LTR	Long Terminal Repeat
LXR	Liver X Receptor
MAPK	Mitogen-Activated Protein Kinase
MDC	Monodansylcadaverine
μM/uM	Micromolar/micromolar (graph legends only)
MMAC1	Mutated in Multiple Advanced Cancers
MMLV	Moloney-Murine Leukaemia Virus
MMP-9	Metalloproteinase-9/Gelatinase B
MPT	Mitochondrial Permeability Transition
MRD	Minimal Residual Disease
NaCl	Sodium Chloride
Na_2HPO_4	Disodium Hydrogen Phosphate
NCoR/SMRT	Nuclear Co-Repressor/Silencing Mediator for Retinoid and Thyroid Receptor
NGF	Nerve Growth Factor
NFκB	Nuclear Factor κB
NP-40	Nonidet NP-40 (Octylphenol-ethylene oxide condensate)
NR	Nuclear Receptor
NRBF	Nuclear Receptor Binding Factor

NRRE	Nuclear Receptor Responsive Element
NSAID	Non-Steroidal Anti-Inflammatory Drug
NSE	Neurone Specific Enolase
OA	Oleic Acid
OER	Oestrogen Receptor
oxLDL	Oxidised Low Density Lipoprotein
PA	Phosphatidic Acid
PARP	Poly-ADP Ribose Polymerase
PBP	PPAR Binding Protein
PBS	Phosphate Buffered Saline
p/CAF	p300/CBP Associated Factor
PCD	Programmed Cell Death
p/CIP	p300/CBP Co-Integrator Associate Protein
PDK1	Phosphatidylinositol 3,4,5 Triphosphate-Dependent Protein Kinase 1
PEG	Polyethylene Glycol
PGC-1	PPARγ Co-Activator-1
PGD_2	Prostaglandin D_2
PIPES	Piperazine-NN'-bis-Ethanesulphonic Acid
PI	Propidium Iodide
PI3K	Phosphatidylinositol 3-Kinase
PIP_2	Phosphatidylinositol 3,4-Bisphosphate
PIP_3	Phosphatidylinositol 3,4,5-Trisphosphate
PKB	Protein Kinase B
PKR	Protein Kinase R
PLZF	Acute Promyelocytic Leukaemia Zinc Finger Protein
PML-RAR	Acute Promyelocytic Leukaemia Oncoprotein
PMSF	Phenylmethylsulphonyl Fluoride
PP2A	Serine-Threonine Phosphatase 2A
PPARα	Peroxisome Proliferator-Activated Receptor Alpha
PPARβ	Peroxisome Proliferator-Activated Receptor Beta
PPARγ	Peroxisome Proliferator-Activated Receptor Gamma
PPARs	Peroxisome Proliferator-Activated Receptors

P-PKB	Phospho-Protein kinase B
PPRE	Peroxisome Proliferator-Activated Receptor Response Element
PRIP	PPAR Interacting Protein
PtdCho	Phosphatidylcholine
PtdEtn	Phosphatidylethanolamine
PtdGro	Phosphatidylglycerol
PtdIns	Phosphatidylinositol
PtdSer	Phosphatidylserine
PUFA	Polyunsaturated Fatty Acid
PVDF	Polyvinyldifluoride
PTEN	Phosphatase and Tensin Homologue Deleted from Chromosome 10
RAC3	Receptor Associated Co-Activator 3
RAR	Retinoic Acid Receptor
RT-PCR	Reverse Transcriptase Polymerase Chain Reaction
RXR	Retinoid X Receptor
S1P	Sphingosine-1-Phosphate
SDS	Sodium Dodecyl Sulphate
SDS-PAGE	SDS-Polyacrylamide Gel Electrophoresis
S.E.M.	Standard Error of the Mean
SIV-1	Simian Immunodeficiency Virus
SRC1/NCoA1	Steroid Receptor Co-Activator 1/Nuclear Co-Activator 1
SREBP-1	Sterol Response Element Binding Protein-1
SSC	Sodium Chloride Sodium Citrate Buffer
SV40	Simian Virus 40
TAE	Tris Acetate
TEMED	N,N,N',N'-Tetramethylenediamide
TEP1	Transforming Growth Factor β Regulated Epithelial Cell Enriched Phosphatase
TE-SLS	Tris-EDTA-Sodium Lauryl Sarcosine
TGZ	Troglitazone
TIF-2	Transcriptional Intermediary Factor-2

TLC	Thin Layer Chromatography
TK	Thymidine Kinase
TNFα	Tumour Necrosis Factor alpha
TR	Thyroid Receptor
TRAM1	TR Activator Molecule 1
TRAP220	Thyroid Hormone Receptor-Associated Protein 220
Tris	Tris(hydroxymethyl)aminomethane
Tris-HCl	Tris(hydroxymethyl)aminomethane Hydrochloride
TNFα	Tumour Necrosis Factor α
Tween-20	Polyoxyethylenesorbitan Mono-Laurate
TZD	Thiazolidinedione
Upa	Urokinase Plasminogen Activator
UTR	Untranslated Region
UV	Ultra-violet
VDR	Vitamin D Receptor
VEGF	Vascular Endothelial Growth Factor
VMA	Vanillomandelic Acid

List of Figures

Chapter 3

Chapter 4

Chapter 6

List of Tables

Chapter 1

Introduction

1 *Neuroblastoma*

1.1 *Epidemiology*

Neuroblastoma is the most common, solid extra-cranial childhood tumour [1, 2], accounting for 8-10 % of all childhood cancers [3]. This relates to an annual incidence of approximately 8-10 children per million world-wide [4, 5, 6]. Neuroblastomas are rarely seen at birth [7], but 50 % of cases occur within the first 2 years of age and 97 % of cases occur within 10 years of age [3]. Neuroblastoma can develop due to spontaneous mutations, however, a subset of neuroblastomas are familial, following an autosomal dominant pattern of inheritance [1]. Neuroblastoma can show a biphasic age incidence with peaks in children under one year of age and between 2 and 4 years of age [8]. The peak incidence of familial neuroblastoma occurs earlier, around 9 months of age and may involve multiple primary tumour sites [3]. Overall, neuroblastoma is also more common in boys than girls, giving a male to female ratio of 1.2:1 [1].

1.2 *Pathology*

Neuroblastomas derive from primitive neuroectodermal cells of neural crest origin and although they may occur at sites throughout the body, they are predominantly found in the sympathetic nervous system and adrenal medulla [3, 9, 10]. However, this does depend upon the age of the patient, as children demonstrate a higher incidence of adrenal tumours and a lower incidence of thoracic and cervical tumours, than infants [11]. Approximately 1 % of cases will present with no detectable primary tumour [11]. Neuroblastomas contain small round or slightly elongated "blue" cells with scant cytoplasm, which grow in solid sheets [3, 9, 10]. 15-50 % of cases contain Homer-Wright rosettes, which are neuroblasts surrounding areas of eosinophilic neuropil [12]. Neuroblastomas morphologic mimic the embryonic character of the tissue of origin and tend to be poorly organised. Ganglioneuroblastoma is similar to neuroblastoma and is characterised by more areas of cellular maturation and also overlaps with ganglioneuromas, which are considered to be further differentiated [1]. Neuroblastoma and ganglioneuroma are though to represent extremes on the

opposite ends of the spectrum of cellular differentiation seen in cases of "neuroblastoma" [1, 3]. Interestingly, neuroblastic nodules have been shown to occur uniformly in foetuses, with peak incidence between 17 and 20 weeks of gestation, and gradually regress by the time of birth or shortly afterwards [13, 14].

1.3 *Disease staging*

There are four main clinical stages to neuroblastoma which have been defined by several systems, including the International Neuroblastoma Staging System described by Brodeur *et al.* [3, 15] and also by Shimada System [16, 17, 18]. Brodeur *et al.*, based their system on other staging methods, but standardised definitions of localised and metastatic neuroblastomas [3, 15], whereas Shimada *et al.*, based their system on an age-linked classification dependent on the differentiation state of the tumour cells [16, 17, 18]. Early stage neuroblastomas (Stages I and II) have good prognosis, with 3-year event-free survival rates of 75-90 %, whereas later stages of the disease (Stages III and IV) have a much poorer prognosis [11]. Early stage neuroblastomas represent localised tumours confined to the area of origin, whereas later stage tumours represent those that have metastasised and involve the lymph nodes [15, 16]. The 3-year event-free survival rate for infants with Stage III neuroblastoma is around 80 % and for those with Stage IV neuroblastoma is around 60 % [11]. However, the 3-year event-free survival rate for children with Stage III neuroblastoma is approximately 50 % and is as little as 10-15 % in children with Stage IV neuroblastoma [11].

1.4 *Clinical markers of prognosis*

Prognosis for neuroblastoma can be determined by patient age at presentation, clinical stage of the disease and site of primary tumour. Patients diagnosed at less than one year of age tend to have a more favourable prognosis (5-year event-free survival of 80 %) than those diagnosed after one year of age (40 % 5-year event-free survival), which is partly related to disease stage [19]. Patients with abdominal primary tumours have a less favourable prognosis than those with cervical, pelvic or thoracic primary tumours in Stage III and IV of the disease, whereas there was no influence of site on survival in early stages of the disease [19]. The involvement

of bone marrow also signals a less favourable outcome and this is further reduced by the presence of multiple bone metastases [19]. Tumour relapse usually occurs within 2 years, with 2-year event-free survival after the first relapse being 10 % and 5-year event-free survival only 5.6 % [19]. Tumour recurrence is usually widespread affecting the bone, primary tumour site and lymph nodes [19]. The degree of tumour differentiation and presence of both biological and genetic markers can also determine prognosis for neuroblastoma.

1.5 *Biological markers of prognosis*

Markers of good prognosis in neuroblastoma include highly differentiated tumour cells [19, 20], which show a more organised cytoplasm and characteristic patterns neurofilaments and microtubules [1]. The expression of nerve growth factor (NGF) receptors is another marker of good prognosis in neuroblastoma [21, 22]. NGF is important for the differentiation and survival of neural crest cells [23]. The expression of the high affinity NGF receptor, trkA, and the low affinity NGF receptor, 75NGFR, correlate with younger patient age, favourable clinical stages and the absence of genetic markers of poor prognosis [21, 22]. Interestingly, in one study, three tumours were shown to co-express trkA and 75NGFR and these tumours regressed without treatment, whereas another tumour expressed trkA and lacked 75NGFR and this had a fatal outcome [22].

Other biological markers, such as neurone specific enolase (NSE) [24], vanillomandelic acid (VMA) [25] and ferritin [26] are markers of poor prognosis, when they are detected at higher than normal levels. NSE is a cytoplasmic protein whose activity is associated with neural cells and is found in higher levels in the serum of patients with neuroblastoma [24, 27]. However, it has also been seen in patients with other paediatric tumours and has more use as a measure of the progress of the disease [1]. Neuroblastomas lack phenylethanolamine *N*-methyltransferase, the enzyme responsible for the breakdown of noradrenaline to adrenaline, and as a result noradrenaline is converted to VMA [3], which can be detected in the urine of patients [1, 25]. 90-95 % of neuroblastomas secrete catecholamines and higher levels of catecholamine metabolites are also seen in patients with Stage IV neuroblastoma [19]. Ferritin is the predominant form of stored iron in the body and levels of ferritin

are increased in patients with actively growing tumours and are elevated in advanced stage neuroblastomas [26].

1.6 *Genetic markers of prognosis*

Common genetic markers of poor prognosis in neuroblastoma include translocation of part of chromosome 17q, NMYC amplification [28, 29] and deletion of part of the short arm of chromosome 1 [30, 31]. Translocations of chromosome 17q are the most common genetic abnormality seen in neuroblastoma, occurring in 65-70 % of cases [32, 33, 34]. They may be associated with many different chromosomes, including chromosome 9p, 10q, 11p, 14q and 16q and the breakpoints usually occur at [32, 33]. There seems to be no prognostic significance of the type of translocation involving 17q, but 17q translocation is associated with other markers of poor prognosis [32]. Gain of 17q leads to reduced survival rates as 3-year event-free survival for neuroblastomas with gain of 17q is 13.5 %, whereas that of neuroblastomas lacking gain of 17q is 100 % [32]. In some tumours, translocation from 17q to 1p may be involved, rather than a simple deletion [35]. Other genetic changes include tumour cell ploidy [36]. Diploid and tetraploid neuroblastomas are associated with later stages of neuroblastoma and poor outcome, whereas hyperdiploid tumours are indicative of early stage neuroblastomas, which respond to chemotherapeutic agents [36].

NMYC amplification at chromosome 2p24 confers a growth advantage to cells *in vitro* [37] and has been correlated with rapid neuroblastoma progression [38]. Amplified NMYC DNA is arranged in a "head-to-tail" configuration, which produces homogeneously staining regions (HSRs) [39]. HSRs are a cytogenic manifestation of gene amplification in which the amplified sequences are chromosomally integrated [40, 41, 42, 43]. Self-replicating extra-chromosomal double-minute chromatin bodies are another feature of gene amplification and are seen in 30 % of primary neuroblastomas [41, 42]. In 50 % of tumours, which are NMYC amplified, the genes NAG and DDX1, which is also oncogenic, are co-amplified [44, 45]. NMYC amplification has been observed in only 5-10 % of Stage I and Stage II neuroblastoma, whereas it occurs in up to 40 % of advanced stage tumours and the presence of more than 10 copies, correlates with poor prognosis [46, 47].

Another common genetic change seen in neuroblastomas is deletion of chromosome 1p [15, 40, 48, 49, 50], which is more common in Stages III and IV of the disease [51, 50, 52, 53, 54]. Deletions of 1p are associated with NMYC amplification, and usually involve only one allele, suggesting the other is inactive [35]. The deletions of chromosome 1 are somewhat variable in their proximal breakpoints, but the region distal to 1p36.1 appears to be deleted in all cases [55]. No tumour suppressor genes have been identified for this region of chromosome 1. However, one candidate gene that maps to the deleted part of chromosome 1p is p73 [56], which is 63 % identical to the tumour suppressor gene, p53 [35]. p73 is predicted to interact with some of the targets of p53, such as p21, which inhibits the cell cycle [56, 57] and loss of p73 expression may reflect a mechanism by neuroblastomas grown unchecked.

A variety of less common mutations are also seen in neuroblastoma [35, 58]. These include deletions in chromosome 9 and 11, losses of chromosome 11, 14q and X and amplifications of several chromosomal regions [35] including 12q13-14, which contains the MDM2 gene, which is amplified in rare cases of neuroblastoma [59]. Interestingly, the only statistically significant indicator of poor prognosis, which was independent of NMYC amplification was a deletion at 9p21 [60]. This region contains part of the tumour suppressor gene, p16 (CDKN2A), which although is rarely mutated in neuroblastoma, it is not expressed in the majority of neuroblastoma cell lines and p16 may be involved in the development of the tumour [61].

1.7 *Current treatments for neuroblastoma*

Treatments for early stage neuroblastoma involve surgery and later stages involve intensive regimes of chemotherapy and radiotherapy [2]. Surgery is the treatment of choice when neuroblastomas are localised and is also used for diagnostic purposes [2]. However, surgery is avoided in infants who tend to have better prognosis and also have more frequent surgical complications [3]. Resection of the primary tumour is generally successful, but despite this, some malignant cells can remain in the body and grow up again. This is known as minimal residual disease (MRD). As a result of MRD and the fact that over 25 % cases of neuroblastoma in infants and 68

% of cases in children have metastasised at presentation [3], neuroblastoma has a high childhood mortality rate.

Chemotherapy using single or combinations of drugs is also a common treatment for neuroblastoma. Some studies of the efficacy of chemotherapeutic agents have shown high initial response rates, with 60-70 % partial remissions and prolonged event-free survival, however long-term prognosis for Stage IV patients is still poor. Other current methods for the treatment of neuroblastoma include radiotherapy, bone marrow transplantation and immunotherapy, but their efficacy in all clinical setting remains to be established [2]. For example, neuroblastoma is a radiosensitive tumour, but the control of *in vivo* neuroblastomas by radiotherapy has proved less successful [62].

1.8 *Stage IVS neuroblastoma*

The prospect for neuroblastoma patients, however, has improved with the characterisation of a separate clinical stage of the disease, known as Stage IVS or 4S (S denotes special) [63]. Stage IVS neuroblastoma has a similar prognosis to Stage I and II neuroblastoma, with 75-90 % survival rate in all children [63, 64, 65, 66] and a better prognosis than Stage III and Stage IV of the disease. Stage IVS neuroblastoma usually occurs in infants under thirteen months of age and displays a characteristic pattern of metastasis. Patients frequently have a large primary adrenal tumour with metastasis to the liver, spleen, skin and bone marrow, with no skeletal involvement [63, 64, 65, 66], as skeletal involvement indicates Stage IV neuroblastoma [63]. This pattern of metastasis is thought to be due an abnormal distribution of neural crest cells during embryonic development [63] and the development of tumours from cells which would normally differentiate into Schwann cells or melanocytes, which develop mutations [67].

Stage IVS neuroblastoma has good prognosis because almost half of these tumours can spontaneously differentiate in non-malignant gangliomas [63, 64, 65, 66, 68]. Regression takes place over 6-12 months [63, 69] and several mechanisms have been proposed, including immunological attack, spontaneous maturation or apoptosis. Hellstrom *et al.*, [70] suggested that the infant's immune system or maternally-

acquired antibodies attack the tumour cells, although Pritchard and Hickman [69] question why this would not cause other tumours to regress. Maturation of Stage IVS neuroblastomas to non-malignant gliomas have been recorded [63, 71], but in some cases, the tumour completely disappears and it has been suggested that this occurs because the cancer cells have undergone apoptosis [69]. Whichever mechanism is responsible for the maturation and regression of Stage IVS tumours, it has lead to a new tactic in the treatment of neuroblastoma, known as differentiation therapy.

2 *Differentiation and nuclear hormone receptors*

2.1 *Differentiation*

Differentiation is the development of cells with specialised structure and function from unspecialised precursor cells. When cancer cells differentiate, they stop proliferating and lose their tumour characteristics and there may be depletion of the tumour stem cell pool [72]. Some skin cancer cells "differentiate" because they are no longer able to proliferate through the loss of nuclei [72]. The treatment of human malignancies by inducing differentiation was first suggested by Pierce in 1961 [73] and currently, differentiation therapy is being used to treat neuroblastoma and acute promyelocytic leukaemia [74, 75]. Agents such as retinoic acids, cyclic nucleotides and phorbol esters have been shown to differentiate neuroblastoma cells *in vitro* [76, 77, 78]. However, attempts to differentiate neuroblastomas with nerve growth factor and pharmacological agents have proved unsuccessful [79, 80, 81]. Clinical trials using 13-*cis* retinoic acid to treat neuroblastoma have produced variable results and have shown that retinoic acid is less effective *in vivo* than *in vitro* [82, 83, 84]. Therefore, there is a need to find a more effective agent than retinoic acid, for differentiating neuroblastoma cells *in vivo*. Despite the disappointing response of patients to 13-*cis* retinoic acid, it does work *in vitro*, and the idea of activating the transcription of growth-inhibitory genes has potential and it is possible that activating other transcription factors with their respective ligands may be more effective at treating neuroblastoma.

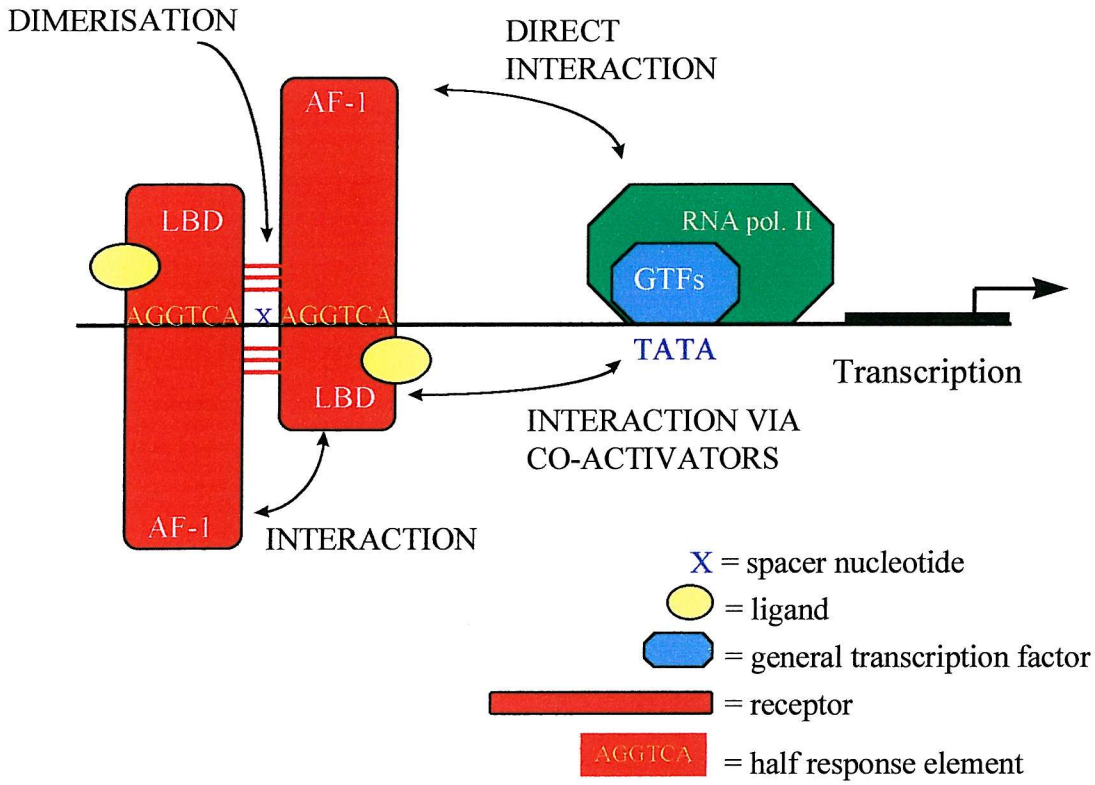

Figure 1.1 Activation of transcription by ligand-induced retinoid acid receptor homodimers and heterodimers. Retinoic acid receptors (RARs) and retinoid X receptors (RXRs) can dimerise with other members of the nuclear hormone receptor super-family to activate gene transcription and a variety of cellular responses.

2.2 *Nuclear hormone receptor superfamily*

Retinoids are derivatives of vitamin A and are the ligands for retinoic acid receptors (RARs) and retinoid X receptors (RXRs) [85, 86, 87, 88], which are members of the nuclear hormone receptor super-family [85, 89]. 13-*cis* retinoic acid isomerises within cells to form all-*trans* retinoic acid, which activates RARs and 9-*cis* retinoic acid, which is the specific ligand of RXRs [85, 86, 87, 88]. Other members of this super-family include the oestrogen receptor (OER) [90, 91], thyroid hormone receptor (TR) [92], peroxisome proliferator-activated receptors (PPARs) [93] and liver X receptors (LXRs) [94]. Nuclear hormone receptors form homodimers or heterodimers with other members of the same super-family when a ligand binds to the ligand binding domain [95, 96]. RARs can heterodimerise with RXRs, and RXRs can homodimerise or heterodimerise with RARs, PPARs, TR and VDR [97, 98, 99, 100, 101, 102, 103]. These dimers then bind to response elements within DNA and either directly, or through co-activators, activate the transcription initiation complex and initiate the transcription of genes (Figure 1.1), which are involved in a variety of cellular responses [104, 105].

3 *Peroxisome-Proliferator Activated Receptors (PPARs)*

Peroxisome proliferator-activated receptors (PPARs) are nuclear hormone receptors [106] and activate transcription by basically the same mechanism as RARs and RXRs. They were discovered in 1990, in mice, by Issemann and Green [107, 108, 109, 110, 111], as the receptors activated by chemicals, which induce proliferation of peroxisomes and liver hyperplasia in rodents [112, 113]. Since then it has been shown that many different organisms express PPARs. There are 3 different isoforms of peroxisome proliferator-activated receptors, α, β (also known as δ, FAAR or fatty acid activated receptor and Nuc-1) and γ [93, 107, 108, 114, 115, 116], which have very different tissue expression and function.

3.1 *Expression of PPARs throughout evolution*

Humans [115, 117], mice [114] and *Xenopus* [118] have been shown to express all three isoforms of PPARs, whereas other organisms have only been shown to express some of the isoforms. PPARα has been cloned from ducks [119, 120] and chickens [121], with a high degree of homology and similar tissue expression with that reported in other species, however, it is also expressed in uropygial glands, which are specific to birds [119, 120, 121]. Guinea pigs express PPARα, which is closely related to rodent and human PPARα, but like humans, it is expressed at lower level than that of rats and mice and may explain why peroxisome proliferators fail to induce a response in guinea pigs [122]. PPARβ has been cloned from rabbit mature osteoclasts [123] and both PPARα and PPARγ have been cloned from pigs [124]. Porcine PPARα occurs in two alternatively spliced transcripts, which are evolutionary distant to rodent PPARα, however, they also express PPARγ1 and γ2, which both have high homology to human and rodent PPARγ [124]. The cloning of PPARγ cDNA has also been reported in other organisms including birds, again in the uropygial glands [119, 120], hamsters [125], cows [126] and Rhesus monkeys [127]. A recent report has shown that Atlantic salmon also express PPARγ and the protein shares 47 % homology with mammalian PPARγ [128]. The protein has high sequence identity in the DNA binding domain (DBD) and ligand binding domains (LBD), but its N-terminal region is very different from that of other PPARs [128]. Salmon PPARγ is expressed as two different transcripts, one being truncated with the loss of the AF-2 activation domain and has an additional nine residues in its DBD, which may reflect different regulation of PPARγ activity in fish [128]. PPARs are therefore conserved throughout evolution, with the DBD and LBD sequences and tissue expression being highly conserved, but there are differences in regulation, function and activity.

3.2 *Tissue expression and function of the three isoforms of PPARs*

The different PPAR isoforms have specific tissue distribution and expression patterns and although most cell types contain PPARs at one level or another, there are cells which do not express one or more of the isoforms. These include cells of cerebellum and brainstem which lack PPARα [129] and KG-1 cells [130] and

keratinocytes [129] which lack PPARγ. Interestingly, oocytes and spermatogonia were shown not to express any of the isoforms of PPARs [129].

3.2.1 *PPARα*

The α isoform of PPAR is encoded on chromosome 22q telomeric to a group of genetic markers situated at 22q12-q13.1, and has a molecular weight of 52 kDa [115]. There are two natural allelic variants of peroxisome proliferator-activated receptor α, PPARα2, which has the mutation, R131Q, and PPARα3, which has the mutation, L162V [131]. Cells that are involved in high mitochondrial and peroxisomal β-oxidation activities, including hepatocytes, cardiomyocytes and epithelial cells from the proximal tubule of the kidney tend to express the highest levels of PPARα [129, 132], whereas it is expressed at lower levels in the brain and nervous system [129]. PPARα is involved in the β-oxidation of fatty acids and also in a broad range of cellular pathways, including fatty acid elongation and the metabolism of reactive oxygen species [133]. PPARα knockout mice appear healthy, but cannot induce genes involved in fatty acid oxidation and are resistant to the effects of peroxisome proliferators [134].

3.2.2 *PPARβ*

The PPARβ isoform has a molecular weight of 50 kDa and is encoded on chromosome 6p21.2 [135]. The PPARβ gene spans 85 KB of DNA including 9 exons and 8 introns [135]. It lacks a TATA box and is transcribed from a unique start site located 380 base pairs upstream of the ATG initiation codon [135]. PPARβ is expressed at low levels in most tissues [129, 132], but is found at higher levels in placenta and skeletal muscle [132]. There is speculation that PPARβ has a housekeeping function or that it acts as a regulator of PPAR activity [136]. PPARβ is capable of inhibiting PPARα activation either by competition for binding sites on DNA [129] or by titrating out a limiting factor required for the transcriptional activity of PPARα [136]. PPARβ has been shown to regulate the expression of acyl-CoA synthetase 2 in the brain, which links it to basic lipid metabolism [137]. It is also

thought to be important in development, and may participate in embryo implantation [138].

3.2.3 *PPARγ*

There are two isoforms of PPARγ, γ1 and γ2, which are produced by alternative promoter usage and mRNA splicing and differ by 30 amino acids at their amino-terminal [110]. PPARγ1 is a 54.2 kDa protein and PPARγ2 is a 55.6 kDa protein, both of which are encoded on chromosome 3p25 [139, 140, 141]. *PPARγ* is expressed at high levels in immune cells, white adipose tissue and skeletal muscle [117, 129, 132]. Expression of *PPARγ1* and *PPARγ2* varies, *PPARγ1* expression is more abundant in all tissues and it is predominantly expressed in adipose tissue, immune cells and skeletal muscle [117]. *PPARγ2* is detected in the liver and adipose tissue, where, in humans, it accounted for 15 % of all *PPARγ* mRNA, however unlike *PPARγ1*, *PPARγ2* is not expressed in skeletal muscle [117]. Two other *PPARγ* transcripts transcribed from different promoters have also been described, *PPARγ3*, which produces a protein identical to *PPARγ1* [142], and *PPARγ4* [143]. *PPARγ3* mRNA is transcribed from a novel promoter localised upstream of exon A2[a] and is its expression is thought by Fajas *et al.*, [142] to be restricted to adipose tissue and the large intestine, whereas Mukherjee *et al.*, show it is also expressed in macrophages [132]. The transcription initiation site for human *PPARγ4* is located at the 5' end of exon 1 and the protein translated from the *PPARγ4* transcript is identical to the one transcribed from the *PPARγ1* and *PPARγ3* transcripts [143].

Human PPARγ1 and γ2 share a coding region of six exons [139] out of a total of nine exons in the human PPARγ gene, which spans more than 100 kilobases [117]. PPARγ1 is encoded by 8 exons and has a 5'-untranslated region (UTR), which is encompassed by exons A1 and A2, whereas PPARγ2 is encoded by 7 exons and its 5'-UTR and N-terminal amino acids are encoded by exon B, found between exon A1 and A2 [117] (Figure 1.2).

[a] Exon nomenclature for the human gene is the same as that used for the mouse gene.

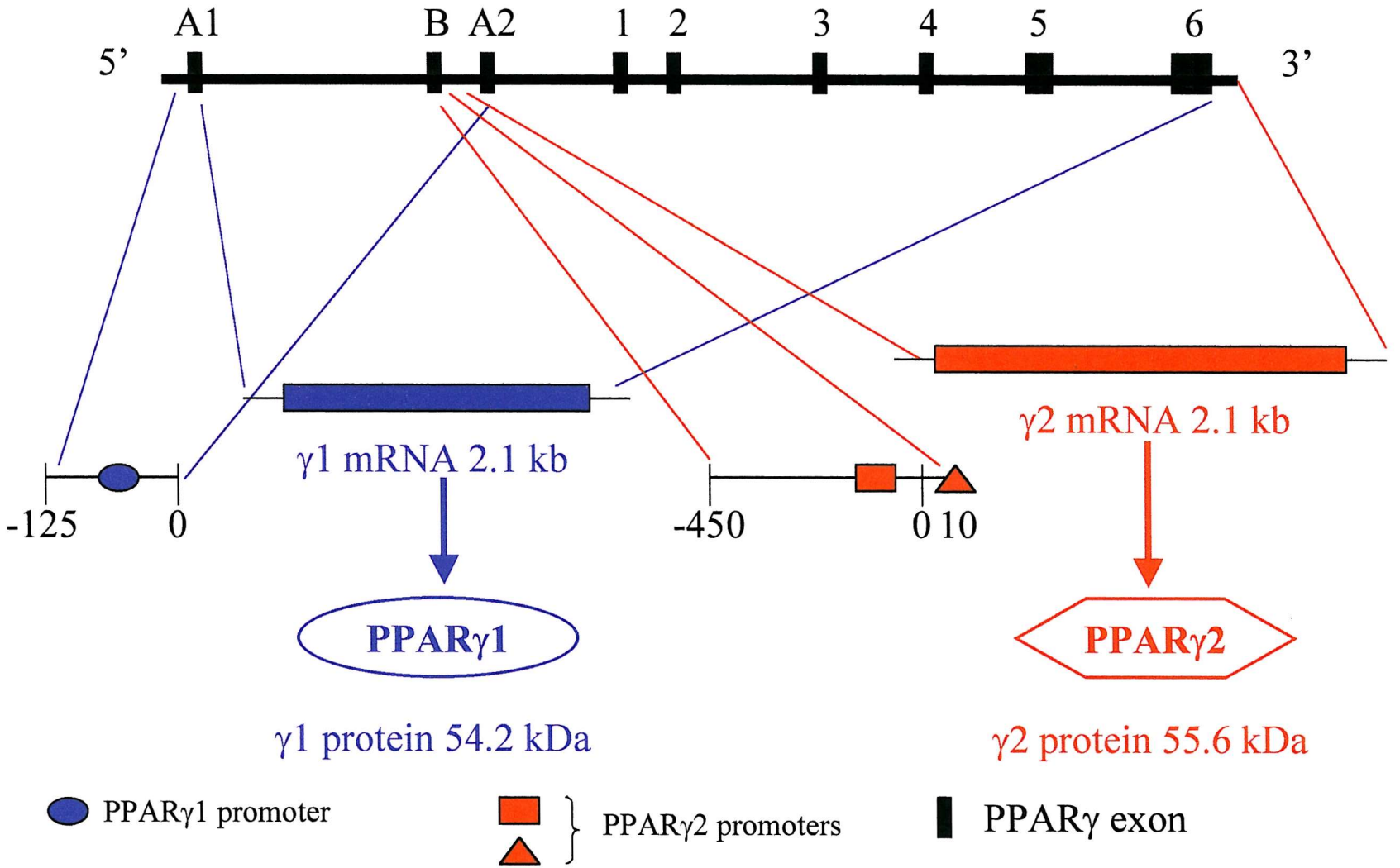

Figure 1.2 The transcription of PPARγ1 and γ2 mRNA from the human PPARγ gene by different promoter usage and the translation of PPARγ1 and γ2 proteins. Exon nomenclature used was originally devised in the mouse.

Human PPARγ has 95 % amino acid sequence identity to mouse PPARγ, but the human sequence is two amino acids longer and uses a different initiation codon [117]. Several groups have published cDNA sequences of PPARγ [139, 140, 141], which differ at three positions and the sequence published by Greene *et al.*, [140] has an insertion at nucleotide 719. PPARγ knockout mice live only briefly after birth and lack visible fat pads [144, 145, 146]. Knocking out PPARγ in mice interferes with terminal differentiation of the trophoblast and placenta vascularisation, leading to myocardial thinning and death by E10-11.5 [144, 145]. Replacement of the placenta with a wild-type placenta results in mice, which die through multiple haemorrhaging and lipodystrophy [144]. Null PPARγ cells also cannot contribute to the formation of adipocytes [145, 146]. Gene dosage also appears to be important as a single PPARγ allele produces an intermediate phenotype between wild-type and null cells [145, 146].

3.3 *Structure of Peroxisome Proliferator-Activated Receptors*

PPARs, like other nuclear hormone receptors are made up of 6 domains designated regions A-F (Figure 1.3). Region A/B is hypervariable and is found at the N-terminal of the protein and contains a ligand-independent transcription transactivation function (AF-1) [91, 134, 147, 148]. Region C is the DNA binding domain and in PPARγ is encoded by exons 2 and 3 [117] and is about 70 amino acids in length [149]. It contains two cysteine zinc finger motifs, in which the zinc ion is tetrahedrally co-ordinated by the cysteine residues [149] (Figure 1.4). These zinc fingers are important in dimer alignment on DNA and amino acid sequences (CEGCKG) known as P-boxes, which are found at the base of the first zinc finger and are involved in DNA recognition [150, 151]. The zinc fingers are followed by α-helical structures, one of which serves as a recognition helix that makes base-specific contacts within the major groove of the core site [152]. The first zinc finger contains four cysteines and several hydrophobic residues [149]. The second zinc finger contains five cysteine residues and many basic amino acids [149].

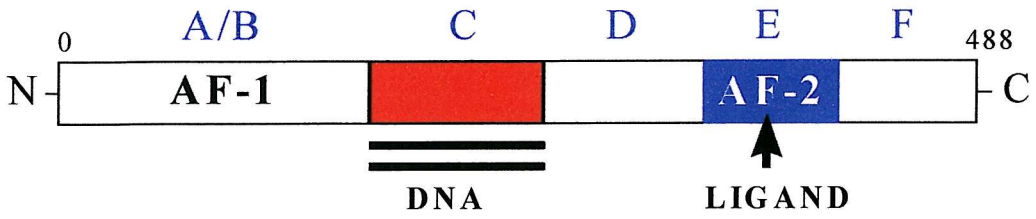

A/B	Hypervariable region
C	DNA binding domain
D	Hinge region
E	Ligand binding domain
F	Small variable domain

Figure 1.3 Domain structure (A-F) of peroxisome proliferator-activated receptors, showing the DNA binding domain (red) and ligand binding domain (blue). AF-1 is the ligand-independent transactivation site and AF-2 is the ligand-dependent transactivation domain.

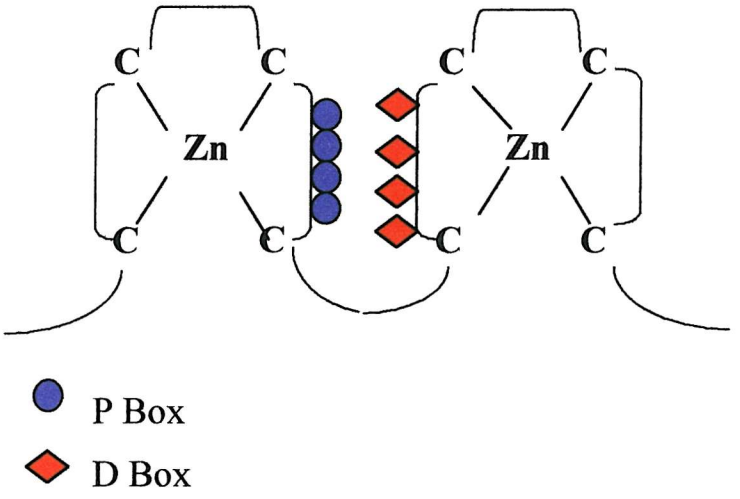

Figure 1.4 Two cysteine zinc fingers of the DNA binding domain (Region C) of PPARs, in which the zinc ion is tetrahedrally co-ordinated by the cysteine residues. These zinc fingers are important in dimer alignment on DNA. They contain amino acid sequences (CEGCKG) known as P-boxes (blue circles), which are involved in DNA recognition and three amino acid sequences known D-boxes (red diamonds), which are involved in receptor dimerisation.

There are also three amino acid sequences known D-boxes, which are involved in receptor dimerisation [104, 105, 149]. PPAR D-boxes differ from those of nuclear hormone receptors, which have D-boxes of five amino acid residues [133].

Region D is encoded by exon 4 and is a non-conserved hinge region, which allows conformational alteration of the protein and is involved in interactions with co-activators and co-repressors [152]. Region E, encoded by exons 5 and 6 in the human PPARγ gene, is the conserved ligand-binding domain (LBD). Region E is made up of 13 α helices in three layers and 4 small β sheets, which form a large "pocket" into which the ligand binds [153]. The PPAR LBD is approximately 1300 $Å^3$ and is much larger than that of other members of the nuclear hormone superfamily, for example the ligand binding domain of RXR is only 470 $Å^3$ [154, 155, 156]. The ligand binding domain of PPARβ is "Y"-shaped [157], whereas that of PPARγ is "T"-shaped [153]. PPARγ has a unique overall tertiary structure compared to other nuclear hormone receptors, due to an extra α helix, designated H2', and its H2 α helix is positioned differently, providing easier access for ligands [153], this may also explain the diverse nature of PPAR ligands. An additional ligand-dependent site (AF-2) is found in region E [158, 159, 160, 161]. Region E also harbours dimerisation surfaces, nuclear localisation signals and heat shock protein association surfaces [91, 96, 104, 148]. No specific function has been attributed to the small variable C-terminal domain known as region F, but it is known to be evolutionarily conserved [152].

4 Activators of PPARs

4.1 *Peroxisome Proliferators*

The name "peroxisome proliferator-activated receptor" is a misnomer, as only the α isoform of the receptor is effectively activated by peroxisome proliferators and fibrates, such as Wy-14643 (Figure 1.7) and the hypolipidaemic agent, clofibric acid [162, 163, 164]. Peroxisome proliferators are similar in structure to fatty acids, possessing both a large hydrophobic moiety and an acid moiety [165]. Clofibric acid maximally activates PPARα at 300 μM, only very weakly activates PPARγ and

does not activate PPARβ [164]. However, a novel fibrate analogue, GW2331, has been shown to activate PPARγ, but to a much lesser extent than PPARα [166]. The synthetic fibrate drug, Wy-14643, is thought to have the highest affinity for PPARα and does not bind to PPARβ, however, in some cases it has been shown to activate PPARγ, whereas other groups have reported no activation of PPARγ [167, 168].

4.2 *Non Steroidal Anti-Inflammatory Drugs (NSAIDs)*

Some non-steroidal anti-inflammatory drugs (NSAIDs) have been shown to be activators of PPARs. Indomethacin, flufenamic acid and fenoprofen all bind PPARα and PPARγ [169]. These drugs are able to inhibit cyclo-oxygenase type 1 (COX-1) and type 2 (COX-2), which is the mechanism by which they exert their anti-inflammatory effects. Inhibition of cyclo-oxygenases prevents the first oxidation step in the production of eicosanoids (except leukotrienes), which play a role in inflammation [170]. PPARα reduces induction of COX-2, which enhances the anti-inflammatory effects of these drugs [171].

4.3 *Fatty acids*

Fatty acids are proposed to be activators of PPARs, with different forms of fatty acids binding to and activating PPARs. Short-chain saturated fatty acids weakly activate PPARα, whereas polyunsaturated fatty acids (PUFAs) bind to and activate PPARα more effectively [116, 157, 166, 172, 173, 174]. Polyunsaturated fatty acids are also activators of the β isoform of PPARs [166] and some mono-unsaturated fatty acids and PUFAs are activators of PPARγ [114, 157, 166]. Fatty acids have been shown to activate reporter genes containing three PPREs [175], however, the long-chain saturated fatty acid, nervonic acid, has actually been shown to inhibit the activation of PPARs using a reporter construct containing three PPAR consensus binding sites [164, 172]. Fatty acids also been shown to act independently of PPARs in some cells, through changing the cellular membrane phospholipids and therefore may activate PPARs, but may not be the natural ligands of these receptors [176, 177].

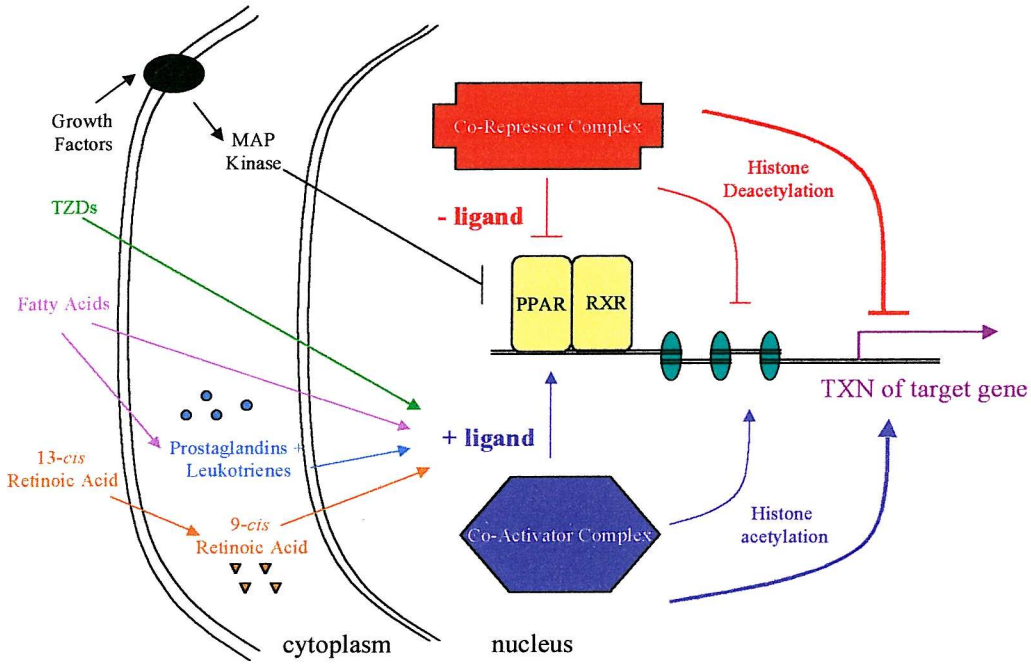

Figure 1.5 Peroxisome proliferator-activated receptors (PPARs) and retinoid X receptors (RXRs) are bound to DNA, but in the absence of a ligand they are bound by the co-repressor complex, which prevents transcription. The co-repressor complex contains SMRT/NcoR, histone deacetylases, sin3, sap48, sap18 and sap30. On addition of a ligand (such as 15-deoxy$\Delta^{12,14}$-prostglandin J_2), the co-repressor complex is released and the co-activator complex is recruited, which promotes transcription of target genes. The co-activator complex contains general co-activators, p160 proteins and CBP and PPAR/RXR specific co-activators including PPAR binding protein (PBP) and PPAR interacting protein (PRIP). The activation of PPARγ can also be reduced by phosphorylation of a serine residue by MAP kinase.

TZDs = thiazolidinedione class of anti-diabetic drugs.

Polyunsaturated fatty acids (PUFAs) are fatty acids which contain more than one carbon=carbon (C=C) double bond within their hydrocarbon backbone. PUFAs activate PPARs (Figure 1.5) [107, 116, 157, 162, 172] and include fatty acids which are important in the development and differentiation of the nervous system, such as docosahexaenoic acid (DHA, n-3) [b] and arachidonic acid (AA, n-6). DHA and AA are required in the foetus for optimal neuronal differentiation and brain functioning [178]. AA is also required for neuronal differentiation and it is a precursor of prostaglandins and leukotrienes [168].

4.4 *Eicosanoids*

PPARα is weakly activated by leukotriene B_4 and potently activated by 8(S)-hydroxyeicosatetraenoic acid (8(S)-HETE) [164, 168]. 8(S)-HETE is a lipo-oxygenase product, produced from cells on treatment with phorbol esters [164, 168]. There is a debate however, as to whether these eicosanoids activate PPARγ or not, as leukotriene B_4 has been shown to activate both PPARα and PPARγ [163]. There is also a debate in the literature as to whether derivatives of fatty acids, such as eicosanoids and prostaglandins are more specific activators of PPARs, than their fatty acid precursors. If these derivatives are more specific PPAR activators, then they may be more effective in inhibiting cancer cell growth through differentiation or apoptosis.

4.5 *Specific Natural Activators of PPARγ*

4.5.1 *J_2 Prostaglandins*

Prostaglandins are derivatives of membrane-bound arachidonic acid. The fatty acid is released from the cell membrane by the action of the enzyme, phospholipase A_2. The free fatty acid can be acted upon by a series of enzymes, to produce prostaglandins (Figure 1.6) such as prostaglandin D_2 (PGD_2) [168].

---

[b] n- numbers are known as ω nomenclature and relate to the position of the double bond within the fatty acid molecule in relation to the terminal methyl group in the fatty acid chain [574].

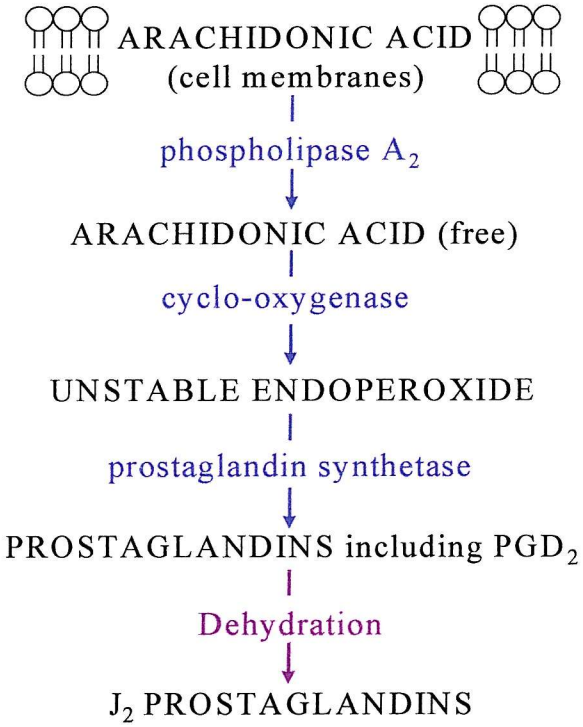

Figure 1.6 The production of J_2 prostaglandins from cell membrane-bound arachidonic acid. Each step is catalysed by an enzyme, except the conversion of prostaglandin D_2 to J_2 prostaglandins, which is thought to involve a dehydration step, as no enzymatic process leading to J_2 prostaglandin production has been reported.

Figure 1.7a) Wy-14643

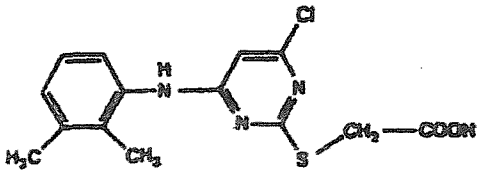

Figure 1.7b) 4 isoforms of 15-deoxy$\Delta^{12,14}$-prostglandin J_2

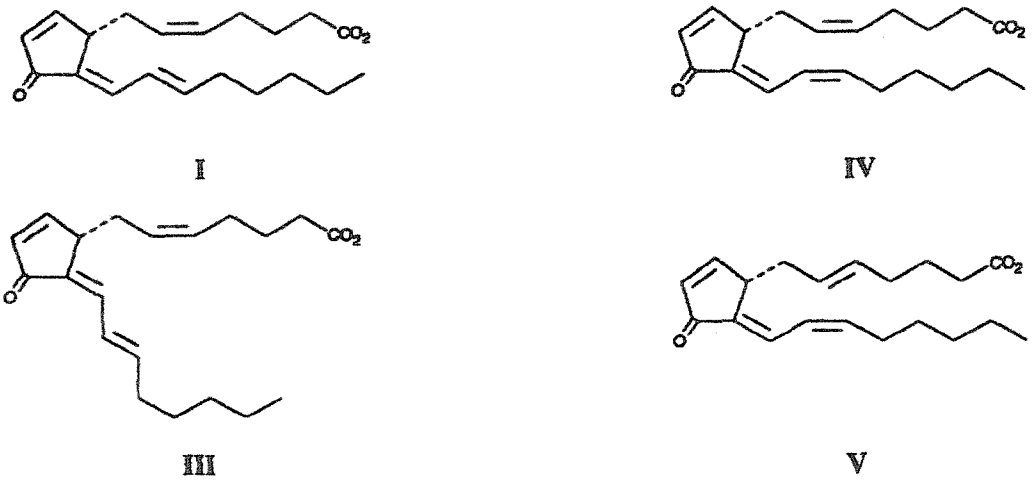

Figure 1.7c) A representative compounds of the thiazolidinedione family of drugs., rosiglitazone.

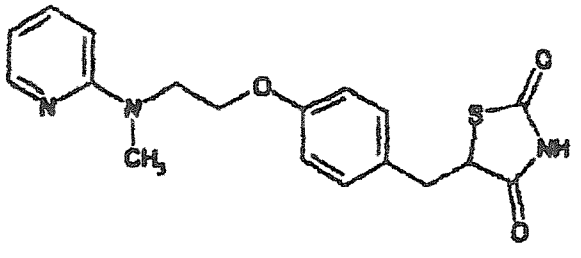

Figure 1.7 The structure of ligands of PPARα and PPARγ. a) PPARα ligand, Wy-14643, b) 4 geometric isoforms of the PPARγ ligand, 15-deoxy$\Delta^{12,14}$-prostaglandin J_2, c) Structure of a thiazolidinedione represented by the original compound discovered, ciglitazone.

PGD_2 undergoes dehydration both *in vitro* and *in vivo* to produce the J_2 series of prostaglandins [179, 180, 181].

J_2 prostaglandins have been shown to inhibit cell cycle progression, such as of colon cancer cells [182], induce endothelial cell apoptosis [183] and differentiate adipocytes [168]. One of these prostglandins, 9-deoxy$\Delta^{9,12}$-13,14-dihydro-prostaglandin D_2 (Δ^{12}-PGJ_2), is actively incorporated into organelles including nuclei [184] and is thought to covalently bind to nuclear proteins of chromatin and the nuclear matrix [184, 185, 186]. The nuclear translocation of J_2 prostaglandins is only thought to occur in cells maintained at 37 °C [185]. It is therefore thought that J_2 prostaglandins may exert their effects on cells through direct interaction with intracellular proteins, such as PPARs (Figure 1.5). The J_2 prostaglandin, 15-deoxy$\Delta^{12,14}$-prostaglandin J_2 ($15dPGJ_2$) (Figure 1.7) is the terminal metabolite of PGD_2 and is the most active [167]. It is also proposed to be the natural ligand for PPARγ [167, 168] and activates PPARγ within two hours of treatment and maximally within 7 hours [167] at an EC_{50} of 2 μM [168]. Activation of PPARγ by 15-deoxy$\Delta^{12,14}$-prostglandin J_2 has been shown to initiate transcription using a reporter construct containing three PPREs [167] and efficiently promote the differentiation of fibroblasts into adipocytes [168].

15-deoxy$\Delta^{12,14}$-prostglandin J_2 exists *in vivo* and has been detected in urine [187], but its precise concentration in PPARγ-target tissues is difficult to determine [181, 188]. The $15dPGJ_2$ obtained by chemical decomposition of PGD_2 consists of a single prominent compound surrounded by isomers with identical molecular weights [189]. These isomers are geometric isomers about the three double bonds, not in the cyclopentenone ring of $15dPGJ_2$ [189]. The major isomer is the 5-*cis*, 12-*trans*, 14-*cis* compound, isomer IV and minor isoforms are I, III, and V (Figure 1.7) [189]. The 4 isomers show different potency, isomers I and IV were shown to induce growth arrest of breast carcinoma cells *in vitro*, whereas cells treated with isomers III and V grew at a faster rate than controls [189]. $15dPGJ_2$ is electrophilic and chemically reactive and has a short half-life [189]. It is able to react within minutes with thiol nucleophiles, including cysteine, glutathione and protein thiols to form Michael adducts [189]. $15dPGJ_2$ is thermally stable, but is very photo-labile. Pure isomers of

$15dPGJ_2$ can be rendered less than 50 % pure by a single day's exposure to ambient light for 24 hours [189]. The *trans*-Δ5 isomers of prostaglandins are usually less potent than the *cis*-isomers, but as PPARγ ligands, they are more than twice as potent [189].

15-deoxy$\Delta^{12,14}$-prostglandin J_2 has also been shown to inhibit the induction of genes involved in inflammation, by a mechanism independent of PPARγ [190]. It directly inhibits NFκB-dependent gene expression through covalent modifications of critical cysteine residues in IκB kinase and the DNA binding domains of the NFκB sub-units [190, 191]. In resting cells, NFκB is bound to the inhibitor of NFκB, IκB, and is sequestered in the cytoplasm [190, 191]. During inflammation, IKK phosphorylates IκB, which becomes degraded and allows NFκB to enter the nucleus and activate gene expression [192]. $15dPGJ_2$ inhibits IKK and prevents NFκB-induced gene expression and it is hypothesised that the receptor-independent effects of $15dPGJ_2$ are due to the reactive cyclopentenone ring [190]. $15dPGJ_2$ was also shown to induce neurite outgrowth in PC12 cells, but other ligands of PPARγ did not induce the same effect and it was suggested that this process may not involve PPARγ [193].

4.5.2 *Oxidised alkyl phospholipids*

Oxidised alkyl phospholipids are specific high affinity ligands for PPARγ [194]. These phospholipids are derived from a small pool of alkyl phosphatidylcholines (PC) in low-density lipoprotein (LDL) and include azelaoyl PC (azPC) [194]. azPC binds to PPARγ in a concentration-dependent manner and can compete with known ligands of PPARγ for the ligand binding domain [194]. azPC can also activate PPAR-dependent transcription using a reporter gene assay [194]. azPC is specific for PPARγ, as it activates a reporter construct to a greater extent in cells over-expressing PPARγ, but does not activate a reporter construct to a greater extent in cells over-expressing PPARα [194].

4.6 *Specific Synthetic Activators of PPARγ*

4.6.1 *Thiazolidinediones*

A class of anti-diabetic compounds with potent adipogenic activity has been shown to be high affinity synthetic ligands of PPARγ [195], which do not activate PPARα or PPARβ [167, 168]. These compounds are called thiazolidinediones (TZDs) and were first discovered in 1982, through research into hypolipidaemic agents, to reduce cholesterol and triglyceride levels (Figure 1.7) [196, 197, 198]. Thiazolidinediones were developed through manipulation of the original compound, ciglitazone, to produce more potent adipogenic compounds, including pioglitazone, rosiglitazone (BRL49653) and troglitazone [198]. Thiazolidinediones have been shown to rapidly activate PPARγ at an EC_{50} of 40 nM [195] and increase expression of the receptor during induction of adipogenesis [195, 199, 200]. Several thiazolidinedione have been used in the clinical setting including, troglitazone (Rezulin™), rosiglitazone (Avandia) and pioglitazone (Actos) [201], however, troglitazone has been associated with side effects including liver failure [202]. TZDs have also been shown to act independently of PPARγ. Troglitazone inhibits cholesterol biosynthesis in a range of cell types independent of PPARγ [203], including 3T3-L1 cells, which have been shown to express high levels of PPARγ [204, 205].

4.6.2 *Phenylacetate*

The aromatic fatty acid phenylacetate and its analogues are structurally similar to the peroxisome proliferator, clofibrate [206]. They activate PPAR-dependent transcription and 4-iodophenylbutyrate is the most potent analogue, whereas phenylacetate is much weaker [206]. These aromatic fatty acids were also shown to increase the mRNA levels of PPAR target genes in the hepatocytes of treated rats [206]. Phenylacetate was also shown to specifically bind to PPARγ with low affinity in human neuroblastoma cell lines [207]. It also activated PPARγ in human neuroblastoma cell lines, as antagonists of PPARγ prevented the phenylacetate from having any effects on the neuroblastoma cells [207].

5 *Mechanism of action of ligand-activated PPARs*

5.1 *Ligand-activated PPARs undergo a conformational change*

In the absence of a ligand, nuclear receptors interact with a co-repressor complex, which includes NcoR/SMRT (nuclear co-repressor/silencing mediator for retinoid and thyroid receptors), Sin3, histone deacetylases and other proteins including sap18, sap48 and p30 [208, 209, 210, 211, 212, 213] (Figure 1.5). On ligand binding the co-repressor complex is released and the co-activator complex is recruited [214] (Figure 1.5). When a ligand binds to a nuclear receptor there is a conformational change in the receptor [215]. This has been shown in retinoic acid receptors, where the omega loop which connects helices 1 and 3 in RARs or helices 2 and 3 in RXRs, flips 180° [215]. Helix 12, which contains the AF-2 domain, then moves 90° from a position away from the ligand binding domain (domain E), towards the ligand binding domain [215]. This change in the AF-2 domain allows the co-repressors to be released and promotes interactions with co-activator proteins [154, 216, 155, 156]. The change in conformation exposes the co-activator binding site, LXXLL, which is orientated via a "charged clamp" formed by conserved lysine and glutamate residues [153]. Research using the novel PPARγ ligand, L-764406, has shown that it was linked to a single cysteine residue, corresponding to cysteine 313 in human PPARγ2 [217]. This residue is located within helix 3 of the ligand binding domain and is also thought to be important in ligand binding [217]. Ligand binding also serves to stabilise PPARγ [218]. In the absence of a ligand, the ligand binding domain (LBD) and co-activator domain are in a mobile conformation, however, on ligand binding there is a chemical shift in the atoms of the ligand binding domain and the conformation is stabilised [218].

5.2 *PPARs – cytoplasmic proteins which translocate to the nucleus on ligand binding or nuclear proteins?*

Nuclear receptors have been shown to translocate from the cytoplasm to the nuclei of cells on ligand binding [219].

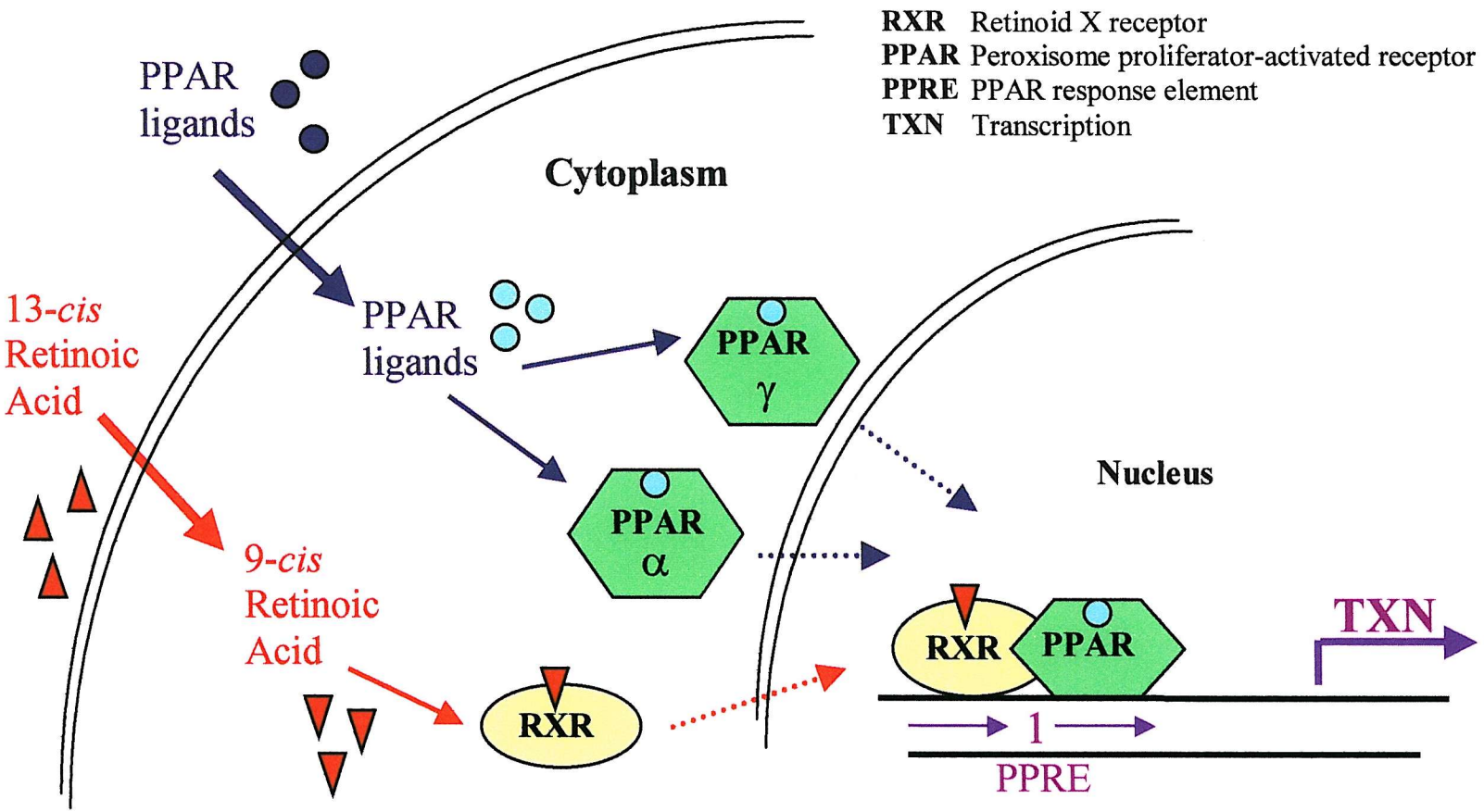

Figure 1.8 Activated PPARs translocate to the nuclei of cells and heterodimerise with retinoid X receptors. The heterodimers bind to PPAR response elements (PPREs) on DNA and activate the transcription of genes.

However, there is increasing evidence that PPARα [220, 221] and PPARγ [214, 222, 223] are predominantly expressed in the nuclei of cells bound to co-repressors and that ligand binding serves to recruit co-activators and release co-repressors and not induce nuclear translocation of the protein (Figure 1.5). In this case, some RXRs must also be expressed in the nucleus for ligands of PPARγ to activate the transcription of genes, as ligands of PPARs alone would not induce nuclear translocation of RXRs. Interestingly some expression of oestrogen receptors has also been reported to occur in the nuclei of cells [219].

However, other reports suggest that PPARγ translocates to the nuclei of cells on ligand binding (Figure 1.8) [152, 224]. This was shown in MCF-7 and MDA MB 231 breast cancer cells treated with γ-linolenic acid [224]. Treatment of both cell types with 75 μM fatty acid resulted in translocation of PPARγ to the nucleus within 30 minutes [224]. Within 6 hours of exposure, the majority of PPARγ was seen in the nuclei of both cell lines, with a concurrent reduction in cytoplasmic staining [224]. This agrees with data showing that treatment of CV-1 cells with 15-deoxy$\Delta^{12,14}$-prostglandin J_2 activates PPARγ, which induces transcription of its target genes within 2 hours of treatment and that this is maximal within 7 hours of treatment [167]. A thiazolidinedione, rosiglitazone, is also able to activate PPARγ within 2 hours in CV-1 cells [167]. Bisphenol A diglycidyl ether (BADGE), which has been shown to be an agonist PPARγ, has also been shown to induce nuclear translocation of PPARγ in the endothelial cell line ECV304 [225].

5.3 *Ligand-activated PPARs dimerise with multiple partners*

On ligand binding, PPAR receptors heterodimerise with other members of the nuclear hormone receptor super-family (Figures 1.5 and 1.8). Nuclear hormone receptors tend to be promiscuous and are able to dimerise with more than one other partner, or homodimerise. PPARs cannot homodimerise or heterodimerise with RARs, but preferentially heterodimerise with RXRs [152] and also form heterodimers with liver X receptors (LXRs) [226]. There is thought to be cross-talk between the PPAR and thyroid hormone receptor signalling pathways [227, 228]. Cross-talk has also been reported between the oestrogen receptor and PPAR pathways in the duck

[119, 120], although no evidence of this in humans has been reported. Little is known about which isoforms of PPARs dimerise with which isoforms of RXRs, although it is known that RXRα is capable of heterodimerising with PPARα and PPARγ and RXRβ is capable of dimerising with PPARα [172, 229, 230].

The PPARγ/RXRα heterodimer has been shown to be asymmetric, with the PPARγ ligand binding domain rotated by 10° in respect to that of RXR [230]. The majority of the heterodimer interactions occur through helix 10 of each of the receptor, which correspond to residues 432-447 in PPARγ and 415-434 in RXRα [230]. The asymmetry of the dimer results in a positively charged region on RXR packing against a negatively charged region of PPARγ and these interactions are stabilised by the formation of a salt bridge [230]. These additional interactions increase the total dimerisation interface and explain the preferential formation of the PPAR/RXR heterodimer over the formation of homodimers [230].

5.4 *Activated PPAR/RXR heterodimers bind to specific response elements (PPREs)*

PPAR/RXR heterodimers bind to PPAR response elements (PPREs) in the DNA sequence. PPREs are typically arranged as direct repeats of motifs separated by 1 spacer nucleotide, known as DR1 elements [231]. Nucleotide spacing between the response elements repeats serve as a determinant of the specificity of binding by different nuclear hormone heterodimers [232]. DR1 elements that bind PPAR/RXR can be either perfect or imperfect repeats. The PPRE of the *Aco* gene is a DR1 element with perfect RG(G/T)TCA repeat motif (AGGACA(A)AGGTCA) and is one of the least promiscuous of binding elements [233, 234]. However, the PPRE of apoAI gene is also DR1 element with a perfect RG(G/T)TCA repeat motif (AGGGCA(G)GGGTCA) and can bind other heterodimers, such as RAR/RXR [234]. DR1 elements with imperfect RG(G/T)TCA motifs include PPREs in the apoB [235] and α1-anti-trypsin genes [236]. DR1 elements with purine or thymidine residues as the spacer nucleotides, are suitable for PPAR/RXR binding and adenine as the spacer nucleotide allows the strongest binding [234]. DR1 elements are found in the

upstream promoters of target genes and the 5' flanking regions around these elements determine heterodimer affinity [227, 237].

The PPARγ2/RXR heterodimer has been shown to induce bending of DNA on binding to its response element [238]. This was seen with the unique response element in the murine lipoprotein lipase promoter and resulted in the DNA bending by 46° [238]. Parallel studies using an artificial response element also showed that the DNA was distorted by binding of PPARγ2/RXR heterodimers, but in this case the distortion was 56° [238]. This indicates that PPARγ2 uses a common mechanism shared by other members of the nuclear receptor superfamily which also induce DNA bending at their DNA binding sites [238].

RXR can heterodimerise with PPARs and other members of the nuclear receptor superfamily. These heterodimers can be permissive or non-permissive [215, 103, 99, 239, 232]. RAR/RXR heterodimers are non-permissive and this is because in some cases RAR prevents RXR ligands from binding to RXR [239]. In other cases, RXR ligands can only bind to their receptor on activation of RAR [232]. This is because RAR activation results in the recruitment of co-activators and a change in the allosteric interactions between RAR and RXR, thus permitting RXR ligands to bind [232]. In contrast, PPAR/RXR heterodimers are permissive [99, 103]. This is because RXR ligands can bind to RXR within PPAR/RXR heterodimers with high affinity and allow RXR-specific transactivation [232].

5.5 *Ligands of PPARs and RXRs can act synergistically*

Activation of PPAR-RXR heterodimers can be maximised when both receptors are bound by their respective ligands [240]. Simultaneous treatment of liposarcoma cells with both PPAR and RXR ligands has been shown to increase cell differentiation [241]. Combinations of troglitazone and all-*trans* retinoic acid in MCF-7 breast cancer cells synergistically and irreversibly inhibit cell growth and induces apoptosis [242] and rosiglitazone and 9-*cis* RA synergistically inhibit the growth of leukaemia cells [243]. Synergistic transactivation may occur by each sub-unit of the dimer contacting different components of a common co-activator complex or by

each receptor activating a different co-activator complex [244, 245]. It is known that the ligand-dependent transcriptional transactivation site, AF-2, in RXR is not required for this synergy [215]. This is because inactivation of RXR AF-2 has no effect on the ability of PPAR/RXR to respond to rosiglitazone, whereas inactivation of the PPARγ AF-2 domain transforms the heterodimer permissive for RXR signalling into a non-permissive heterodimer [215]. This suggests that binding of a ligand to RXR induces a conformational change throughout the dimer, which facilitates transactivation by PPARγ [215]. This conformational change also increases the recruitment of co-activators by the heterodimer [215].

5.6 *Co-activators and co-repressors*

5.6.1 *Co-activators*

PPAR-RXR heterodimers and RXR-RXR homodimers interact with DNA and through DNA binding proteins known as co-activators, and non-DNA binding accessory proteins [152] (Figure 1.5). Co-activators are thought to interact with the D-box motif at the base of the second zinc finger in the nuclear hormone receptor DNA binding domain [152]. Non-DNA binding accessory proteins may act as "bridging factors" between the basal transcription machinery and the nuclear receptors [152]. Co-activators function by forming a bridge with the basal transcription machinery and confer a local increase in histone acetylation [246, 247]. PPAR and RXR function separately within the heterodimer conformation to recruit co-activators. Activation of the PPAR-RXR heterodimer by RXR ligands induces the recruitment of p160 coactivators, whereas PPARγ ligands exclusively recruited the DRIP205 co-activator complex to PPARγ, but not p160 proteins [248].

5.6.1.1 *p160 proteins*

The co-activator complex, which binds to the PPAR/RXR heterodimer, contains cAMP responsive element binding protein (CREB) binding protein (p300/CBP) [244]. It also contains three p160 proteins, one of which is steroid receptor co-activator

1/nuclear co-activator 1 (SRC1/NcoA1) [249]. The second p160 protein is known as transcriptional intermediary factor-2 (TIF2) in humans [250] and glucocorticoid receptor interacting protein/nuclear co-activator 2 (GRIP1/NcoA2) in mice [251]. The other p160 protein in the co-activator complex in humans is called activator of the thyroid and retinoic acid receptor/receptor associated co-activator 3/amplified in breast cancer 1/TR activator molecule 1 (ACTR/RAC3/AIB1/TRAM1) [252, 253, 254, 255]. The mouse homologue of ACTR/RAC3/AIB1/TRAM1 is called p300/CBP co-integrator associate protein or p/CIP [251]. ACTR/RAC3/AIB1/TRAM1 is also known as PPAR interacting protein (PRIP) and contains two LXXLL motifs, of which one at amino acid position, 892-896 is able to bind PPARγ [256]. PRIP is ubiquitously expressed in and is able to potentiate the transcriptional activity of PPARγ and RXRα in mammalian cells [256].

CBP/p300 binds to PPARγ in both a ligand-dependent and -independent manner, at two docking sites in its N-terminal region at residues 1-113 and 1099-1460 [257]. CBP/p300 constitutively binds PPARγ, but on activation by a ligand, the co-activator binds to PPARγ at the second binding site [257]. CBP/p300 possesses intrinsic histone acetyltransferase activity and is therefore thought to influence the chromatin structure and also establish a contact between nuclear receptors such as PPARγ and the basal transcription machinery [257]. It has also been shown to be associated with RNA polymerase II via RNA helicase A [258] and is also known to bind to other nuclear hormone receptors [154]. These include retinoid X receptors [244, 259] and PPARα [260]. CBP/p300 acts as a platform for a large number of proteins, including CBP/p300 associated factor (p/CAF), another histone acetyltransferase [261]. p/CAF also interacts with SRC-1/NcoR-1 at its N-terminal and another domain on the protein interacts with p/CIP/ACTR/RAC3/AIB-1/TRAM-1 [252].

p160 proteins have highly conserved interaction domains and contain 3 repeated motifs of the consensus sequence, LXXLL [251, 253, 262]. These are also known as NR (nuclear receptor) boxes and are involved in direct interaction with the ligand binding domain of the receptor [257]. p160 proteins interact with PPARγ in a ligand-dependent and -independent manner and also with CBP/p300 through one of the transactivation domains [244, 251, 262, 263, 264]. Like the other co-activators, p160

proteins possess histone acetyltransferase activity [247, 265] and can co-activate synergistically with CBP/p300 [263]. Amino acid residues in helix 3 (K301), helix 4 (V315), helix 5 (Y320) and helix 12 (L468 and E471) on PPARγ are essential for ligand induced co-activator interaction of CBP/p300 and SRC-1/NcoA-1 with PPARγ [266].

5.6.1.2 *PPARγ co-activator-1 (PGC-1)*

PGC-1 is a co-activator of PPARγ, which is induced on exposure to cold temperatures in thermogenic tissues such a brown fat and skeletal muscle [267, 268]. It is not a histone acetyltransferase, but is thought to exist in a complex with CBP/p300 and SRC-1/NcoA-1 [267]. It binds to SRC-1/NcoA-1 at residues 782-1139, which encompasses the binding sites for CBP/p300 and p/CAF [267]. The binding of PGC-1 to PPARγ has been described as the "spring trap model" by Puigserver *et al.*, [267]. In this model, PGC-1 has low transcriptional activity and ability to complex with other co-activators, when it is not bound to PPARγ [267]. On ligand binding, there is a change in conformation of PPARγ allowing PGC-1 to bind and increases its ability to enhance transcription and complex with CBP/p300 and SRC-1 [267]. PGC-1 also increases the transcriptional activity of PPARγ and the expression of key enzymes in the respiratory chain [268].

5.6.1.3 *PPARγ binding protein (PBP)*

PPAR binding protein (PBP) is ubiquitously expressed, but highly expressed in the germinal epithelium of mouse testis [256]. It serves as a co-activator of PPARγ and other nuclear hormone receptors, including PPARα and RXR in a ligand-dependent manner [256]. However, PBP only modestly increases PPARγ transcriptional activity [256]. PBP contains two LXXLL motifs, which are required for binding of cofactors to nuclear hormone receptors and binds to the 12 C-terminal amino acids of PPARγ [256]. It is known that PBP does not interact with SRC-1, but any interactions with CBP/p300 have yet to be investigated [256].

5.6.1.4 *Other co-activators*

A range of other co-activators bind to PPARs including thyroid hormone receptor-associated protein 220 (TRAP220) [269], DRIP205 complex [248], nuclear receptor binding factors 1 and 2 (NRBF-1 and NRBF-2) [270, 271] and androgen receptor co-activator, ARA70 [272]. TRAP220 is recruited to the ligand binding domain of PPARγ on ligand binding through one LXXLL motif in the AF-2 region [265]. TRAP220 anchors a complex of 14-16 proteins to PPARγ [265, 269] and also recruits RNA polymerase II to the site of transcription [265]. DRIP205 is a distinct, multi-subunit coactivator complex containing TRAP220 and other co-activators [248]. DRIP205 binds directly to PPARγ, but not RXR, in a ligand-dependent manner [248]. NRBF-1 [270] and NRBF-2 [271] interact with several nuclear receptors, including PPARα . Both the hinge and ligand-binding domains of PPARα are required for the interaction with NRBF-1, which seems to be translocated to the nucleus by a "piggyback" mechanism, together with PPARα [270]. ARA70 is expressed in a wide range of tissues including adipose tissue [272]. It interacts with PPARγ in the absence of the $15dPGJ_2$, although the addition of exogenous ligand enhances this interaction [272]. This suggests that there is some cross-talk between the androgen and PPAR signalling pathways [272].

5.6.2 *Co-repressors*

Receptor interacting protein 140 (RIP140) is a co-repressor of PPARs and binds to the C-terminal of the proteins [273, 274]. Ligands of PPARs enhance the interaction of RIP140 with PPARα and PPARγ in solution but not with PPAR/RXR heterodimers on DNA [273], however RIP140 does bind efficiently to PPARα in the absence of any added ligand [274]. In contrast, RIP140 only interacts with RXR in the presence of 9-cis retinoic acid [274]. Binding of RIP140 and co-activators such as SRC-1 to nuclear receptors is competitive and RIP140 is thought to antagonise receptor activity in mammalian cells [273, 274] and specifically down-regulate coactivation mediated by SRC-1 [273]. Nuclear co-repressor/silencing mediator for retinoid and thyroid

receptors (NcoR/SMRT) is a strongly interacting co-repressor for many nuclear receptors, including retinoic acid receptors and thyroid hormone receptors, however, it only weakly interacts with PPARγ and RXR [215]. This is consistent with the fact that PPARs lack conserved co-repressor boxes [232], to which N-COR would bind, seen in other members of the nuclear receptor family [208, 214].

6 *Regulation of PPARs*

PPARs can be regulated by a variety of factors, including ligand-binding, interactions with both co-activators and co-repressors [152], binding to DNA, phosphorylation and interactions with heat shock proteins. PPARα has also been shown to be inhibited by growth hormone [275]. Growth hormone stimulates Janus kinase-signal transducer and activator of transcription 5b (JAK2/STAT5b) and this inhibited PPARα-dependent transcription by up to 80-85 % [275]. It is thought that STAT5b may act through an indirect inhibition mechanism, such as competition for an essential PPARα coactivator or STAT5b-dependent synthesis of a more proximal PPARα inhibitor [275].

6.1 *Regulation of PPARs by PPAR ligands*

6.1.1 *Up-regulation of PPARγ*

Some thiazolidinediones have been shown to up-regulate the expression of PPARγ [276, 277]. Troglitazone was shown to increase PPARγ mRNA and protein expression in hepatocytes, whereas ciglitazone, rosiglitazone, $15dPGJ_2$ and other ligands of PPARs had no effect [276]. Troglitazone is therefore thought to regulate PPARγ at the level of gene expression in these cells and is not thought to induce an increase in protein stability [276]. Likewise pioglitazone was shown to increase the levels of PPARγ mRNA and protein expression in pre-adipocytes, however, it down regulated PPARγ expression in mature adipocytes [277]. Interestingly, retinoic acid receptor mRNA expression is also increased on treatment with its ligands [278].

6.1.2 *Down-regulation of PPARγ*

In contrast to the results seen in hepatocytes [276], troglitazone, rosiglitazone and $15dPGJ_2$ have also been shown to reduce the expression of PPARγ mRNA in 3T3-L1 adipocytes [279, 280]. Recent data published by Hauser *et al.*, [280] also suggest that the PPARγ protein may be regulated by feedback system, whereby ligand-induced activation of the receptor results in degradation of the protein. Interestingly, degradation of PPARγ correlates well with the ability of PPARγ ligands to activate this receptor and is seen on treatment of fibroblasts and adipocytes with both natural and synthetic ligands of PPARγ, but not PPARα [280]. The non-phosphorylated form of PPARγ is preferentially lost, however, the phosphorylated form of PPARγ is not degraded [280].

Ligand-induced activation of PPARγ results in ubiquitin-dependent degradation of the protein at the proteasome [280]. Ubiquitination involves attachment of ubiquitin to lysine residues in the protein to be degraded, by three enzymes, ubiquitin-activating enzyme (E1), ubiquitin-conjugating enzyme (E2) and ubiquitin protein ligase (E3) [281]. The ubiquitinated protein is then delivered to the proteasome where it is degraded [281]. Ubiquitination has already been shown to be involved in the turnover of other nuclear hormone receptors, including thyroid hormone receptors [282] and retinoic acid receptors [278]. PPARγ is ubiquitinated on ligand binding and this degradation is dependent on the conformation of the AF-2 domain and may involve co-activators [280]. It is possible that one or more proteins in the ubiquitin pathway are able to bind to the AF-2 domain only in the ligand-bound conformation [280]. However, RIP140, a ligand-dependent co-repressor of PPARγ blocks ubiquitination of the protein and therefore ligand binding is not the only prerequisite for ubiquitination, and it is thought that ubiquitination of PPARγ is closely associated with a transcriptionally active form of the receptor [280].

6.2 *Phosphorylation of PPARα and PPARγ*

Phosphorylation has been shown to be important in the regulation of nuclear hormone receptors including the progesterone receptor [283] and retinoic acid receptor [278]. Likewise, PPARα is a phosphoprotein, which can be phosphorylated by treatment of cells with insulin [284]. Treatment of rat adipocytes and CV-1 cells, with insulin induced a time-dependent increase in phosphorylation of PPARα and a three-fold increase within 30 minutes [284]. This change in phosphorylation enhanced the transcriptional activity of PPARα two-fold [284] and may explain some of the cross-talk between insulin signalling and PPAR activity. PPARα is also phosphorylated by p38 MAPK in A/B N-terminal region in response to stress stimuli and this also significantly enhanced ligand-dependent transactivation by PPARα [284].

In contrast, the activity of PPARγ is reduced or inhibited by phosphorylation by protein kinases. Mitogen-activated protein kinases (MAPKs) including extra-cellular signal regulated kinases (ERKs) have been shown to phosphorylate PPARγ1 and PPARγ2 [285, 286, 287, 288]. PPARγ1 has also been shown to be strongly phosphorylated by c-Jun N-terminal kinase (JNK) [285, 288] and weakly by p38 MAPK [288]. Both basal and ligand-dependent transcription induced by PPARγ is down regulated on phosphorylation of PPARγ [285, 288]. The N-terminal of PPARγ1 and PPARγ2 contain a consensus MAP kinase site ($PX^{S}/_{T}P$) at serine^{84} of PPARγ1 and serine^{112} of PPARγ2 in humans [285, 286, 287, 288]. Phosphorylation of this residue by activated MAP kinases significantly inhibits ligand-dependent and ligand-independent transcriptional transactivation [285]. Mutation of serine 84 to alanine results in increased transcriptional activity and adipogenic activity of the receptor [285]. It is thought that phosphorylation of serine 84 acts to prevent interaction of PPARγ with co-activators and accessory proteins, as it does not affect stability or DNA binding [285]. The prostaglandin F_2 is also thought to negatively regulate PPARγ through an indirect mechanism involving MAP kinase [289]. Inhibitors of MAP kinase, such as PD89059 have also been shown to increase transcriptional activity of PPARγ and in combination with PPARγ ligands such as troglitazone [290].

6.3 *Interactions with heat shock proteins*

Rat PPAR has been shown to co-precipitate with the heat shock protein, Hsp72, in a clofibric acid-dependent manner [291]. It has been suggested that Hsp72 may be involved in the folding of PPARs, sub-cellular localisation or the signalling pathways of PPARs [291]. However, no reports of interactions between other heat shock proteins and PPARs have been described in human cells and neither have any interactions between PPARs and Hsp72 been reported in response to ligands of PPARγ. Other members of the nuclear receptor superfamily have been shown to interact with hsp90 and other minor species [292].

7 *Involvement of PPARα and PPARβ in normal cell function and human disease*

7.1 *Normal cells*

Activated PPAR-RXR heterodimers and co-activators activate transcription of genes through the transcription initiation complex. Many of these target genes are known to involved in lipid metabolism [152], although there are a few genes involved in cell cycle control whose transcription is induced by PPAR activators [293]. Peroxisome proliferators have been shown to induce oncogenes such as *c-jun* and *c-myc* and their ability to induce these genes correlates with tumour-promoting potential [294, 165]. Other activators of PPARα such as Wy-14643 are known to induce the oncogenes *c-fos* and *junB*/erg-1 [165].

Target genes of PPARα include those encoding enzymes in the peroxisomal β-oxidation pathway [152]. This pathway includes enzymes whose activities are up-regulated in response to peroxisome proliferators, such as acyl CoA oxidase and 3-ketoacyl-CoA thiolase [295, 296]. The increased activities are due to increases in the rates of gene transcription [297]. Acyl CoA oxidase has a well-characterised PPRE in its promoter [233] whereas no functional PPRE has been identified in the ketoacyl-CoA thiolase gene promoter [152]. Genes encoding proteins belonging to the family

of cytochrome *P*-450 IV enzymes are also targets of PPARα and their activity is related to rates of transcription [298]. These enzymes catalyse the ω-hydroxylation of substrates which include fatty acids and prostaglandins [299, 300] and their promoters also contain functional PPREs [301]. The processes of ketogenesis and mitochondrial β-oxidation are examples of other processes enhanced by increased transcription rates due to the action of peroxisome proliferators [302, 303]. PPARα controls the activity of (3-hydroxy-3-methylglutaryl coenzyme A) HMG-CoA synthase, an important ketogenesis enzyme [304] and is also known to be involved in activation of cytosolic proteins, such as fatty acid binding proteins [233, 305] and malic enzyme [306].

7.2 *Cancer*

PPARα is involved in peroxisome proliferation and the development of hepatic, pancreatic and testicular cancers in rodents [112, 152], but activation of PPARα has also been shown to inhibit the promotion of skin tumours [307] and colorectal cancer [308] in mice. Activation of PPARα has not been associated with peroxisome proliferation and the development of cancers in humans [309]. However, PPARα is either not expressed or is weakly expressed in normal prostate epithelial cells, whereas is it highly expressed in poorly differentiated prostate carcinomas [310].

Little is known of the function of PPARβ in normal cells, although it has been implicated in embryo implantation [138] and the regulation of other PPARs [136]. However in 1999, a link between PPARβ and colon cancer was established [311]. PPARβ is a negative target of the APC gene, which is mutated in familial adenomatous polyposis, an inherited disease characterised by numerous colorectal adenomas [311]. It is also antagonised by a non-steroidal anti-inflammatory drug (NSAID), which is known to suppress colorectal tumourigenesis [312]. Genetic disruption of the PPARβ gene has also been shown to reduce the tumourigenecity of human colon cancer cells [313]. As well as being shown to be over-expressed in many colorectal cancers, with normal tissue expressing lower levels of the isoform [313, 314], PPARβ has been shown to be highly expressed in uterine endometrial adenocarcinomas [315].

8 *Involvement of PPARγ in normal cell function and human disease*

8.1 *Lipid metabolism, lipid storage, obesity and diabetes*

PPAR-induced transcription is involved in both intracellular and extracellular metabolism of triglyceride-rich lipoproteins. High density lipoprotein contains both Apo I and Apo II, which are involved in cholesterol transport from the liver to the tissues and are important in prevention of atherosclerosis [316]. Both proteins have functional PPREs in their promoters and are synthesised as a result of PPAR-induced transcription [152]. Within cells, enzymes involved in the process of lipoprotein metabolism, e.g. lipoprotein lipase (LPL), are also activated through the action of fatty acids and fibrates on a PPRE in the LPL gene promoter [152]. PPAR-mediated transcription is also involved in fatty acid transport within cells through genes such as acyl CoA synthetase (ACS), which esterifies fatty acids ensuring they remain within the cell [317] and several proteins involved in this process, including ACS, have PPREs in their promoters [152].

PPARγ has been shown to be important in the storage of lipids and along with CAAT enhancer binding protein (C/EBP) and adipocyte determination and differentiation factor/sterol-response element binding protein (ADD-1/SREBP-1), promotes the differentiation of adipocytes [110, 146, 168, 205]. These factors act synergistically and it is thought that C/EBP is elevated during the early stages of adipocyte differentiation in response to adipogenic factors, such as insulin and glucocorticoids [318]. C/EBP then induces the expression of PPARγ [318, 319], which is the central trigger for adipogenesis, which acts to stimulate the uptake of glucose and fatty acids and their conversion to triglycerides [312]. An excess of adipose tissue leads to obesity, whereas its absence is associated with lipodystrophic syndromes [133]. In the fasting state, the expression of PPARγ is decreased and the expression of PPARα is increased, resulting in lipolysis and fatty acid oxidation.

Both PPARγ and SREBP-1 are regulated by insulin [320] and PPARγ is phosphorylated on treatment of cells with insulin [287]. In diabetes, a lack of insulin

may lead to a reduction in the expression of PPARγ, resulting in a decrease in the glucose and fatty acid uptake, leading to hyperglycaemia [312]. It is somewhat contradictory that PPARγ orchestrates adipocyte differentiation and yet thiazolidinediones, which are ligands of PPARs, have been used to treat insulin resistance, which occurs on excess adipogenesis and obesity [133]. However, adipose tissue is required for a patient to respond to insulin, as patients lacking adipose tissue can be severely insulin resistant [321]. Thiazolidinediones are thought to mediate their effects on insulin sensitivity through PPARγ, as receptor activation correlates with this ability [322].

Several amino acid substitutions involving insulin insensitivity and obesity within the human PPARγ gene have been described, including P12A and P115G. The substitution of alanine^{12} for proline^{12} is the most common substitution found [323, 324, 325]. It is associated with reduced receptor activity, increased insulin insensitivity and a lower body-mass index [326]. The Proline^{115}-Glycine^{115} substitution, which is in the MAP kinase target sequence of PPARγ, has been associated with changes in body mass indices and is a rare cause of morbid obesity [327, 328]. This mutation prevents the phosphorylation of PPARγ at serine^{112} leading to increased activity, accelerated adipocyte differentiation and severe obesity [327]. Two other mutations have been described in patients suffering from severe insulin insensitivity, but not obesity [329]. Some cases of severe insulin resistance are due to mutations within helix 12 of PPARγ, which produce a dominant negative protein [330]. The mutations affect the co-activator docking sites, so that, even on ligand binding, the dominant negative PPARγ cannot recruit co-activators or release co-repressors, so that it cannot activate transcription of its target genes [330]. Therefore adipocyte differentiation cannot occur and the patient develops diabetes, severe insulin resistance and hypertension at an unusually early age [330].

8.2 *Inflammation*

PPARγ is markedly upregulated in activated macrophages and inhibits the inflammatory response [331]. The expression of interleukins, tumour necrosis factor α (TNFα), matrix metalloproteinases and scavenger receptor A are inhibited in

macrophages and monocytes treated with natural or synthetic ligands of PPARγ [331]. PPARγ has also been shown to reduce non-lipopolysaccharide-induced excretion of interleukin 2 and interleukin 6 from monocytes [224]. Matrix metalloproteinases are involved in tissue damage and scavenger receptor A has a role in cell adhesion during inflammation [331]. The promoters of these genes contain binding sites for the transcription factors, AP-1, NFκB and STAT-1, and the inhibition of inflammation is thought to occur in part by PPARγ antagonising the activities of the transcription factors AP-1, STAT and NFκB [331]. However, the concentrations of ligands of PPARγ required to modulate cytokine production through antagonism of NFκB far exceed those required to activate the receptor, and it has been suggested that additional PPARγ pathways may be involved [332]. Another link between PPARγ and inflammation is that NSAIDs are ligands of PPARγ, as well as PPARα [169] and it is thought that part of the anti-inflammatory effects of NSAIDs are mediated through PPARs.

PPARγ is undetectable in circulating monocytes, but activation of monocytes with a combination of PPAR and RXR ligands, results in the expression of the cell surface marker, CD14, which is a marker of monocyte differentiation [333, 334]. However, PPARγ expression itself, is only seen several hours post-differentiation of the monocytes and RXR may be the more important transcription factor in this process [335]. PPARγ-mediated transcription also has a negative effect on T-lymphocyte activation, through inhibition of interleukin-2 (IL-2) expression [336]. The transcription factor NFAT plays a role in IL-2 expression, which in turn governs most of the early lymphocyte proliferation responses [336]. Activated PPARγ directly interacts with NFAT and down-regulates the IL-2 promoter, resulting in the inhibition of T-lymphocyte activation [336].

8.3 *Atherosclerosis*

PPARs have been implicated in inflammation and the development of atherosclerosis. Atherosclerosis is a complex disease characterised by a gradual build-up of lipids in the arterial wall, known as atherosclerotic plaques [312]. These plaques can rupture leading to the sudden obstruction of blood-flow. The

development of atherosclerosis involves endothelial dysfunction, chronic inflammation, proliferation of smooth muscle cells and the formation of foam cells [337, 338]. PPARα and PPARγ are involved in the inflammatory response and may be useful in the treatment of atherosclerosis. PPARγ has been shown to reduce the expression of the metalloproteinase, MMP-9, which is important in destabilisation of atherosclerotic plaques [339]. The anti-inflammatory effects of PPARγ, including inhibition of inflammatory cytokines known to be involved in the progression of atherosclerotic lesions, may be beneficial in the treatment of atherosclerosis [312]. However, PPARγ stimulates the uptake of oxidised low density lipoprotein (oxLDL) by enhancing expression of the scavenger receptor, CD36, which is important in the formation of foam cells [333, 334]. OxLDL and some of its metabolites have also been shown to induce PPARγ, which would initiate a positive feedback loop, leading to increased expression of CD36, oxLDL uptake and further foam cell formation [333, 334]. Therefore, ligands of PPARγ have potential as treatments of atherosclerosis and other inflammatory diseases such as rheumatoid arthritis [331], but all the effects of these ligands on cells needs to be elucidated before they can be developed further.

8.4 *Cancer*

8.4.1 *Expression in cancer cells*

PPARγ is expressed at high levels in some cancer cell lines and primary tumours including those of colon [182], liposarcoma [241], breast [242, 290] gastric [340] and lung [341], as well as in the corresponding normal tissue. However, prostate cancer cells express high levels of PPARγ, whereas the normal tissue had very low expression levels [130]. Human neuroblastoma cell lines and primary tumours have been shown to express high levels of PPARγ, however the expression of the protein decreases with advanced stages of the disease [342]. Interestingly, human neuroblastoma cell lines have been shown to express very different levels of PPARγ [343].

Mutations and polymorphisms have been found in some cancer cell types, although PPARγ null cells have been shown to be embryonic lethal [144, 145, 146]. These mutations include somatic loss-of-function mutations in sporadic colorectal carcinomas (detailed below) and somatic translocation of PAX8 and PPARγ in follicular thyroid carcinoma, but not other related cancers [344]. The PAX8PPARγ1 translocation results in the formation of a dominant negative PPARγ protein, which is proposed to be involved in the development of this cancer [344]. Over-representation of a PPARγ variant, H449H, has also been found in patients with glioblastoma multiforme and it has been suggested that PPARγ contributes common, low-penetrance alleles for cancer susceptibility [345]. The PPARγ variant, P12A, was shown to be under-represented in renal cell carcinoma patients, but in contrast, the H449H variant was over-represented in endometrial carcinoma [345].

8.4.2 *Activation of PPARγ has potential as anti-cancer therapy*

Activation of PPARγ in cancer cells results in inhibition of cancer cell growth [130, 182, 241, 242, 290, 346]. PPARγ-induced growth inhibition has been shown to occur through mechanisms including differentiation [207, 342], apoptosis [223, 347, 340, 341] and more recently shown, autophagy or type II programmed cell death [346]. This has been mainly achieved by using 15-deoxy$\Delta^{12,14}$-prostglandin J_2 ($15dPGJ_2$), the natural ligand of PPARγ [168, 167], phenylacetate [207] or the thiazolidinediones [290]. The exact mechanisms by which PPARγ induces growth inhibition in cancer cells are unclear. However pre-adipocytes, which express PPARγ, differentiate on treatment with PPARγ ligands and this is associated with loss of DNA binding for the growth-related E2F/DP transcription complex and exit from the cell cycle at G_1 [348]. This is because activation of PPARγ decreases the expression of the catalytic sub-unit of the serine-threonine phosphatase, PP2A, and as a consequence, the phosphorylation of E2F/DP is increased, reducing binding to DNA and transcriptional activities of the protein complex [348]. It is therefore thought that PPARγ ligands could have potential as a non-toxic therapy for treating cancers. This is because the natural ligand $15dPGJ_2$ exists in cells and would not be toxic

and TZDs, although having some side effects would be an improvement on current treatments, such as chemotherapy, which have many side effects.

The role of PPARγ in colon cancer is less clear, however, as conflicting reports on the effect of PPARγ-induced transcription in colon cancer cells have been published. Sarraf *et al.*, [182] and Brockman *et al.*, [349] reported that PPARγ is highly expressed in colon cancer cells and that activation of PPARγ using troglitazone resulted in cell growth arrest, cellular differentiation and the slowing of tumour cells grown in Swiss nude mice. However, in a mouse model of familial adenomatous polyposis coli and sporadic colon cancer (C57BL/6J-APC^{min}/+ mice), activation of PPARγ resulted in the growth of tumour cells being promoted [350, 351]. $15dPGJ_2$ has also been linked to the proliferation of a cyclo-oxygenase depleted human colorectal cancer cell line, but it is not known whether this occurs by a PPARγ-dependent or -independent mechanism [188].

Another twist in the complex involvement of PPARγ in colon cancer was found when Sarraf *et al.*, [352] reported that four somatic mutations were found in primary colon tumours. These include a nonsense mutation, a frame-shift mutation and two mis-sense mutations, each of which impaired the function of the protein [352]. Three of the mutations (c.472delA, Q286P and K319X) affected the ligand binding domain and the fourth mutation, R288H, decreased binding of PPARγ to DNA and therefore, transcription [352]. These results confirm previous work by Sarraf *et al.*, [182] and Brockman *et al.*, [353] and suggest that PPARγ is important in sporadic colon cancer. The high frequency of genetic alterations in *RAS* in colon cancer can also lead to inhibition of PPARγ, through hyper-activation of kinase pathways [354] leading to hyper-activation of MAP kinase and inhibition of PPARγ activity through direct phosphorylation [285, 286]. Therefore, it is important to establish the precise roles of PPARγ in tumour growth and tumour cell death, before any ligands of PPARγ would prove useful as anti-oncogenic treatments.

8.4.3 *Activated PPARγ induces a variety of cellular responses in cancer cells*

Activation of PPARγ has been shown to induce the differentiation of some cancer cell types. These include liposarcomas [241] and neuroblastomas [207, 342], which have been shown to express markers of differentiation on treatment with ligands of PPARγ. Liposarcomas undergo terminal differentiation in response to pioglitazone, characterised by accumulation of intracellular lipid, induction of adipocyte-specific genes, and withdrawal from the cell cycle [241]. Troglitazone was also shown to be successful in differentiating liposarcomas in clinical trials, as it reduced markers of cellular proliferation and increased lipid accumulation [355]. The level of NMYC expression decreases in neuroblastoma cell lines treated with $15dPGJ_2$ [342] and phenylacetate [207] and this has previously been shown to occur on differentiation of neuroblastoma cells with retinoic acid [356]. The cells also extended their neurites and increased acetylcholinesterase activity, which are also markers of neuroblastoma cell differentiation [77, 342]. Differentiation of neuroblastoma cells has been suggested as a mechanism for the regression of Stage IVS neuroblastoma and therefore, if PPARγ ligands induced differentiation then they would have potential as neuroblastoma therapies [63, 71].

PPARγ-induced apoptosis (type I programmed cell death) has been observed in many types of cancer cells including breast cancer, non-small cell lung cancer, gastric cancer and choriocarcinoma cells [182, 242, 340, 341, 347, 357]. Apoptosis occurs during embryonic development, regulation of immune responses and at the end of the lifespan of normal cells [358]. Apoptosis involves several processes including the release of cytochrome C from mitochondria, the activation of caspases, the activation of an endogenous endonuclease that cleaves internucleosomal DNA and specific morphological changes in the cytoplasm and cell nucleus [359, 360] (Figure 1.9). These include contraction of cellular volume, chromatin condensation, fragmentation of the nucleus and the formation of apoptotic bodies [359, 360, 361]. In cancer cells in which PPARγ ligands induce apoptosis, activation of PPARγ would seem to be an ideal treatment, as apoptosis would result in the destruction of the tumour cells and without invoking an inflammatory response. Apoptosis has also been seen in neuroblastoma cells and cortical neurones treated with $15dPGJ_2$ [362].

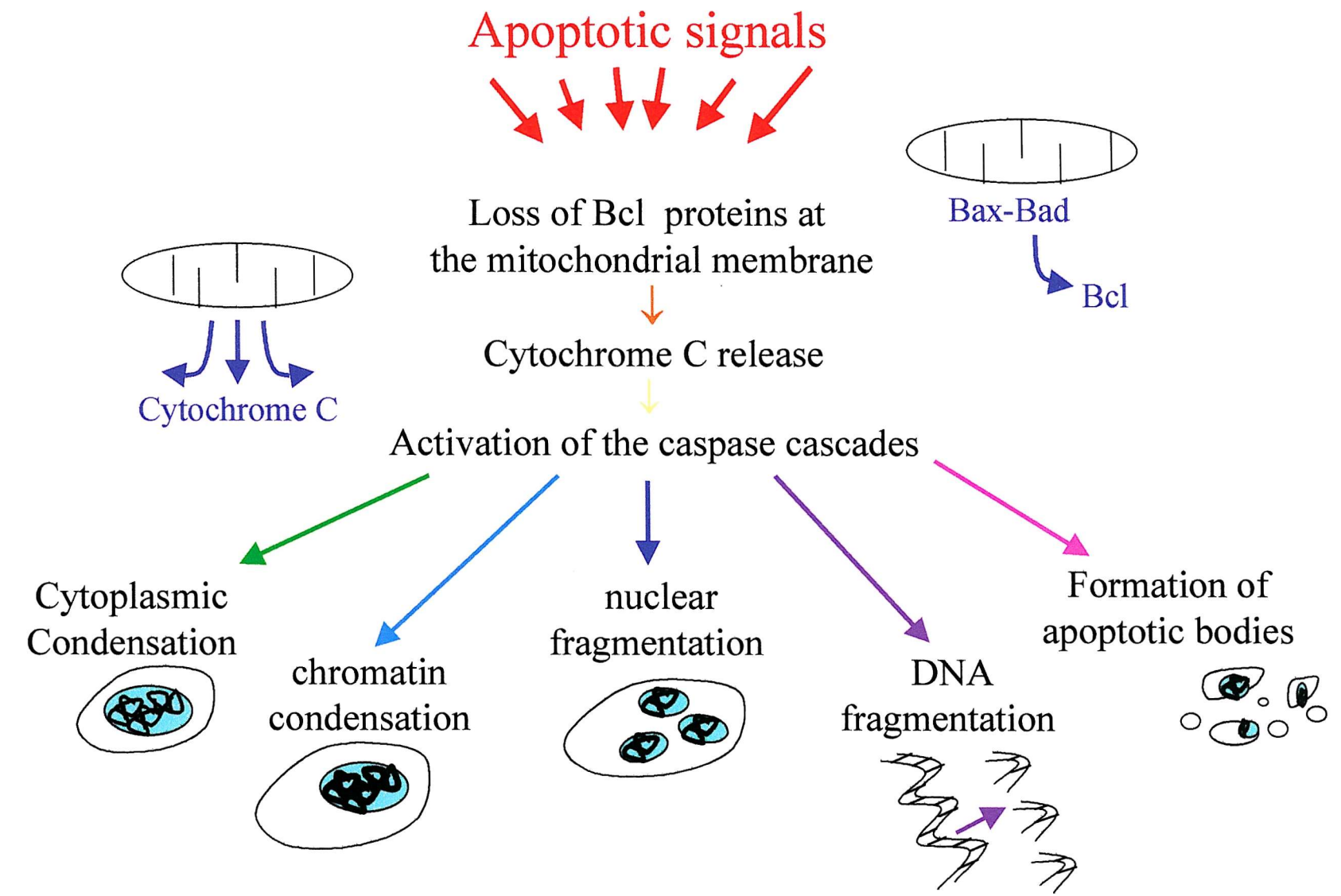

Figure 1.9 Overview of the apoptotic pathway

PPARγ was also cleaved in these cells and Rohn *et al.*, [362] suggested that PPARγ is therefore a target of caspases.

Another form of programmed cell death, Type II or autophagy has also been shown to be induced through activation of PPARγ by 15-deoxy$\Delta^{12,14}$-prostglandin J_2 in prostate cancer cells [346]. Autophagy occurs naturally and is involved in processes such as cellular ageing and remodelling during differentiation [363]. Autophagy involves the destruction of cytoplasm and organelles within the cell by fusion with the lysosomes, which eventually results in cell death (Figure 1.10) [364, 365]. Once autophagy is triggered, the rough endoplasmic reticulum envelops parts of the cytoplasm and organelles, including mitochondria and forms double-membrane-bound vacuoles, called the nascent autophagic vacuoles or autophagosomes [364, 365]. These vacuoles then fuse with pre-existing lysosomes and golgi bodies to form single membrane-bound vacuoles called degradative vacuoles or autolysosomes [364, 365]. Autolysosomes fuse with late endosomes or lysosomes to destroy the vacuolar contents [364, 365]. Both autophagosomes and autolysosomes contain hydrolases, but only the degradative vacuoles contain acid phosphatases [364, 365]. It was initially thought that autophagy and apoptosis were distinct processes [366], but has since been shown that they overlap [367], and that cells undergoing autophagy are more likely to apoptose [368]. It is possible that ligands of PPARγ may cause autophagy in cancer cells other than prostate cancer cells and this too would be a suitable treatment, as autophagy, like apoptosis, would not invoke an inflammatory response and would hopefully be specific for tumour cells.

Another important mechanism in the development of tumours, which involves PPARγ, is angiogenesis. Angiogenesis is the formation of new blood vessels from pre-existing blood vessels and is important in the pathology of diabetes, rheumatoid arthritis and cancer. Angiogenesis was originally described by Folkman in 1971 [369] and is thought to be important in the maintenance of solid tumour cell growth and metastasis, as growing cells require factors such as oxygen, which can only be accessed from a local capillary network [369, 370]. It is thought that by inhibiting angiogenesis, tumour cells will be unable to respire, divide or metastasise [369, 370].

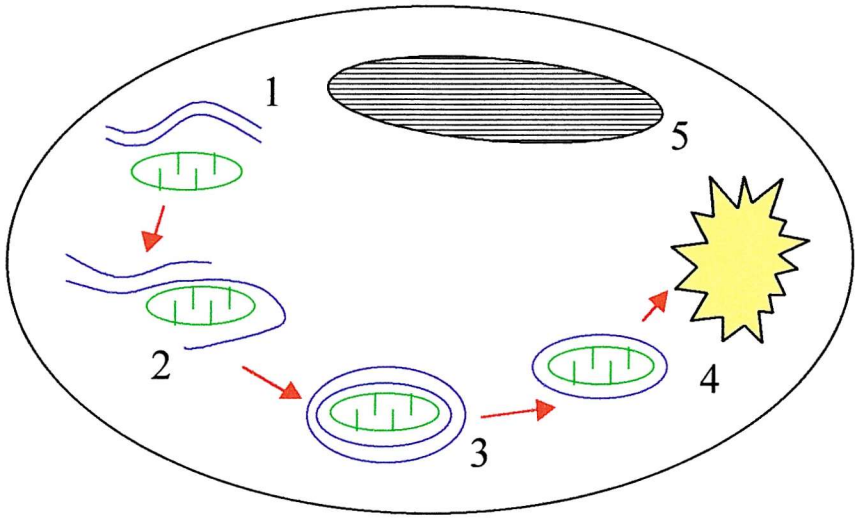

1.Autophagic cell death is triggered.

2.The endoplasmic reticulum envelopes mitochondria and cytoplasm.

3.The endoplasmic reticulum forms a double-membrane vacuole around the cellular contents, called an autophagosome.

4.The autophagosome matures and becomes a single-membrane bound autolysosome.

5.The autolysosome fuses with a lysosome to degrade the cellular contents.

Figure 1.10 Overview of the process of autophagy. Autophagy is a form of programmed cell death, which is distinct from apoptosis, as it lacks DNA laddering, the nucleus remains virtually intact and the cells do not fragment into apoptotic bodies. In autophagy, the cytoplasm and organelles are sequestered into vacuoles, are destroyed by lysosomal degradation.

Human umbilical vein endothelial cells (HUVECs) have been shown to express PPARγ and treatment of these cells with $15dPGJ_2$ *in vitro*, results in growth arrest and inability to form new blood vessels [371]. PPARγ-induced transcription in HUVECs results in increased expression of plasminogen activator inhibitor-1 mRNA and reduced expression of vascular endothelial growth factor (VEGF) receptor 1 and 2 and urokinase plasminogen activator (uPa) mRNA [371]. VEGF receptor-1 functions as a transducer to signal endothelial cell proliferation and VEGF receptor-2 is involved in endothelial cell morphogenesis, both of which are required for angiogenesis [372, 373, 374]. It has also been shown that the production of proteases, such as uPa is correlated with degradation of the endothelial cell matrix and endothelial cell migration, which are also important in the angiogenic process [375]. PPARγ-induced repression of angiogenesis has also been shown in an *in vivo* model of angiogenesis in the cornea [371]. These facts point to the potential of PPARγ ligands in the treatment of cancer. If these ligands can induce growth arrest and cell death, as well as inhibit the formation of a new blood supply for growing tumour cells, then they would be a specific and efficient method of treatment.

8.5 *Involvement of PPARγ in other diseases*

In recent years the involvement of PPARs, notably PPARγ, has been reported in many diseases. These include Alzheimer's disease, osteopaenia, hepatitis and HIV, which are discussed below. However, PPARs are constantly being reported as playing key roles in diseases and this list is not exhaustive, as PPARs have also been shown to be involved in skin conditions and diseases of the digestive system. For example, troglitazone has been shown to inhibit the proliferation of keratinocytes in patients and models of psoriasis [376] and thiazolidinediones markedly reduced colonic inflammation in a mouse model of inflammatory bowel disease [377].

8.5.1 *Alzheimer's Disease*

Alzheimer's disease is a neurodegenerative disease characterised by extracellular deposition of beta-amyloid fibrils within the brain and the subsequent association

and activation of microglial cells associated with amyloid plaques [378, 379]. This is thought to involve inflammatory events and therefore anti-inflammatory drugs have been used to treat Alzheimer's disease [378, 379]. NSAIDs, which are ligands of PPARs [169] have been shown to be efficacious in reducing the incidence and risk of Alzheimer's disease and significantly delaying disease progression [379]. Interestingly, the levels of PPARγ are altered in the brains of patients with Alzheimer's disease [379]. It is thought that NSAIDs bind to and activate PPARγ, which inhibits the secretion of pro-inflammatory products by microglia and monocytes which is responsible for neurotoxicity and astrocyte activation seen in Alzheimer's disease [378]. It is therefore proposed that ligands of PPARγ could be novel therapies for the treatment of Alzheimer's and possibly other neurodegenerative diseases [378, 379].

8.5.2 *Osteopaenia*

Stromal cells have the ability to convert between an osteoblast and adipocyte phenotype, depending on conditions [380, 381, 382]. The osteoblast specific gene, Osf2/Cbfa1, is a target gene of PPARγ2 and its expression is suppressed by PPARγ2 activity [383]. This suppression of Osf2/Cbafl activity inhibits the differentiation of bone marrow cells into osteoblasts and the cells terminally differentiate into adipocytes instead [383]. This mechanism may be important in osteopaenia, as a mouse model of this disease shows increased adipogenesis at the expense of osteoblastogenesis, resulting in decreased bone formation and bone mass [384, 385].

8.5.3 *Hepatitis B*

Functional PPREs have been described in some viral promoters including the hepatitis B virus 1 enhancer [386], prompting suggestions of a link between PPARs and hepatocarcinomas [152], as chronic hepatitis B infection can lead to liver cancer. PPAR/RXR heterodimers have been shown to interact with a retinoic acid response element in the hepatitis B virus promoter [386] and PPAR/RXR heterodimers also activated the synthesis of the pre-genomic viral RNA [387]. It is thought that

appropriate ligands to nuclear receptors may be useful in the treatment of hepatitis B virus infection [387].

8.5.4 *HIV*

A response element that interacts with multiple nuclear receptors has been identified in the long terminal repeat (LTR) of human immunodeficiency virus-1 (HIV-1), but not in simian immunodeficiency virus (SIV) isolates [388]. LTRs are a sequence repeated at each end of the integrated retroviral pro-virus generated by the mode of insertion [388]. It has been suggested that this nuclear receptor responsive element (NRRE) may allow HIV-1 to utilise other signalling pathways and enhance viral adaptation [152]. Ciglitazone, a synthetic agonist of PPARγ is also able to inhibit the replication of HIV-1 in U937 bone derived macrophages, through suppressing HIV-1 promoter activity, mRNA stability and affecting the expression of HIV-1 genes prompting suggestions that ligands of PPARγ may have potential in HIV therapy [389].

In conclusion, peroxisome proliferator-activated receptors are involved in many cellular processes and in many human disease states. Each isoform has specific roles, but it seems that PPARγ is most important in human cancers and may be involved in neuroblastoma. If so, then there is potential for studying the effects of activation of PPARγ in neuroblastoma cells, which could lead the way to the development of new treatments for the disease.

Chapter 2

Materials and Methods

2.1 MATERIALS

Chemicals were obtained from Sigma-Aldrich (Poole, Dorset, UK) unless otherwise stated. α^{32}P-dATP were acquired from Amersham Pharmacia Biotech Limited (Little Chalfont, Buckinghamshire, UK). Tissue culture plastics and culture medium were obtained from Invitrogen Limited (Paisley, Scotland). Antibodies were obtained from Santa Cruz (Autogen Bioclear UK limited, Calne, Wiltshire, UK), CN Biosciences (UK) Limited (Nottingham, UK) Novocastra Laboratories (Vector Laboratories Limited, Peterborough, UK) and Upstate Biotechnology UK (Botolph Claydon, Buckinghamshire, UK).

2.2 METHODS

2.2.1 *Bacterial Growth Medium*

2.2.1.1 *Lennox L Broth (LB) Medium*

20 g LB medium was dissolved into 1 litre of distilled water and autoclaved under standard conditions. Once cooled, LB medium was made into LB^{amp} medium, by the addition of ampicillin to give a final concentration of 100 μg/ml.

2.2.1.2 *LB Agar*

Prepared as LB medium with 1.5 % (w/v) agar added prior to autoclaving. When agar had cooled sufficiently ampicillin was added to give a final concentration of 100 μg/ml.

2.2.2 *Glycerol Stocks*

10 ml of LB was inoculated with *Escherichia coli* cells (DH5α) [390] and 10 ml LB^{amp} was inoculated with DH5α cells containing vectors. Culture was incubated with shaking at 37 °C overnight. 500 µl of overnight culture was mixed 1:1 with sterile glycerol and vortexed gently to mix. Stock was stored at ⁻80 °C until use.

2.2.3 *DNA Maxi Preparations*

10 ml cultures of DH5α cells containing vector DNA were grown in LB^{amp} were incubated with shaking at 37 °C for 6 hours. The cultures were used to inoculate 500 ml LB^{amp} and these cultures were incubated at 37 °C with shaking, overnight. Overnight cultures were pelleted at 1800 *g* for 15 minutes at 4 °C in Sorvall RC-3B centrifuge (Kendro Laboratory Products Limited, Bishop's Stortford, Hertfordshire, UK). The pellets were resuspended in 4 ml Sucrose-Tris buffer (730 mM sucrose, 50 mM *Tris*(hydroxymethyl)aminomethane hydrochloride (Tris-HCl)) containing 188,000 Units of lysozyme. The suspensions were put on ice for 15 minutes, then 500 mM ethylenediamine tetra-acetic acid (EDTA) was added to make a final concentration of 10 mM and the suspensions were returned to the ice for a further 15 minutes. ½ volume of 3x Triton buffer (150 mM Tris-HCl pH 8, 187.5 mM EDTA, 3 % (v/v) Triton X-100) was added and the samples were mixed on ice for 10 minutes until lysis occurred. Samples were spun at 25000 *g* for 1.5 hours at 4 °C in a Beckman J2-21 centrifuge (Beckman Coulter Inc., Fullerton, California) and supernatant was collected. The supernatant was made up to 500 mM sodium chloride (NaCl), washed 1:1 with 1:1 phenol:chloroform and centrifuged at 1100 *g* for 10 minutes. The top layer was decanted to a fresh tube and chloroform was added to make a 1:1 mix. The preparation was mixed vigorously with the chloroform and centrifuged at 1100 *g* for 10 minutes. The top layer was collected and 16.7 mM polyethylene glycol (PEG) was dissolved into it by mixing at 37 °C and left at 4 °C overnight. The preparation was centrifuged at 16667 *g* for 20 minutes at 4 °C to obtain a pellet. The pellet was resuspended in 500µl Tris-HCl pH 8 and treated with 10 Units RNAse A at 37 °C for 30 minutes. 500 µl PEG buffer (33.4 mM PEG 6000, 1 M NaCl, 1 mM EDTA, 10 mM Tris pH 8) was

added to the preparation and it was put on ice for 1 hour. A pellet was obtained by centrifugation at 13000 *g* for 15 minutes and it was resuspended into 400 µl Tris-NaCl (10 mM Tris-HCl pH 8, 500 mM NaCl). It was re-treated with RNAse A at 37° C for 30 minutes and washed twice with 1:1 phenol:chloroform. The DNA was then ethanol precipitated, washed with 70 % ethanol and dissolved into 100 µl tissue-culture sterile water. Optical density was measured as a ratio of absorbance at 260 nm and 280 nm to confirm purity of DNA.

2.2.4 *Preparation of Fatty Acid Supplementation*

Sodium salts of arachidonic acid (AA), docosahexaenoic acid (DHA) and γ-linolenic acid (γLA) were prepared by the addition of 100 mM sodium hydroxide to 30 µmoles fatty acid in ethanol. Fatty acid-sodium salts were dried under nitrogen at 40 °C and dissolved in Hank's Balanced Salt Solution (HBSS) without phenol red, calcium or magnesium by heating to 90 °C. 100 mg/ml ice cold fatty acid-free bovine serum albumin (BSA) in HBSS was then added to the fatty acid salts and the solution stirred at room temperature until clear. Fatty acid-albumin complexes were diluted with HBSS to 300 µM filter sterilised and stored at ⁻20 °C. Recovery of fatty acid-albumin conjugates was 95-100 %.

2.2.5 *Preparation of PPAR ligands and Retinoic Acids*

2.2.5.1 *PPARα Ligands*

Wy-14643 ([4-chloro-6-(2,3-xylidino)-2-pyrimidinylthio]acetic acid, pirinixic acid) was dissolved in DMSO at 40 mg/ml and was diluted 1:100 with DMSO before use and used at 5 µM.

2.2.5.2 *PPARγ Ligands*

15-deoxy$\Delta^{12,14}$-prostglandin J_2 (11-oxoprosta-5*Z*,9,12*E*,14Z-tetraen-1-oic acid) was obtained from Cayman Chemicals (Alexis Corporation, Bingham, UK) supplied in methyl acetate. Solvent was removed by evaporation under N_2 and 15dPGJ$_2$ was

resuspended in 100 µl dimethyl sulphoxide (DMSO). It was diluted 1:10 with DMSO before use and used at 5 µM.

2.2.5.3 *Retinoic Acids*

9-*cis* retinoic acid (9-*cis* RA) was dissolved in DMSO to make a 4 mM stock solution. The solution was diluted with DMSO prior to use and used at 4 µM.

2.2.6 *Cell Culture*

The established NMYC amplified neuroblastoma cell lines, IMR-32 [391] and Kelly [28], were used for all experiments. IMR-32 cells were maintained in Dulbecco's Modified Eagle's Medium (DMEM) and Kelly cells were maintained in RPMI-1640 medium, both containing 10 % (v/v) foetal calf serum (FCS) and 100 mM glutamine, supplemented with 0.1 mg/ml penicillin-streptomycin and Fungizone® (2.5 µg/ml amphotericin B). Cells were incubated in a humidified atmosphere containing 5 % (v/v) CO_2 and were passaged by incubation with 1x Trypsin-EDTA (500 Units Trypsin, 0.53 mM EDTA). 3T3-L1 pre-adipocytes and Hep G2 cells were cultured under the same conditions.

IMR-32 cell line was derived from the abdominal neuroblastic tumour, which occurred in a 13-month old Caucasian male in 1967 [391]. The cell line consists of two morphologically distinct cell types, with fibroblast or neuroblast-like morphologies. The predominant cell type is a small, neuroblast-like cell, which grows densely forming focal accumulations. The minor cell type is the fibroblast-like cell, which are relatively large and well spread and occur in small numbers. IMR-32 cells grow slowly and the minor cell type has a finite lifespan. The cells also vary in their ultra-structure, with the minor cell type having rough endoplasmic reticulum (RER) and mitochondria with ordered internal structures, whereas the predominant neuroblast-like cell having poorly developed RER and mitochondria, which also varied dramatically in size and tended to have longitudinally orientated cristae. The fibroblast-like cells also exhibit many cell surface projections. The cells have a deletion in chromosome 1, chromosome 16 is absent and they have

amplification of the NMYC gene, which all relate to poor prognosis in neuroblastoma. Kelly cells are also NMYC amplified [28] and like IMR-32 cells can be induced to differentiate in the presence of retinoic acid [392], but less details of this cell line are available.

2.2.7 *Freezing Cells in Liquid Nitrogen and Resuscitation of Frozen Cells*

Adherent cells were pelleted at 500 *g* for 3.5 minutes and culture medium was decanted off. Cells were resuspended in 1 ml of freezing culture medium (10 % (v/v) DMSO in complete medium) and frozen on dry ice for 1 hour. Cells were then transferred to ⁻80 °C overnight and then to liquid nitrogen stores. For resuscitation, cells were rapidly defrosted and diluted into 10 ml of complete culture medium. Cells were pelleted and resuspended in 10 ml fresh complete medium and grown as described above.

2.2.8 *DNA Transfection of Cultured Cells*

Cells were plated out at 5 x 10^5 cells per 96 mm dish in Fungizone®-free medium and allowed to attach overnight. Two tubes were set up per sample: tube A contained 5 μg reporter plasmid DNA and 31 μl 2M $CaCl_2$ in 250 μl total and tube B contained 250 μl 2x Hepes Buffered Saline (HBS) (280 mM NaCl, 50 mM *N*-(2-Hydroxyethyl)piperazine-*N*'-(2-ethanesulphonic acid)(Hepes free acid), 2.8 mM disodium hydrogen phosphate (Na_2HPO_4), pH 7.12). The contents of tube A were added drop-wise to the contents of tube B to form a translucent precipitate. The precipitate was transferred to the cell culture medium and gently agitated. The cells were incubated at 37 °C for 6 hours, when the medium containing the precipitate was removed, the cells were washed and 5 ml fresh complete medium was added to the cells. The cells were then incubated at 37 °C, with or without treatments for 72 hours and then harvested.

	Vector	Size (Kb)	Supplier	Promoter	Insert	Resistance Gene	Reporter Gene	Reference/Patent
β-Galactosidase	pSV-β-Galactosidase	6.8	Promega	Simian Virus 40 (SV40)	-	-	*lac*Z gene	393
pBL_2CAT	pBL_2CAT	4.5	-	Minimal Herpes Simplex Virus Thymidine Kinase	-	-	Chloramphenicol acetyl transferase	394
pLTRPoly	pLTRPoly	5.2	-	Simian Virus 40 (SV40)	-	-	-	395
pGL_3Basic	pGL_3Basic	4.8	Promega	None	-	-	Luciferase	U.S. Patent Number 5,670,356. Recombinant expression of *Coleoptera* luciferase – U.S. Patent Numbers 5,583,024, 5,674,713 and 5,700,673
pcDNA3.1+©	pcDNA3.1+	5.4	Invitrogen	Human Cytomegalovirus (CMV)	-	Neomycin phosphotransferase	-	Invitrogen Limited

3PPRE-TK-CAT	pBL_2CAT	4.6	-	Minimal Herpes Simplex Virus Thymidine Kinase	Triple repeat of a consensus PPAR binding site (rat *Aco*-PPRE: AGGAGAAAGGTCA)	-	Chloramphenicol acetyl transferase	122
pGL3-5xκB (NFκB)	pGL3-Luciferase	4.8	Promega	None	5 consensus NFκB binding sites (GGGGACTTTCC)	-	Luciferase	Gift from Dr. R. Hofmeister, Universität Regensburg, Regensburg, Germany
pSG5PPARγ1	pSG5	4.1	Stratagene	Simian Virus 40 (SV40)	cDNA for Human PPARγ1	-	-	141
Pax8PPARγ1	pCR3.1-BI	5.1	Invitrogen	Human Cytomegalovirus (CMV)	2.5Kb cDNA encoding – Pax8 exons 1-7 + 9 fused in-frame to PPARγ1 exons 1-6	Neomycin phosphotransferase	-	344

Table 1 Details of expression, reporter and control vectors used for DNA transfection of IMR-32 cells.

2.2.9 *Establishment of Stable Cell Lines*

IMR-32 cells were seeded at 5 x 10^5 cells per 96 mm culture dish and allowed to attach overnight. Cells were transfected with 5 μg DNA using the method described above (2.2.8). For PAX8PPARγ1 dominant negative experiments, IMR-32 cells were transfected with 5 μg pCR®3.1CMV expression vector (Invitrogen, Paisley, Scotland) containing a cDNA encoding the PAX8PPARγ1 chimeric protein, (a kind gift from Dr. T. Kroll, Brigham and Women's Hospital, Harvard Medical School, Boston, USA) and 5 μg pcDNA3.1+© (Promega, Chilworth, UK) was used as the vector control. For expression experiments, cells were transfected with 5 μg pSG5 vector (Stratagene Europe, Amsterdam, Netherlands) containing PPARγ1 (a kind gift from Dr. A. Elbrecht, Merck Research Laboratories, New Jersey, USA), 5 μg pLTRPoly (control for SV40 promoter) and 5 μg pcDNA3.1+©, as pSG5-PPARγ1 lacks neomycin resistance gene. Control cells for expression experiment were transfected with 5 μg pLTRPoly and 5 μg pcDNA3.1+©. Transfected cells were cultured for 72 hours and then treated with 800 mM Geneticin® disulphate salt (G418) in fresh complete DMEM. Cells were selected by treatment of cells with subsequent doses of 800 mM G418 in fresh medium, until clones were visible with the naked eye. Individual clones were "picked" using Trypsin-EDTA and cultured as separate cell lines.

2.2.10 *Preparation of cDNA for Reverse Transcriptase Polymerase Chain Reaction (RT-PCR)*

Total RNA was isolated from treated and untreated IMR-32 cells, Kelly cells, 3T3-L1 pre-adipocytes and HepG2 liver cells using TRIZOL® reagent (Invitrogen Limited, Paisley, Scotland). TRIZOL®-chloroform mixes of cell suspensions were centrifuged at 13000 *g* at 4 °C for 10 minutes. The aqueous layer was isolated and the RNA was precipitated with isopropyl alcohol and collected by centrifugation. The RNA pellet was air-dried resuspended in 30 μl of autoclaved, 0.1 % (v/v) diethyl pyrocarbonate (DEPC)-treated water.

cDNA was synthesised from total cell RNA. 1 μg RNA was heated to 65 °C for 2 minutes and chilled on ice. RNA was mixed with cDNA synthesis mix (2 μl 10x PCR buffer (100 mM Tris-HCl pH 8.3, 500 mM potassium chloride), 2 μl 100 mM magnesium chloride, 2 μl 100 mM dNTP mix (Promega, Chilworth, UK), 1 μl 90 OD Units/ml random hexamers in Tris-EDTA (Amersham Pharmacia Biotech Limited, Little Chalfont, UK), 20-40 Units RNAsin® (Promega, Chilworth, UK), 100 Units Moloney-Murine Leukaemia Virus (M-MLV) reverse transcriptase (Invitrogen Limited, Paisley, Scotland) and 0.1 % (v/v) DEPC-water to total volume with RNA of 20 μl). cDNA was synthesised at 37 °C for 1 hour.

2.3.1 *Reverse Transcriptase-Polymerase Chain Reaction (RT-PCR)*

cDNA was amplified using cyclophilin, PPARα, PPARγ, PAX3 or PAX8 specific primers obtained from MWG (MWG Biotech, Milton Keynes, UK) and Invitrogen Limited (Paisley, Scotland). 500 ng of primers were used to generate RT-PCR products of the cyclophilin, PPARα, PPARγ or PAX3 genes. Cyclophilin was used as a control to normalise for cDNA levels. For PAX8PPARγ1 RT-PCR, 1 μg of PAX8 forward primer and 1 μg of PPARγ reverse primer were used to yield a product of 772 base pairs. Reactions (5 μl cDNA, 10 μl PCR buffer, 10 μl 100m M magnesium chloride, 2 μl 100 mM dATP, 2 μl 100 mM dCTP, 2 μl 100 mM dGTP, 2 μl 100 mM dTTP, forward primer, reverse primer and 62.5 μl 0.1 % (v/v) DEPC-treated water) were incubated in Omnigene PCR thermocycler (Hybaid, Ashord, UK) for optimum number of cycles using 2.5 Units Taq polymerase (Sigma, Poole, UK). The optimum number of cycles was determined by analysing PCR products on an agarose gel every 5 cycles, after an initial measurement at 30 cycles. 30 cycles was used as for initial measurement because the PCR products needed to be observed in the exponential phase of amplification, where differences in levels of expression could be seen. If the amplification reached plateau phase, then lower expressed mRNA would be amplified up to a similar level as more highly expressed mRNA, which had reached a plateau of expression that could be reached within the limits of the reaction mix. PCR products were run on 1.5 % (w/v) agarose gel and were visualised by UV light. Unique restriction sites within the amplified sequence were used to confirm the identity of the PCR product.

Primers	Forward Primer Sequence 5' – 3'	Reverse Primer Sequence 5' – 3'	Size of RT-PCR product
Cyclophilin	TTG GGT CGC GTC TGC TTC GA	5'-GCC AGG ACC TGT ATG CTT CA-3'	250 bp
PPARα	GCC TCA GGC TAT CAT TAC G	5'-CTT CTA TGT CAT GTT CAC AG-3'	225 bp
PPARγ	TGC AGA TTA CAA GTA TGA C	5'-TCG ATA TCA CTG GAG ATC-3'	385 bp
PAX3	GGA ATA AAA GAG AGA ACC GG	5'-CTT CAT CTC ACT GAG GTG CAG-3'	300 bp
PAX8-PPARγ1	CTC AGG GCG AGA GAT G (PAX8)	5'-TCG ATA TCA CTG GAG ATC-3' (PPARγ)	772 bp

Table 2a Primer sequences for RT-PCR of cyclophilin, PPARα, PPARγ, PAX3 and PAX8PPARγ1.

Primers	Denature	Time (seconds)	Anneal	Time (seconds)	Extension	Time (seconds)	No. of Cycles
Cyclophilin	95°C	30	54°C	30	72°C	30	30
PPARα	95°C	30	55°C	30	72°C	30	35
PPARγ	95°C	30	50°C	30	72°C	30	35
PAX3	95°C	30	60°C	30	72°C	30	35
PAX8PPARγ1	94°C[c]	40	52°C	40	72°C	50	50

Table 2b Conditions for RT-PCR of cyclophilin, PPARα, PPARγ, PAX3 and PAX8PPARγ1. Optimum number of cycles was determined by analysis of PCR products on an agarose gel every 5 cycles after an initial measurement at 30 cycles.

[c] PAX8PPARγ1 dominant negative vector was used as a positive control and for RT-PCR reactions included an initial denaturation step of 94°C for 2 minutes.

2.3.2 *Labelling of Probe for Southern Blotting*

Probe was boiled for 3 minutes and then 10 µl probe was incubated with labelling reaction at room temperature for 5 hours. The labelling reaction contained 10 µl oligonucleotide labelling buffer (20 µl solution A (1 ml solution O (1.25 M Tris HCl pH 8 and 125 mM magnesium chloride), 18 µl β-mercaptoethanol, 5 µl 100 mM dCTP, 5 µl 100 mM dGTP and 5 µl 100 mM dTTP), 50 µl solution B (2 M Hepes pH6.6) and 30 µl solution C (90 OD Units/ml random hexamers in Tris-EDTA)), 37µl 0.1 % (v/v) DEPC-treated water, 2 µl α^{32}P-dATP and 1 µl Klenow. The reaction was stopped using 200 µl stop solution (20 mM NaCl, 20 mM Tris HCl pH 7.5, 2 mM EDTA, 0.25 % (w/v) sodium dodecyl sulphate (SDS) and 1 µM dATP). Labelled probe was separated from unincorporated α^{32}P-dATP by passing down G50 sephadex column.

2.3.3 *Southern Blot*

20 µl PCR reactions were run on 1.5 % (w/v) agarose gel and blotted onto Hybond™-N membrane (Amersham Life Sciences, Little Chalfont, UK). The agarose gel was inverted onto filter paper wicks with their ends soaked in 0.1 % (v/v) DEPC-treated 20x SSC (3M NaCl and 300 mM sodium citrate). The membrane was soaked in 0.1 % (v/v) DEPC-treated 20x SSC and placed onto the inverted gel and any air bubbles removed. A layer of filter paper was placed on top of the membrane, followed by several layers of paper (around 5 cm deep). Finally, a weight was used to enhance blotting and the blotting set up was left overnight at room temperature. After blotting the membrane was baked in an oven at 80 °C for 2-3 hours and stored at room temperature. All solutions were treated with 0.1 % (v/v) DEPC overnight and autoclaved under standard conditions before use.

Membrane was blocked with pre-hybridisation buffer (6x SSC, 2x Denhart's Solution (25 µM Ficoll 400, 1 mM polyvinylpyrrolidine and 10 mg/ml Fraction V bovine serum albumin (BSA), 0.5 % (w/v) SDS) for 2 hours at 65 °C. The membrane was then incubated with hybridisation buffer (pre-hybridisation buffer,

100 mg/ml dextran sulphate sodium salt (ICN Biomedicals Inc., Ohio, USA) and 100 μg/ml denatured fragmented salmon sperm DNA, containing α^{32}P-dATP-labelled fragment of PPARγ) at 65 °C overnight. The membrane was washed twice with 2x SSC and 0.1 % (v/v) SDS at 65 °C for 10 minutes each and then autoradiographed overnight.

2.3.4 *Cell Growth*

IMR-32 cells were seeded at 2 x 10^4 into 6 well plates and incubated overnight to facilitate attachment. Cells were supplemented daily with 2ml fresh DMEM and treatments during the experiment. For fatty acid experiments, the treatments were HBSS, 30 μM AA, 30 μM DHA, 30 μM or 75μM γLA and 30 μM oleic acid (OA). For PPAR ligand experiments, the treatments were DMSO, 5 μM Wy-14643 and 5 μM 15dPGJ$_2$. Untreated cells were also counted. For synergy experiments, cells were treated with 5 μM 15dPGJ$_2$ and 30 μM DHA or 4 μM 9-*cis* retinoic acid.

Cells were counted by harvesting after a brief wash with phosphate buffered saline (PBS) (140 mM NaCl, 2.7 mM potassium chloride (KCl), 9.2 mM Na_2HPO_4, 1.84 mM potassium dihydrogen phosphate (KH_2PO_4), pH 7.2) (Oxoid, Basingstoke, UK) using Trypsin-EDTA. The cells were resuspended in DMEM and pelleted by centrifugation at 750 *g* for 3 minutes in a Centurion 4000 series centrifuge (Centurion Scientific Limited, West Sussex, UK). Cell pellets were resuspended in 25 μl PBS and 25 μl 0.4 % trypan blue and counted using a haemacytometer. Live cells and "dead" cells (trypan blue positive) were counted separately. Four counts were made per treatment per day and an average calculated. The average number of cells counted on the haemacytometer grid refers to the number of cells x 10^4 per ml and as the volume of cell suspension was known, the total number of cells could be determined.

2.3.5 *Cell Proliferation (Bromodeoxyuridine incorporation)*

IMR-32 cells expressing increased levels of PPARγ were seeded at 5 x 10^2 cells per well in a 96 well plate and treated with DMSO or increasing concentrations of

15dPGJ$_2$ with a change of medium daily for 72 hours. Cellular proliferation was measured using the Biotrak™ Bromodeoxyuridine (BDU) Cell Proliferation Elisa System Version 2 (Amersham Pharmacia Biotech UK Limited, Little Chalfont, Buckinghamshire, UK). The BDU labelling reagent was diluted 1:100 in sterile complete tissue culture medium to produce a concentration of BDU of 100 μM. The labelling solution was added to the cells to give a final concentration of 10 μM BDU and the cells were incubated at 37 °C for 4 hours. The labelling medium was then removed by tapping, and the cells and controls were fixed in 200 μl fixative per well at room temperature for 30 minutes. The fixative was then removed and 200 μl blocking buffer (solution B – 1 % (w/v) protein in 50 mM Tris-HCl, 150 mM NaCl, pH 7.4) was added to each well and the cells were blocked at room temperature for 30 minutes. Blocking buffer was removed and 100 μl peroxidase-labelled anti-BDU working solution (solution D) was added to each well and incubated at room temperature for 90 minutes. The working solution was removed and the wells were washed three times with 200 μl washing solution (solution E). 100 μl of TMB substrate (Amersham Pharmacia Biotech UK Limited, Little Chalfont, Buckinghamshire, UK), which had been equilibrated to room temperature, was aliquoted into the washed wells. The wells were covered, mixed and incubated at room temperature for 5 minutes when the colour development was sufficient for optical density measurement. The reaction was stopped using 25 μl 1 M sulphuric acid per well and the colour change was measured immediately at 450 nm.

2.3.6 *Cell Death (Trypan Blue)*

Adherent and non-adherent cells were collected by centrifugation and resuspended in 25 μl PBS and 25 μl 0.4 % trypan blue. 250 cells were counted per sample and cell death expressed as percentage of trypan blue positive cells.

2.3.7 *DNA Fragmentation*

IMR-32 cells were seeded at 2 x 10^5 into 96 mm tissue culture dishes and grown and treated as described above. Adherent and non-adherent cells were pooled and

examined for internucleosomal fragmentation using variation of methods by Sellins and Cohen [396], Gunji *et al.*, [397] and Ritke *et al.* [398]. Briefly, cell pellets were resuspended in 10 µl PBS and 20 µl Tris-EDTA-sodium lauryl sarcosine (TE-SLS) (10 mM EDTA, 50 mM Tris-HCl pH 8, 17 mM sodium lauryl sarcosinate) was added. Cell suspensions were incubated at 50 °C with 0.3 mUnits proteinase K (Promega, Chilworth, UK) for 1 hour, then further incubated for 1 hour at 50 °C with 1 Unit RNAse A. Temperature was increased to 70 °C for addition of loading buffer (10 mM EDTA pH 8, 1 % (w/v) low melting point agarose (Helena Biosciences, Sunderland, UK), 3.7 mM bromophenol blue, 1.2 M sucrose) and samples were loaded into dry wells of 1 % (w/v) agarose gel. Samples were allowed to set and gel was run in 1x Tris-acetate (TAE) (400 mM Tris acetate, 1mM EDTA) at 80V for 2-3 hours. DNA was visualised under UV illumination. Neuroblastoma cells treated with betulinic acid (43.8 µM) for 24 hours were used as a positive control for apoptotic laddering.

2.3.8 *Flow Cytometry*

Pellets of adherent and non-adherent cells were resuspended in 50 µl PBS and counted. 1 x 10^6 cells were prepared using modifications of methods by Krishan [399] and Nicoletti *et al.*, [400]. Cells were diluted into 1 ml flow cytometry buffer (3.4 mM sodium citrate, 78.4 µM propidium iodide and 0.1 % (v/v) Triton X-100) and incubated for 30 minutes in the dark. 5000 events were measured for forward and side scatter on FACScalibur® flow cytometer (Beckton Dickinson Diagnostic Systems, Oxford, UK) at 258 nm λ and analysed using Cellquest™ software. The cell cycle inhibitor, aphidocolin, which blocks G_1 to S was used at 30 µM to treat IMR-32 cells. Aphidocolin was used as a control to confirm cell cycle phases and position of G_1 cell cycle phase of flow cytometry histogram. The number of cells in each stage of the cell cycle were analysed by selecting for live cells and setting markers to outline each stage (Figure 2.1).

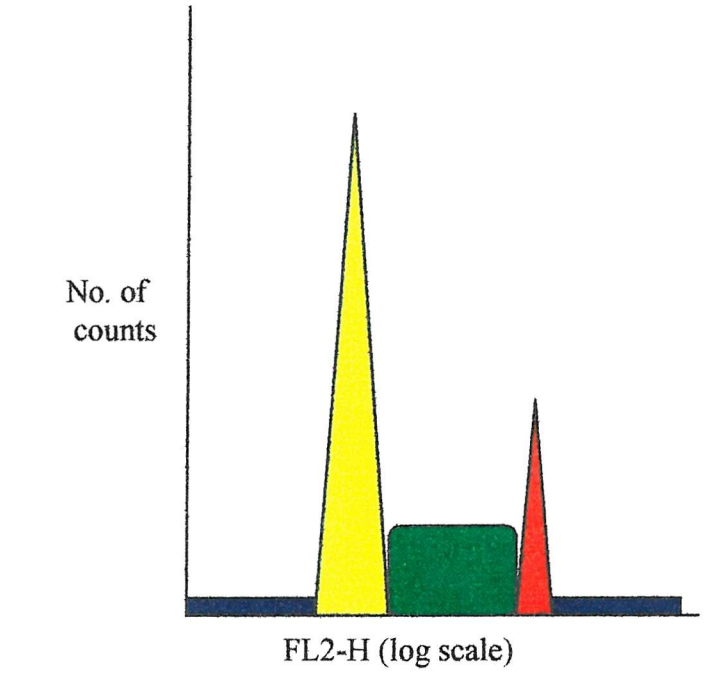

Figure 2.1 Scheme of flow cytometry scan showing areas measured for each phase of the cell cycle, which were converted to graph form.

2.3.9 *Caspase 3 Assay*

Adherent and non-adherent cells were harvested and pooled. Cell pellets were washed in PBS, re-pelleted and then assayed by a modification of the method by Datta *et al.*, [575]. Cell pellets were resuspended in 60 µl caspase assay lysis buffer (50 µM Hepes, 100 µM NaCl, 0.01 % (v/v) NP-40, 10 µM dithiothrietol (DTT), 0.1 % (v/v) glycerol, 1 µM EDTA) and put on ice for 1 hour. Cell debris was pelleted at 13000 *g* for 20 minutes and extracts measured for protein. The caspase 3 substrate (ac-DEVD-pNA) (a kind gift from Dr. R. Broadbridge, University of Southampton) was diluted into fresh lysis buffer to produce a substrate concentration of 100 µM. 20 µl of lysate was mixed with 180 µl of diluted substrate to produce a final substrate concentration of 90 µM. Reactions were set up in 96 well plates and incubated at 37 °C overnight. Optical density of reactions was measured at 410 nm. Controls used for the caspase assay were lysis buffer and cell lysate without substrate and lysis buffer and substrate without cell lysate.

2.3.10 *Electron Microscopy*

IMR-32 cells were grown on Thermenox coverslips (Miles Scientific, Naperville, Illinois, USA) treated with fibronectin (1.8 µM fibronectin, 500 mM NaCl, 50 mM Tris HCl pH 7.5). Cells were treated as for cell growth experiment, for 72 hours, and fixed initially in main fixative (0.3 M glutaraldehyde (Agar Scientific, Stanstead, UK), 1.3 M formaldehyde and PIPES buffer (5 M sodium hydroxide and 100 mM piperazine-NN'-bis-ethanesulphonic acid pH 7.2) [401]. Cells were washed with PIPES buffer (pH 7.2) and post-fixed with 40 mM osmium tetroxide (Oxkem, Oxford, UK) in PIPES buffer (pH 7.2). Cells were dehydrated with ethanol, infiltrated and embedded in 100 % TAAB resin (TAAB Laboratories, Aldermaston, UK).

Resin blocks were produced by turning the layer of cells in resin 90° and reattaching them to the resin block. Green sections (0.5 µM) were initially cut with an Ultracut E microtome (Leica Instruments, Milton Keynes, UK) to prepare block face and check sections. Green sections were dried onto glass slides, stained with

30 mM toludine blue O (Sigma, Poole, UK), washed and mounted in DPX mountant (BDH laboratory Supplies, Poole, UK). Sections were observed under light microscopy (not shown).

Silver sections (60-90 nm) were also cut with an Ultracut E microtome, dried on to copper grids and stained with saturated uranyl acetate solution in 50 % (v/v) ethanol (Agar Scientific, Stanstead, UK) at room temperature in the dark for 15 minutes. Sections were washed with fresh double-distilled water and subsequently stained with Reynolds's lead citrate stain (110 mM lead nitrate, 20 mM sodium citrate and 200 mM sodium hydroxide) [402] in carbon dioxide-free environment at room temperature for 5 minutes. Grids were washed as before and allowed to dry. Cells were observed using Hitachi H7000 transmission electron microscope (Hitachi Instruments, Finchampstead, UK) at 75 kV.

2.4.1 *Fluorescent Microscopy (Monodansylcadaverine)*

Cells were observed using a digital camera RS linked to an Axioplan 2 microscope and analysed using Metamorph® software (Roper Scientific™, Marlow, Buckinghamshire, UK). Cells were seeded at 1 x 10^4 cells per 13 mm coverslips, which had been sterilised with 70 % ethanol and treated with fibronectin to facilitate cell attachment. 50 μM monodansylcadaverine was added to the culture medium and cells were incubated at 37° C for one hour. Cells were washed with PBS 3 times for 5 minutes and fixed in 40 mg/ml paraformaldehyde at room temperature for 20 minutes. Cells were washed with PBS 3 times for 5 minutes, mounted in 10 % (v/v) glycerol in PBS and observed as described above.

2.4.2 *Mini Nuclear and Cytoplasmic Extracts*

Cells were pelleted and washed with PBS. Cells were resuspended in 400 μl Buffer A (10 mM Hepes pH 7.9, 10 mM KCl, 100 μM EDTA, 1 mM DTT, 500 μM Phenylmethanesulphonyl fluoride (PMSF)) and put on ice for 15 minutes. 25 μl of 10 % (v/v) NP40 was added, the suspension was vortexed for 15 seconds and centrifuged at 13000 *g* for 30 seconds. The supernatant (cytoplasmic fraction) was

removed to a fresh tube and stored at ⁻80 °C until use. The pellet (nuclear fraction) was resuspended in 40 µl Buffer C (200 mM Hepes, 400 mM NaCl, 1 mM EDTA, 1 mM DTT, 1 mM PMSF) and incubated on ice with mixing for 4 hours. Nuclear extract was cleared by centrifugation at 13000 *g* for 10 minutes at 4 °C and stored at ⁻80 °C.

2.4.3 *Bicinchoninic Acid (BCA) Protein assay*

Cell extracts were assayed for protein using bicinchoninic acid protein assay reagent (Pierce, Rockford, Illinois). 5 µl extracts were mixed into 1 ml of 1 part reagent B and 50 parts reagent A. Assay was incubated at 37 °C for 30 minutes and measured at 562 nm λ. Standard curves of protein concentration were produced using BSA.

2.4.4 *Western Blotting*

20 µg cell extracts were denatured by boiling for 2 minutes with 2x sample buffer (100 mM Tris-HCl pH8, 200 mM DTT, 4 % (v/v) SDS, 20 % (v/v) glycerol, 3 mM bromophenol blue) and were resolved on a 10 % sodium dodecyl sulphate polyacrylamide gel (SDS-PAGE). SDS-PAGE gel was run in 1x SDS-Tris running buffer (250 mM Tris-HCl, 1.92 M glycine, 1 % (w/v) SDS) at 35V for 45 minutes. Resolved proteins were transferred to polyvinyl difluoride (PVDF) membrane (Amersham Life Sciences, Little Chalfont, UK), which had been primed with methanol for 1 minute and then equilibrated with transfer buffer (48 mM Tris-HCl, 39 mM glycine, 0.037 % (w/v) SDS, 20 % methanol, pH 8.3) for 20 minutes. Transfer was run at 100 mAmps for 1 hour. The membrane was then blocked in blocking buffer and transferred straight into blocking buffer containing primary antibody. After incubation with the primary antibody, the membrane was washed and probed with a horseradish peroxidase (HRP)-conjugated secondary antibody in blocking buffer (Sigma-Aldrich, Poole, Dorset). After probing with the HRP-conjugated secondary antibody, the membrane was washed and then developed using Super-Signal® West Dura Extended Duration Substrate (Pierce, Rockford, Illinois) and autoradiography.

Antigen	Blocking Buffer	Primary Antibody	Wash	Secondary Antibody	Wash
PPARγ	5 % milk + 0.1 % PBS-Tween 20 overnight[d]	1:200 (Santa Cruz) x 1 hour	3 x 5' 0.1 % PBS-Tween 20	1:5000 anti-rabbit x 1 hour	3 x 5' 0.1 % PBS-Tween 20 + 3 x 5' PBS
p21	5 % milk + 0.1 % PBS-Tween 20 x 1 hour	1:500 (Santa Cruz) overnight	3 x 5' 0.1 % PBS-Tween 20	1:5000 anti-rabbit x 1 hour	3 x 5' 0.1 % PBS-Tween 20 + 3 x 5' PBS
p53	5 % milk + 0.01 % PBS-Tween 20	1:2000 (Novocastra) x 1 hour	3 x 5' 0.01 % PBS-Tween 20	1:2000 anti-rabbit x 1 hour	3 x 5' 0.1 % PBS-Tween 20 + 3 x 5' PBS
c-Myc	5 % milk + 0.1 % PBS-Tween 20 overnight	1:500 (Calbiochem) x 1 hour	3 x 5' 0.1 % PBS-Tween 20	1:5000 anti-mouse x 1 hour	3 x 5' 0.1 % PBS-Tween 20 + 3 x 5' PBS
N-Myc	5 % milk + 0.1 % PBS-Tween 20 overnight	1:2000 (Calbiochem) x 1 hour	3 x 5' 0.1 % PBS-Tween 20	1:10000 anti-rabbit x 1 hour	3 x 5' 0.1 % PBS-Tween 20 + 3 x 5' PBS
MAD 1	5 % milk + 0.1 % PBS-Tween 20 overnight	1:2000 (Santa Cruz) x 1 hour	3 x 5' 0.1 % PBS-Tween 20	1:10000 anti-rabbit x 1 hour	3 x 5' 0.1 % PBS-Tween 20 + 3 x 5' PBS
MAD 3	5 % milk + 0.1 % PBS-Tween 20 overnight	1:2000 (Santa Cruz) x 1 hour	3 x 5' 0.1 % PBS-Tween 20	1:10000 anti-rabbit x 1 hour	3 x 5' 0.1 % PBS-Tween 20 + 3 x 5' PBS
Phospho-Protein kinase B	3 % milk + 0.05 % PBS-Tween 20 X 1 hour	1:1000 (Calbiochem) overnight	2 x 1' Water	1:4000 anti-rabbit x 1.5 hours	3 x 5' 0.05 % PBS-Tween 20
Poly-ADP Ribose polymerase (PARP)	3 % milk + 0.05 % PBS-Tween 20 X 1 hour	1:1000 (Upstate Biotechnology) overnight	2 x 1' Water	1:10000 anti-rabbit x 1.5 hours	3 x 5' 0.05 % PBS-Tween 20

Table 3 Conditions used for Western blotting with various antibodies.

[d] All 1 hour incubations at room temperature with mixing on spiramixer. All overnight incubations at 4°C with mixing on spiramixer.

2.4.5 *Preparation of Membrane Phospholipids*

A pellet of known number of cells was resuspended in 200 µl HBSS in a 1.5-ml eppendorf and sonicated in a sonicating waterbath for 2 minutes. 15 nmoles dimyristoyl phosphatidylcholine (PtdCho 14:0/14:0), 4 nmoles dimyristoyl phosphatidylethanolamine (PtdEtn 14:0/14:0) and 0.5 nmoles dimyristoyl phosphatidic acid (PA 14:0/14:0) were added for each 10^7 cells as internal standards.

The cell suspension was added drop-wise to 1 ml ice-cold methanol with vortexing in a screw-top tube and the residual suspension in the tube was pooled in the methanol, by rinsing the tube with 800 µl HBSS. 1 ml methanol, then 1 ml chloroform was added to the suspension and vortexed to achieve a solution as one phase. 1 ml chloroform, then 1 ml distilled water was added to the suspension and vortexed, to yield a two phase solution with the upper layer being aqueous. Sharp resolution of the phases was achieved by centrifugation at 500 *g* for 10 minutes. The lower chloroform layer was carefully decanted to a clean tube and dried under nitrogen at 40 °C for approximately 2 hours. The residue was dissolved into 1 ml chloroform and applied to a Bond-Elut NH_2 disposable solid phase extraction column, which had been equilibrated with 1 ml chloroform wash prior to use, and allowed to percolate under gravity. The eluted liquid and two subsequent 1 ml chloroform washes, collected under vacuum, were discarded and the PtdCho 14:0/14:0 fraction was eluted by washing the columns with 1 ml 60:40 chloroform:methanol under vacuum.

The PtdEtn 14:0/14:0 fraction was collected by elution with 1 ml methanol under vacuum. The acid phospholipid fraction was eluted with three 1 ml washes of methanol:water:phosphoric acid (96:4:1) containing 40 mM choline chloride. The eluted fraction was dried down under nitrogen and back-extracted to remove choline chloride by adding 100 µl water, then 200 µl methanol, then 200 µl chloroform and then finally another 100 µl water. The lower chloroform layer from the back-extraction was dried down under nitrogen into insert vials within amber vials prior to analysis on the mass spectrometer.

The phosphatidylcholine and phosphatidylethanolamine fractions were dried under nitrogen and re-dissolved in 100 µl chloroform before transfer to insert vials and dried again under nitrogen for mass spectrometry analysis.

2.4.6 *Electrospray Ionisation Mass Spectrometry*

Electrospray ionisation mass spectrometry (ESI MS) was performed on Micromass Quattro Ultima triple quadropole mass spectrometer (Micromass, Wythenshaw, UK) equipped with an electrospray ionisation interface. Samples of phosphatidylcholine (PtdCho), phosphatidylethanolamine (PtdEtn) and acid phospholipids were extracted from control-treated, fatty acid-treated and PPAR ligand-treated IMR-32 cells and were dissolved in methanol:chloroform:water (7:2:1 v/v). The samples were introduced into the mass spectrometer via a syringe pump. PtdEtn and acid phospholipid samples were analysed by ESI^{-ve} mass spectrometry. Samples of PtdCho were fragmented with argon gas in the collision cell and tandem ESI^{+ve} MS was used to analyse the parents of 184 fragments. All samples were detected by sensitive photomultiplier and mass spectra for each phospholipid type were shown as mass/charge (m/z).

2.4.7 *Chloramphenicol Acetyl Transferase Reporter Assay*

Cells transfected with reporter plasmids were pelleted and cell pellets were washed with PBS and then resuspended in 100 µl 0.25 mM Tris-HCl pH 7.8. Cell membranes were disrupted by 5 cycles of freeze-thaw. Cell debris was pelleted at 14083 *g* for 5 minutes and supernatant collected and assayed for protein. Extracts were assayed for chloramphenicol acetyl transferase (CAT) activity [403] at 37 °C for 6 hours in a reaction mix (120 mM Tris HCl pH 7.8, 4 mM acetyl CoA, 1 µl ^{14}C chloramphenicol) with a total volume of 146 µl. Chloramphenicol was extracted in 1 ml ethyl acetate by vortexing for 30 seconds. Samples were spun down at 5416 *g* for 3 minutes and top layer collected.

This was dried down under vacuum for 2 hours in an evacuated spinning centrifuge or Uniscience Univap. The dried residue was resuspended in 15 µl ethyl acetate and spotted onto a thin layer chromatography (TLC) plate (Whatman International Limited, Maidstone, UK). The TLC plate was developed in a TLC tank containing 100 ml of 95:5 chloroform:methanol. The plate was air dried and autoradiographed overnight. Quantification of the CAT assay was achieved using a Storm 860 Phosphoimager (Molecular Dynamics Limited, Chesham, Buckinghamshire, UK) and an image quantifier programme to calculate percentage conversions of the ^{14}C chloramphenicol to its acetylated products.

2.4.8 *Luciferase Reporter Assay*

IMR-32 cells were transfected with 5 µg pGL_3Basic (Promega, Chilworth, UK) as a control and 5 µg of a construct, pGL3-5xκB-luc, containing a Nuclear Factor κB (NFκB) DNA binding site linked to a luciferase reporter gene (a kind gift from Dr. R Hofmeister, Universität Regensburg, Regensburg, Germany). The cells were treated with DMSO or 5 µM $15dPGJ_2$ in fresh medium post-transfection. Luciferase activity was measured using Promega luciferase assay kit (Promega, Chilworth, UK). Briefly, cells were lysed in lysis buffer and freeze-thawed once. Cell debris was pelleted and the supernatant was assayed for protein. The supernatant was mixed with luciferase substrate and each sample was measured three times in a TD-20/20 luminometer (Turner Designs, Sunnyvale, California) and an average calculated.

2.4.9 *Decoy Assay*

IMR-32 cells were seeded at 5 x 10^5 cells per 96 mm tissue culture dish and allowed to attach overnight. Cells were transfected in Fungizone®-free tissue culture medium with 0, 10 or 20 µg of vector containing the decoy sequence, which was a triple repeat of a consensus peroxisome proliferator-activated receptor DNA binding site (rat ACO-PPRE: AGGAGAAAGGTCA).

The insert had been previously cloned into a pBl_2CAT reporter construct upstream of a thymidine kinase promoter (3PPRE-TK-CAT) for 6 hours at 37 °C [233]. Control cells were transfected with 0, 10 or 20 μg vector alone (pBl_2CAT) for 6 hours at 37 °C. The DNA content was normalised using β-galactosidase vector. Cells were washed and 5 ml fresh medium was added and the cells were incubated at 37 °C for 1 hour. Cells were then treated with DMSO or 5 μM $15dPGJ_2$ and live and dead cells were counted after 24, 48 and 72 hours. Treatments were reapplied daily in fresh complete medium.

2.4.10 *Delipidation of Foetal Calf Serum*

Batches of foetal calf serum (FCS) (Invitrogen Limited, Paisley, Scotland) were mixed with 1 litre of butan-1-ol:di-isopropylether (40:60 v/v) (Fischer Scientific UK, Loughborough, UK) and vortexed using magnetic stirrer in a fume cupboard for one hour, in a modification of the technique previously described by Cham and Knowles, [404].

The lower aqueous fraction was decanted and dialysed in batches of 50 ml against two changes of Hanks Balanced Salt Solution to remove excess organic solvent (predominantly butan-1-ol). 70-75 % volume of the delipidated foetal calf serum was recovered and was filter sterilised through 0.2 μM filters. Delipidated foetal calf serum was used as previously described for normal foetal calf serum, i.e. at 10 % (v/v) in complete tissue culture medium.

2.5.1 *Preparation of Lysophosphatidic Acid and Sphingosine-1-Phosphate*

2.5.1.1 *Lysophosphatidic acid (LPA)*

Oleoyl-lysophosphatidic acid (LPA) was dried down under N_2 and calcium-free, magnesium-free HBSS was added to the residue. The oleoyl-LPA mixture was sonicated in a water bath for 5 minutes until in the oleoyl-LPA was resuspended.

The oleoyl-LPA suspension was added to ice cold fatty acid-free bovine serum albumin and mixed on a spiramixer for 1 hour at room temperature to make a 500 μM solution. The oleoyl-LPA-bovine serum albumin solution was filter sterilised and used at 5 μM. Oleoyl-LPA-BSA was stored at ˉ20 °C and once defrosted was stored at 4 °C.

2.5.1.2 *Sphingosine-1-Phosphate*

1 mg sphingosine-1-phosphate (S1P) was dried down under N_2 and 5 ml calcium-free, magnesium-free Hanks Balanced Salt Solution was added. The S1P mixture was sonicated in a water bath for 5 minutes until in suspension. The S1P mixture was added to ice cold fatty acid-free bovine serum albumin and mixed on a spiramixer for 1 hour at room temperature to make a 500 μM solution. The S1P-BSA solution was filter sterilised and used at 5 μM. The S1P-BSA solution was stored at ¯20 °C and once defrosted was stored at 4 °C.

2.5.2 *Cell Culture using Delipidated Cell Culture Medium*

Cell culture experiments were repeated using Dulbecco's Modified Eagle's Medium (DMEM) containing 10 % (v/v) delipidated foetal calf serum (FCS) and 100 mM glutamine, supplemented with 0.1 mg/ml penicillin/streptomycin and Fungizone® (2.5 μg/ml amphotericin B) under the conditions described above. Cells were initially plated out using tissue culture medium with normal foetal calf serum to facilitate attachment. The medium was replaced after 24 hours with tissue culture medium containing delipidated FCS and appropriate treatments (30 μM fatty acids or 5 μM PPAR ligands). The treatments, but not the tissue culture medium, were replaced daily, as changes of medium caused premature cell detachment from the tissue culture plastic.

2.5.3 *Statistics*

All experiments were completed in duplicate, with duplicate wells of cells counted per sample per day for cell growth and cell death experiments. Duplicate samples per treatment per day were analysed for flow cytometry experiments and mass spectrometry spectra are representative of duplicate samples for the fatty acid and PPAR ligand experiments.

The errors on the graphs represent standard errors of the mean. Statistics were calculated using analysis of variance (ANOVA) for time course experiments and the student's t test was used for single time point experiments. For all analysis p values of 0.05 and under are represented as * and p values of 0.01 and under are represented as **.

Chapter 3

The Effects of Polyunsaturated Fatty Acids on IMR-32 Cells *In Vitro*

3.1 *Introduction*

Polyunsaturated fatty acids (PUFAs) are fatty acids which contain more than one carbon=carbon (C=C) double bond within their hydrocarbon backbone. PUFAs include fatty acids which are important in the development and differentiation of the nervous system, such as docosahexaenoic acid (C22:6, n-3)[e] and arachidonic acid (C20:4 n-6) [178]. PUFAs have been shown to inhibit the growth of some types of cancer cells and tumours and they have also been shown to induce apoptosis in some cancer cell types, without affecting normal cells [405]. Docosahexaenoic acid (DHA) induces apoptosis in HT-29 colon cancer cells [406] and Jurkat cells [407]. It has also been shown to reduce both the size of breast and epithelial tumours implanted into mice as well as reducing the number of metastases [176, 408]. Arachidonic acid (AA) has been shown to reduce the number of metastases in mice implanted with colon cancer cells [177]. Both AA and γ-linolenic acid (γ-LA) inhibit the growth of chronic myeloid leukaemia cells and AA is also able to induce apoptosis in these cells [409]. These effects may occur through changes to membrane lipids, as it has been shown that the anti-metastatic activity of DHA was associated with pronounced changes in the fatty acid composition of breast cancer cell membranes [176] and colon cell membranes [177].

Fatty acids are proposed to be activators of all three isoforms of peroxisome proliferator-activated receptors (PPARs), α, β and γ. PUFAs bind to and activate PPARα, whereas short-chain saturated fatty acids weakly activate PPARα, and very long chain fatty acids fail to bind or to activate PPARα [116, 157, 166, 172, 173, 174]. Polyunsaturated fatty acids are also activators of the β isoform of PPARs [166] and some monounsaturated fatty acids and PUFAs are activators of PPARγ [114, 157, 166]. PUFAs have also been shown to activate reporter constructs containing PPAR consensus binding sites, suggesting that they are able to activate PPAR-induced transcription [175]. However, the long-chain monounsaturated fatty acid, nervonic acid, has actually been shown to inhibit the activation of PPARs using a reporter construct containing three PPAR consensus binding sites [164, 172].

---

[e] C22:6 relates to a fatty acid molecule with 22 carbon atoms and 6 C=C double bonds. n- numbers are known as ω nomenclature and relate to the position of the double bond within the fatty acid molecule in relation to the terminal methyl group in the fatty acid chain [574].

The effects of PUFAs on cancer cells may be linked to activation of peroxisome proliferator-activated receptors (PPARs), as PUFAs activate PPAR-induced transcription [175] and activation of PPARγ can inhibit the growth of some cancer cells [177, 408].

The expression of all three isoforms of PPAR can differ between normal and malignant cells. PPARα is either not expressed or is weakly expressed in normal prostate epithelial cells, whereas is it highly expressed in poorly differentiated prostate carcinomas [310]. PPARβ is highly expressed in uterine endometrial adenocarcinomas [315] and has been shown to be over-expressed in many colorectal cancers, with normal tissue expressing lower levels of the isoform [351]. PPARγ has been shown to be expressed at high levels in several cancer cell lines and primary tumours, including breast [290], colon [349] and liposarcoma [241] and the corresponding normal tissue. However, prostate cancer cells express high levels of PPARγ, whereas the normal tissue had very low expression levels [130].

Therefore to determine whether polyunsaturated fatty acids were able to inhibit the growth of neuroblastoma cells, the human neuroblastoma cell line, IMR-32, was treated with physiological concentrations of fatty acids [166, 410] and the effects on cell growth determined. The mechanism of action of the fatty acids was investigated to determine whether any effects they had involved changes to membrane phospholipids or through activation of PPARs. The expression of PPARs in IMR-32 cells and another human neuroblastoma cell line, Kelly, was also determined.

3.2.1 *Some PUFAs inhibit the growth of IMR-32 cells*

Polyunsaturated fatty acids have been shown to inhibit growth of some cancer cell lines. To assess the whether PUFAs affected neuroblastoma cell proliferation, IMR-32 cells were treated with PUFAs, including AA, DHA, OA (18:1, n-9) and γ-LA (22:3, n-3). 30 μM fatty acids were used for these experiments, as this is thought to be the approximate physiological concentration of PUFAs in normal serum [166, 410].

Figure 3.1 30 μM polyunsaturated fatty acids (PUFAs) have a marginal effect on IMR-32 cell growth. IMR-32 cells were seeded at 2 x 10^4 cells per well. The tissue culture medium was supplemented with 30 μM PUFAs and was replaced daily with fresh PUFAs. IMR-32 cell growth was measured as increasing cell number over 120 hours and compared to control cells treated with Hank's balanced salt solution (HBSS). Two samples were measured per treatment per day and experiments were completed in duplicate and error bars represent standard error of the mean (s.e.m.).

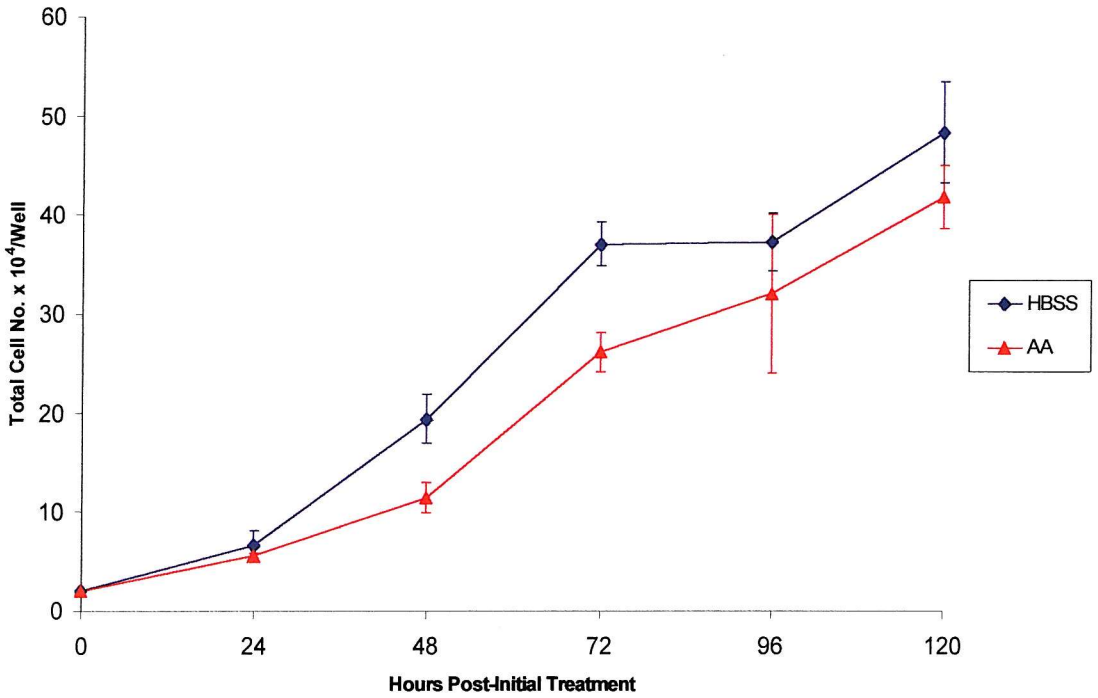

Figure 3.1a Arachidonic Acid (AA)

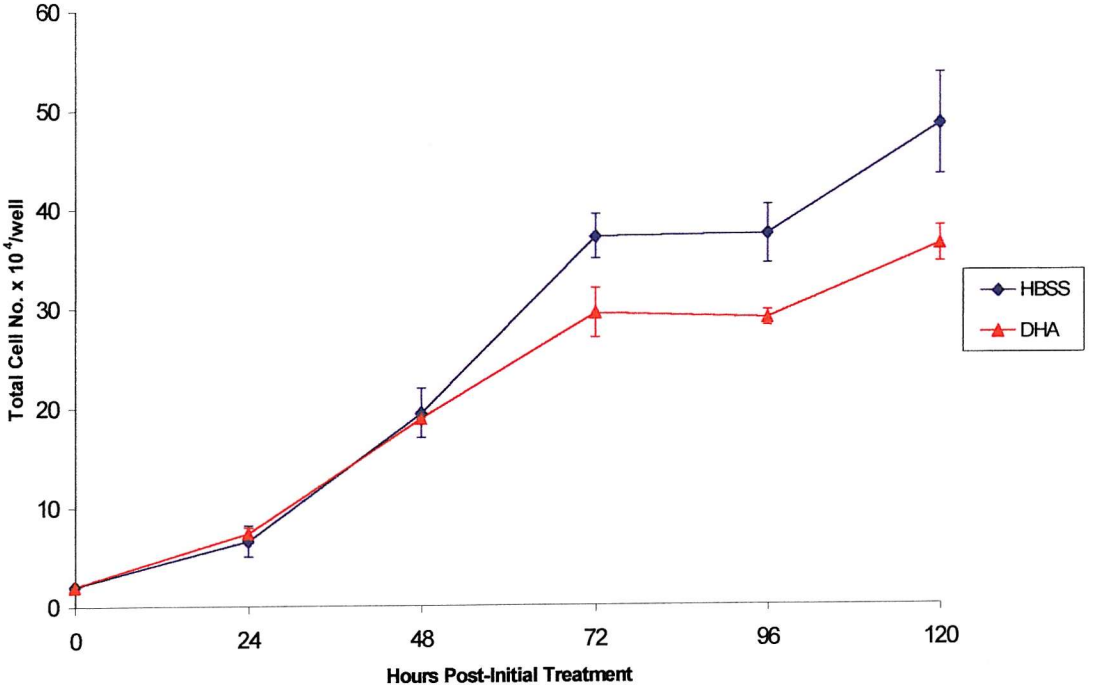

Figure 3.1b Docosahexaenoic Acid (DHA)

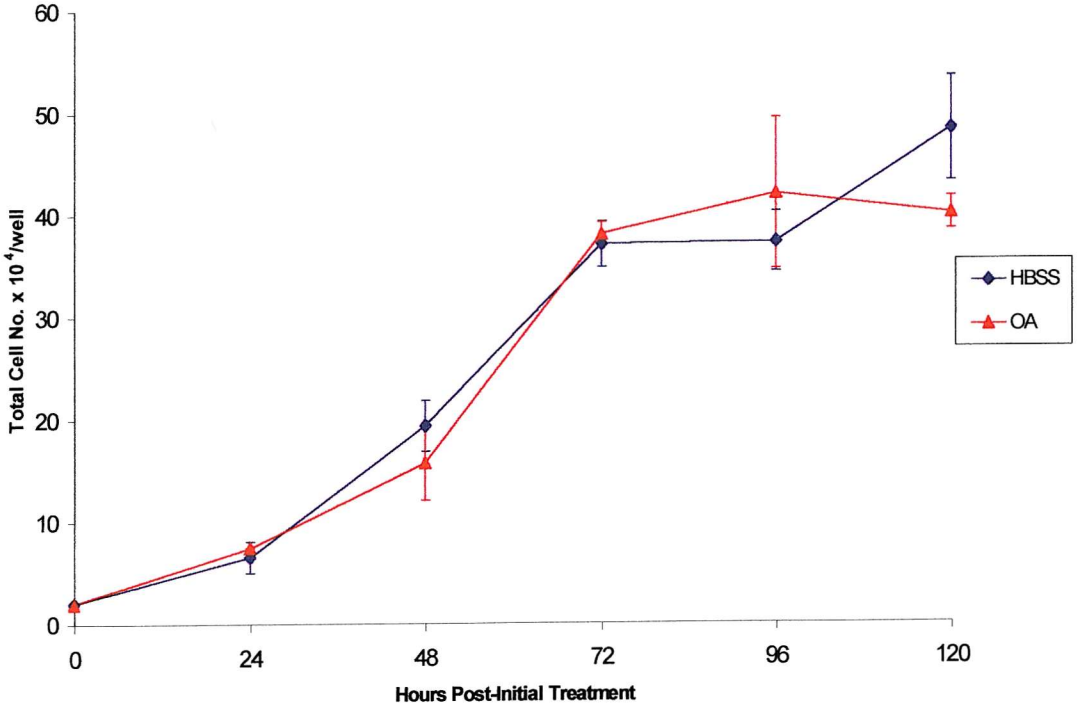

Figure 3.1c Oleic Acid (OA)

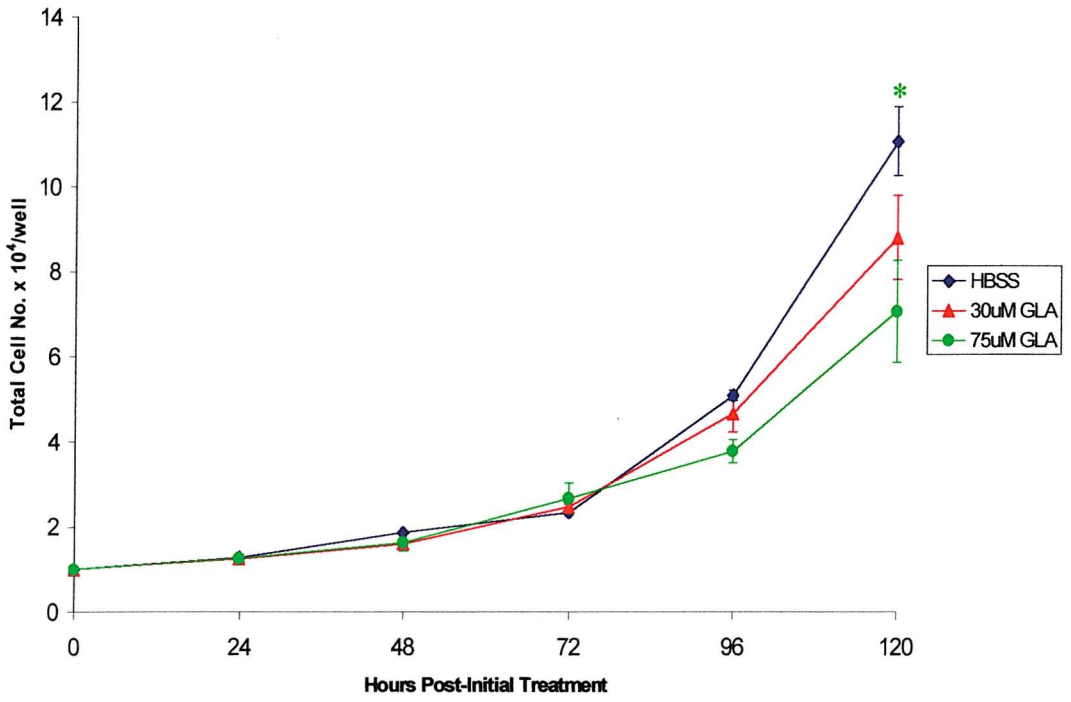

Figure 3.2 75 μM γ-linolenic acid marginally affects IMR-32 cell growth. IMR-32 cells were plated out 2 x 10^4 cells per well and the tissue culture medium was supplemented with 30 μM or 75 μM γ-linolenic acid (GLA or γLA in text). Fresh medium and treatments were applied daily and cell growth measured over 120 hours as an increase in cell number. Two samples were measured per treatment per day and experiments were completed in duplicate. Error bars represent standard errors of the mean. Statistics were calculated using an ANOVA and showed no significant difference between samples throughout the experiment. However, a student's t test showed a significant difference between control samples and 75 μM γLA, but only after 72 hours treatment, where $p<0.05$ (*).

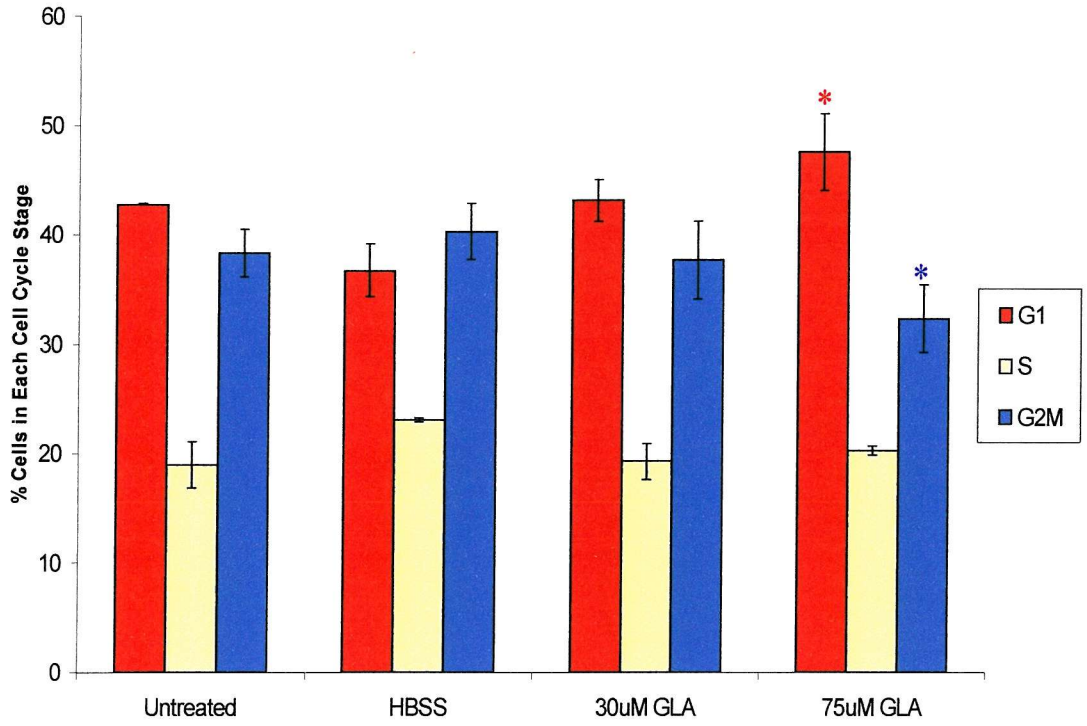

Figure 3.3 75 μM γ-linolenic acid marginally increases number of IMR-32 cells in G_1 phase of the cell cycle. IMR-32 cells were treated with 30 μM or 75 μM γ-linolenic acid (γLA/GLA). 1 x 10^6 cells were stained with propidium iodide and analysed by flow cytometry after 120 hours treatment. Experiments were run in duplicate and error bars represent s.e.m. Statistics were calculated using a student's t test and a significant increase in the number of cells G_1 ($p < 0.05$ *) and decrease in the number of cells in G_2/M ($p < 0.05$ *) were seen.

Concentrations of more than 30 μM fatty acids results in accumulation of the fatty acids as lipid droplets within cells [411]. IMR-32 cells were treated for 120 hours, with daily supplements of 30 μM PUFAs in fresh culture medium, and the effects on cell growth were investigated. IMR-32 cells treated with the control treatment, Hank's balanced salt solution (HBSS), increased in number throughout the experiment (Figures 3.1a-c). AA (Figure 3.1a) and DHA (Figure 3.1b) reduced the growth of IMR-32 cells but only after more than 48 hours continual treatment, and at later time points AA was not effective. The addition of oleic acid, however, had no effect on the growth of the cells, with cell growth similar to that of controls over the whole time period (Figure 3.1c). Some inhibition of growth was achieved using 30 μM γ-LA, compared to control-treated cells (Figure 3.2). A higher concentration of γ-LA, 75 μM, was also used to treat IMR-32 cells, as 75 μM γ-LA has been shown to activate PPARγ in breast cancer cells [224]. When the cells were treated with 75 μM γ-LA for 120 hours, there was a decrease in growth rate compared to controls (Figure 3.2). This reduction in cell growth was also seen as an increase in the percentage of cells found in G_1/G_0 of the cell cycle and a decrease in those found in G_2/M (Figure 3.3). No changes in the cell cycle distribution were seen with 30 μM AA, DHA, OA or γ-LA (Figure 3.3 and data not shown).

3.2.2 *PUFAs do not induce cell death in IMR-32 cells*

PUFAs have been shown to induce apoptosis in some cancer cells including leukaemia cells [409] and colon cancer cells [406]. The marginal effects of 30 μM AA, DHA and γ-LA on IMR-32 cell growth could have been due to an increase in cell death. To determine whether the PUFA treatments induced cell death in neuroblastoma cells, IMR-32 cells were treated with 30 μM AA, DHA, OA or γ-LA for 120 hours and cell death measured using the trypan blue exclusion assay. Only cells in which the membrane integrity has been lost take up this dye, as it is excluded by those cells with intact membranes, and this can be used to determine the number of dead cells within a population. Less than 5 % of control-treated IMR-32 cells took up trypan blue throughout the experiment, suggesting the cells were remaining viable *in vitro*.

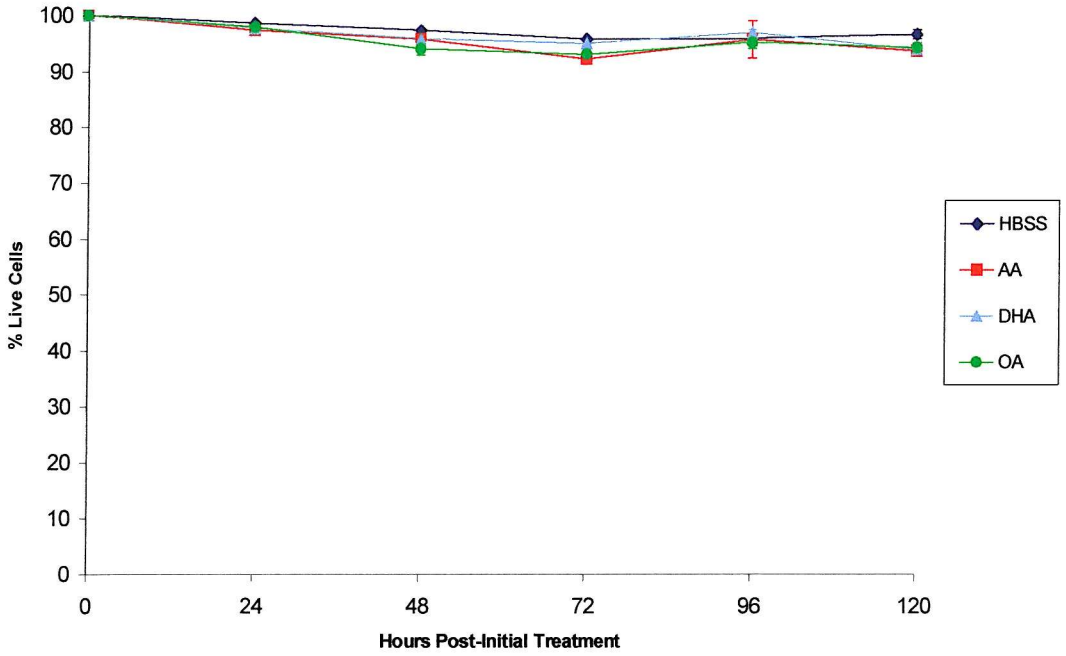

Figure 3.4 PUFAs do not induce death of IMR-32 cells. IMR-32 cells were plated out at 2 x 10^4 cells per well and treated as previously described for cell growth experiments. The cells were treated with 30 μM arachidonic acid (AA), docosahexaenoic acid (DHA) or oleic acid (OA). The cells were harvested, stained with 0.4 % trypan blue solution and the proportion of live and dead cells determined over 120 hours. Two samples were measured per treatment per day and experiments were run in duplicate and error bars represent s.e.m.

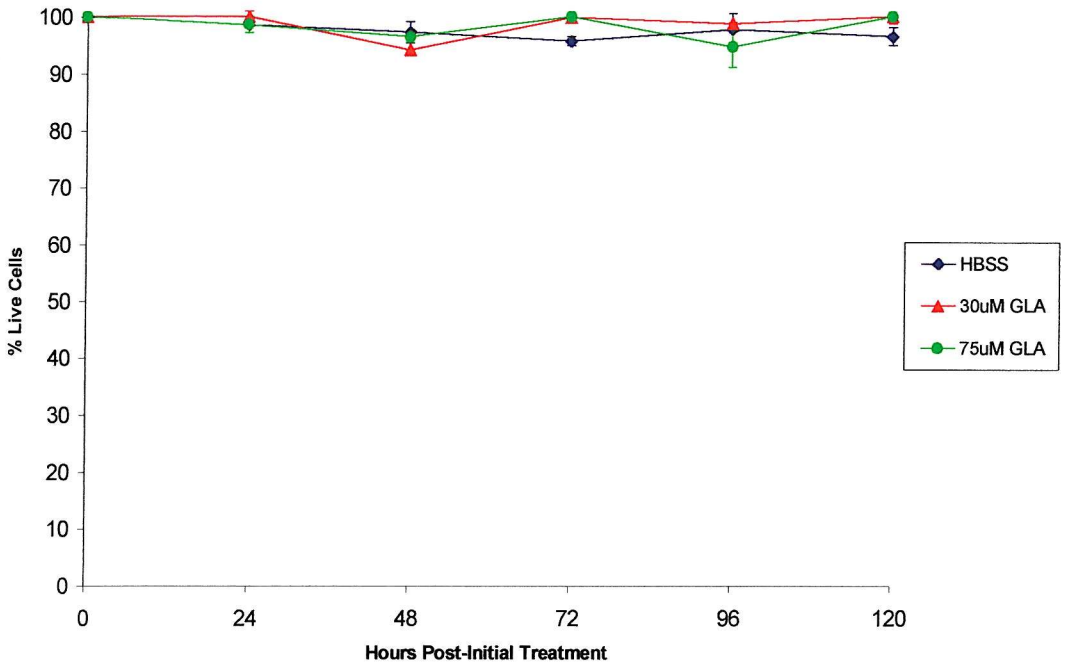

Figure 3.5 γ-linolenic acid does not induce death of IMR-32 cells. IMR-32 cells were plated out at 2 x 10^4 cells per well and treated as previously described for cell growth experiments, with 30 μM or 75 μM γ-Linolenic acid (γ-LA/GLA). The cells were harvested, stained with 0.4 % trypan blue solution and the proportion of live and dead cells determined over 120 hours. Two samples were measured per treatment per day and experiments were completed in duplicate and error bars represent s.e.m.

None of the PUFAs (AA, DHA, OA and γ-LA) increased cell death over the time course (Figures 3.4 and 3.5), suggesting that any decrease in growth rate seen was not due to cell death. IMR-32 cells were also treated with 75 μM γ-LA and stained with trypan blue and compared to HBSS-treated controls. Despite this concentration of γ-LA inhibiting cell growth more than 30 μM γ-LA, it did not induce an increase in cell death compared to controls or IMR-32 cells treated with 30 μM γ-LA (Figure 3.5).

3.2.3 *IMR-32 cells treated with PUFAs undergo changes in membrane phospholipid composition*

The marginal effects of PUFAs on IMR-32 cell growth may occur through changes to membrane phospholipids. The anti-metastatic activity of PUFAs have been associated with pronounced changes in the fatty acid composition of breast cancer cell membranes [176] and colon cell membranes [177]. Therefore extracts of phosphatidylcholine (PtdCho), phosphatidylethanolamine (PtdEtn) and acid phospholipid (PA) species were made from the membranes of treated IMR-32 cells and analysed by electrospray ionisation mass spectrometry (ESI-MS), to determine whether 30 μM PUFAs altered the membrane composition.

Treatment of IMR-32 cells with 30 μM AA resulted in an increase in arachidonyl-containing PtdCho species from 11.9 % to 44.3 % (Figure 3.6). The major changes to the AA-containing PtdCho species were increases in palmitoyl-arachidonyl PtdCho (16:0/20:4) and stearoyl-arachidonyl PtdCho (18:0/20:4). There was also a concurrent increase in the more saturated dipalmitoyl PtdCho (16:0/16:0). Treatment of IMR-32 cells with 30 μM DHA for 72 hours resulted in an increase in DHA-containing species of phosphatidylcholine from 10.9 % to 28.1 % (Figure 3.6). The major changes to species of PtdCho containing DHA, were a large increase in palmitoyl-docosahexaenyl PtdCho (16:0/22:6) and an increase in stearoyl-docosahexaenyl PtdCho (18:0/22:6). This was concurrent with an increase in disaturated PtdCho species, such as dipalmitoyl PtdCho (16:0/16:0).

Figure 3.6 PUFAs mediate changes to the membrane phosphatidylcholine composition of IMR-32 cells. IMR-32 cells were treated with 30 μM AA or DHA for 72 hours and phosphatidylcholine (PtdCho) species were isolated from the cell membranes. The PtdCho samples were analysed by tandem electrospray ionisation $^{+ve}$ mass spectrometry (ESI^{+ve} MS) and spectra of parent species of m/z 184 were produced. 184 is the mass of the phosphocholine headgroup. Mass spectra were shown as peak intensity and mass/charge (m/z) and each spectrum is representative of duplicate samples.

Control IMR-32 cell membrane PtdCho molecular species composition

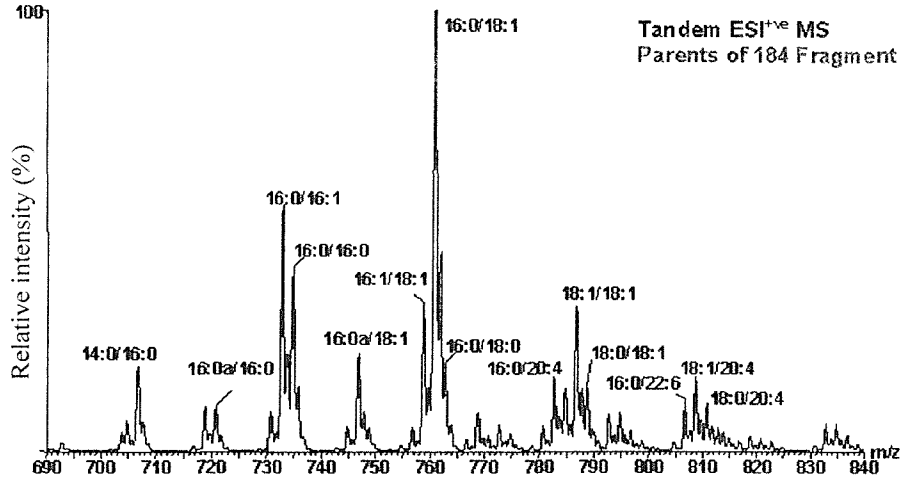

IMR-32 cell membrane PtdCho molecular species composition after 72h DHA supplementation

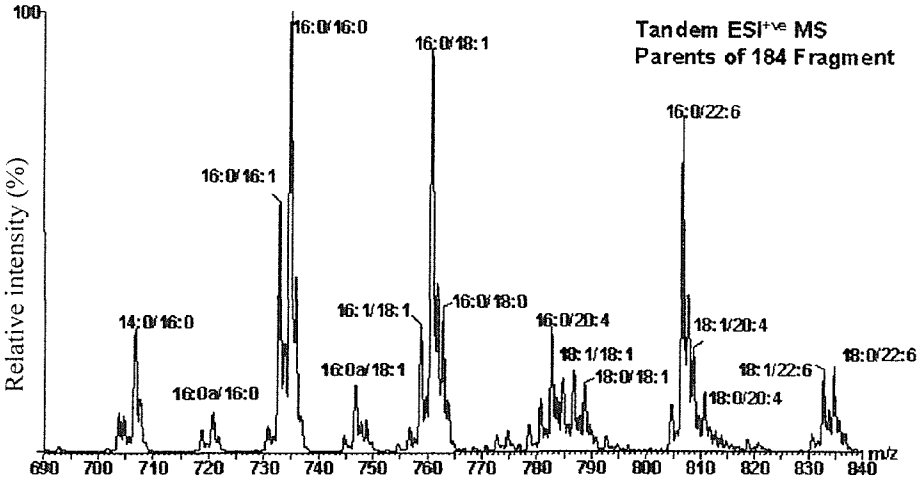

IMR-32 cell membrane PtdCho molecular species composition after 72h AA supplementation

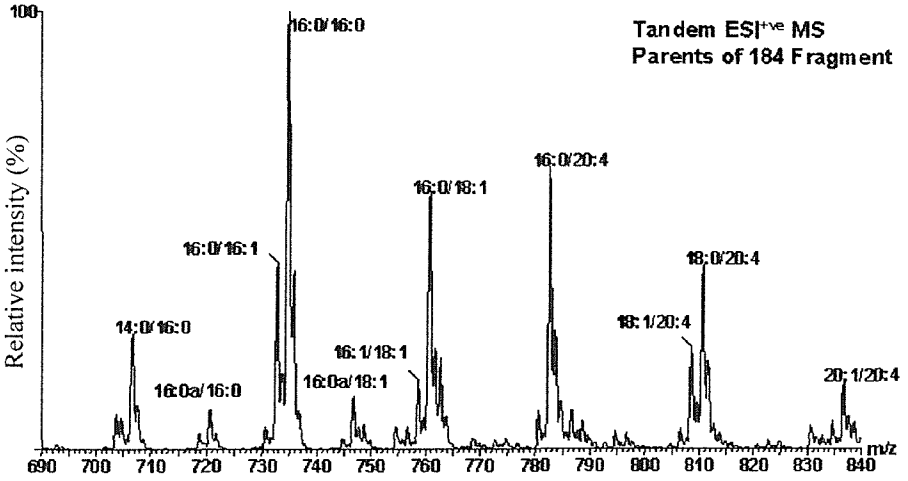

Figure 3.7 PUFAs mediate changes to the membrane phosphatidylethanolamine composition of IMR-32 cells. IMR-32 cells were treated with 30 μM AA or DHA for 72 hours and phosphatidylethanolamine (PtdEtn) species were isolated from the cell membranes. The PtdEtn samples were analysed by electrospray ionisation $^{-ve}$ mass spectrometry (ESI^{-ve} MS) and mass spectra were shown as peak intensity and mass/charge (m/z) and each spectrum is representative of duplicate samples.

Control IMR-32 cell membrane PtdEtn molecular species composition

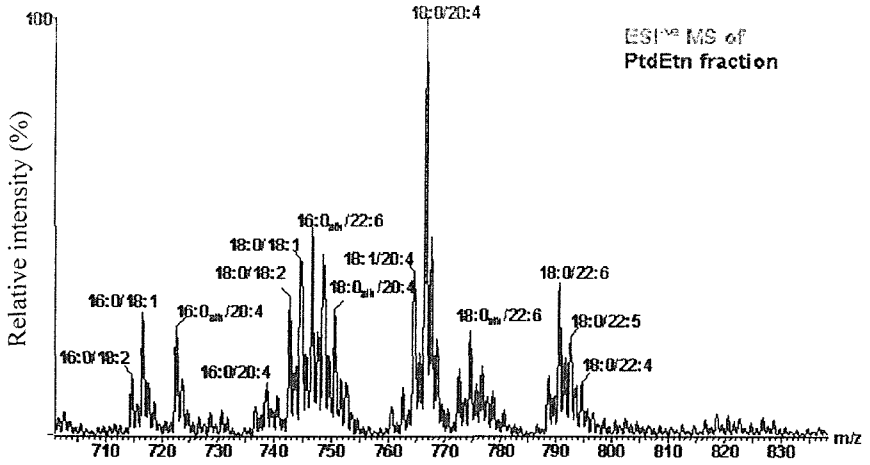

IMR-32 cell membrane PtdEtn molecular species composition after 72h DHA supplementation

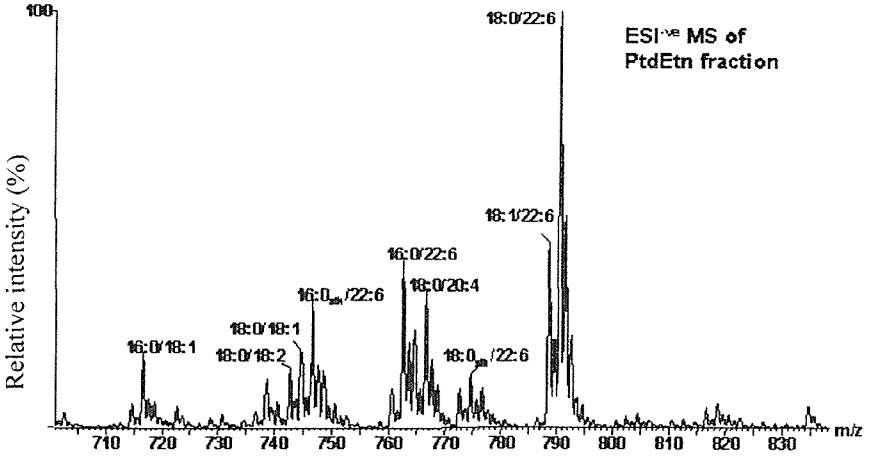

IMR-32 cell membrane PtdEtn molecular species composition after 72h AA supplementation

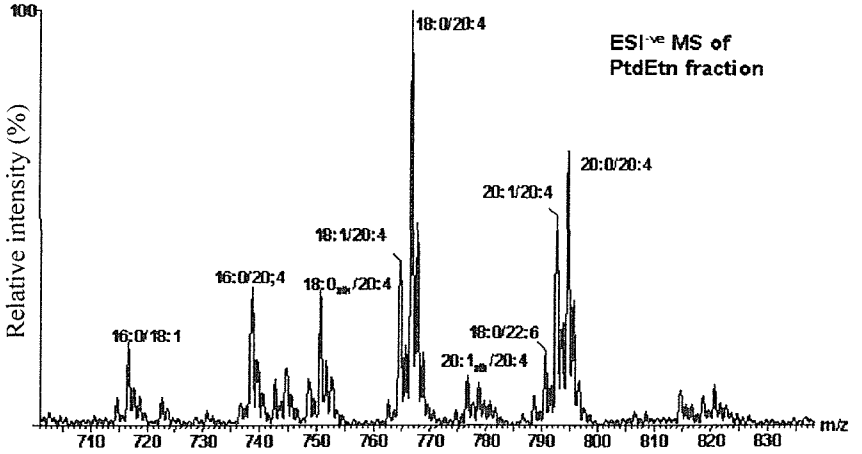

Figure 3.8 PUFAs mediate changes to the membrane acid phospholipid composition of IMR-32 cells. IMR-32 cells were treated with 30 μM AA or DHA for 72 hours and acid phospholipid species were isolated from the cell membranes. The acid phospholipid samples were analysed by electrospray ionisation $^{-ve}$ mass spectrometry (ESI^{-ve} MS) and mass spectra were shown as peak intensity and mass/charge (m/z). Each spectrum is representative of duplicate samples.

Control IMR-32 cell membrane acidic phospholipid molecular species composition

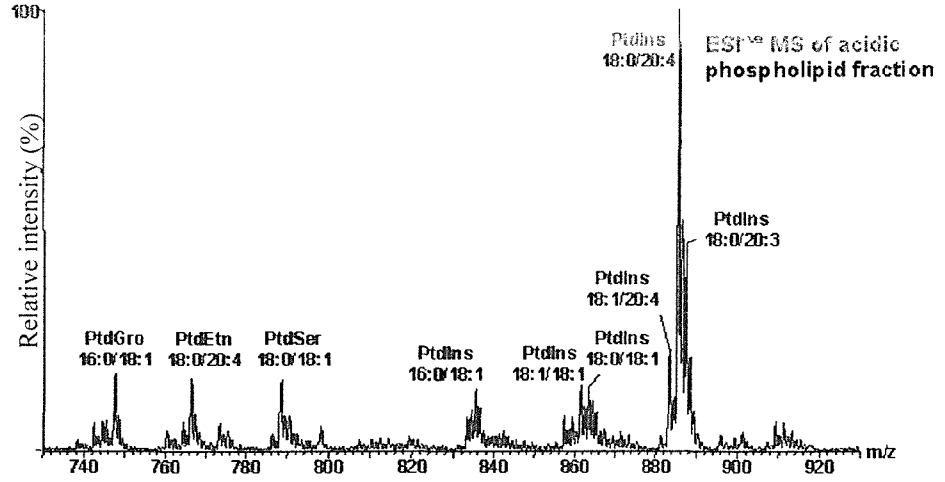

IMR-32 cell membrane acidic phospholipid molecular species composition after 72h DHA supplementation

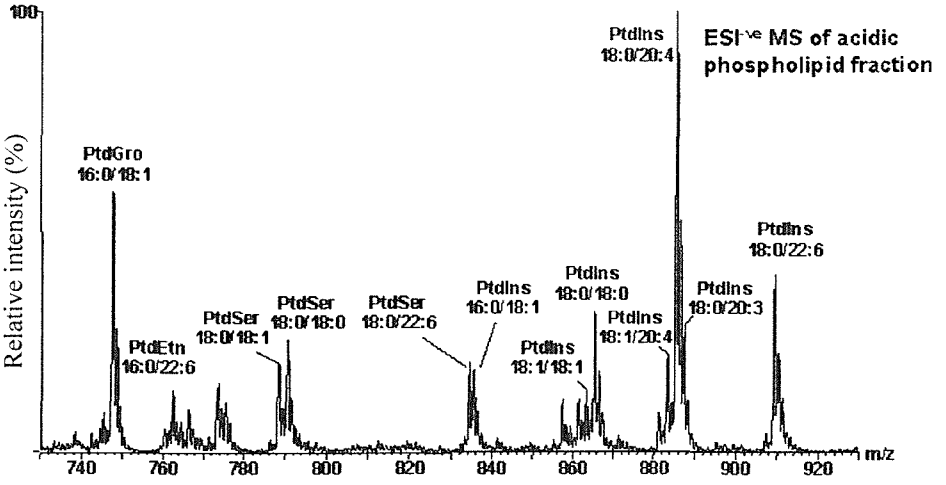

IMR-32 cell membrane acidic phospholipid molecular species composition after 72h AA supplementation

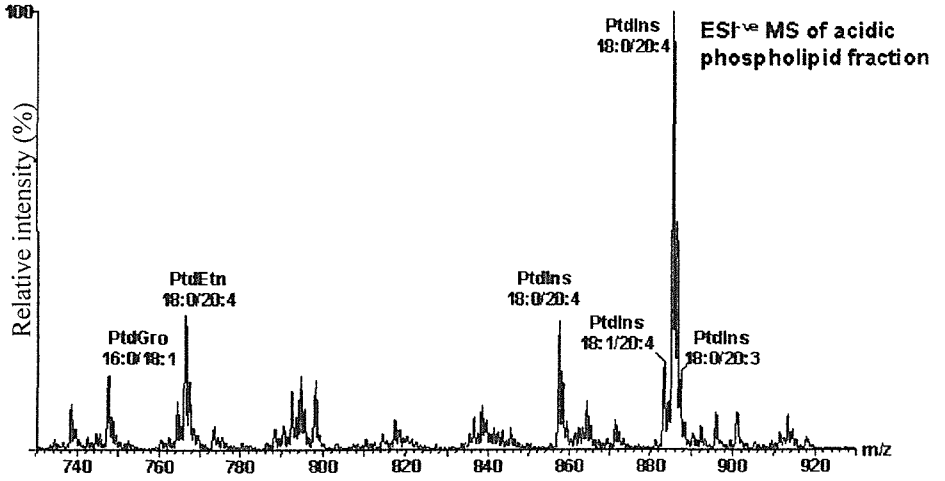

Treatment of IMR-32 cells with 30 μM AA resulted in an increase in arachidonoyl-containing PtdEtn species from 37.8 % to 46.6 % (Figure 3.7). The major changes to the AA-containing PtdEtn species were increases in palmitoyl-arachidonoyl PtdEtn (16:0/20:4) and arachidoyl-arachidonoyl PtdEtn (20:0/20:4). Some of the PtdEtn species are alkenyl PtdEtn species, which means that the fatty acid at position 1 has an ether bond instead of an ester bond, which increases stability. Treatment with 30 μM AA did not affect any of the alkenyl PtdEtn species, but did reduce the amount of DHA-containing PtdEtn species present from 19.8 % to 7.6 %. Treatment of IMR-32 cells with 30 μM DHA for 72 hours resulted in an increase in DHA-containing species of PtdEtn from 19.8 % to 55.1 % (Figure 3.7). The changes to species of PtdEtn containing DHA included were an increase in palmitoyl-docosahexanoyl PtdEtn (16:0/22:6) and oleoyl-docosahexanoyl PtdEtn (18:1/22:6). There was also a large increase in stearoyl-docosahexanoyl PtdEtn (18:0/22:6). This was at the expense of arachidonoyl-containing PtdEtn species from 37.8 % to 20.1 %, which included a large reduction in the amount of stearoyl-arachidonoyl PtdEtn (18:0/20:4). Like AA treatment, 30 μM DHA did not alter the amount of alkenyl PtdEtn species.

The acid phospholipid species detected in the membranes of IMR-32 cells included phosphatidylinositol (PtdIns), phosphatidylglycerol (PtdGro) and phosphatidylserine (PtdSer) with some PtdEtn species (Figure 3.8). The major species found was stearoyl-arachidonoyl PtdIns (18:0/20:4), which is not affected by treatment with 30 μM AA or DHA for 72 hours. On treatment with 30 μM AA for 72 hours, there was an increase in AA-containing acid phospholipid species, including palmitoyl-arachidonoyl PtdIns (16:0/20:4) (Figure 3.8). There was also suppression of DHA-containing acid phospholipid species, with no increase in more saturated acid phospholipid species. On treatment with 30 μM DHA, there was an increase in DHA-containing acid phospholipid species (Figure 3.8), including stearoyl-docosahexanoyl PtdIns (18:0/22:6), and stearoyl-docosahexanoyl PtdSer (18:0/22:6). There was also an increase in the more saturated palmitoyl-oleoyl PtdGro (16:0/18:1) and distearoyl PtdIns (18:0/18:0).

3.2.4 *Neuroblastoma cells express PPARα and PPARγ*

To determine the possible mechanisms by which PUFAs may affect cell growth, neuroblastoma cells were investigated for the expression of peroxisome proliferator-activated receptors (PPARs). The neuroblastoma cell lines used were IMR-32 and Kelly. The IMR-32 cell line was derived from the abdominal neuroblastic tumour, which occurred in a 13-month old Caucasian male in 1967 [391]. The cell line consists of two morphologically distinct cell types [391]. The predominant cell type is a small, neuroblast-like cell, which grows densely forming focal accumulations. The minor cell type is the fibroblast-like cell, which are relatively large and well spread and occur in small numbers. The fibroblast-like cells also exhibit many cell surface projections. The cells have a deletion in chromosome 1, chromosome 16 is absent and they have amplification of the NMYC gene [391], which are markers of poor prognosis in neuroblastoma [40]. Less information is available about the origins or details of the Kelly neuroblastoma cell line (personal communication, Garrett Brodeur, Children's Hospital of Pennsylvania). However, the Kelly cells used in this study tended to grow in focal accumulations and the cells formed only short neurites and tended to have an almost rectangular-shaped morphology. Like IMR-32 cells, Kelly cells have amplification of the NMYC gene [28].

To show the expression of PPARs within neuroblastoma cells, IMR-32 cells and Kelly cells were analysed by RT-PCR with PPARα and PPARγ specific primers. Total cellular RNA was made from IMR-32 cells and Kelly cells and 1 μg RNA was reversed transcribed into cDNA. The cDNA was then amplified initially using primers specific for the housekeeping gene, cyclophilin, to ensure equal amounts of cDNA were made. To ensure the RT-PCR reactions were in the exponential phase of amplification, 5 μl of the reactions were analysed after 30, 35 and 40 cycles.

Both NMYC amplified neuroblastoma cell lines, IMR-32 and Kelly, expressed PPARα (Figures 3.9 and 3.10) and PPARγ (Figures 3.11 and 3.12). PPARβ was not studied as little was known about its function or ligands at the start of the project.

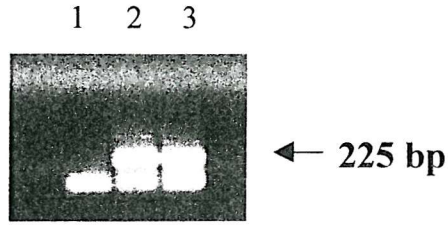

PPARα

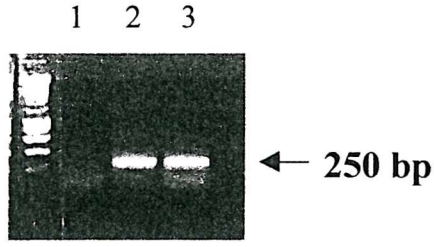

Cyclophilin

Lane 1	Negative control
Lane 2	IMR-32 cells
Lane 3	HepG2 cells

Figure 3.9 The human neuroblastoma cell line, IMR-32, expresses PPARα. PPARα expression was analysed by RT-PCR using cDNA made from total cellular RNA and PPARα-specific primers. A liver cell line, HepG2, was used as a positive control. cDNA levels were normalised by RT-PCR using cyclophilin primers as a control.

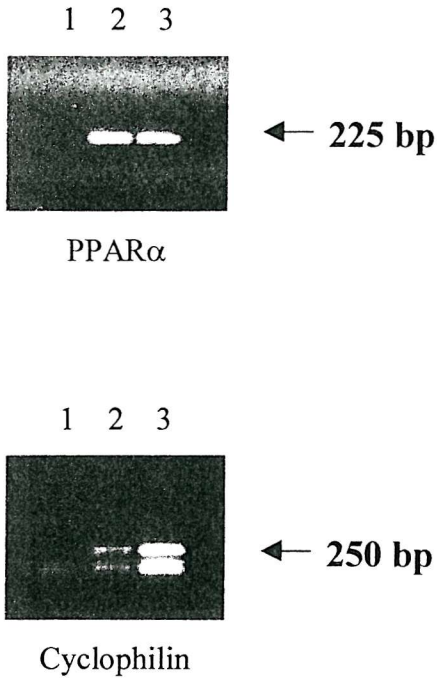

Lane 1	Negative control
Lane 2	Kelly cells
Lane 3	HepG2 cells

Figure 3.10 The human neuroblastoma cell line, Kelly, expresses peroxisome proliferator-activated receptor α. PPARα expression was analysed using cDNA made from total cellular RNA and RT-PCR analysis using PPARα-specific primers. A liver cell line, HepG2, was used as a positive control. cDNA levels were normalised by RT-PCR using cyclophilin primers as a control.

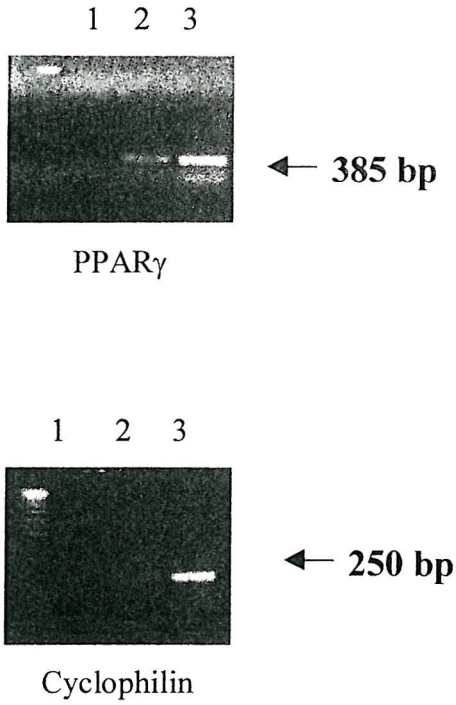

Lane 1	Negative control
Lane 2	IMR-32 cells
Lane 3	3T3-L1 cells

Figure 3.11 The human neuroblastoma cell line, IMR-32, expresses peroxisome proliferator-activated receptor γ. PPARγ expression was analysed by RT-PCR using cDNA made from total cellular RNA and PPARγ-specific primers. An adipocyte cell line, 3T3-L1, was used as a positive control. cDNA levels were normalised by RT-PCR using cyclophilin primers as a control.

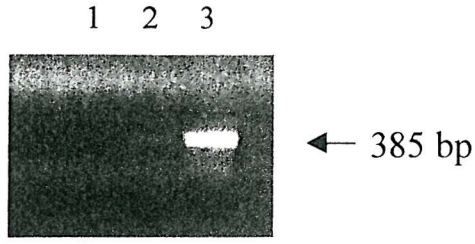

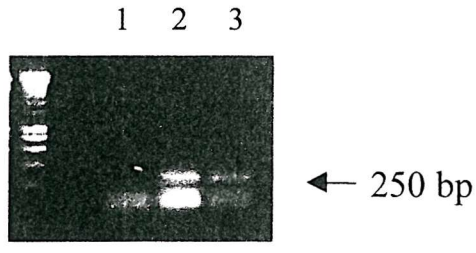

Lane 1	Negative control
Lane 2	Kelly cells
Lane 3	3T3-L1 cells

Figure 3.12 The human neuroblastoma cell line, Kelly, expresses peroxisome proliferator-activated receptor γ. PPARγ expression was analysed using RT-PCR with PPARγ-specific primers and an adipocyte cell line, 3T3-L1, was used as a positive control. cDNA levels were normalised by RT-PCR using cyclophilin primers as a control.

Expression of PPARα was confirmed by using a liver cell line, human HepG2, as a control and PPARγ expression was confirmed using 3T3-L1 adipocyte control, which have previously been shown to express high levels of PPARγ [110, 204]. Both PCR products were cut using unique restriction sites within their sequences (data not shown). IMR-32 cells and Kelly cells expressed high levels of PPARα equivalent to that of the liver cell line and both cell lines expressed PPARγ. The housekeeping gene, cyclophilin, was used as a control for levels of cDNA (Figures 3.9 - 3.12).

3.2.5 *PUFAs activate PPARs and PPAR-induced transcription in IMR-32 cells*

To investigate whether PUFAs could activate PPAR-induced transcription in neuroblastoma cells, IMR-32 cells were transiently transfected with a CAT reporter construct containing three consensus PPREs cloned upstream of a TK promoter (3PPRE-TK-CAT) [233]. The transfected cells were treated with 30 μM fatty acids and CAT activity measured [403]. 30 μM AA, DHA, γ-LA and OA were able to activate PPAR-induced transcription in IMR-32 cells measured as an increase in reporter gene activity above that of controls-treated cells. Control-treated cells were transfected with PPRE-TK-CAT and supplemented with HBSS and CAT activity in these cells was set at 100 %. All transfections were normalised by co-transfection of pCMV-β galactosidase. AA induced the greatest amount of reporter gene activity with an increase in nearly nine-fold compared to controls, whilst OA increased transcription rates by seven-fold (Figure 3.13). DHA only induced transcription rates to around half the amount of transcription induced by AA and γ-LA barely increased levels of PPAR-induced transcription above those of controls (Figure 3.13). None of the PUFAs increased CAT activity when a reporter construct, which lacks the triple PPRE sequence, pBL_2CAT, was transfected into the cells and the cells subsequently treated (Figure 3.14). This shows that AA was most effective at activating PPARs than PUFAs in the n-3 and n-9 series.

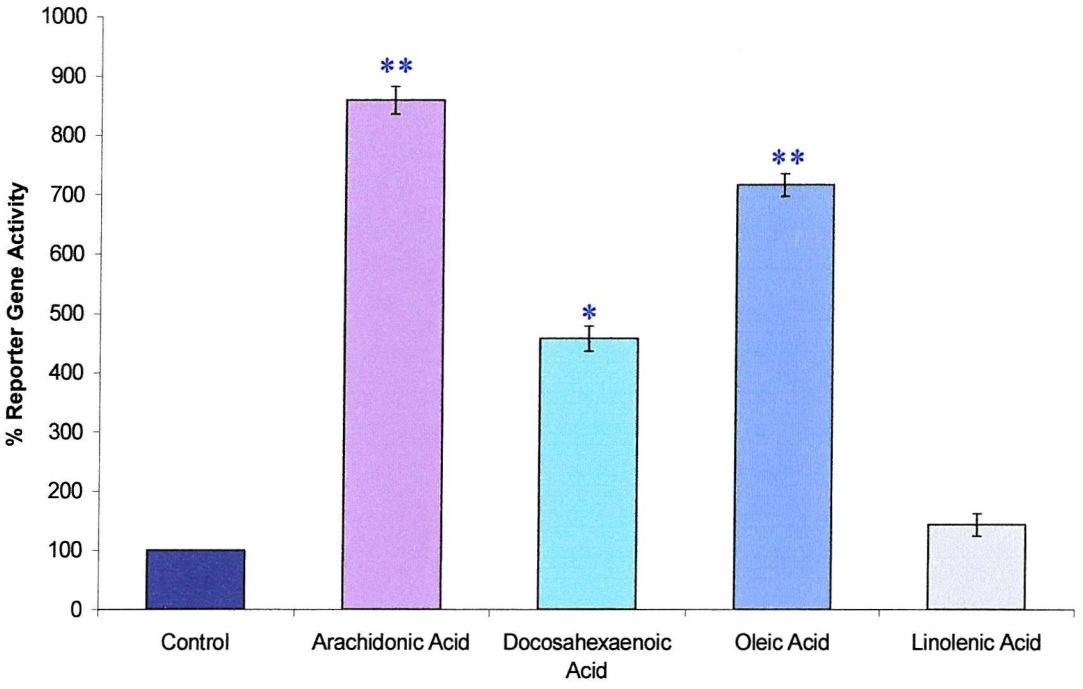

Figure 3.13 PUFAs activate PPAR-induced transcription in IMR-32 cells. IMR-32 cells were transfected with 5 μg 3PPRE-TK-CAT for 6 hours and the culture medium was supplemented with 30 μM arachidonic acid (AA), docosahexaenoic acid (DHA), oleic acid (OA) or γ-linolenic acid (γLA). Reporter gene activity in HBSS-treated cells (controls) was taken as 100 % to normalise the level of CAT activity seen and CAT activity in treated cells was measured by a CAT assay and compared to this level. Statistics were calculated using a t test and significance represented as follows - $p<0.05$ (*), $p<0.01$ (**).

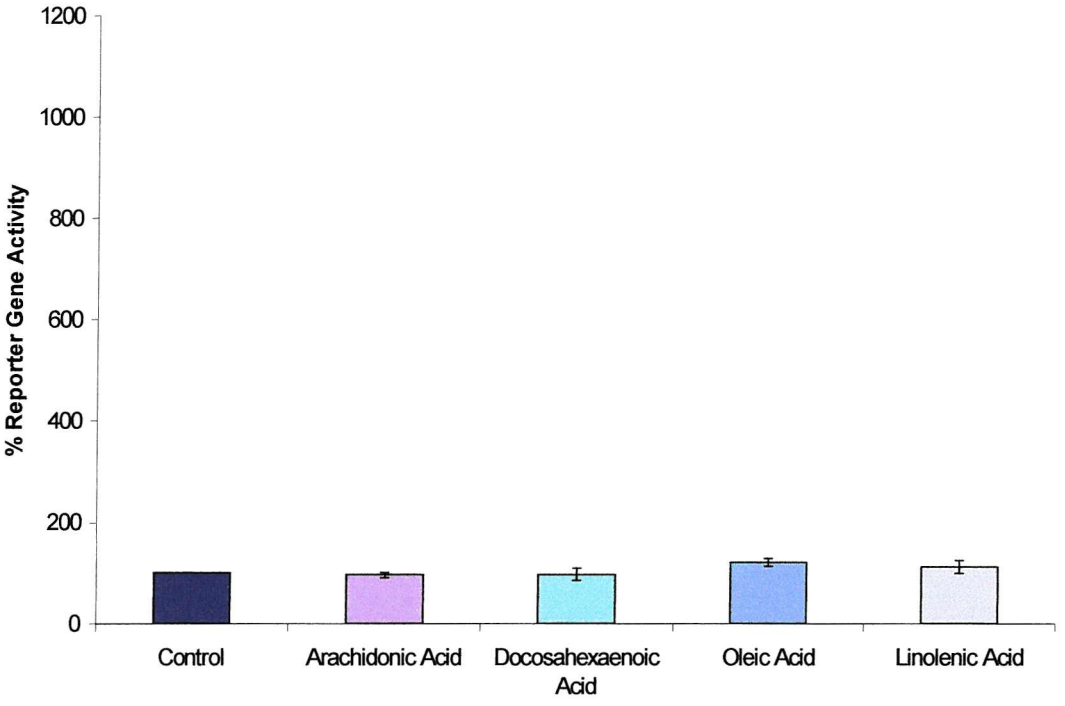

Figure 3.14 PUFAs do not activate transcription from control vectors lacking PPREs. Cells were transfected with 5 μg pBL_2CAT for 6 hours and the culture medium was supplemented with 30 μM arachidonic acid (AA), docosahexaenoic acid (DHA), oleic acid (OA) or γ-linolenic acid (γLA). Activation seen in HBSS-treated cells (controls) was taken as 100 % to normalise the level of CAT activity seen and CAT activity in treated cells was measured by a CAT assay and compared to this level.

3.3 *Discussion*

PUFAs have been shown to inhibit the growth of many types of cancer cell types, by mechanisms including growth inhibition and apoptosis. Arachidonic acid (AA) has also been shown to induce terminal differentiation in HL-60 cells with concurrent down-regulation of cMYC [412], whilst γ-linolenic acid (γ-LA) is able to morphologically differentiate human oesophageal carcinoma cell lines [413]. Cells of the neuroblastoma cell line, IMR-32, were treated with PUFAs, including AA, DHA, OA and γ-LA to determine the effects of these fatty acids on cell growth. AA, and γ-LA were able to marginally inhibit the growth of neuroblastoma cells (Figures 3.1a and 3.2), agreeing with data showing that AA and γ-LA are able to inhibit the growth of other cancer cell lines [412, 413]. However, AA was less effective after 96 hours treatment (Figure 3.1a) and γ-LA was more effective at 75 μM, than at 30 μM (Figure 3.2). DHA was the most effective at inhibiting IMR-32 cell growth (Figure 3.1b) and has also been shown to effectively inhibit the growth of malignant melanoma cell lines [414]. Oleic acid has no effect on the growth of IMR-32 cells (Figure 3.1c), however it has been shown to inhibit the growth of lung metastatic nodules [177]. Therefore, different cancer cell types may respond differently to different types of fatty acids.

As well as inhibiting the growth of cancer cells, PUFAs can induce cancer cells to undergo apoptosis. DHA is a potent inducer of apoptosis in HT-29 colon cancer cells [406] and Jurkat cells, where it is thought to induce apoptosis through a pathway involving protein phosphatases, PP1 and PP2B [407]. However DHA did not induce death of IMR-32 cells (Figure 3.4). In Jurkat cells, similar concentrations of AA and OA were used to that of the DHA (60 μM and 90 μM) and had no effects [407], suggesting that it is not just the concentrations of PUFAs that are important in inducing cellular response, but also the type of PUFA. For example, 50 μM γ-LA and 100 μM AA have both been shown to induce apoptosis in a chronic myeloid leukaemia cell line with no effect on non-transformed cells [409]. These concentrations of PUFAs are greater than physiological concentrations, which are thought to be around 30 μM [166], as the concentration of total non-esterified fatty acids in human serum is 1 mM and the most prevalent fatty acids account for

approximately 30 % of this [410]. None of the PUFAs induced death of IMR-32 cells, with levels of cell death equivalent to that of controls within 120 hours (Figures 3.4 and 3.5). The effects of AA, DHA, OA and γ-LA seen in IMR-32 cells were achieved at lower concentrations (30 μM) than those used in the Jurkat and leukaemia cell experiments, however, even at 75 μM, γ-LA did not induce death of IMR-32 cells (Figure 3.5). 75 μM γ-LA was also used as it has been shown to activate PPARγ and induce translocation of PPARγ to the nucleus in breast cancer cells at this concentration [224]. However, it is not known whether 75 μM γ-LA activates PPAR-induced transcription or alters membrane phospholipids to a greater extent than 30 μM γ-LA. This suggests that although these PUFAs have the capability to induce apoptosis in certain cancer cells, in IMR-32 cells they only slowed cell growth or induced a low level of cell cycle arrest, but did not induce cell death. However, concentrations above that of 75 μM were not used, and these levels of PUFAs may cause apoptosis in IMR-32 cells.

Membrane fluidity of tumour cells is different to that of normal cells and the ability of cancer cells to metastasise is related to the degree of membrane fluidity. Neural tumour cells, leukaemia and lymphoma cells all have increased membrane fluidity compared to the equivalent normal cells, however, hepatoma cell membrane fluidity decreases compared to that of normal liver cells [415]. PUFA-treatment of cancer cells also induces a change in their membrane phospholipid composition. Rose *et al.*, fed nude mice, which had breast cancer cells implanted into their thoracic cavity, on diets containing high levels of DHA and observed that not only did their tumour cells grow slower, but that the occurrence and severity of metastases was reduced [176]. This was proposed to be due to the increases in proportion of DHA in the tumour phospholipids and a decrease in arachidonic acid concentrations [176]. DHA and OA have been shown to exert an anti-metastatic effect due to changes in the PUFA-component of the cells in the highly metastatic colon carcinoma 26 model [177]. This suggests that the growth inhibitory effects of polyunsaturated fatty acids may be due to their influence on membrane phospholipids.

30 μM AA and DHA treatment altered the membrane phospholipid composition of IMR-32 cells after 72 hours (Figures 3.8 - 3.10). Addition of AA resulted in an increase in arachidonoyl-containing PtdCho species (Figure 3.8), which would increase the fluidity of the cell membrane if it occurred alone, however, the concurrent increase in disaturated PtdCho species would compensate for this increase, by reducing the membrane fluidity back to normal. A similar effect was seen with DHA treatment, in that an increase in DHA-containing PtdCho species, resulted in a compensatory increase in disaturated PtdCho species (Figure 3.8). An increase in AA and DHA-containing phospholipid species, on treatment with the respective PUFAs, were also seen in mouse models of breast cancer [176] and colon cancer [177].

Similarly to PtdCho species, AA induced an increase in AA-containing PtdEtn species and DHA supplementation induced an increase in DHA-containing PtdEtn species (Figure 3.9). However, unlike with the PtdCho species, AA treatment suppressed the DHA-containing PtdEtn species and DHA suppressed the AA-containing PtdEtn species within the cell membrane (Figure 3.9). This effect was also seen in mouse models of breast cancer [176] and colon cancer [177] and it is suggested that an increase in DHA-containing membrane phospholipid species reduces the metastatic capability of tumour cells [177] and the size of tumours [176]. Interestingly, DHA treatment, which increased DHA-containing species in IMR-32 cell membranes was the most effective PUFA at inhibiting IMR-32 cell growth, although AA, which suppressed DHA-containing species, marginally inhibited IMR-32 cell growth at 24 to 48 hours post-initial treatment.

Fewer changes were seen in the acid phospholipid membrane fraction of IMR-32 cells treated with 30 μM AA and DHA, than with the PtdCho and PtdEtn fraction (Figure 3.10). This may be because phosphatidylinositol, especially stearoyl-arachidonoyl PtdIns (18:0/20:4) is involved in cell signalling and the cell manages to maintain the same levels of PtdIns species, as much as possible. DHA was unable to suppress AA-containing acid phospholipid species, however, AA seemed to suppress DHA-containing acid phospholipid species, which are not as prevalent in the cell membranes initially (Figure 3.10). PUFAs dramatically altered the

membrane phospholipid composition of IMR-32 cells, but not the PtdIns component. Therefore, some of the effects of PUFAs on IMR-32 cells may be due to these changes rather than activation of PPARs and decoy oligonucleotides could be used to prove whether PPARs are involved or not.

The marginal effects of fatty acids on IMR-32 cell growth may have been due to changes in the membrane phospholipids or low level activation of PPARs. To determine whether neuroblastoma cells express PPARs, total RNA was made from IMR-32 and Kelly cells and reversed transcribed to cDNA. The cDNA was amplified by RT-PCR reactions using PPARα or PPARγ-specific primers and primers for the housekeeping gene, cyclophilin, were used to control for cDNA amounts. In both IMR-32 cells and Kelly cells, PPARα was expressed at levels equivalent to that of the human liver cells line HepG2 (Figures 3.11 and 3.12). Han *et al.*, showed that the Lan-5 neuroblastoma cell line expresses PPARβ and PPARγ, but does not express the α isoform of PPAR [342].

The γ isoform of PPAR was also expressed in both IMR-32 cells and Kelly cells (Figures 3.13 and 3.14). This agrees with published data suggesting that malignant cells do express PPARγ. PPARγ is expressed in both human neuroblastoma cell lines and primary cells and its expression correlates with the degree of differentiation of the neuroblastoma cells. Poorly differentiated neuroblastomas, representing later stage disease express lower levels of PPARγ [342]. Several groups have shown that prostate cancer cell lines express different levels of PPARγ, which may reflect different disease stages of the tumour cells from which the cell lines were derived, and that levels of expression were lower than those of freshly isolated prostate cancer cells [130].

To determine whether the effects of fatty acids on IMR-32 cells were due to an increase in PPAR-mediated transcription, IMR-32 cells were transfected with a CAT reporter gene from a construct containing 3 consensus PPAR binding sites (PPREs) upstream of a thymidine kinase promoter [175], treated and CAT activity measured [233]. CAT activity increased when PPARs were activated by PUFAs within the IMR-32 cells (Figure 3.15) and several groups have shown that PUFAs

activate PPARs [172, 175]. Keller *et al.*, showed that PUFAs activated a reporter construct containing three consensus PPREs around ten-fold, whereas monounsaturated and saturated fatty acids were less potent activators of PPARs [172]. Arachidonic acid has been shown to activate PPAR-induced transcription, but to a lesser extent than some of its metabolites [167, 168]. Oleic acid has also been shown to be a weak activator of PPARs using competition assays with a radiolabelled high affinity ligand for both PPARα and PPARγ, GW2331 [166]. The PPRE used in these experiments did not distinguish between the different isoforms, as all three isoforms bind to the same sequences. However, differences in activation of PPARs can be observed using expression vectors for the three isoforms co-transfected with reporter plasmids [166]. In IMR-32 cells, AA and OA showed the greatest effect on PPAR activity followed by DHA and γ-LA had the least effect (Figure 3.15). This suggests that some of the effects of the PUFAs may be mediated through activation of PPARs and the resulting transcription of PPAR target genes. The differences in levels of activation of PPARs may be related to the hydrocarbon chain shape and stearic interactions, as oleic acid is a "bent" molecule and may not be able to make strong hydrophobic interactions with PPAR ligand binding domains that are required for stable ligand binding [157]. However, PUFAs such as AA, which is more a "hairpin" structure may be able to make these connections and may activate PPARs more effectively [157]. 30 μM of the PUFAs, AA, DHA, γ-LA, and OA were sufficient to activate PPAR-induced transcription, so should be sufficient to induce any PPAR-induced effects on the cells. However Maehle *et al.*, [408] have shown that very different concentrations of fatty acid are required to achieve the same growth inhibitory effects in similar epithelial tumour cell lines and therefore different cancer cell types may also require different concentrations of fatty acids to achieve the same effects.

Therefore, in conclusion PUFAs only had a marginal effect on the growth of IMR-32 cells and this effect is more likely to be mediated through the changes to the membrane phospholipids than through activation of PPARs. This is because DHA had the greatest effect on membrane phospholipid composition, activated PPARs to a lesser extent than most of the other PUFAs used, but had the greatest affect on cell growth. Likewise, OA activated PPARs more than DHA, but had no effect on

IMR-32 cell growth and also AA activated PPAR-induced transcription to a greater extant than DHA, but had less of a growth-inhibitory effect and was only slightly more effective than OA at activating PPARs, but had more effect on cell growth. Therefore activation of PPARs with 30 μM PUFAs did not correlate with the cellular effects of the PUFAs. In contrast, fatty acid supplementation altered the membrane composition of IMR-32 cells considerably and therefore a large proportion of the fatty acids may be integrated into the membrane, rather than activating PPARs and inhibiting cell growth. Indeed DHA suppressed the amount of arachidonyl-containing phospholipid species in IMR-32 cells, and suppression of AA-containing, but not DHA-containing, species was involved in the inhibition of colon cancer cell growth [177]. Therefore, considerable changes to the membrane phospholipids are required to have a marginal effect on cell growth. Interestingly, PUFAs activate PPARα and PPARγ and the activity seen in the reporter assay could have been mainly due to activation of the α isoform, which has not be shown to be involved in the growth inhibition of cancer cells. Therefore, other more potent and specific activators of the γ isoform of PPARs, such as J_2 prostaglandins, may be more suited to inhibiting the growth of neuroblastoma cell lines and will be fully investigated in the following chapters.

UNIVERSITY OF SOUTHAMPTON LIBRARY

Chapter 4

The Effects of PPAR Ligands on Neuroblastoma Cells *In Vitro*

4.1 *Introduction*

Fatty acids only marginally inhibited the growth of IMR-32 cells and this effect was not due to activation of PPARs, but was more likely due to changes in the membrane phospholipid composition. There is debate in the literature as to whether fatty acids are ligands of PPARγ, or whether fatty acid metabolites are actually true PPARγ ligands. Therefore the effectiveness of another reportedly high affinity ligand of PPARγ, a J_2 prostaglandin, 15-deoxy$\Delta^{12,14}$-prostglandin J_2 ($15dPGJ_2$), was assessed as an inhibitor of neuroblastoma cell growth. The three isoforms of PPARs, α, β/δ and γ have specific patterns of tissue expression and function [129]. PPARα is involved in the development of cancers in rodents [112], but has not been associated with the development of cancers in humans [309]. PPARβ is frequently over-expressed in many colorectal cancers [314] and genetic disruption of the PPARβ gene reduces the tumourigenicity of human colon cancer cells [313].

A number of groups have demonstrated that activation of PPARγ by its ligands results in the inhibition of cell growth in many other cancer cell types. This growth inhibition can occur through mechanisms including differentiation [207, 342], apoptosis [340, 341, 347] and, more recently shown, autophagy or type II programmed cell death [346]. However, activation of PPARγ has been shown to both inhibit [350, 351] and promote [182, 349] the development of colon cancer in mouse models. $15dPGJ_2$ has also been linked to the proliferation of a human colorectal cancer cell line, but this may occur through PPARγ-dependent or -independent mechanisms [188]. The inhibition of cancer cell growth through activation of PPARγ has been achieved by using $15dPGJ_2$ [167, 168], phenylacetate [207] or the thiazolidinedione (TZD) class of anti-diabetic drugs [130, 243]. It is therefore proposed that PPARγ ligands could have potential as a therapy for treating cancers. Ligands of PPARα, including the fibrate drug, Wy-14643, are suitable controls, as activation of PPARα has not been implicated in the development of human cancer [309]. $15dPGJ_2$ is a metabolite of arachidonic acid and exists naturally within cells [187, 189]. It would therefore be a suitable treatment for cancer as it is non-toxic.

4.2.1 *The PPARγ ligand, 15-deoxy$\Delta^{12,14}$-prostglandin J_2 inhibits the growth of IMR-32 cells*

To test whether ligands of PPARs are more effective inhibitors of neuroblastoma cell growth than PUFAs, IMR-32 cells were seeded at 2 x 10^4 cells and treated with increasing concentrations of PPAR ligands for 72 hours and the effect on cell growth was determined. The ligands used were Wy-14643, which potently activates PPARα, and 15dPGJ$_2$, the natural ligand of PPARγ. Increasing concentrations of Wy-14643 did not inhibit IMR-32 cell growth up to 25 μM, but at concentrations of 50 μM and above there was a small decrease in cell number, which could reflect some toxicity of Wy-14643 in susceptible cells (Figure 4.1). However, even at high concentrations (50-100 μM), Wy-14643 was not effective at inhibiting neuroblastoma cell growth. In complete contrast, the growth of IMR-32 cells treated with more than 1 μM 15dPGJ$_2$ was inhibited by 72 hours, compared to controls (Figure 4.1). Increasing concentrations of 15dPGJ$_2$ above that of 1 μM inhibited cell growth with increasing effectiveness, so that at concentrations above 7.5 μM, no viable IMR-32 cells were observed at 72 hours post-initial treatment (Figure 4.1).

The effect of a constant concentration of 15dPGJ$_2$ over time was also measured. The concentration of 15dPGJ$_2$ chosen was 5 μM, as the EC_{50} is 2 μM and most published experiments used concentrations between 2.5 μM and 10 μM 15dPGJ$_2$. 15dPGJ$_2$ inhibited the growth of IMR-32 cells from 24 hours post-initial treatment (Figure 4.2). The effect was marked from 72 hours onwards, with numbers of 15dPGJ$_2$-treated cells increasing from 2 x 10^4 cells to 4 x 10^4 cells and control cells increasing in number to 2 x 10^5 (Figure 4.2). To determine whether the effect of 15dPGJ$_2$ was unique to IMR-32 cells, the effect on another NMYC amplified neuroblastoma cell line, Kelly was determined. Both cell lines tested were representative of neuroblastoma with poor prognosis, which is the type of neuroblastoma that requires an effective treatment. As seen with IMR-32 cells, the growth of Kelly cells treated with 5 μM 15dPGJ$_2$ was inhibited and yet control-treated Kelly cells grew almost ten-fold (Figure 4.3).

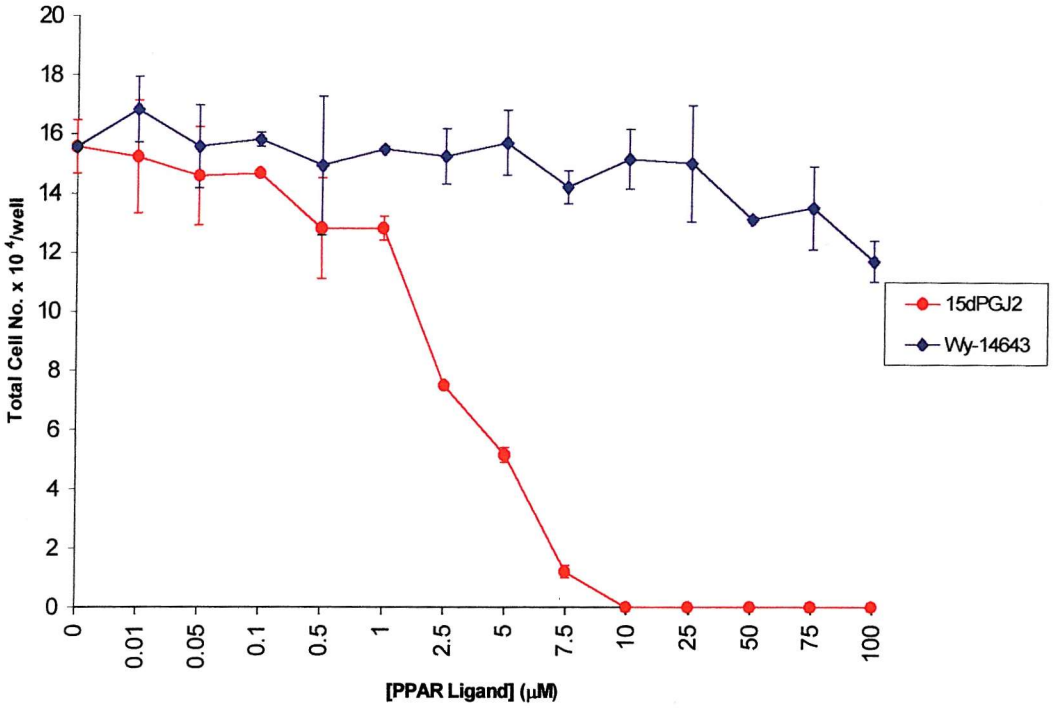

Figure 4.1 Dose response of IMR-32 cells to the PPARα ligand, Wy-14643 and PPARγ ligand, 15-deoxy$\Delta^{12,14}$-prostglandin J_2. IMR-32 cells were plated out at 2 x 10^4 cells and their response to increasing concentrations of the PPARα ligand, Wy-14643 and the PPARγ ligand, 15-deoxy$\Delta^{12,14}$-prostglandin J_2 were measured after 72 hours treatment. Two samples were measured per concentration of treatment and the experiments were completed in duplicate and the error bars represent s.e.m.

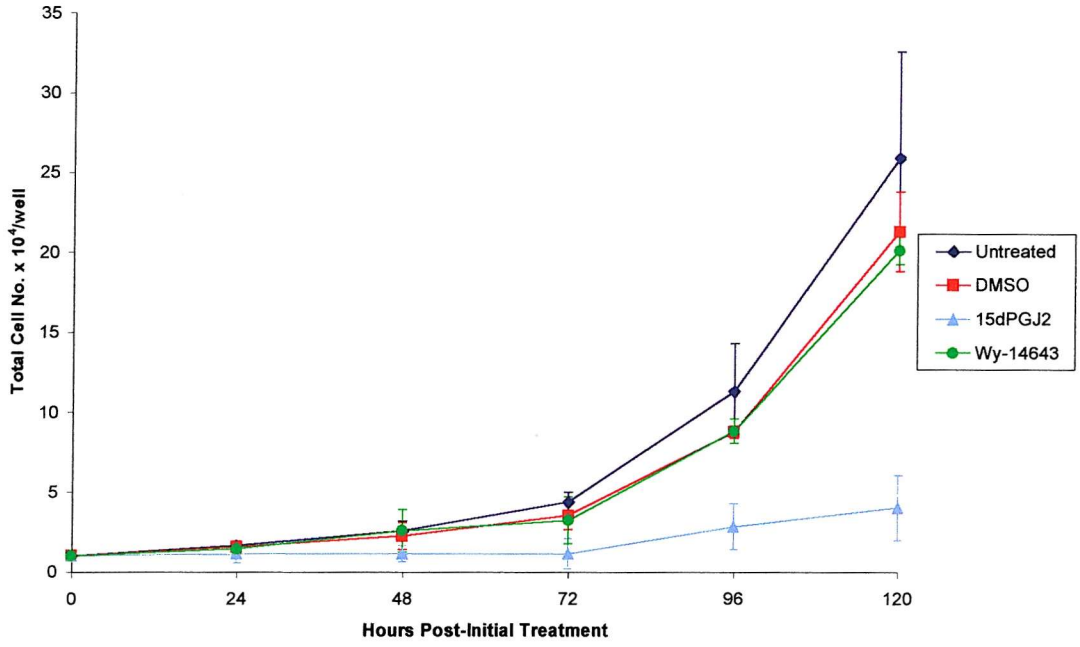

Figure 4.2 Ligands of PPARγ, but not PPARα inhibit the growth of IMR-32 cells. To determine whether ligands of PPARs inhibited the growth of IMR-32 cells, the cells were plated out at 2 x 10^4 cells, treated with 5 μM of each ligand and the effects on cell growth measured over 120 hours. Two samples were counted per treatment per day and experiments were completed in duplicate. Statistics were calculated using an ANOVA, which showed that $15dPGJ_2$ significantly inhibited cell growth compared to DMSO controls at a significance of $p<0.01$.

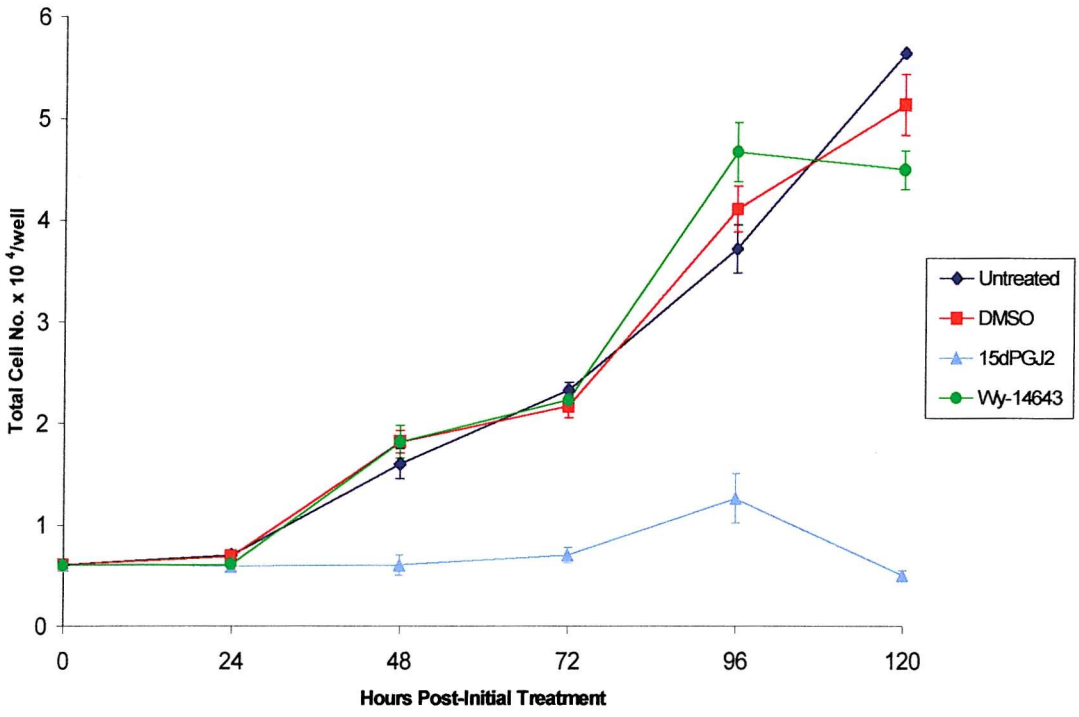

Figure 4.3 Ligands of PPARγ, but not PPARα inhibit the growth of Kelly cells. Kelly cells were plated out at 2 x 10^4 cells treated with 5 μM $15dPGJ_2$ or 5 μM Wy-14643 and the effects on cell growth measured over 120 hours. Two samples were counted per treatment per day and experiments were performed in duplicate and error bars represent standard errors. Statistics were calculated using an ANOVA, which showed that $15dPGJ_2$ significantly inhibited cell growth compared to DMSO controls at a significance of $p<0.05$.

This effect on cell growth was restricted to the ligand of PPARγ as the PPARα ligand, Wy-14643, did not inhibit the growth of Kelly cells either (Figure 4.3). This shows that a ligand of PPARγ, $15dPGJ_2$, but not a potent activator of PPARα, was able to inhibit neuroblastoma cell growth *in vitro*.

4.2.2 *15-deoxy$\Delta^{12,14}$-prostglandin J_2 induces cell cycle arrest in IMR-32 cells and Kelly cells*

The growth inhibition induced in neuroblastoma cells in response to $15dPGJ_2$ may have involved cell cycle arrest and therefore the cell cycle profiles of the treated cells were analysed by flow cytometry. The neuroblastoma cells were treated with DMSO, 5 μM $15dPGJ_2$ or 5 μM Wy-14643 and were then stained with propidium iodide. Live cells were selected, and dead cells and degraded DNA were discounted using markers. The cells were analysed at a wavelength of 258 nm and the number of cells with the correct fluorescence were counted. No changes in the cell cycle distribution were seen with IMR-32 cells treated with $15dPGJ_2$ at 24 hours (Figure 4.4). However, at 72 hours, there were significantly fewer cells in the G_1/G_0 stage of the cell cycle and a significant increase in cells in the G_2/M phase of the cell cycle (Figures 4.5 and 4.6). The number of cells in G_1/G_0 was reduced compared to controls and treatment with Wy-14643 (Figure 4.6). This suggests that in IMR-32 cells, $15dPGJ_2$ induced cell cycle arrest at G_2/M between 24 and 72 hours. However, in Kelly cells, the only significant change in the cell cycle distribution of the cells was an increase in cells in G_1/G_0 after 72 hours (Figures 4.7 and 4.8), suggesting that growth inhibition of Kelly cells might actually occur through a different mechanism to that seen in IMR-32 cells.

4.2.3 *15-deoxy$\Delta^{12,14}$-prostglandin J_2 induces morphological changes in IMR-32 cells*

Differentiating neuroblastoma cells extend their neurites, form connections with other cells and exit the cell cycle [416], and PC12 cells treated with $15dPGJ_2$ extend their neurites [24]. To establish whether 5 μM $15dPGJ_2$ induced any morphological changes, such as neurite output, treated cells were observed by light microscopy.

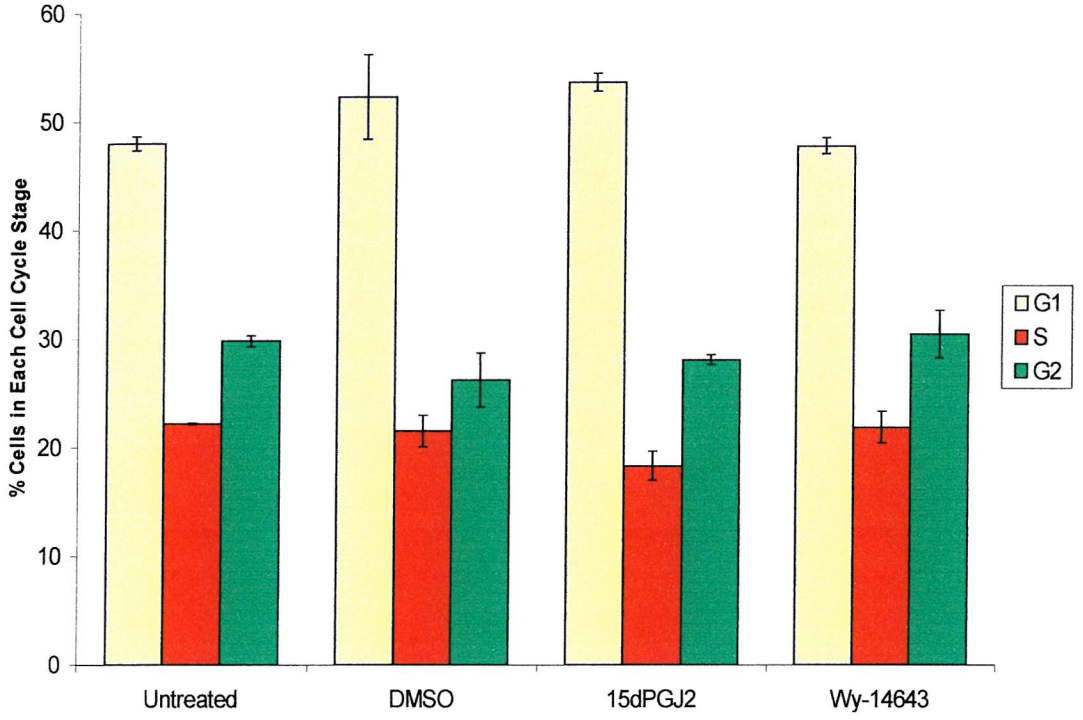

Figure 4.4 Ligands of PPARα and PPARγ do not affect the IMR-32 cell cycle after 24 hours. IMR-32 cells were treated with 5 μM Wy-14643 or 5 μM 15-deoxy$\Delta^{12,14}$-prostglandin J_2 for 24 hours and the cells were stained with propidium iodide. The cells were analysed by flow cytometry and dead cells and degraded DNA were excluded. Graph represents duplicate experiments and errors are standard errors of the mean.

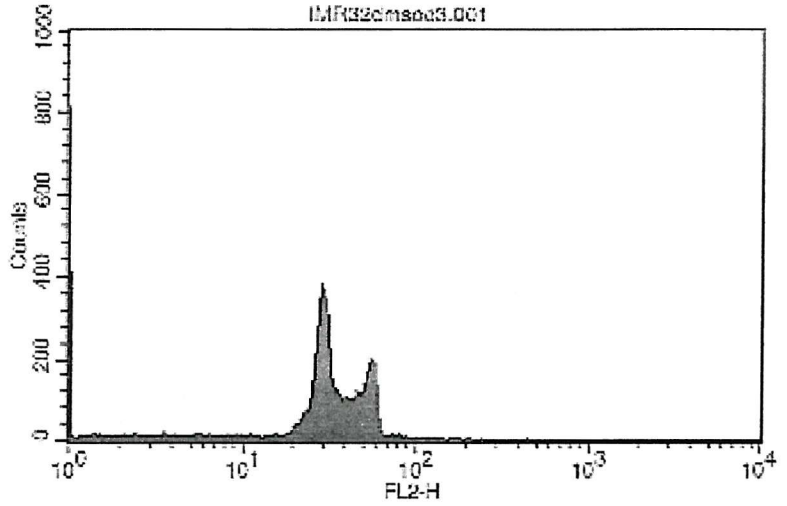

Dimethyl sulphoxide

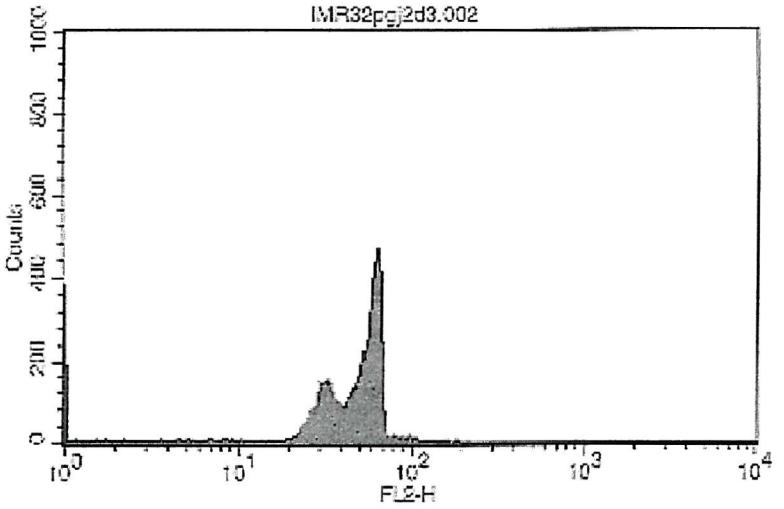

15-deoxy$\Delta^{12,14}$-prostglandin J_2

Figure 4.5 Flow cytometry scan showing 15dPGJ$_2$ arrests IMR-32 cells at G$_2$/M of the cell cycle after 72 hours treatment. IMR-32 cells were treated with DMSO or 5 μM 15-deoxy$\Delta^{12,14}$-prostglandin J$_2$ (15dPGJ$_2$) for 72 hours. The cells were stained with propidium iodide and analysed by flow cytometry. The scans are representative of the effects of 15dPGJ$_2$.

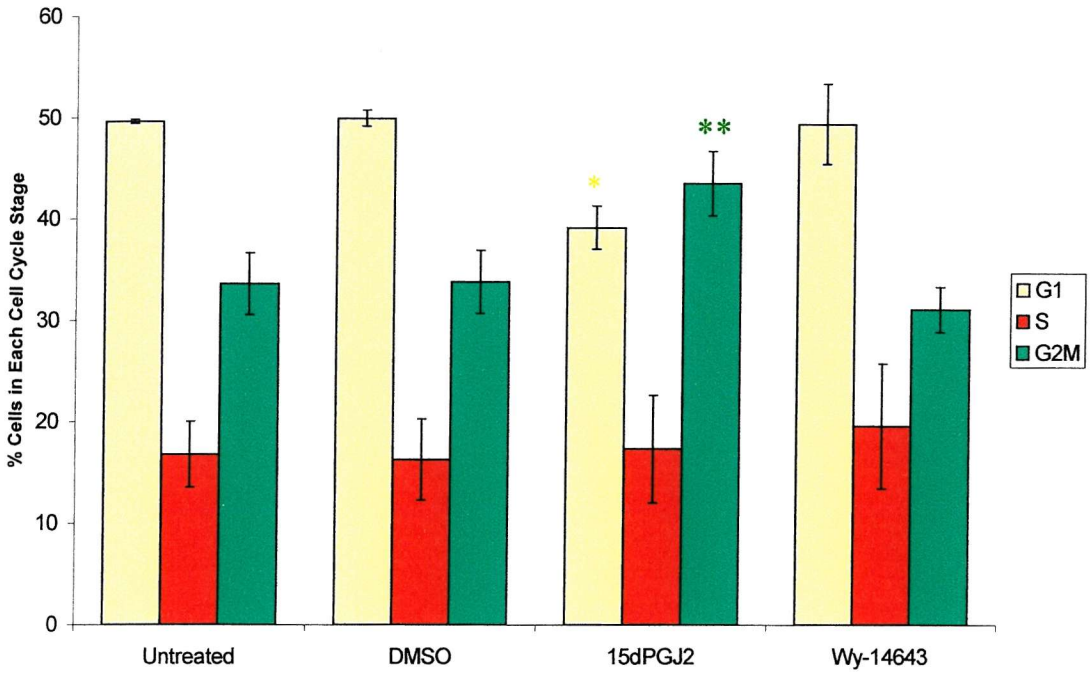

Figure 4.6 15dPGJ$_2$ arrests IMR-32 cells at G$_2$/M of the cell cycle after 72 hours treatment. IMR-32 cells were treated with 5 μM Wy-14643 or 5 μM 15-deoxy$\Delta^{12,14}$-prostglandin J$_2$ for 72 hours and the cells were labelled with propidium iodide. The cell cycle was analysed by flow cytometry and the graph represents duplicate experiments with one sample per experiment and the errors are standard errors of the mean. Statistics were calculated using a t test – $p<0.05$ (*) and $p<0.01$ (**).

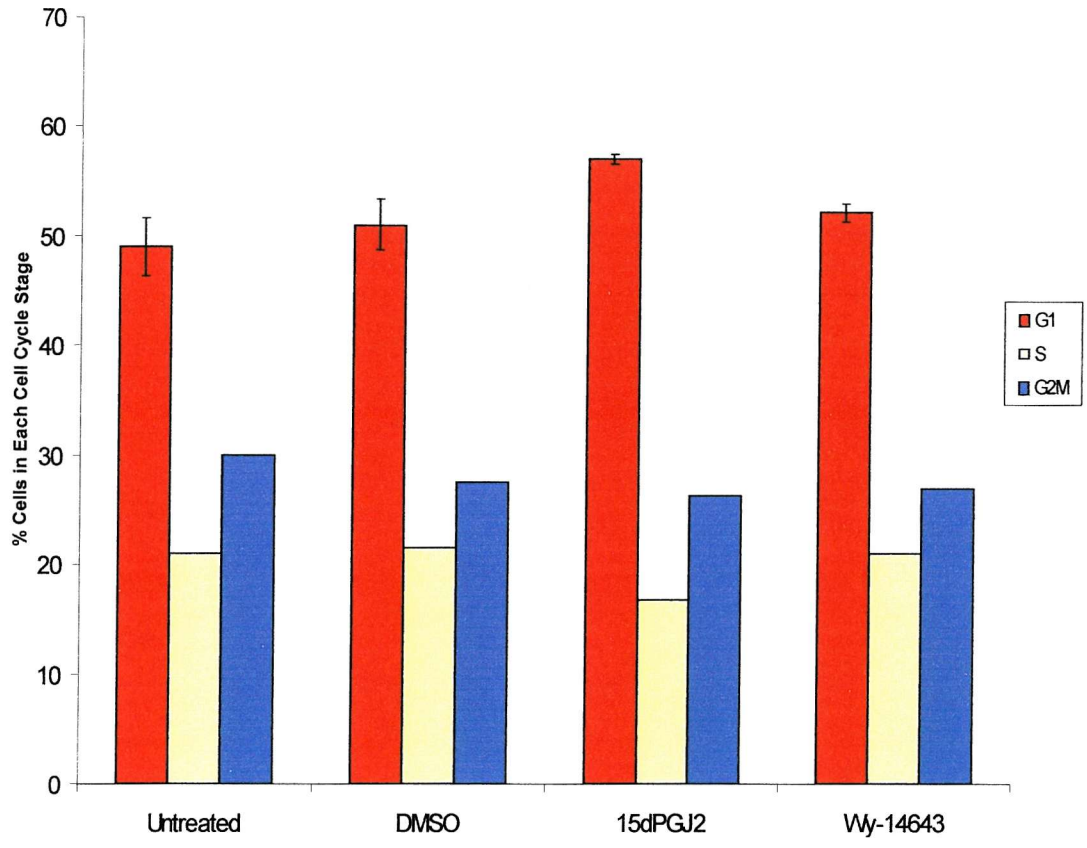

Figure 4.7 Ligands of PPARα and PPARγ do not affect Kelly cell cycle after 24 hours. Kelly cells were treated with 5 μM Wy-14643 or 5 μM 15-deoxy$\Delta^{12,14}$-prostglandin J_2. The cells were stained with propidium iodide and analysed by flow cytometry after 24 hours treatment. The graph represents duplicate experiments and the errors are s.e.m.

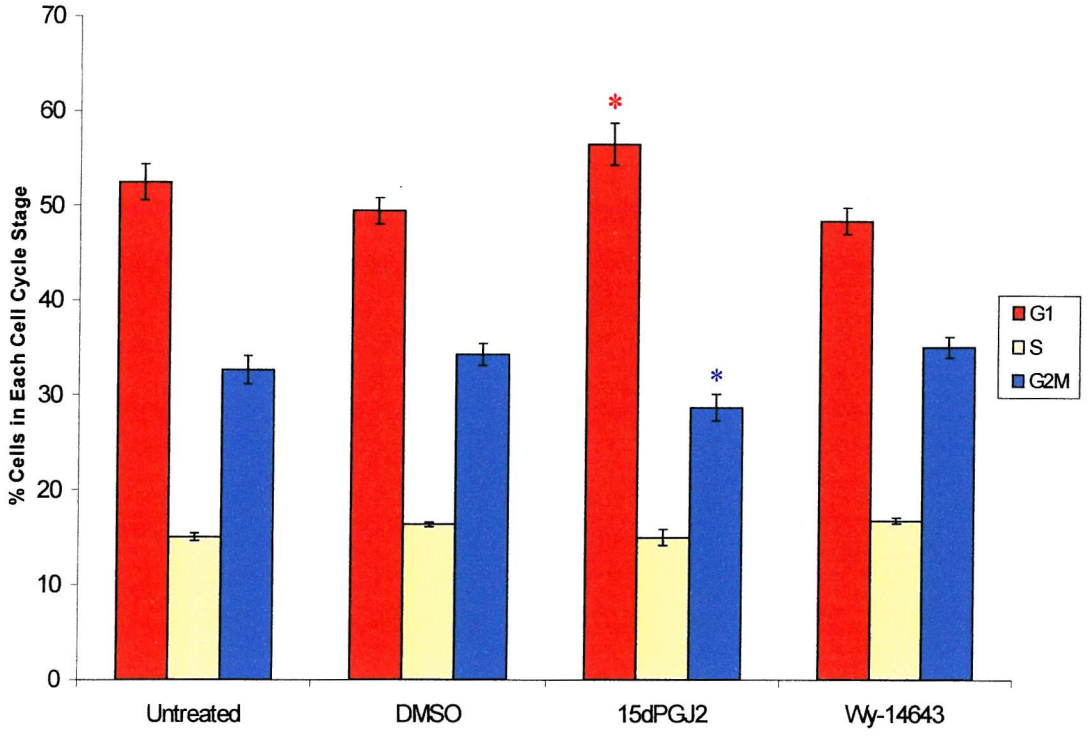

Figure 4.8 $15dPGJ_2$ has an effect on the Kelly cell cycle after 72 hours treatment, by increasing the number of cells in G_1/G_0. Kelly cells were treated with 5 μM Wy-14643 or 5 μM 15-deoxy$\Delta^{12,14}$-prostglandin J_2 ($15dPGJ_2$). The cells were stained with propidium iodide and analysed by flow cytometry after 72 hours treatment. The graph represents duplicate experiments with one sample per experiment and the error bars show the standard errors. Statistics were calculated by a t test – $p<0.05$ (*).

IMR-32 cells treated with $15dPGJ_2$ rounded up and retracted their neurites (Figure 4.9) rather than extending their neurites. The same effect was not seen in IMR-32 cells treated with Wy-14643 or in Kelly cells treated with $15dPGJ_2$ or Wy-14643 (data not shown). However, Kelly cells extended fewer, shorter neurites than IMR-32 cells and therefore, it is more difficult to determine whether the cells were retracting their neurites or not.

4.2.4 *15-deoxy$\Delta^{12,14}$-prostglandin J_2 induces a form of cell death, requiring de novo protein synthesis in IMR-32 cells*

$15dPGJ_2$ induces growth inhibition and cell cycle arrest in IMR-32 cells and a series of assays measuring cell death were employed to determine whether the arrested cells died. A general measure of cell death is the uptake of trypan blue, which penetrates into cells with compromised plasma membranes. Live cells have intact plasma membranes and should therefore exclude the dye. Neuroblastoma cells were treated with ligands of PPARα and PPARγ and the percentage of live and dead cells measured over 120 hours. Increasing numbers of IMR-32 cells treated with $15dPGJ_2$ took up trypan blue over the time course, with the greatest increase occurring between 48 and 72 hours (Figure 4.10). This suggests that treatment with $15dPGJ_2$ compromised the integrity of the plasma membrane. It also shows that the inhibition of neuroblastoma cell growth involved cell cycle arrest followed by cell death, as the greatest increases in trypan blue uptake occurred after 48 hours, whereas growth inhibition was seen within 48 hours. As expected, IMR-32 cells treated with 5 μM Wy-14643 did not stain with trypan blue at numbers greater than control cells and therefore Wy-14643 did not induce cell death (Figure 4.10). Treatment of Kelly cells with 5 μM $15dPGJ_2$ also increased the number of cells taking up the trypan blue dye (Figure 4.11), although to a lesser extent than IMR-32 cells. As expected Wy-14643 did not induce cell death in Kelly cells compared to control-treated cells over 120 hours (Figure 4.11).

Trypan blue uptake does not distinguish between protein synthesis-dependent cell death (programmed cell death) and protein synthesis-independent cell death.

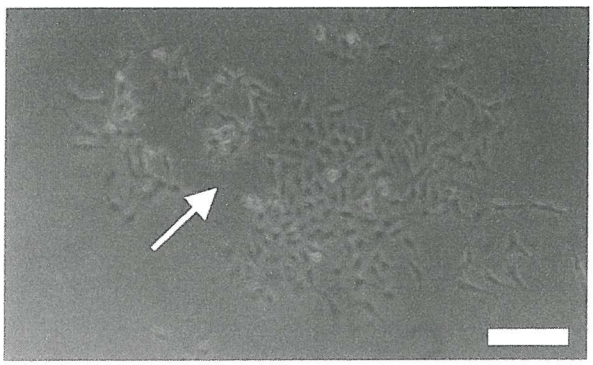

Dimethyl sulphoxide

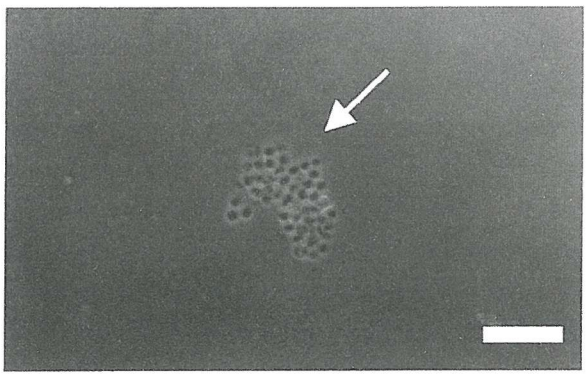

15-deoxy$\Delta^{12,14}$-prostglandin J_2

Figure 4.9 15dPGJ$_2$ induces neurite retraction in IMR-32 cells after 72 hours. IMR-32 cells were treated with DMSO or 5 μM 15dPGJ$_2$ for 72 hours and the cellular morphology was assessed using light microscopy. Scale bar represents 50 μM.

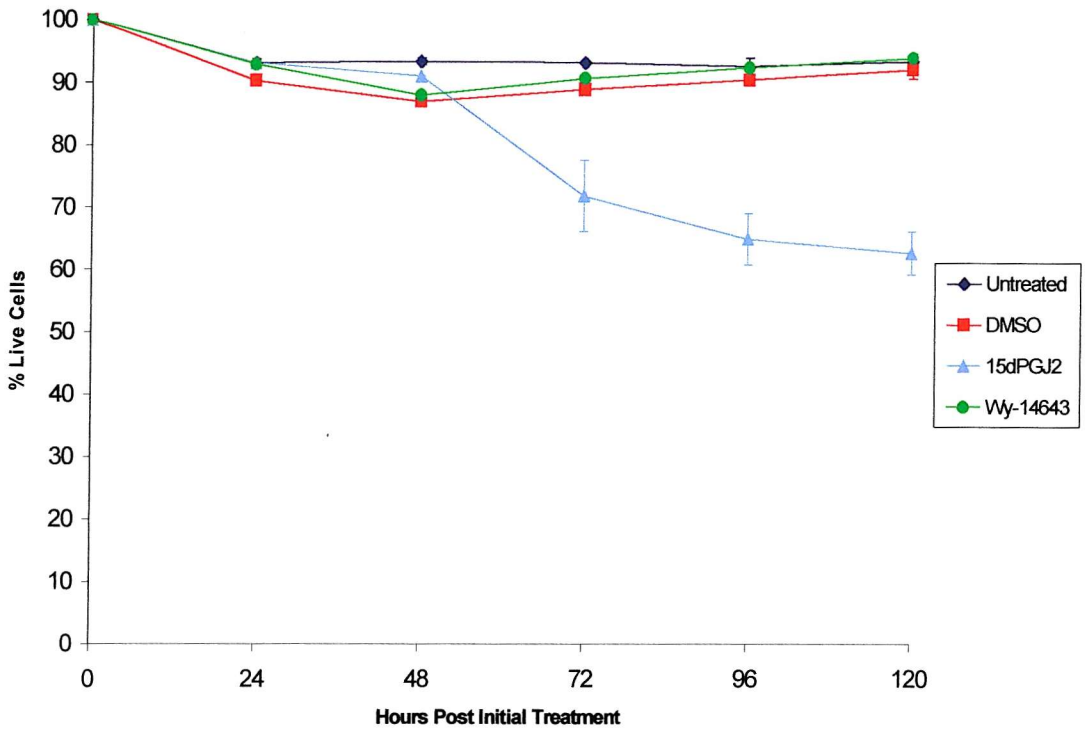

Figure 4.10 $15dPGJ_2$, but not Wy-14643 induces death of IMR-32 cells. IMR-32 cells were treated with 5 μM Wy-14643 or $15dPGJ_2$ and stained with 0.4 % trypan blue solution. The proportion of live cells was determined over 120 hours. Two samples were counted per treatment per day and the experiments were completed in duplicate and the error bars represent s.e.m. Statistics were calculated by an ANOVA, which showed that $15dPGJ_2$ significantly induced cell death compared to controls at a significance of $p<0.05$.

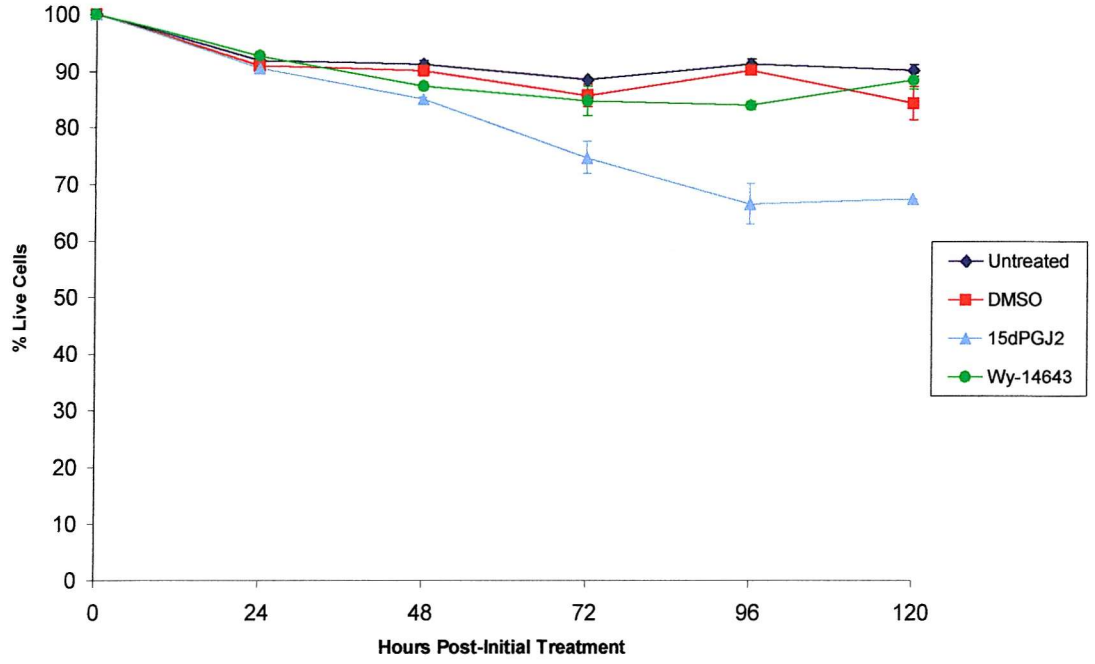

Figure 4.11 15dPGJ$_2$, but not Wy-14643 induces death of Kelly cells. Kelly cells were treated with 5 μM Wy-14643 or 15dPGJ$_2$ and stained with 0.4 % trypan blue solution. The proportion of live cells was determined over 120 hours. Two samples were counted per treatment per day and the experiments were run in duplicate and the error bars represent s.e.m. Statistics were calculated by an ANOVA, which showed that 15dPGJ$_2$ induced cell death compared to controls at a significance of $p<0.05$.

Therefore the protein synthesis inhibitor, cycloheximide, was used to determine whether the death induced by $15dPGJ_2$ in IMR-32 was protein synthesis-dependent. Cells were treated with DMSO or 5 μM $15dPGJ_2$ for 72 hours, with or without the addition of 10 μg/ml cycloheximide for 24 hours prior to counting. IMR-32 cells treated with $15dPGJ_2$ alone were stained by trypan blue at a greater rate than controls. However, when the treatment was combined with cycloheximide, the number of cells taking up the dye was decreased at all time points, but was most noticeable at 72 hours, when cell death was reduced by almost 25 % (Figure 4.12). As necrosis is not dependent on protein synthesis, this suggests that $15dPGJ_2$ did not induce necrosis in IMR-32 cells, but induced a form of cell death, which required *de novo* protein synthesis.

4.2.5 *15-deoxy$\Delta^{12,14}$-prostglandin J_2 does not induce apoptosis of IMR-32 cells or Kelly cells*

Active or programmed cell death, which requires *de novo* protein synthesis, can occur by several mechanisms, the most widely studied being apoptosis. To determine whether the active cell death seen in neuroblastoma cells was due to apoptosis, several assays for apoptosis were employed including DNA fragmentation, caspase activity and PARP cleavage. Both IMR-32 cells and Kelly cells were treated with DMSO, 5 μM $15dPGJ_2$ or 5 μM Wy-14643 and assayed at 24 and 72 hours for apoptosis. These time points were chosen as virtually no growth inhibition is seen at 24 hours and the greatest reduction in cell growth is seen between 48 and 72 hour time points. DNA from the neuroblastoma cell lines was electrophoresed to determine whether it produced a "ladder" on an agarose gel. This is because, during apoptosis, nucleases cause inter-nucleosomal fragmentation of DNA, producing characteristic multiples of 180-200 base pair lengths of DNA, which appear as a ladder on a gel [396, 397, 398]. DNA was isolated from neuroblastoma cells treated with DMSO, 5 μM $15dPGJ_2$ or 5 μM Wy-14643. Betulinic acid was used as a positive control [417] and induced DNA fragmentation in IMR-32 cells (Figure 4.13). However, despite betulinic acid being reported as a universal inducer of apoptosis it did not produce DNA laddering in Kelly cells [417].

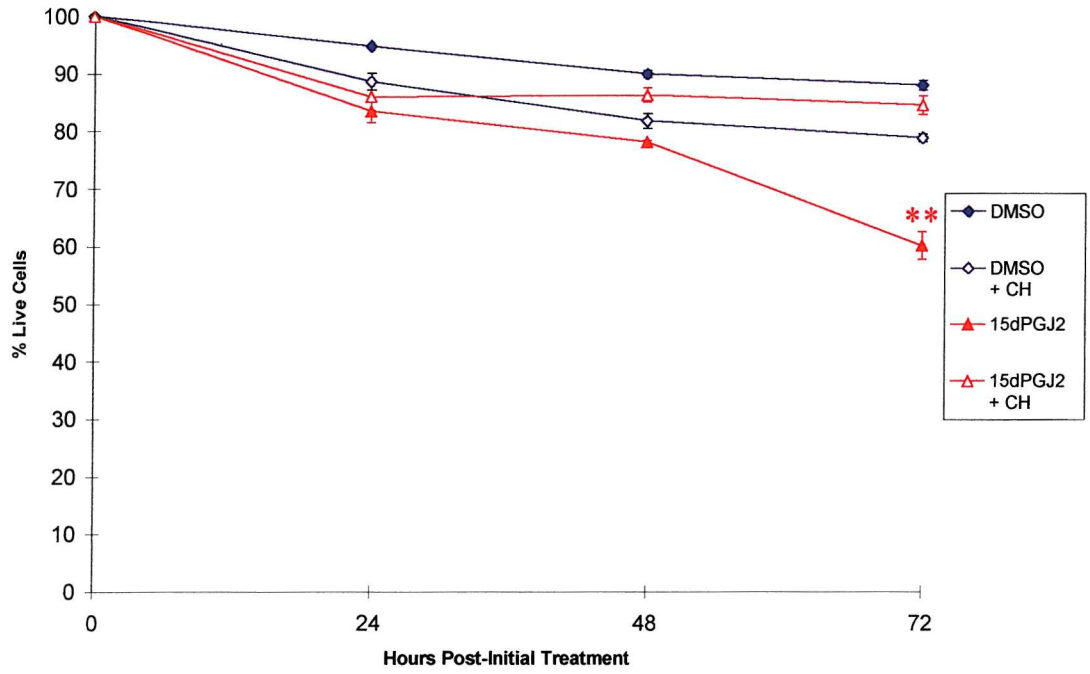

Figure 4.12 15dPGJ$_2$ induces cell death in IMR-32 cells, which requires *de novo* protein synthesis. IMR-32 cells were treated with 5 μM 15dPGJ$_2$ and the cells were also treated with the inhibitor of protein synthesis, cycloheximide (CH) and the effect on cell death measured by trypan blue exclusion assay. Two samples were counted per treatment per day and the graph represent duplicate experiments and the error bars represent s.e.m. Statistics were calculated by using an ANOVA and showed that cycloheximide did not significantly prevent 15dPGJ$_2$-induced cell death throughout the experiment. However, after 72 hours only, when maximal cell death was occurring, a student's t test showed that cycloheximide did have a significant effect, with a significance of $p<0.01$ (**).

No DNA ladders were seen in control cells or cells treated with Wy-14643 (Figures 4.14 and 4.15), consistent with these treatments having no effect on cell growth or inducing cell death. Importantly, although $15dPGJ_2$ induced an active form of cell death in IMR-32 cells, it caused neither DNA fragmentation nor apoptosis in either IMR-32 cells (Figure 4.14) or Kelly cells (Figure 4.15). No fragmentation of DNA was seen in IMR-32 cells or Kelly cells treated with 10 μM $15dPGJ_2$ (data not shown). However, some cell types do not undergo DNA fragmentation during apoptosis [418] and therefore other methods for detecting apoptosis were used.

Cytochrome C is released from mitochondria in response to apoptotic signals and activates caspase 9, which then interacts with APAF-1 to activate the caspase cascade [419]. Caspases are a family of cysteine proteases, which specifically cleave proteins at aspartic acid residues [420]. Activation of the caspase cascade results in the cleavage of various substrates causing morphological changes and degradation, which are characteristic of the cellular features seen in apoptosing cells [420]. One of the substrates of caspase 9, is caspase 3, which cleaves substrates containing the amino acid sequence DEVD [420] and is required for some of the morphological changes seen in apoptosis [421]. To establish whether $15dPGJ_2$ induced apoptosis by activating caspase 3 in neuroblastoma cells, total cell lysates from treated cells were mixed with a synthetic caspase 3 substrate, ac-DEVD-pNA. Ac-DEVD-pNA fluoresces when cleaved and the degree of fluorescence directly relates to the activity of caspase 3. No caspase 3 activity was seen in IMR-32 cells or Kelly cells at either 24 or 72 hours (Figures 4.16 and 4.17), suggesting that apoptosis was not occurring. To confirm that neuroblastoma cells contain functional caspase 3, staurosporine and betulinic acid were used positive controls (Figures 4.16 and 4.17). However, as seen with DNA fragmentation, betulinic acid did not activate caspase 3 or induce apoptosis in Kelly cells.

Several caspases are activated during apoptosis and therefore caspases other than caspase 3 may have been involved in the cell death induced in IMR-32 cells treated with $15dPGJ_2$. In addition, MCF-7 cells lack caspase 3 [422], but are able to undergo apoptosis, presumably through activation of other caspases [421].

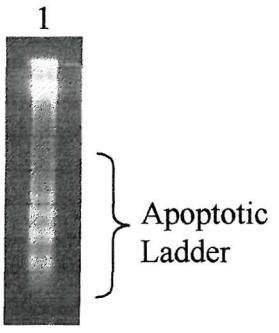

Figure 4.13 Betulinic acid induces DNA fragmentation in IMR-32 cells. IMR-32 cells were treated with 20 μg/ml betulinic acid for 24 hours (lane 1), total DNA was isolated from the cells and electrophoresed to look for a DNA ladder.

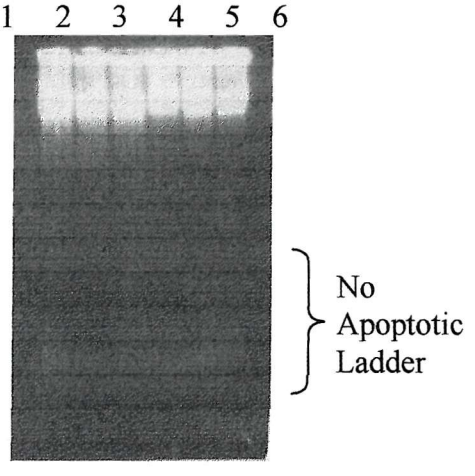

Lane 1	Untreated
Lane 2	DMSO
Lane 3	4 μM 9-*cis* retinoic acid
Lane 4	4 μM all-*trans* retinoic acid
Lane 5	5 μM 15-deoxy$\Delta^{12,14}$-prostglandin J_2 (15dPGJ$_2$)
Lane 6	5 μM Wy-14643

Figure 4.14 15dPGJ$_2$ and Wy-14643 do not induce DNA fragmentation in IMR-32 cells after 72 hours. IMR-32 cells were treated with 4 μM retinoic acid, 5 μM 15dPGJ$_2$ and 5 μM Wy-14643 for 72 hours and total DNA was extracted and electrophoresed to look for a DNA ladder.

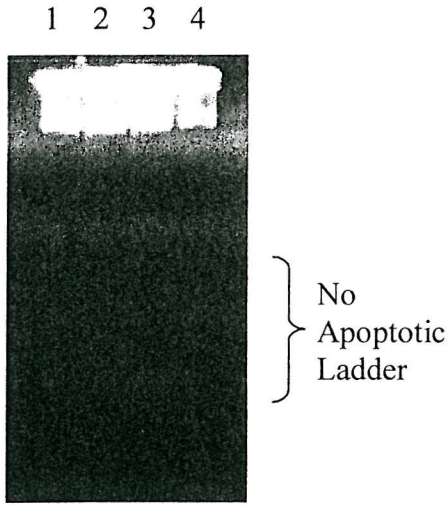

Lane 1	Untreated
Lane 2	DMSO
Lane 3	5 μM 15-deoxy$\Delta^{12,14}$-prostglandin J_2 (15dPGJ$_2$)
Lane 4	5 μM Wy-14643

Figure 4.15 15dPGJ$_2$ and Wy-14643 do not induce DNA fragmentation in Kelly cells after 72 hours. Kelly cells were treated with 5 μM 15dPGJ$_2$ and 5 μM Wy-14643 for 72 hours and total DNA was extracted. The DNA was electrophoresed to look for the presence of a DNA ladder.

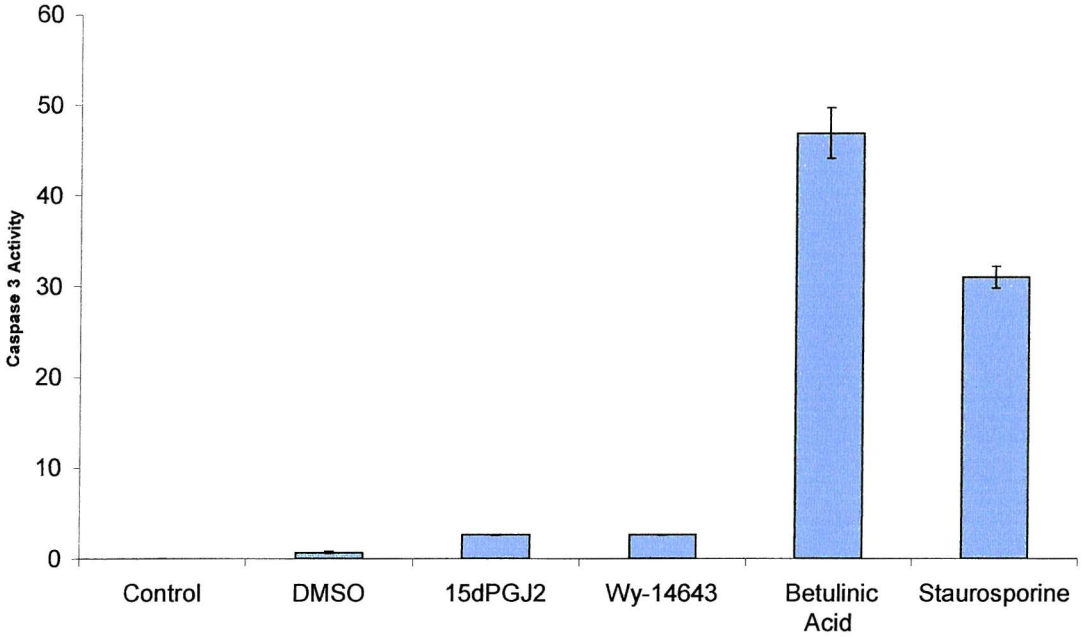

Figure 4.16 15dPGJ$_2$ and Wy-14643 do not activate caspase 3 in IMR-32 cells after 72 hours. IMR-32 cells were treated with 5 μM 15dPGJ$_2$ or 5 μM Wy-14643 and caspase 3 activity was measured in treated cells by measuring cleavage of the synthetic caspase 3 target, acDEVD-pNA. IMR-32 cells do have caspase 3, which can be activated by treating the cells with betulinic acid, which has previously been shown to induce apoptosis in neuroblastoma cells and by staurosporine, the general inducer of apoptosis.

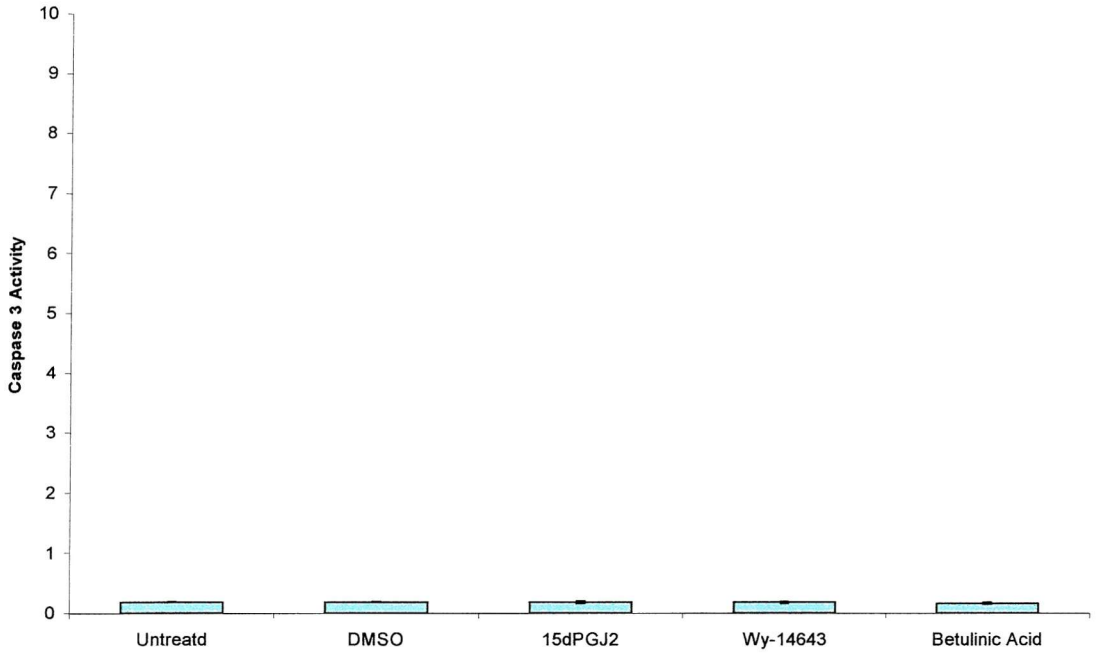

Figure 4.17 15dPGJ$_2$ and Wy-14643 do not activate caspase 3 in Kelly cells after 72 hours. Kelly cells were treated with 5 μM 15dPGJ$_2$ or 5 μM Wy-14643 and caspase 3 activity was measured in treated cells by measuring cleavage of the synthetic caspase 3 target, acDEVD-pNA. Betulinic acid is not a positive control for apoptosis in Kelly cells.

Therefore cleavage of poly ADP ribose polymerase (PARP) was also studied to confirm whether apoptosis was occurring or not. PARP is the substrate for several caspases including caspase 7 and cleavage of PARP is a marker for early apoptosis [423]. The larger 85 kDa fragment of PARP binds to DNA and prevents repair enzymes from repairing the DNA and rescuing the cell from apoptosis [424, 425]. Extracts of IMR-32 cells treated with PPAR ligands for 24 or 72 hours were resolved by SDS-PAGE and probed with an anti-PARP antibody (Upstate Biotechnology, New York) which recognises the full-length protein and its cleavage products. No cleavage of PARP was seen with any of the treatments at any time point in IMR-32 cells and the levels of full-length protein remained constant between treated and control cells at both 24 and 72 hours (Figure 4.18). Together these data suggest that $15dPGJ_2$ was not inducing apoptosis in IMR-32 cells.

4.2.6 *15-deoxy$\Delta^{12,14}$-prostglandin J_2 induces autophagy in IMR-32 cells*

Apoptosis is not the only form of programmed or active cell death. Autophagy or type II programmed cell death was first described in 1990 and involves lysosomal destruction of cellular contents such as mitochondria [364, 365]. Butler *et al.*, reported that $15dPGJ_2$ induces prostate cancer cell lines to undergo cell cycle arrest at S phase and autophagic cell death subsequent to the cell cycle arrest [346]. IMR-32 cells also underwent autophagic cell death, but arrested at G_2/M and not at S phase of the cell cycle. Despite this they showed similar characteristics to the prostate cancer cells in that the cell death occurred with intact nuclei and without DNA fragmentation, caspase activation or PARP cleavage.

To determine whether autophagy was occurring in neuroblastoma cells treated with $15dPGJ_2$, IMR-32 cells treated with DMSO or 5 μM $15dPGJ_2$ for 24 or 72 hours were stained with 50 μM monodansylcadaverine, fixed and observed by fluorescent microscopy. Monodansylcadaverine (MDC) is a fluorescent compound with a dansyl group conjugated to cadaverine, a diamine pentan which specifically accumulates in autophagic vesicles [426]. Untreated and DMSO-treated IMR-32 cells had no autophagic vesicles at 24 or 72 hours (Figure 4.19 and data not shown).

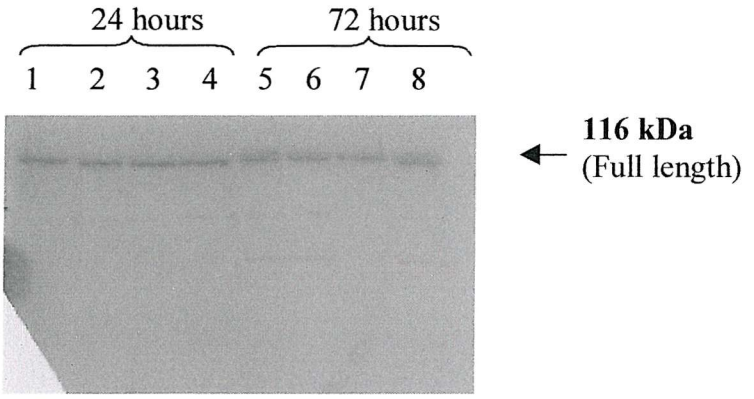

SDS-PAGE membrane

Lane 1 + 5	IMR-32 cells – untreated
Lane 2 + 6	IMR-32 cells + DMSO
Lane 3 + 7	IMR-32 cells + 15-deoxy$\Delta^{12,14}$-prostglandin J_2
Lane 4 + 8	IMR-32 cells + Wy-14643

Figure 4.18 Treatment of IMR-32 cells with 15dPGJ$_2$ and Wy-14643 does not result in the cleavage of PARP. IMR-32 cells were treated with 5 μM 15dPGJ$_2$ or 5 μM Wy-14643 and nuclear extracts made of the cells after 24 and 72 hours. Cleavage of poly-ADP ribose polymerase (PARP), a caspase target, was determined by resolving the extracts by SDS-PAGE Western blotting with an antibody to full-length and cleaved PARP.

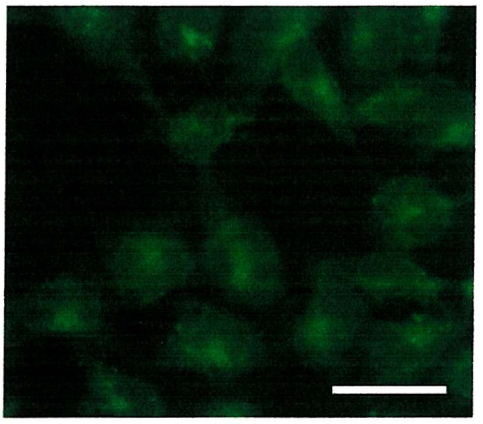

DMSO

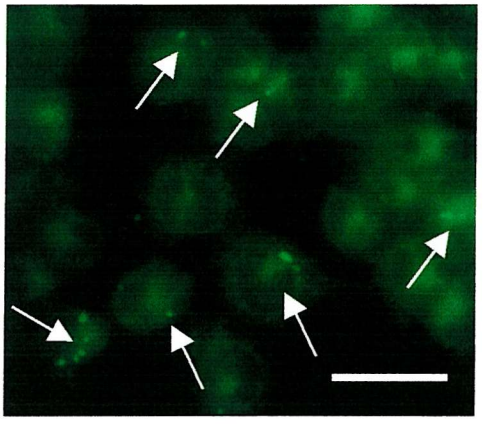

$15dPGJ_2$

Figure 4.19 $15dPGJ_2$ induces the formation of autophagic vesicles, stained by MDC in IMR-32 cells after 72 hours. IMR-32 cells were treated for 72 hours with 5μM 15dPGJ2 or DMSO. The cells were stained with monodansylcadaverine, a dye which stains autophagic vesicles and visualised by fluorescent microscopy. Scale bars represent 30 μM.

A few vesicles were visible in cells treated with 5μM $15dPGJ_2$ for 24 hours (data not shown), but after 72 hours treatment there was an accumulation of autophagic vesicles in most IMR-32 cells (Figure 4.19). This suggests that autophagy occurred in IMR-32 cells. If IMR-32 cells treated with $15dPGJ_2$ were undergoing autophagic cell death, observing ultrastructural changes to the cells would confirm this. Autophagy is characterised by formation of autophagic vesicles, which sequester cytoplasm and organelles from the rest of the cell and are destroyed by fusing with lysosomes [364, 365]. Organelles, especially mitochondria, are degraded during autophagy and a reduction in mitochondrial functioning results in cell death [364, 365, 427]. Autophagic cell death has been previously shown using electron microscopy to observe autophagic vesicles in cells treated with $15dPGJ_2$ [346] and in rat sympathetic neurones deprived of nerve growth factor [427].

Silver sections of IMR-32 cells treated with 5 μM $15dPGJ_2$, DMSO or left untreated for 72 hours, were cut and stained to observe any ultra-structural changes occurring in these cells upon treatment, which may indicate autophagy. Untreated and DMSO-treated cells appeared to have a normal cellular ultra-structure, with intact nuclei and random distribution of intact intracellular organelles, without chromatin condensation, condensation of cytoplasm or loss of cellular membrane integrity (Figures 4.20a and 4.20b). However, cells treated with $15dPGJ_2$ for 72 hours, showed contraction of the cellular volume, with many organelles such as mitochondria becoming arranged in densely packed formations at one side of the nucleus with little intervening cytoplasm (Figure 4.20c). Such densely packed formations are a feature of apoptosis and may reflect overlapping of cytoplasmic changes seen with apoptosis and autophagy [368]. These organelles appeared to have moved or been moved within the cell, leaving large areas of the cell with very few or no organelles. All of the organelles appeared intact and had not undergone swelling (a feature of necrosis), except possibly some of the endoplasmic reticulum (ER), which appeared slightly distended (Figure 4.20d). This may reflect an early part of the mechanism of autophagic cell death, where membranes of ER envelop parts of the cell. Another feature of autophagy is the presence of "whorls" of ER membrane within the cell [364], which were seen $15dPGJ_2$-treated cells at 72 hours (Figure 4.20e).

Figure 4.20 15dPGJ$_2$ induces features of autophagic cell death in IMR-32 cells after 72 hours. Silver sections of IMR-32 cells treated with DMSO, 5 μM 15dPGJ$_2$ or left untreated for 72 hours were stained with uranyl acetate and lead citrate and analysed by transmission electron microscopy. Whole untreated and DMSO-treated IMR-32 cells are shown in Figure 4.20a and 4.20b. Whole IMR-32 cells treated with 15-deoxy$\Delta^{12,14}$-prostglandin J$_2$ (15dPGJ$_2$) for 72 hours are shown in Figure 4.20c. Figures 4.20d – 4.20h show higher magnification of IMR-32 cells treated with 5 μM 15dPGJ$_2$ for 72 hours. Figure 4.20d shows endoplasmic reticulum, Figure 4.20e shows a "whorled" autophagic vesicle and Figure 4.20f shows an autophagic vesicle containing cellular components. Figure 4.20g shows a degradative autophagic vesicle and Figure 4.20h shows the intact nucleus of an IMR-32 cell treated with 5 μM 15dPGJ$_2$ for 72 hours. Scale bars represent 10 μM for whole cell pictures (Figures 20a-c) and 1 μM for pictures of parts of cells (Figures 20d-h).

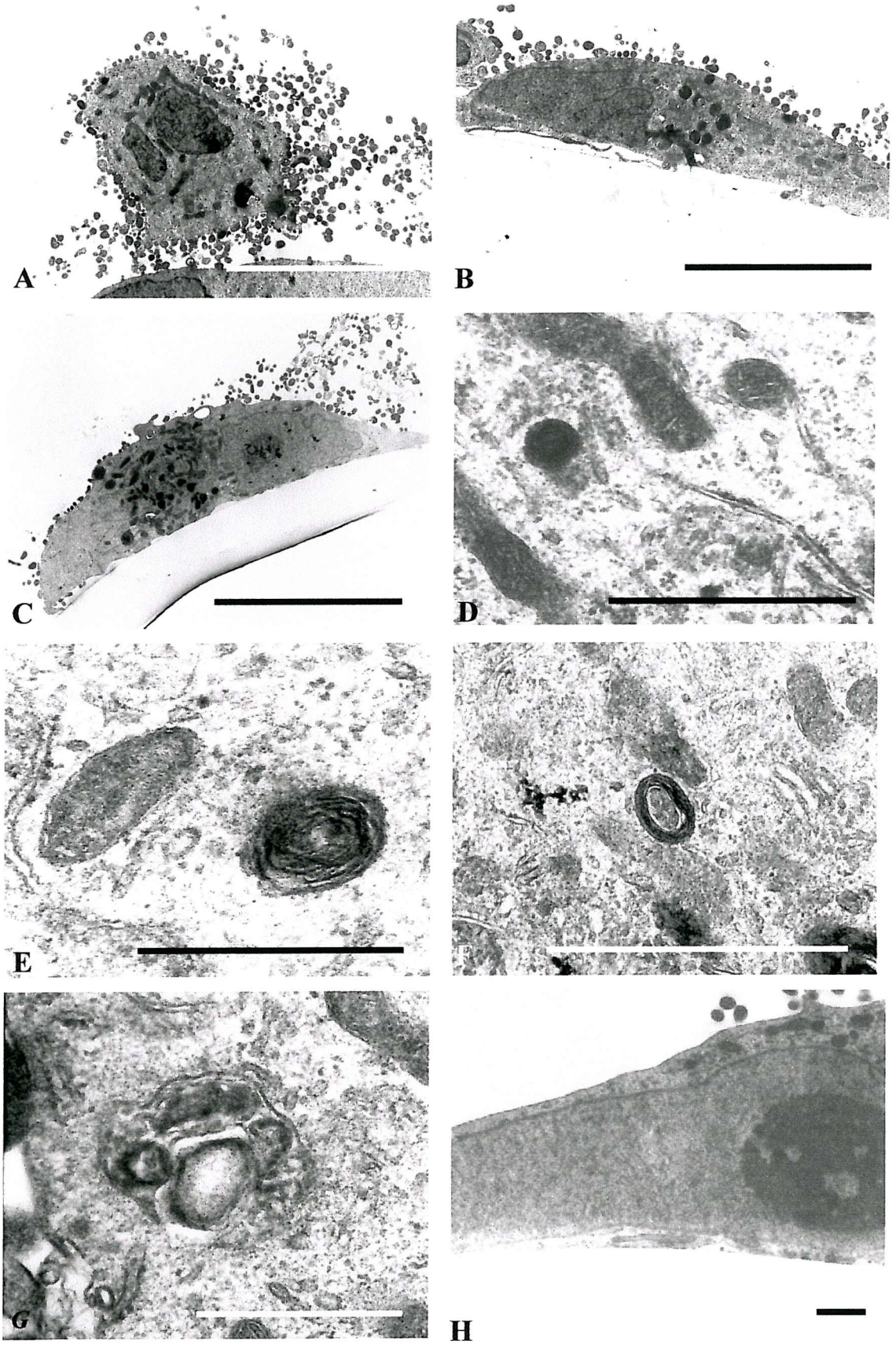
A
B
C
D
E
G
H

These may represent a later stage in the autophagic process, where an organelle has been enveloped (Figure 4.20f). The final stage in the autophagic process is the formation of the single membrane-bound vesicle [365], which may contain parts of the cell. This was also be seen in the $15dPGJ_2$-treated IMR-32 cells at this time point, where the vesicle appeared to contain cellular components, possibly organelles (Figure 4.20g). No chromatin condensation was seen in IMR-32 cells treated with $15dPGJ_2$, the nuclei and nucleoli appeared intact and there were no apoptotic bodies (Figure 4.20h).

4.2.7 *Treatment of IMR-32 cells with ligands of PPARγ and Retinoid X Receptor (RXR) do not synergistically inhibit cell growth or induce death*

Simultaneous treatment with ligands of PPARγ and retinoid X receptors (RXRs) has been shown to be synergistic, resulting in further increases in growth inhibition of some cancer cells. This includes prostate cancer cells [130], leukaemia cells [243] and gastric cancer cells [428]. Breast cancer cells treated with a combination of troglitazone (TGZ), a thiazolidinedione (TZD), which activates PPARγ, and the RXR ligand, 9-*cis* retinoic acid, have also been shown to undergo synergistic increases in cell growth inhibition with increased apoptosis [242]. Docosahexaenoic acid (DHA) activates PPARs [175], but is also a ligand of retinoid X receptors (RXRs) in mouse brain [429]. DHA was found in the hippocampus, striatum, motor cortex and cerebellum of day 13.5 mouse embryos and when used to supplement tissue culture medium, it was shown activate RXR heterodimerised with the orphan receptor, Nurr1 [429]. The binding of DHA to RXR was sensitive to mutations in the ligand binding domain of RXR, suggesting that it was a true ligand of DHA, but it was less effective than 9-*cis* retinoic acid (9-*cis* RA) at activating RXR [429]. Ligands of PPAR and RXR have both been shown to inhibit neuroblastoma cell growth [342, 77]. Therefore, IMR-32 cells were treated with 5 μM $15dPGJ_2$ and 4 μM 9-*cis* retinoic acid or 30 μM docosahexaenoic acid (DHA) for 120 hours and cell numbers counted, to establish whether $15dPGJ_2$ and RXR ligands synergistically inhibited IMR-32 cell growth. 4 μM retinoic acid was used as it has been shown to differentiate neuroblastoma cells [430].

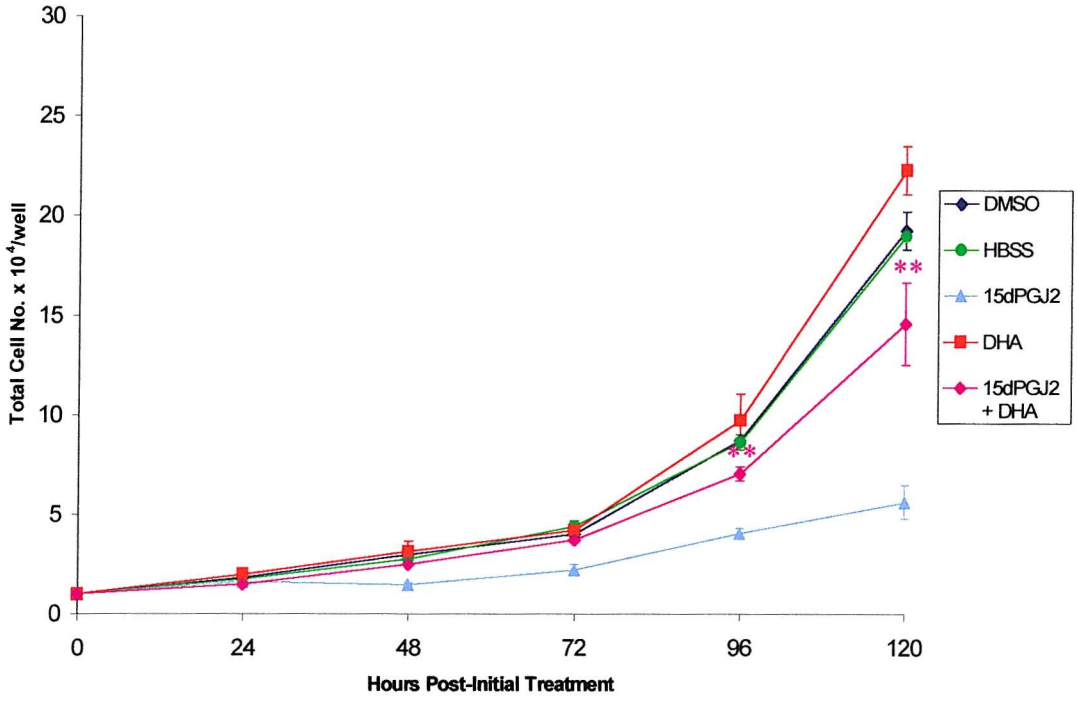

Figure 4.21 DHA protects IMR-32 cells from 15dPGJ$_2$-induced cell death. IMR-32 cells were treated with 30 μM DHA and 5 μM 15dPGJ$_2$ and the effect on cell growth measured over 120 hours. Two samples were counted per treatment per day and the experiments were completed in duplicate and error bars represent standard errors of the mean. Statistics were calculated by an ANOVA and showed that DHA did not significantly protect cells from 15dPGJ$_2$-induced cell death throughout the experiment, but student's t test showed that it significantly protected the cells only after 96 hours treatment, at a significance of $p<0.01$.

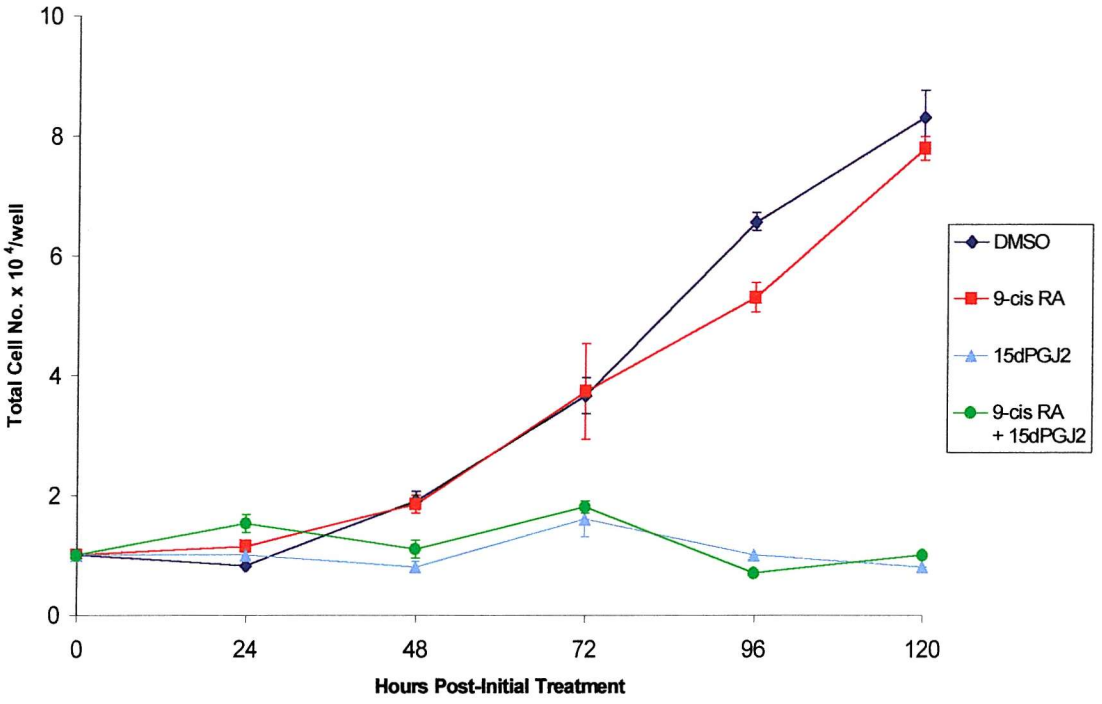

Figure 4.22 9-*cis* retinoic acid and 15dPGJ$_2$ do not synergistically inhibit the growth of IMR-32 cells. IMR-32 cells were treated with 4 μM 9-*cis* retinoic acid and 5 μM 15dPGJ$_2$ and the effect on cell growth measured over 120 hours. Two samples were counted per treatment per day and the experiments were completed in duplicate and error bars are standard errors of the mean.

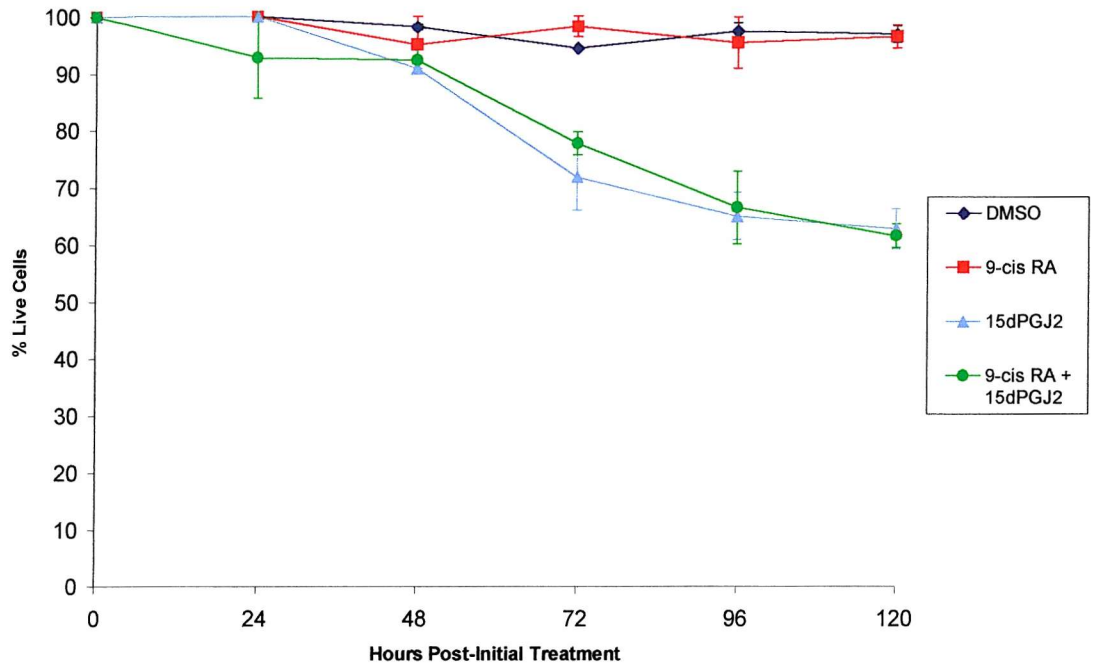

Figure 4.23 9-*cis* retinoic acid and 15dPGJ$_2$ do not synergistically induce death of IMR-32 cells. IMR-32 cells were treated with 4 μM 9-*cis* retinoic acid and 5 μM 15dPGJ$_2$ and the effect on cell death measured over 120 hours using the trypan blue exclusion assay. Two samples were counted per treatment per day and the experiments were performed in duplicate and error bars represent standard errors.

30 μM DHA had a marginal effect on IMR-32 cell growth, but at 120 hours there was an increase in IMR-32 cell growth compared to controls (Figure 4.21). $15dPGJ_2$ inhibited IMR-32 cell growth over 120 hours, but when used in combination with DHA it was less effective, with cell growth rates increasing to 76 % of that of control-treated cells, rather than 30 % when $15dPGJ_2$ was used as a treatment alone (Figure 4.21). This suggested that in IMR-32 cells, DHA did not act synergistically with $15dPGJ_2$ to inhibit the growth of IMR-32 cells and in fact antagonised the growth inhibitory effects of the prostaglandin. It also suggested that in IMR-32 cells, DHA may not have activated RXR and it may have bound to PPARγ, thus preventing activation of the receptor by $15dPGJ_2$, or it may have activated RXR, but there was no synergistic effect of activating both receptors simultaneously.

To determine whether 9-*cis* retinoic acid acts synergistically with $15dPGJ_2$ in IMR-32 cells, cells were treated as described above. 9-*cis* RA had no growth inhibitory effect on IMR-32 cells compared to controls cells (Figure 4.22). Like the DHA, 9-*cis* RA did not act synergistically with $15dPGJ_2$ to inhibit the growth of IMR-32 cells (Figure 4.22). The $15dPGJ_2$ alone inhibited most of the growth of IMR-32 cells, but not completely, and although a synergistic effect may not have been seen at these low cell numbers, the combination of treatments could have inhibited cell growth totally, which they did not do. The level of cell death of IMR-32 cells treated with $15dPGJ_2$ and 9-*cis* RA in combination did not differ from that of $15dPGJ_2$ alone (Figure 4.23), although the combination of ligands may have induced further growth arrest.

4.3 *Discussion*

PPARs are activated by a wide range of natural and synthetic ligands, by virtue of their large ligand binding domains [153]. This in contrast to other members of the nuclear hormone super-family, which have much smaller ligand binding domains and a more limited range of ligands [104]. PPARγ is activated by the arachidonic acid metabolite, 15-deoxy$\Delta^{12,14}$-prostglandin J_2 ($15dPGJ_2$) [167, 168], phenylacetate [206], oxidised phospholipids [334] and thiazolidinediones (TZDs). Ligands of PPARγ have

been to be shown to be growth inhibitory in a number of cancer cell lines and in some primary tumours [312, 342, 355], although, no inhibition of cell growth has been so far reported for oxidised phospholipids. Conflicting results, however, have been seen in mouse models of colorectal cancer [350, 351] and in one human colorectal cancer cell line [188], where PPARγ ligands enhanced cell growth. As yet no ligands of PPARα have been shown to inhibit the growth of any human cancer cells, but treatment of C57BL/6J-APC^{min}/+ mice, a model of familial adenomatous polyposis coli, with doses of methylclofenapate resulted in a reduction in PPARα expression and intestinal polyp area [308]. Therefore, the fact that the potent activator of PPARα, Wy-14643, does not inhibit the growth of IMR-32 cells or Kelly cells (Figures 4.1 – 4.3) is consistent with published data.

5 μM of the PPARγ ligand, 15dPGJ$_2$ inhibited the growth of IMR-32 cells and Kelly cells *in vitro* (Figures 4.2 and 4.3). A similar effect was seen by Han *et al.*, in the Lan-5 neuroblastoma cell line, although they used a higher concentration of 15dPGJ$_2$ [342]. In their experiments, a significant reduction in Lan-5 cell growth was only seen with 10 μM 15dPGJ$_2$ after 6 days of continual treatment [342], whereas in IMR-32 cells, 5 μM 15dPGJ$_2$ inhibited growth of IMR-32 cells within 48 hours. This may be related to the levels of PPARγ expression in different neuroblastoma cell lines [343], as neuroblastoma cells are thought to express different levels of PPARγ [343]. A higher level of PPARγ expression in neuroblastoma cells may require higher concentrations of 15dPGJ$_2$ to induce cell death, than in cells expressing lower levels of PPARγ, if for example, a certain proportion of the receptors needed to be activated to result in cell death as opposed to differentiation. 15dPGJ$_2$ also induced cell cycle arrest at G$_2$/M within 72 hours in a significant number of IMR-32 cells (Figure 4.5 and 4.6), followed by cell death, but it is not known whether more cells arrest at G$_2$/M following treatment with 15dPGJ$_2$ for 120 hours. This contrasts some of the cell cycle arrest in prostate cancer cells seen with 15dPGJ$_2$, as two of the cell lines arrested at S phase of the cell cycle, but another cell line, DU145, did arrest at G$_2$/M [346]. Therefore 15dPGJ$_2$ may activate PPARγ, but that the resulting transcription of genes and growth arrest may be cell-type specific and depend on the expression for example, of cell cycle inhibitors within these cells which may be downstream targets of PPARγ.

In contrast to the effects of $15dPGJ_2$ on IMR-32 cells, Clay *et al.* [431, 432] showed that very different responses to $15dPGJ_2$ can be seen in the same cell line, just by varying the concentration of the ligand. Concentrations of $15dPGJ_2$ of less than 2.5 μM actually induced cellular proliferation of MDA-MB-231 breast cancer cells, whereas concentrations of $15dPGJ_2$ of less than 10 μM induced them to differentiate, seen as an increase in the expression of CD36, a marker of differentiation. A relatively high concentration (10 μM) of $15dPGJ_2$ induced the breast cancer cells to undergo S-phase arrest and to develop characteristics consistent with those seen during apoptosis, but had no further effect on CD36 expression [431, 432]. Similar effects were seen in the same breast cancer cell line in response to the synthetic PPARγ ligand, troglitazone (TGZ). Concentrations of TGZ of less than 5 μM increased cellular proliferation, whereas 100 μM TGZ slowed cell cycle progression and induced CD36 expression. In contrast to this, no increase in cell proliferation was observed in IMR-32 cells treated with low concentrations (<2.5 μM) of $15dPGJ_2$ (Figure 4.1). The morphological characteristics consistent with apoptosis seen in MDA-MB-231 cells treated with 10 μM $15dPGJ_2$ were not seen in IMR-32 cells treated with 5 μM $15dPGJ_2$ or with 10 μM $15dPGJ_2$ (data not shown).

$15dPGJ_2$ did not induce G_2/M arrest in Kelly cells and the only change to the distribution of cells throughout the cell cycle was an increase in the number of cells in G_1/G_0 (Figures 4.7 and 4.8). This may be because the cells were differentiating, which has also been seen in liposarcoma cells [241] and breast cancer cells [290] treated with ligands of PPARγ, although no morphological differentiation of Kelly cells was seen (data not shown). Some cancer cells actually undergo apoptosis following G_1/G_0 cell cycle arrest, such as L1210 murine leukaemia cells in response to prostaglandin A_1 and A_2 [433]. $15dPGJ_2$ induces cell cycle arrest in several cell types, mainly at the G_1 phase of the cell cycle. This occurs in adipocytes, where cell cycle withdrawal was associated with a loss of DNA binding to the growth-related E2F/DP transcription complex [241]. $15dPGJ_2$ is also able to induce G_1 cell cycle arrest in cancer cells, including bladder cancer cells [434] and non-small lung cancer cells [341].

Unlike Kelly cells, $15dPGJ_2$ induced IMR-32 cells to retract their neurites (Figure 4.9). $15dPGJ_2$ also induces the degeneration of neurites in primary rat cortical neurones and SHSY5Y neuroblastoma cells [362]. However not all neuroblastoma cells retract their neurites in response to ligands of PPARγ. Lan-5 neuroblastoma cells actually extend their neurites in response to $15dPGJ_2$, phenylacetate and GW1929, a synthetic agonist of PPARγ, within 48 hours of culture [342]. They also exhibit decreased expression of NMYC and increased expression of acetylcholinesterase activity, both of which are markers of neuroblastoma cell differentiation [342]. This suggests that $15dPGJ_2$ differentiated Lan-5 cells, but unlike the effect seen in IMR-32 cells and SHSY5Y cells, it did not induce growth arrest and cell death. The $15dPGJ_2$-induced morphological changes occurring in these neuroblastoma cells may have been due to changes to the cytoskeleton and a cytoskeletal component could possibly be a downstream target of PPARγ. On the other hand, neurite retraction could just be a response to the activation of the cell death programme. Interestingly, $15dPGJ_2$ also induced neurite outgrowth in PC12 cells, but troglitazone did not induce the same effect and it was suggested that this effect might not involve activation of PPARγ [193]. However, differences in PPARγ-activation have been seen in cells treated with $15dPGJ_2$ and TZDs [352].

In response to 5 μM $15dPGJ_2$, IMR-32 cells underwent cell cycle arrest at G_2/M and neurite retraction followed by cell death, shown as an increase in the number of cells taking up trypan blue (Figure 4.10). This is consistent with the effects of $15dPGJ_2$ on prostate cancer cells, which also increased trypan blue uptake on treatment with $15dPGJ_2$ [346]. Fewer Kelly cells treated with $15dPGJ_2$ took up trypan blue than IMR-32 cells treated with $15dPGJ_2$ and may reflect a different response to ligand (Figure 4.11). For activation of PPARγ by ligands to have potential in the treatment of neuroblastoma, the ligand used must induce either differentiation, cell cycle arrest or a form of programmed cell death (PCD), but not necrosis. This is because necrosis ends with lysis of the cell and the released cellular contents would invoke an inflammatory response. However, the cell death induced in IMR-32 cells by $15dPGJ_2$ was protein-synthesis-dependent, as the protein synthesis inhibitor, cycloheximide prevented $15dPGJ_2$-induced cell death, suggesting that $15dPGJ_2$

induced a form of programmed cell death in IMR-32 cells (Figure 4.12). It is not known whether the cell death seen in Kelly cells treated with $15dPGJ_2$ was dependent on *de novo* protein synthesis and this should be established in future studies.

J_2 prostglandins, including $15dPGJ_2$, have been shown to cause cell cycle arrest and apoptosis in endothelial cells [183] and some cancer cells [130, 341]. To determine whether $15dPGJ_2$ induced apoptosis in IMR-32 cells, the cells were treated with $15dPGJ_2$ or Wy-14643 and apoptosis was measured using a variety of assays. Propidium iodide staining revealed intact nuclei and no condensation of chromatin in IMR-32 cells or Kelly cells treated with $15dPGJ_2$ (data not shown). However, Rohn *et al.*, showed that 10 μM $15dPGJ_2$ induced fragmentation of the nuclei of cortical neurones [362] and this may reflect cell-type specific responses to $15dPGJ_2$. DNA fragmentation gels also showed that the DNA of treated IMR-32 cells and Kelly cells had not been cleaved into the characteristic "ladder" indicative of apoptosis [396, 397, 398] (Figures 4.14 and 4.15). Neither was the DNA randomly cleaved to form a smear on an agarose gel which would indicate that the cells had undergone necrosis, where nucleases randomly cut nucleic acids in the cell. However, apoptosis has been observed without the characteristic laddering of DNA and this has even been seen in IMR-32 treated with 3 μM *N*-(4-Hydroxyphenyl) retinamide, a synthetic retinoid with limited toxicity, which also undergo apoptosis without DNA fragmentation after treatment for 72 hours [435]. Likewise, in IMR-32 treated with staurosporine, the general inducer of apoptosis, DNA does not become fragmented during apoptosis. This may be a general feature of IMR neuroblastoma cell lines, as IMR-5 cells also do not undergo DNA fragmentation in response to staurosporine, but display other features of apoptotic cell death such as chromatin condensation [436]. IMR-32 cells have a deletion in the short arm of chromosome 1, commonly at 1p36 [40] and it is predicted that two tumour suppressor genes lie in this region [437, 438]. The gene encoding DNA fragmentation factor 45 (DFF45) maps to chromosome band 1p36.2-1p36.3 and is deleted in one neuroblastoma cell line [439]. The mouse homologue of DFF45 is called inhibitor of caspase activated DNAase (ICAD) [440]. DFF45/ICAD is the substrate of caspase 3 and dimerises with DNA fragmentation factor 40 (DFF40)/caspase activated DNAase (CAD). During

apoptosis, caspase 3 cleaves DFF45/ICAD, releasing DFF40/CAD, which degrades DNA into the characteristic ladder pattern [440, 441, 442]. Novel variant transcripts have been found in several neuroblastoma cell lines, including IMR-32 cells [439] and this may explain why some cells, including neuroblastoma cells do not undergo DNA fragmentation even during apoptosis.

Therefore to confirm that 15dPGJ$_2$ was not inducing apoptosis in IMR-32 cells or Kelly cells, the treated cells were measured for caspase 3 activity and cleavage of the caspase substrate poly-ADP ribose polymerase (PARP), which is an early event in the apoptotic pathway [423]. No caspase 3 activity was observed in the 15dPGJ$_2$–treated IMR-32 cells (Figure 4.16), however, they can undergo apoptosis as betulinic acid, which has previously been shown to induce apoptosis in neuroblastoma cells [417], activated caspase 3. The lack of caspase 3 activity also indicated that the cell death seen in IMR-32 cells, is similar to that seen in prostate cancer cells treated with 15dPGJ$_2$ by Butler *et al.*, who used an inhibitor of caspases but were unable to prevent 15dPGJ$_2$-induced cell death [346]. They also observed that 15dPGJ$_2$ treatment did not result in cleavage of PARP [346]. Likewise, nuclear extracts of IMR-32 cells were probed with an anti-PARP antibody and showed that despite 15dPGJ$_2$-inducing an active cell death in IMR-32 cells, apoptosis was not occurring (Figure 4.18). However, cortical neurones and SHSY5Y neuroblastoma cells treated with 10 μM 15dPGJ$_2$ undergo features of apoptosis including cleavage of full-length PARP and this can be prevented by pre-treatment with the general caspase inhibitor Z-VAD [362]. Therefore in these cells, 15dPGJ$_2$ activates caspases and the cells exhibit features of apoptosis in response to the prostaglandin [362]. Like IMR-32 cells, Kelly cells did not undergo DNA fragmentation on treatment with 15dPGJ$_2$ and may not have been apoptosing. There was also no cleavage of the caspase 3 substrate in Kelly cells treated with 15dPGJ$_2$ (Figure 4.17). However, unlike in IMR-32 cells, betulinic acid does not seem to induce apoptosis in Kelly cells as it does not induce DNA fragmentation or activation of caspase 3, though it is possible that Kelly cells do not have active caspase 3. Interestingly, caspase 8 has been shown to be deleted or silenced by methylation in neuroblastomas with poor prognosis [443] and it is possible that caspase 3 may not be present or may not be active in Kelly cells. As apoptosis can

also occur in the absence of caspase 3 [422, 421] and to further establish the effects of $15dPGJ_2$ on Kelly cells, PARP cleavage should also be determined.

Butler *et al.*, also reported that $15dPGJ_2$ induced prostate cancer cells to undergo an active non-apoptotic cell death, known as autophagy or type II programmed cell death [346]. Autophagy occurs in normal cells and is involved in processes during mammalian embryogenesis and the regression of inter-digital webs [366, 444], as well as the normal turnover of mitochondria in non-proliferating cells and the removal of damaged organelles [363, 445]. Autophagic cell death has also been associated with neurodegenerative diseases including Alzheimer's disease [446] and Parkinson's disease [447]. Cancer cells have been shown to undergo autophagy in response to different treatments, including breast cancer cells in response to tamoxifen [448] and acute T-lymphoblastic leukaemia cells in response to tumour necrosis factor alpha (TNFα) [368]. Autophagy is a process whereby the endoplasmic reticulum envelopes parts of the cell, especially mitochondria, into autophagic vesicles and destroys the vesicles and contents by fusion with lysosomes [364, 365]. This process, like apoptosis, would not invoke an inflammatory response and could explain results seen in IMR-32 cells, especially as studies with staurosporine have indicated that IMR-32 cells do undergo an autophagic-like cell death [436]. Neuroblastoma cells are undifferentiated cells of neural crest origin, which cause tumours in the sympathetic nervous system [1, 3]. Autophagy also occurs in sympathetic neurones deprived of nerve growth factor (NGF) [427]. Sympathetic neurones, like neuroblastoma cells also derive from neural crest cells, suggesting that it may also occur in the neuroblastoma cell line, IMR-32. The effects of $15dPGJ_2$ in IMR-32 cells differ from those seen in sympathetic ganglia, where apoptotic features such as the activation of caspase 9 and DNA fragmentation were observed during autophagy [427] and in SHSY5Y cells where cell death induced by $15dPGJ_2$ can be inhibited by caspase inhibitors [362]. Clarke [366] and others [346] reported that autophagy and apoptosis are distinct processes. Likewise, Chi *et al.* [449] proposed that the oncogene *ras* might be involved in triggering autophagy without apoptosis in cancer cells. They expressed oncogenically mutated *ras* in human glioma and gastric cancer cells, as unlike many human tumours, these tumours rarely have mutated *ras* genes and it was thought that this is because the mutated *ras* may initiate a cell death

programme which cannot be overcome in these tumour types [449]. Despite degeneration of the cancer cells with the formation of cytoplasmic vesicles, the nuclei remained intact and there was an absence of caspase activation [449]. It was suggested that mutated *ras* induced autophagic cell death without apoptosis occurring, although the cell lines used were able to undergo apoptotic cell death [449].

In complete contrast several groups have shown that apoptosis and autophagy are overlapping mechanisms of programmed cell death [368, 450] and the differences between the processes may depend on cell type. In acute lymphoblastic leukaemia cells, TNFα induces apoptosis and this requires some of the early stages of autophagy, such as condensed positioning of mitochondria [368]. It is therefore proposed that cells undergoing autophagy have a greater tendency to apoptose [368]. In fact, both type I (apoptotic) and type II (autophagic) programmed cell death share features of the stress response of cells, such as the translocation of the heat shock protein, Hsp90 [451]. However, the processes involve very different fates for the components of the cytoskeleton. In apoptosis, cytoskeletal elements are degraded very early in the process, but in autophagy intermediate and microfilaments are largely preserved, leading to the suggestion that cytoskeleton is required during autophagy [452]. It is thought that the cytoskeleton is redistributed during autophagy [452] and this may explain the morphological changes to IMR-32 cells, such as neurite retraction, seen on treatment with $15dPGJ_2$.

IMR-32 cells and Kelly cells treated with $15dPGJ_2$ were stained with monodansylcadaverine (MDC) to establish the presence of autophagic vesicles within the cells [426]. Only IMR-32 cells treated with $15dPGJ_2$ for 72 hours had autophagic vesicles, indicating that these cells were undergoing autophagy (Figure 4.19). MCF-7 breast cancer cells undergoing tamoxifen-induced autophagy also have increased numbers of vesicles staining positive for monodansylcadaverine [448]. In contrast to IMR-32 cells, Kelly cells did not undergo autophagic cell death in response to $15dPGJ_2$, reflecting differences between the cell lines. It would be of interest to establish the mechanism by which $15dPGJ_2$ inhibits the growth of Kelly cells and to determine whether they behave in a similar manner to other

neuroblastoma cell lines, such as Lan-5, which differentiate or SHSY5Y cells, which apoptose or whether they act via another mechanism.

IMR-32 cells treated with $15dPGJ_2$ for 72 hours were analysed by transmission electron microscopy look for autophagic vesicles. The cells had vesicles which appeared as whorls of membrane sometimes containing electron-dense material, which were nascent autophagic vesicles, or single-membrane-bound vesicles containing organelles, which were degradative autophagic vesicles [364, 365] (Figure 4.20). The degradative vesicles contained parts of the cell, but no whole mitochondria were observed inside them, although this does not suggest that mitochondria were not being degraded. The degradative vesicles contain enzymes, including acid hydrolases [365], which start degrading the vesicle contents before they fuse with lysosomes and therefore the contents may not be easily recognisable. Autophagic vesicles have also been observed in both sympathetic neurones [427] and in prostrate cancer cell treated with $15dPGJ_2$ [346].

The other notable change to the $15dPGJ_2$-treated cells was a difference in the distribution of organelles such as mitochondria, which grouped at one end of the cell with little intervening cytoplasm (Figure 4.20c). A similar observation was made by Butler *et al.* [346] who noted that in prostate cells treated with $15dPGJ_2$, the pattern of mitochondrial distribution changed from random cytoplasmic, to a tightly packed peri-nuclear distribution. The re-distribution of cytoskeletal components without any degradation is thought to be an important part of the autophagic process and may be occurring in IMR-32 cells treated with $15dPGJ_2$, as the mitochondria tended to pack into a peri-nuclear confirmation. Mitochondria and microtubules have been shown to co-localise [453, 454] and when cells are treated with microtubule destabilising agents, the distribution of mitochondria within cells also changes [453, 454]. Interestingly, the disruption of the activity of the microtubule-based motor protein, kinesin, also causes peri-nuclear clustering of mitochondria [455, 456]. Kinesin hydrolyses adenosine triphosphate (ATP) and uses the energy produced to move components, such as organelles, around the cell [457]. Therefore $15dPGJ_2$-induced activation of PPARγ may result in the transcription of a protein which affects kinesin resulting in a reduction in the movement of mitochondria to

the cell periphery, or it is possible that kinesin may be a downstream target of PPARγ and this warrants further study.

Butler *et al.* [346] suggested that $15dPGJ_2$ may affect the mitochondria themselves, resulting in membrane depolarisation and uncoupling of oxidative phosphorylation, which would abolish the production of ATP and prevent kinesin from maintaining the distribution of organelles throughout the cell. This membrane depolarisation is known as the mitochondrial permeability transition (MPT) [445], which represents an abrupt increase in permeability of the mitochondrial inner membrane to solutes of molecular mass of less than 1500 Daltons (Da). Mitochondria which spontaneously or are induced to depolarise, undergo autophagic cell death [445]. It is thought that autophagy occurs if a few mitochondria are involved, but if the numbers increase then the MPT may induce apoptosis, partly due to the release of pro-apoptotic substances from the degrading mitochondria [445]. If the MPT involves all the mitochondria in a cell then the cell undergoes necrosis [445]. Therefore, in IMR-32 cells, $15dPGJ_2$ may induce a small number of mitochondria to depolarise, resulting in autophagic cell death. This may also be related to the level of PPARγ expression in cells. $15dPGJ_2$ may be able to induce apoptosis in cells expressing higher levels of PPARγ, as it may induce depolarisation of more mitochondria. Interestingly, SHSY5Y cells which undergo apoptosis in response to $15dPGJ_2$, express more PPARγ than IMR-32 cells, which undergo autophagy in response to $15dPGJ_2$ (personal communication, Dr. Cimini, University of L'Aquila, Coppito, Italy). Impairment of the function of mitochondria can be measured by using fluorescent probes, such as JC-1. JC-1 is a lipophilic cation, which exists as a monomer emitting green fluorescence, but in a reaction driven by mitochondrial membrane potential, forms dimeric "J-aggregates" that emit red fluorescence [458, 459]. Changes in fluorescence between treated and control cells could be compared to look at potential changes in mitochondrial function. As autophagic cell death involves changes in the cytoskeleton [452], the redistribution of cytoskeletal components could also be studied.

$15dPGJ_2$ induced autophagic cell death in neuroblastoma cells and therefore may have potential as a therapy for neuroblastoma. However, increasing the efficacy of

activation of PPAR-induced transcription would also be advantageous, as long as it did not increase toxicity. Activation of peroxisome proliferator-activated receptor-retinoid X receptor (PPAR-RXR) heterodimers can be maximised when both receptors are bound by their respective ligands. Simultaneous treatment of liposarcoma cells with both PPAR and RXR ligands has been shown to increase cell differentiation [241]. Combinations of troglitazone and *all-trans* retinoic acid in MCF-7 breast cancer cells synergistically and irreversibly inhibit cell growth and induces apoptosis [242] and rosiglitazone and 9-*cis* RA synergistically inhibit the growth of leukaemia cells [243]. However, a combination of $15dPGJ_2$ and 9-*cis* RA were not able to synergistically inhibit the growth of IMR-32 cells or synergistically increase IMR-32 cell death (Figures 4.22 and 4.23). This is in contrast to data showing that $15dPGJ_2$ and 9-*cis* RA inhibited the growth of bladder cancer cells [434] and synergistically activated a reporter construct containing a PPRE cloned upstream of a luciferase reporter gene [434]. In bladder cancer cells, it is thought that the RXR ligand sensitises the cells to death induced by the $15dPGJ_2$ or synthetic PPARγ ligands [434]. However, one group has shown that combinations of troglitazone and retinoic acids are not synergistic, as they do not inhibit the growth of prostate cancer cells [130].

Combinations of DHA and $15dPGJ_2$ also were not synergistic in inhibiting the growth of IMR-32 cells, but instead DHA antagonised some of the growth inhibitory effects of the prostaglandin (Figure 4.21). Both DHA and $15dPGJ_2$ bind to PPARs and DHA could have been competing with $15dPGJ_2$ for PPARγ and preventing the prostaglandin from activating PPAR-induced transcription. This suggests that DHA may bind to PPARs more strongly than $15dPGJ_2$, but does not necessarily induce stronger growth inhibitory effects. Differences in binding of PPAR ligands to PPARγ have also been proposed as a mutant form of PPARγ, PPARγR288H, has an affinity for troglitazone equivalent to that of the wild type PPARγ, however, this mutant has reduced binding affinity for $15dPGJ_2$ compared to the wild type [352]. DHA has only been shown to activate RXR in mouse brain [307] and it may not activate RXR in human cells or activation of both partners within the heterodimer may not produce a synergistic effect in IMR-32 cells.

It is interesting that $15dPGJ_2$ also has diverse effects in different neuroblastoma cell lines, including apoptosis in SHSY5Y cells, differentiation in Lan-5 cells and autophagy in IMR-32 cells. This may reflect differences between the cell lines, as SHSY5Y cells are derived from SK-N-SH neuroblastoma cells and are non-NMYC amplified Schwannian-type neuroblastoma cells [460], whereas IMR-32 cells and Lan-5 cells are both NMYC amplified neuroblast-like neuroblastoma cell lines [77]. Lan-5 cells and IMR-32 cells have previously been shown to respond differently to retinoic acid [77]. Lan-5 cells were more susceptible to growth inhibition by 1 μM retinoic acid than IMR-32 cells and Lan-5 cells also extended their neurites in response to treatment with 3 μM retinoic acid, whereas IMR-32 cells underwent cellular enlargement and vacuolisation [77]. SHSY5Y cells have low cell motility an invasiveness, whereas, IMR-32 cells are high invasive and have high cell motility [461]. IMR-32 cells are also more sensitive to the effect of the chelating agent, desferroxamine than SHSY5Y cells [462]. It is also interesting to note that the distinct effects of $15dPGJ_2$ on the different neuroblastoma cells lines require different concentrations of $15dPGJ_2$. Lan-5 cells differentiate [342] and SHSY5Y cells apoptose [362] in response to 10 μM $15dPGJ_2$, whereas little effects are seen at 5 μM $15dPGJ_2$ and below. However, at 5 μM $15dPGJ_2$, IMR-32 cells underwent autophagic cell death and at 10 μM no IMR-32 cells remained viable, but had not undergone apoptosis, at 3 days post-initial treatment, whereas over 60 % of Lan-5 cells can withstand treatment with 20 μM $15dPGJ_2$ for 6 days [342]. This may reflect differences in levels of expression of PPARγ, differences in gene expression downstream of PPARγ or differences in regulation of the receptor. Importantly, SHSY5Y cells express higher levels of PPARγ than IMR-32 cells and therefore this suggests that levels of PPARγ expression are important in influencing the effects of $15dPGJ_2$ on cells (personal communication, Dr. Cimini, University of L'Aquila, Coppito, Italy).

It would be an exciting prospect to look at the effects of ligands of PPARγ on primary cancer cells and in models of cancer. Obviously, to have potential in the treatment of cancer ligands of PPARγ need to be effective against primary cancer cells and also to have limited toxicity to normal cells. Studies using animal models of cancer or soft agar assays could be used to establish the efficacy of PPARγ

ligands, however, a note of caution should be taken when considering the value of animal models for studying PPARs. This is because it has been shown that rodents and humans respond differently to ligands of PPARs [112, 309], and activation of PPARγ can induce proliferation of cancer cells and increase polyp formation in animal models of familial human colon cancer [350, 351]. The soft agar assay has the advantage of using human cells, but also has the disadvantage of not involving all of the environmental features, which would influence the growth of a tumour, such as blood vessels. Excitingly, $15dPGJ_2$ potently inhibits angiogenesis [371], the formation of new blood vessels from pre-existing ones, which is involved in cancer, where unrestricted tumour growth is dependent on angiogenesis [369, 370]. Preventing angiogenesis therefore is a method of treating cancers. The effect of $15dPGJ_2$ on angiogenesis can be determined using human endothelial cells in a collagen matrix culture, which form tubes and this may be inhibited by $15dPGJ_2$. Artificial tumours grown in nude mice will develop blood vessels and it would be of interest to see whether $15PGJ_2$ can reduce both cancer cell growth and blood vessel formation *in vivo*, acting as a double-edged treatment for cancer. It would also be interesting to look at the effects of other ligands of PPARγ on neuroblastoma cells.

In conclusion, the natural ligand of PPARγ effectively inhibited the growth of neuroblastoma cell lines and induced autophagic cell death, without features of apoptosis in IMR-32 cells. Therefore, PPARγ ligands, such as $15dPGJ_2$ have potential as a treatment for neuroblastoma however combinations of drugs to activate both PPARs and RXRs may not be the answer. TZD drugs also activate PPARγ and could have potential in the treatment of neuroblastoma. However, neuroblastoma affects young children and the use of drugs, which have already been marketed for diabetes therapy, to treat their cancer could have side effects, therefore the natural ligand for PPARγ, $15dPGJ_2$ may be a better candidate. In addition, the effects of ligands of PPARγ need to be confirmed as PPARγ-dependent and the mechanism of action of PPARγ established. This is because the downstream pathways of activated PPARγ have yet to be fully elucidated. These would need to be known before its suitability as a drug target could be confirmed and this will be covered in the following chapter.

Chapter 5

Mechanism of action of PPAR Ligands in IMR-32 cells

5.1 *Introduction*

The peroxisome proliferator-activated receptor γ ligand, 15-deoxy$\Delta^{12,14}$-prostglandin J_2 ($15dPGJ_2$), effectively inhibited the growth of the human neuroblastoma cell lines, IMR-32 and Kelly. In IMR-32 cells, this was achieved through growth arrest at G_2/M and subsequent autophagic cell death. However, before ligands of PPARγ can be considered as potential therapies for the treatment of cancer, their mode of action should be fully established. This is because PPARγ ligands including $15dPGJ_2$ and thiazolidinediones (TZDs) such as troglitazone (TGZ), can induce cellular effects by mechanisms independent of PPARγ [190, 463]. These receptor-independent effects are though to be due to the reactive cyclopentenone ring found in $15dPGJ_2$ [192, 464]. $15dPGJ_2$ also inhibits the synthesis of prostaglandin E_2 in rheumatoid arthritis [465] and inhibits the production of matrix metalloproteinase 9 and interleukins during inflammation [331] independently of PPARγ.

Troglitazone inhibits cholesterol biosynthesis [203] and activates glucocorticoid-mediated transcription in osteosarcoma cells independently of PPARγ [466]. It also inhibits cell proliferation and tumour growth in a PPARγ-independent manner, through cell cycle arrest at G_1 in wild-type PPARγ (+/+) and null PPARγ (-/-) mouse embryonic stem (ES) cells and cells which express different levels of PPARγ [463]. TGZ inhibits translation initiation by depleting intracellular calcium stores, resulting in activation of protein kinase R (PKR) [463]. Active PKR phosphorylates and inactivates elongation initiation factor 2 (eIF2), preventing the exchange of GDP for GTP by eIF2B, thus inhibiting the formation of the pre-initiation complex required for translation [463]. Fatty acids [467] and peroxisome proliferators [468] can also act independently of PPARα and therefore it is important to establish effect on cancer cells induced by PPAR ligands are occurring through PPARs and how they inhibit cell growth.

Different levels of PPARγ expression have been seen in neuroblastoma cells (personal communication, Dr. Cimini, University L'Aquila, Coppito, Italy) [343, 342] and primary neuroblastomas, with decreasing expression of PPARγ in cells of a

more undifferentiated phenotype, which represent a later stage of the disease [342]. One case of neuroblastoma with predominantly primitive neuroblasts showed no expression of PPARγ [342]. Interestingly, post-mitotic cells of the peripheral and central nervous system have been shown to express high levels of PPARγ [129, 339]. Different neuroblastoma cell lines have been shown to respond differently to the ligand of PPARγ, $15dPGJ_2$. SHSY5Y cells undergo apoptosis [362], Lan-5 cells differentiate [342] and IMR-32 cells undergo autophagic cell death and this may relate to differences in the levels of PPARγ between cell lines.

Therefore, reducing the levels of PPARγ would presumably promote cell growth at a faster rate than that of normal cells. Indeed, loss-of-function mutations of PPARγ have been associated with the development of colon cancer [352] where the lack of wild-type PPARγ may prevent any restraint on cell growth, allowing the cells to proliferate at an accelerated rate. This may also occur in follicular thyroid carcinoma, where over 60 % of cases have the chromosomal translocation t(2;3)(q13;p25) [344]. This translocation results in an in-frame fusion of the PAX8 gene to the PPARγ gene and the formation of the PAX8PPARγ1 fusion protein, which has dominant negative activity [344]. One patient with follicular thyroid cancer had an in-frame fusion of PPARγ to an unknown protein [344]. The dominant negative effect of PAX8PPARγ1 may be one mechanism in the formation of follicular thyroid cancer. This dominant negative PPARγ provides a useful tool to prove the involvement of PPARγ in the $15dPGJ_2$-induced effects on IMR-32 cells.

The target genes of PPARγ need to be established, as little is known about the downstream effects of activated PPARγ, which are specifically involved in the inhibition of cancer cell growth. However, the expression of some cell cycle regulators are altered in cells treated with PPARγ ligands, including $p21^{CIP1/SDI1/WAF1}$ expression, which is increased in bladder cancer cells treated with troglitazone [434] and cMYC, which is down-regulated in HL-60 cells treated with $15dPGJ_2$ [469]. Ligands of PPARγ also have very different effects on cancer cells [183, 207, 342, 346, 371] in addition to their role in normal cells [133, 152] and activation of PPARγ by different concentrations of $15dPGJ_2$ induces different responses in breast cancer

cells [431, 432]. Therefore, the precise role of PPARs and the action of their ligands should be fully investigated in each cell type, before the value of PPAR ligands as therapies can be determined.

5.2 *Mechanism of Action of PPAR Ligands*

5.2.1 *PPARγ mRNA and protein expression levels are not altered on treatment with ligands of PPARs*

Treatment of 3T3-L1 adipocytes with troglitazone, rosiglitazone or $15dPGJ_2$ reduces the expression of PPARγ mRNA [279] and therefore, IMR-32 cells were treated with $15dPGJ_2$ and the effect on PPARγ mRNA and protein expression determined. IMR-32 cells were treated with 5 μM $15dPGJ_2$ or 5 μM Wy-14643 for 24 or 72 hours and total RNA was isolated from the cells. 1 μg RNA was reversed transcribed to cDNA, which was analysed for expression of PPARγ using RT-PCR with PPARγ specific primers. 5 μl of the RT-PCR reactions were electrophoresed after 30, 35 and 40 cycles of RT-PCR to ensure that the reactions were in the exponential phase. No changes in PPARγ mRNA were seen in IMR-32 cells treated with any of the ligands or at any time point (Figure 5.1), suggesting that in these cells there is no auto-regulation of PPARγ transcripts.

Hauser *et al.*, [280] showed that PPARγ is regulated at the protein level on treatment with both $15dPGJ_2$ and synthetic PPARγ ligands. In adipocytes, PPARγ was degraded on receptor activation because the receptor was ubiquitinated and degraded by the proteasome, which is also thought to be involved in the normal turnover of PPARγ [280]. To assess whether PPARγ protein levels were down-regulated on treatment with PPARγ ligands, IMR-32 cells were treated with DMSO, 5 μM $15dPGJ_2$ or 5 μM Wy-14643 and protein extracts of the cells were probed with a PPARγ antibody. The PPARγ protein was not down-regulated on treatment with PPARγ ligands after 72 hours (Figure 5.2).

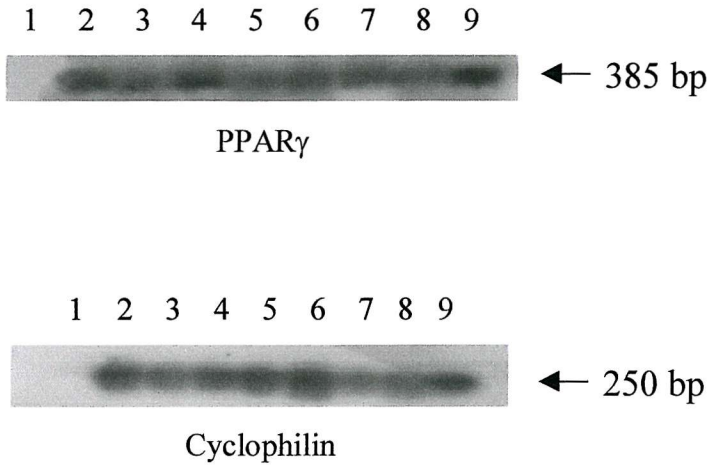

Lane 1	Negative control
Lane 2	Untreated
Lane 3	DMSO (24 hours)
Lane 4	DMSO (72 hours)
Lane 5	5 μM 15-deoxy$\Delta^{12,14}$-prostglandin J_2 (24 hours)
Lane 6	5 μM15-deoxy$\Delta^{12,14}$-prostglandin J_2 (72 hours)
Lane 7	5 μM Wy-14643 (24 hours)
Lane 8	5 μM Wy-14643 (72 hours)
Lane 9	3T3-L1 cells

Figure 5.1 Ligands of PPARs do not induce auto-regulation of the PPARγ transcript in IMR-32 cells. IMR-32 cells were treated with 5 μM 15dPGJ$_2$ or Wy-14643 for 24 or 72 hours and total RNA was isolated from the cells. PPARγ was detected by 35 cycles of RT-PCR using cDNA made from total cellular RNA and PPARγ-specific primers. The cDNA levels were normalised for using 30 cycles of RT-PCR and cyclophilin primers as a control.

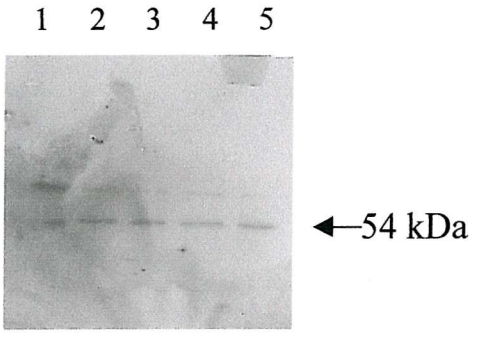

SDS-PAGE membrane

Lane 1	HaCaT cells
Lane 2	Untreated
Lane 3	DMSO
Lane 4	5 μM 15-deoxy$\Delta^{12,14}$-prostglandin J_2
Lane 5	5 μM Wy-14643

Figure 5.2 Ligands of PPARs do not induce auto-regulation of the PPARγ protein in IMR-32 cells. IMR-32 cells were treated with 5 μM 15dPGJ$_2$ or 5 μM Wy-14643 for 72 hours and cellular extracts were made. The cell extracts were resolved by SDS-PAGE and probed with an anti-PPARγ antibody.

This suggests that in IMR-32 cells, PPARγ was not targeted for destruction by the proteasome and may be degraded by a different mechanism. Interestingly, PPARα is degraded by proteasomes in a ligand-dependent manner [470].

5.2.2 *Ligands of PPARα and PPARγ activate PPAR-induced transcription in IMR-32 cells*

Ligands of PPARs bind to and activate PPARs, resulting in the transcription of genes, which can be measured using reporter gene assays. To establish whether PPAR ligands activated PPAR-induced transcription in neuroblastoma cell lines, IMR-32 cells were transiently transfected with a chloramphenicol acetyl transferase (CAT) reporter construct containing three consensus peroxisome proliferator response elements (PPREs) cloned upstream of a thymidine kinase promoter [233]. The cells were then treated with DMSO, 5 μM $15dPGJ_2$ or 5 μM Wy-14643 for 72 hours and assayed for CAT activity. CAT activity in control treated cells was taken as 100 % and CAT activity in treated cells was corrected for this value. Wy-14643 activated the reporter construct 4-fold (Figure 5.3) showing that ligands of PPARα activated PPARs within IMR-32 cells. $15dPGJ_2$ increased the reporter gene activity 7-fold (Figure 5.3), showing that it activated PPARs more strongly than Wy-14643. The PPRE used in this experiment was not specific for the individual isoforms of PPAR and was therefore a measure of the activity of all isoforms. The experiment was repeated with a plasmid lacking the 3PPRE sequence, pBL_2CAT, to demonstrate that the activation of the reporter gene required the presence of the 3PPRE sequence (Figure 5.4).

5.2.3 *The effects of 15-deoxy$\Delta^{12,14}$-prostglandin J_2 on IMR-32 cells are not mediated through changes in membrane phospholipid composition*

PUFAs and $15dPGJ_2$ inhibit the growth of cancer cells through activation of PPARγ and PUFAs also inhibit cancer cell growth through altering the composition of membrane phospholipids [177, 408].

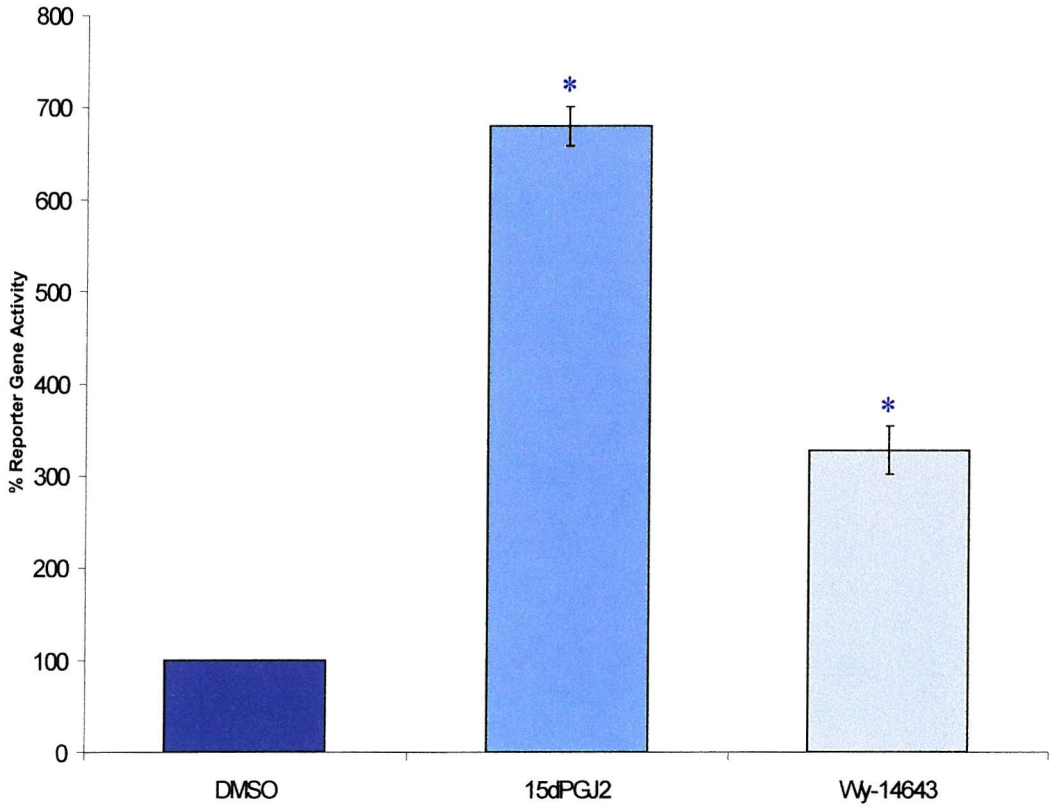

Figure 5.3 Ligands of PPARs activate PPAR-induced transcription in IMR-32 cells. IMR-32 cells were transiently transfected with a CAT reporter construct containing three consensus PPAR binding sites cloned upstream of a thymidine kinase promoter. Cells were treated with DMSO, 5 μM $15dPGJ_2$ or 5 μM Wy-14643 for 72 hours and CAT activity measured. Graphs represent two independent experiments with two samples per experiment. Values were normalised by transfection with β-galactosidase. Statistics were calculated using a t test and significance is represented as follows: $p<0.05$ (*).

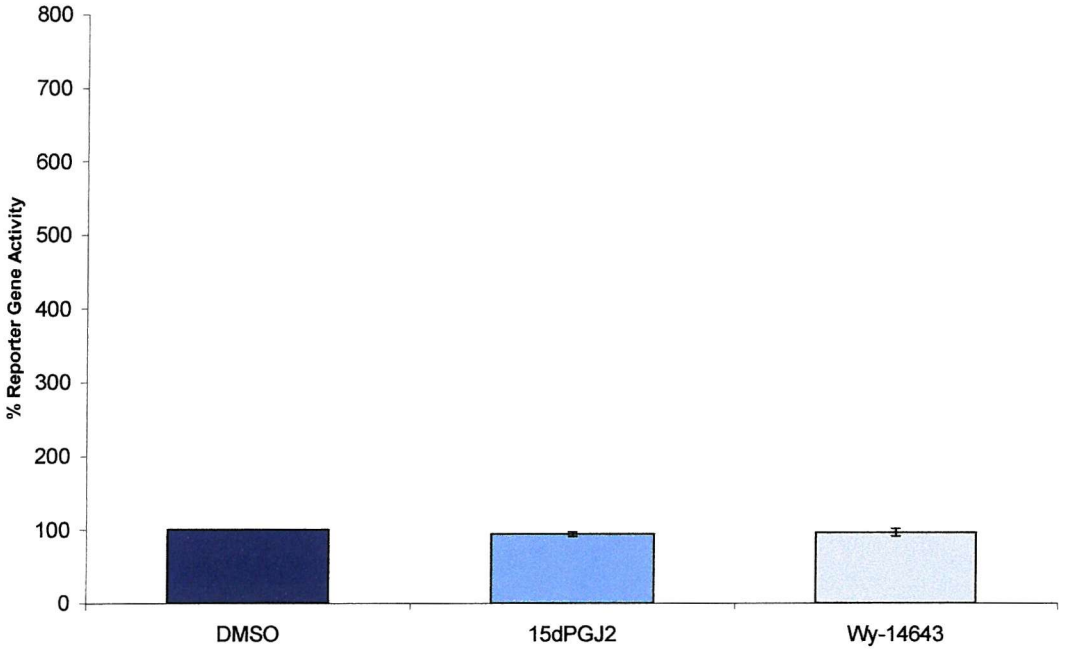

Figure 5.4 Ligands of PPAR do not activate transcription from control vectors lacking PPREs. IMR-32 cells were transiently transfected with a CAT reporter construct without an insert, as a control. Cells were treated with DMSO, 5 μM $15dPGJ_2$ or 5 μM Wy-14643 for 72 hours and CAT activity measured. Graphs represent two independent experiments with two samples per experiment. Values were normalised by transfection with β-galactosidase.

Membrane phospholipids of neuroblastoma cells treated with 5 μM $15dPGJ_2$ or Wy-14643 were extracted and analysed by electrospray ionisation mass spectrometry (ESI-MS) to determine whether the composition of phospholipids changed upon treatment. Samples of phosphatidylcholine (PtdCho) species, phosphatidylethanolamine (PtdEtn) and acid phospholipid species, which include phosphatidylinositol (PtdIns), phosphatidylglycerol and phosphatidylserine species were analysed. IMR-32 cells treated with 5 μM $15dPGJ_2$ for 24 and 72 hours resembled spectra of control-treated cells, with no changes in the composition of PtdCho species with either length of treatment and palmitoyl-oleoyl PtdCho (16:0/18:1) being the major species (data not shown and Figure 5.5). Likewise, no changes in the PtdEtn phospholipid fraction were observed in $15dPGJ_2$-treated IMR-32 cells at either 24 hours or 72 hours, with the major peak being stearoyl-arachidonyl PtdEtn (18:0/20:4) and no differences between the minor peaks (data not shown and Figure 5.6). Similarly, there were no differences in the acid phospholipid composition in IMR-32 cell membranes treated with $15dPGJ_2$ (data not shown and Figure 5.7). The major species of acid phospholipids seen were stearoyl-arachidonyl PtdIns (18:0/20:4) and palmitoyl-oleoyl phosphatidylglycerol (16:0/18:1) (Figure 5.7). This suggests that the growth inhibitory effects of PPARγ are not mediated through changes to the membrane phospholipid composition of IMR-32 cells. Unsurprisingly, Wy-14643 had no effect on the membrane phospholipids of IMR-32 cells (Figures 5.5 and 5.7).

5.2.4 *$15dPGJ_2$-induced growth inhibition of IMR-32 cells involves activation of not antagonism of NFκB*

Some of the effects of PPARγ in macrophages occur through inhibition of gene expression through antagonising the activities of transcription factors such as AP-1 and NFκB [190]. NFκB is a transcription factor, involved in regulation of genes involved in inflammation [471], apoptosis [472] and neuronal development and differentiation [473]. NFκB is activated prior to retinoic acid-induced differentiation of SHSY5Y cells [473] and bromodeoxyuridine-induced differentiation in IMR-32 cells [474].

Figure 5.5 Ligands of PPARs do not mediate changes to IMR-32 cell membrane phosphatidylcholine composition. IMR-32 cells were treated with 5 μM $15dPGJ_2$ or 5 μM Wy-14643 for 72 hours and phosphatidylcholine (PtdCho) species were isolated from the cell membranes. The PtdCho samples were analysed by tandem electrospray ionisation $^{+ve}$ mass spectrometry (ESI^{+ve} MS) and spectra of parent species of 184 were produced. 184 is the mass of the phosphocholine head group. Mass spectra were shown as peak intensity and mass/charge (m/z) and each spectrum is representative of duplicate samples.

Control IMR-32 cell membrane PtdCho molecular species composition after 72h DMSO vehicle

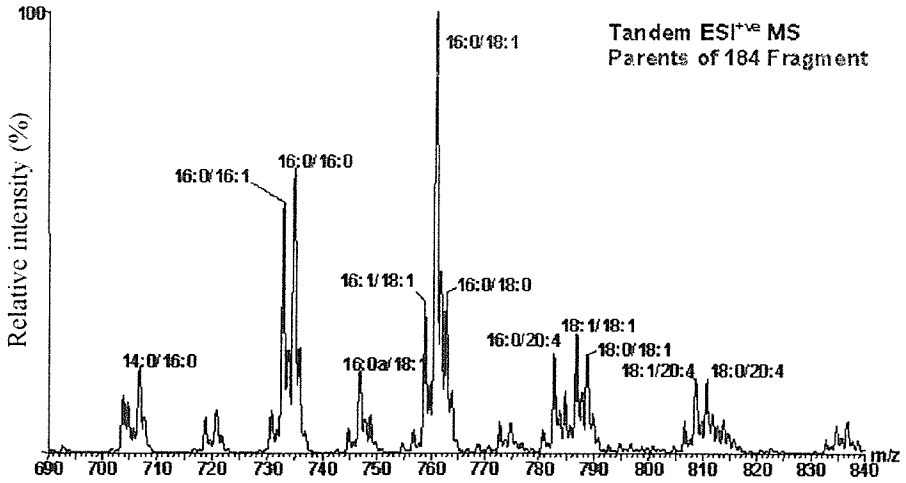

IMR-32 cell membrane PtdCho molecular species composition after 72h 15dPG J_2 exposure

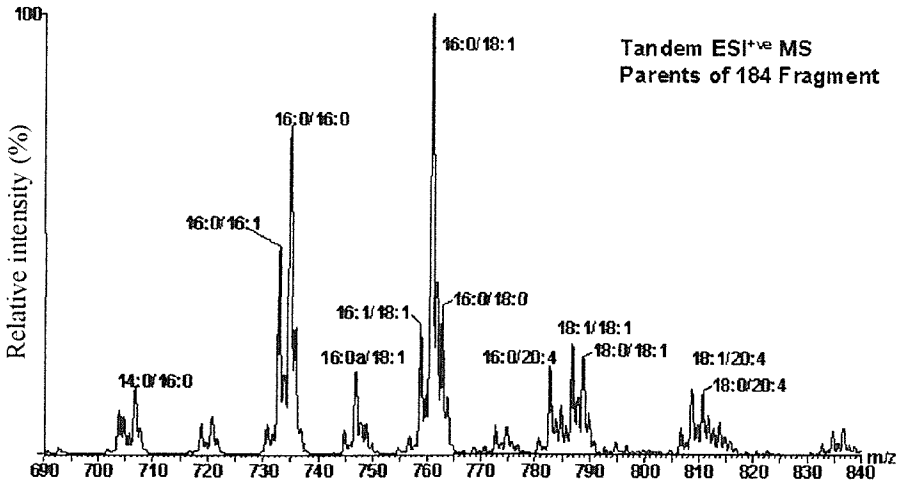

IMR-32 cell membrane PtdCho molecular species composition after 72h WY-14,643 exposure

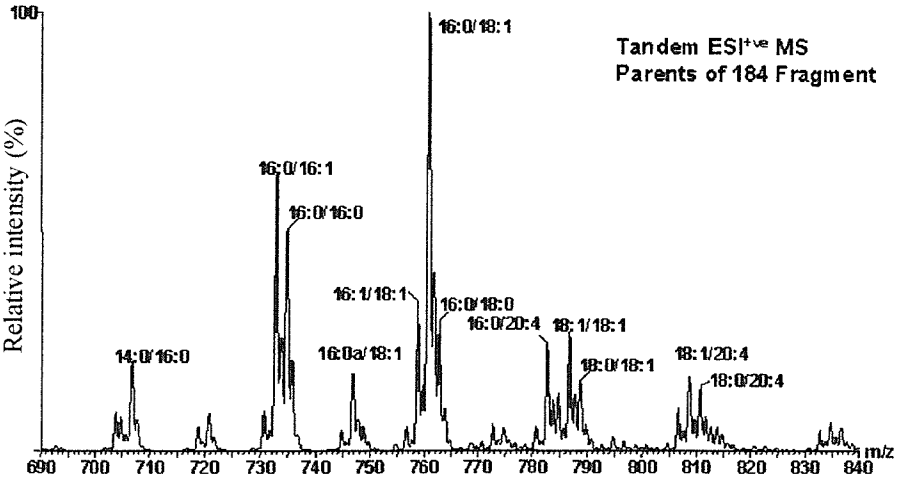

Figure 5.6 Ligands of PPARs do not mediate changes to IMR-32 cell membrane phosphatidylethanolamine composition. IMR-32 cells were treated with 5 μM 15dPGJ$_2$ or 5 μM Wy-14643 for 72 hours and phosphatidylethanolamine (PtdEtn) species were isolated from the cell membranes. The PtdEtn samples were analysed by electrospray ionisation $^{-ve}$ mass spectrometry (ESI^{-ve} MS) and mass spectra were shown as peak intensity and mass/charge (m/z). Each spectrum is representative of duplicate samples.

Control IMR-32 cell membrane PtdEtn molecular species composition after 72h DMSO vehicle

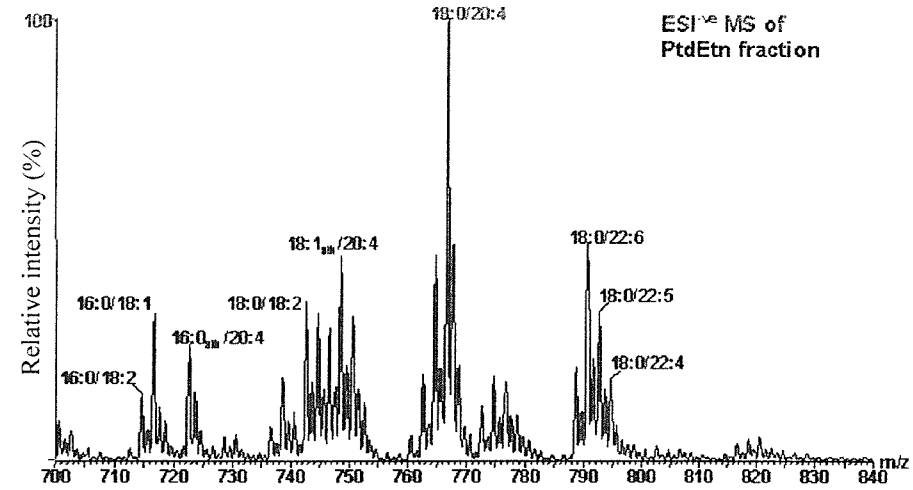

IMR-32 cell membrane PtdEtn molecular species composition after 72h 15dPG J_2 exposure

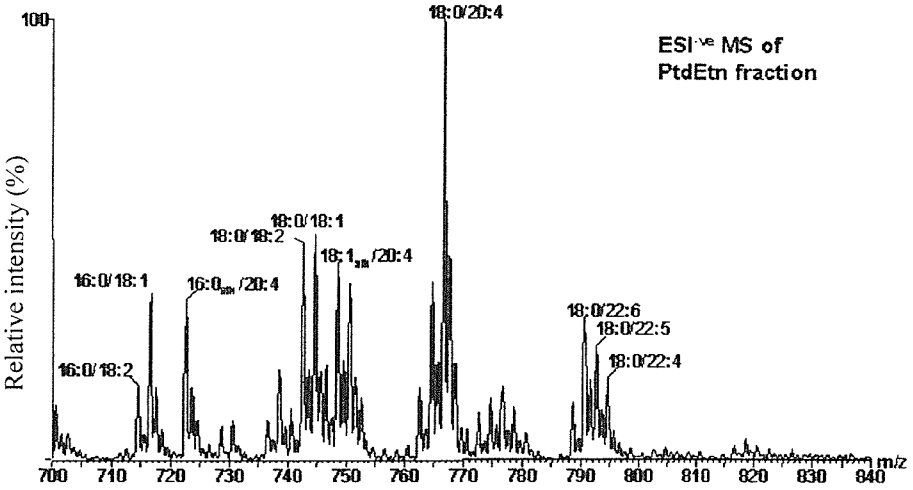

IMR-32 cell membrane PtdEtn molecular species composition after 72h WY-14,643 exposure

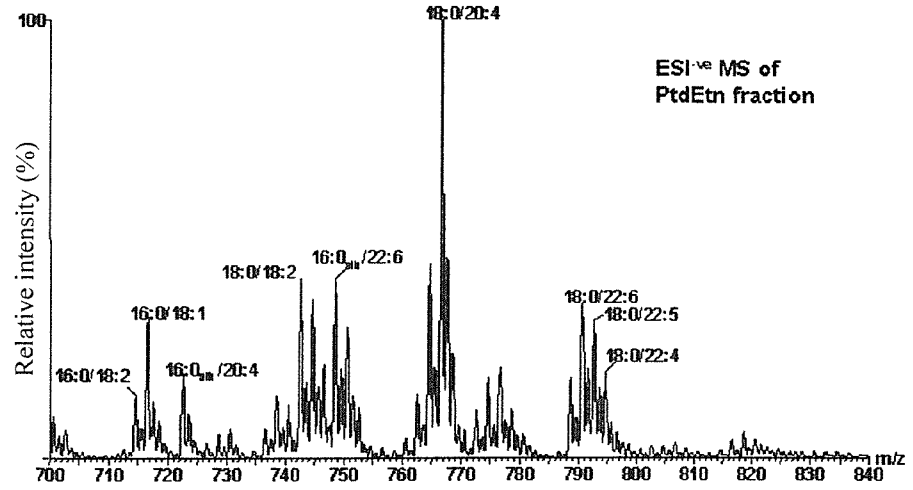

Figure 5.7 Ligands of PPARs do not mediate changes to IMR-32 cell membrane acid phospholipid composition. IMR-32 cells were treated with 5 μM $15dPGJ_2$ or 5 μM Wy-14643 for 72 hours and acid phospholipid species were isolated from the cell membranes. The acid phospholipid samples were analysed by electrospray ionisation $^{-ve}$ mass spectrometry (ESI^{-ve} MS) and mass spectra were shown as peak intensity and mass/charge (m/z). Each spectrum is representative of duplicate samples.

Control IMR-32 cell membrane PtdIns molecular species composition after 72h DMSO vehicle

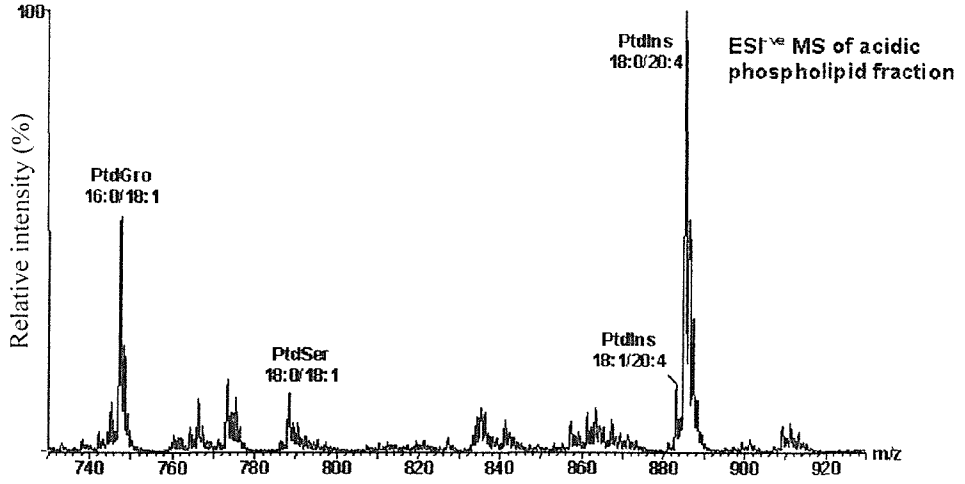

IMR-32 cell membrane PtdIns molecular species composition after 72h 15dPG J_2 exposure

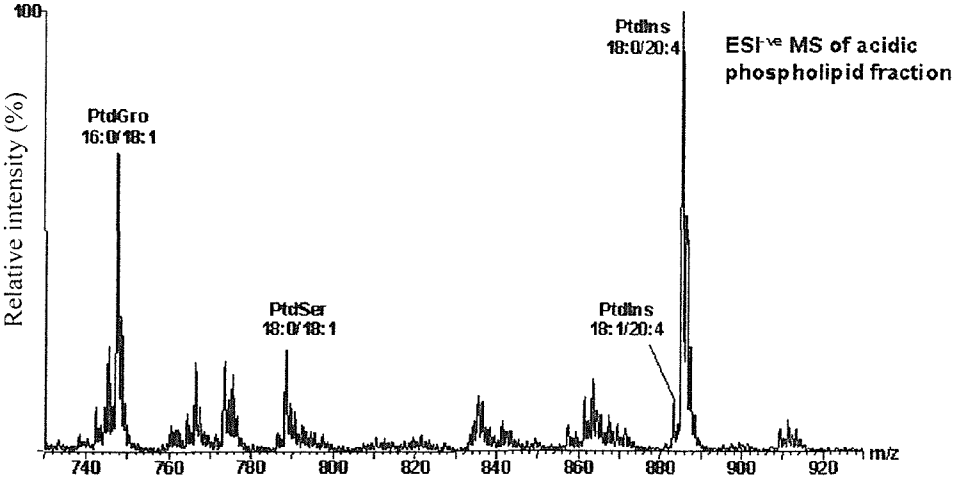

IMR-32 cell membrane PtdIns molecular species composition after 72h WY-14,643 exposure

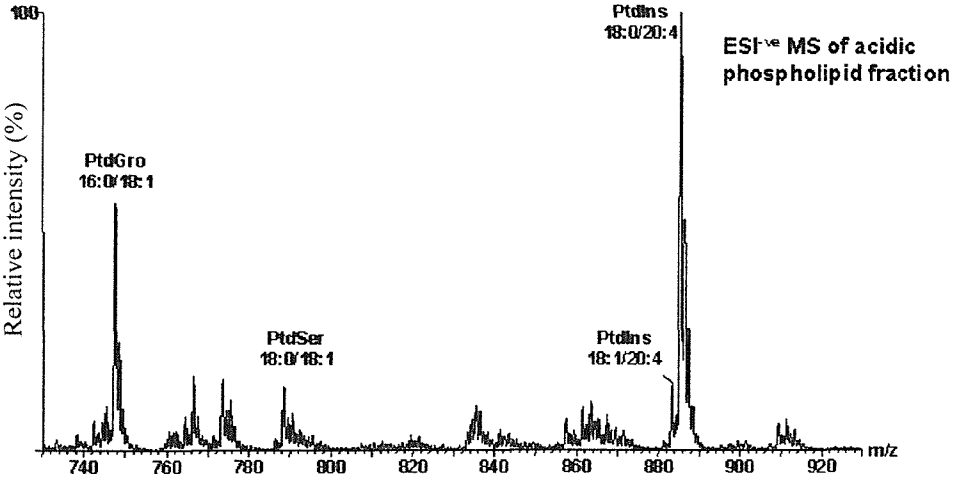

To determine whether $15dPGJ_2$ antagonised NFκB in IMR-32 cells, the cells were transiently transfected with 5 μg of a luciferase reporter construct containing a binding site for NFκB linked to a luciferase reporter gene. IMR-32 cells were also transfected with 5 μg pGL_3Basic as a control. After transfection, the cells were treated with DMSO or 5 μM $15dPGJ_2$ and luciferase activity measured after 72 hours. No changes were seen in the levels of NFκB-induced transcription in the IMR-32 cells treated with DMSO, however, in IMR-32 cells treated with $15dPGJ_2$ for 72 hours, there was an increase in NFκB-induced transcription by 3 fold (Figure 5.8). This suggests that PPARγ does not act by antagonising NFκB in IMR-32 cells, but through activation of NFκB. It is not known whether $15dPGJ_2$ antagonises or activates NFκB-induced transcription in Kelly cells.

5.2.5 *The growth inhibitory effects of 15-deoxy$\Delta^{12,14}$-prostglandin J_2 on IMR-32 cells are mediated through PPARs*

The decoy method was employed to show that $15dPGJ_2$ acts through PPARs. Decoy oligonucleotides can be used to prevent binding of a transcription factor to DNA and activating transcription (Figure 5.9) and this method was used by Bishop-Bailey and Hla [183] to prove that $15dPGJ_2$ induces endothelial cell apoptosis through activation of PPARγ. They transfected an endothelial cell line with oligonucleotides containing DNA binding sequences for PPARs (PPREs) and scrambled controls and treated the cells with natural and synthetic PPARγ ligands [183]. They showed that this method specifically prevented transcription of a reporter gene, linked to a PPRE, in cells treated with $15dPGJ_2$, using the decoy oligonucleotide, but not in the cells transfected with the control or scrambled oligonucleotide [183].

To confirm $15dPGJ_2$ acted through PPARs in IMR-32 cells, the cells were transiently transfected with decoy plasmids and treated with 5 μM $15dPGJ_2$. The plasmid used as a "decoy" (3PPRE-TK-CAT) contains a triple repeat of a consensus PPAR binding site (rat *Aco*-PPRE: AGGAGAAAGGTCA) [233] (the decoy sequence) (Figure 5.9) and the control plasmid (pBL_2CAT) lacks this sequence.

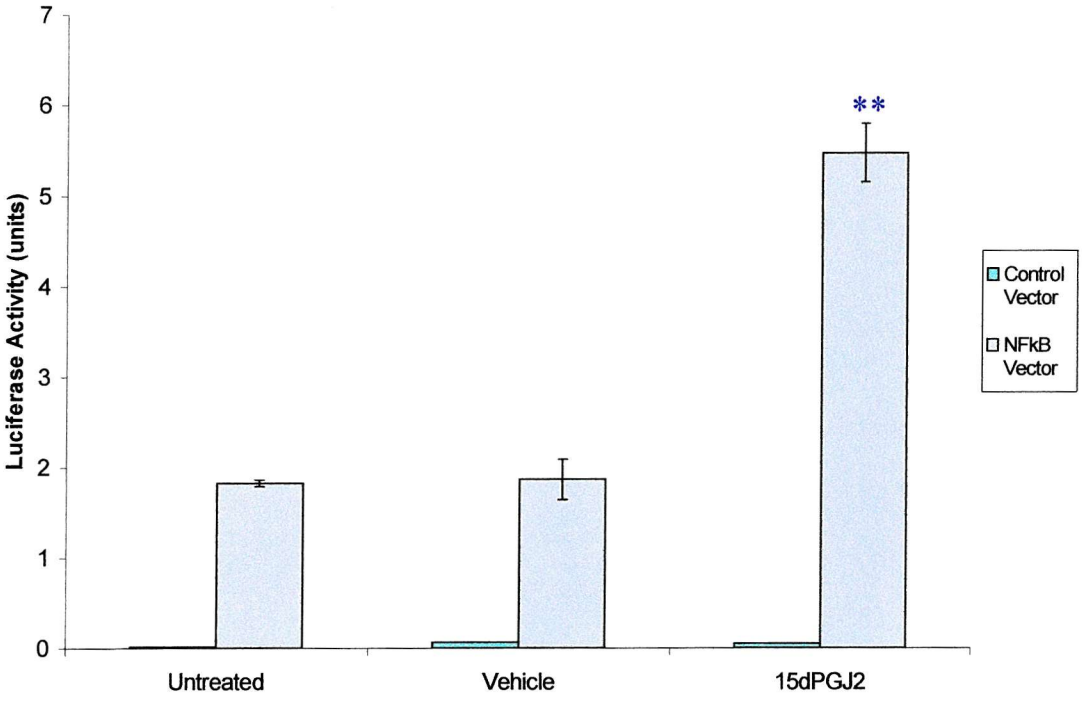

Figure 5.8 15dPGJ$_2$ does not act-independently of PPARγ through antagonism of NFκB, but actually activates NFκB-induced transcription. IMR-32 cells were transiently transfected with 5 μg of a reporter construct containing an NFκB binding site. The cells were treated with 5 μM 15dPGJ$_2$ for 72 hours and NFκB activity measured by increases in reporter gene activity. Graphs represent two independent experiments with two samples per experiment. Control cells were transfected with 5 μg pGL$_3$Basic. Statistics were calculated using a t test and $p < 0.01$ (**).

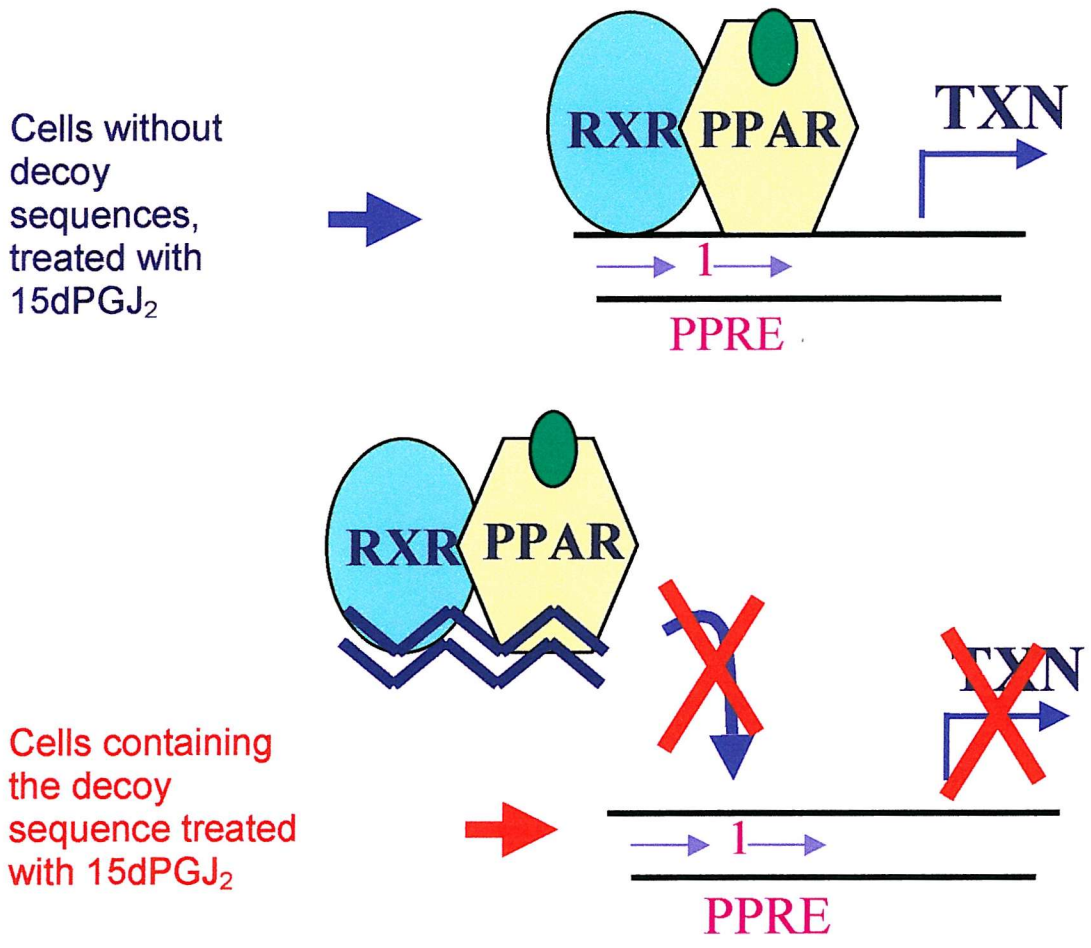

Figure 5.9 Theory of the decoy method. Decoy sequences (a DNA sequence to which the receptor binds) are transfected into cells to "bind out" PPARs, preventing them from binding to DNA and activating transcription. The decoy sequence used can simply be an oligonucleotide or the sequence can be contained within a plasmid, as was used for the experiments described in this chapter.

20 μg of DNA was transfected in each case, with 0 μg, 10 μg and 20 μg decoy used, and the remainder being made up using a β-galactosidase vector, to control for the amounts of DNA transfected. After transfection, the cells were treated with DMSO or 5 μM $15dPGJ_2$, every 24 hours and total cell numbers determined. DMSO-treated IMR-32 cells transfected with increasing amounts of decoy plasmid, increased in number throughout the experiment, even when 20 μg of the decoy plasmid was transfected into the cells (Figure 5.10). IMR-32 cells transfected with 20 μg β-galactosidase and 0 μg decoy plasmid and treated with 5 μM $15dPGJ_2$ grew slowly with only a small increase in cell number within 72 hours (Figure 5.10). However, when IMR-32 cells were transfected with 10 μg decoy plasmid and 10 μg β-galactosidase and treated with $15dPGJ_2$, cell growth increased throughout the experiment. Therefore, despite treatment with $15dPGJ_2$, these cells continued to grow, so that within 72 hours, 10 μg of the decoy plasmid reduced $15dPGJ_2$-induced growth inhibition by almost 50 %. IMR-32 cells transfected with 20 μg decoy plasmid showed even greater increases in number throughout the experiment and the numbers of cells at all time points were not significantly different from the numbers of DMSO-treated IMR-32 cells transfected with 20 μg decoy plasmid (Figure 5.10).

IMR-32 cells transfected with increasing concentrations of the control plasmid (pBl_2CAT) and treated with DMSO, increased in number throughout the experiment, from 5×10^5 to 36×10^5 cells (Figure 5.11). However, the growth of IMR-32 cells transfected with increasing amounts of control plasmid and treated with 5 μM $15dPGJ_2$ was inhibited, as cell number only reached 15×10^5 cells (Figure 5.11). Even IMR-32 cells transfected with 20 μg of the control plasmid and treated with 5 μM $15dPGJ_2$ grew similarly to those treated with $15dPGJ_2$ and not transfected with any plasmid, indicating that this effect was specific to the PPRE. This shows that increasing amounts of decoy plasmid specifically prevented PPAR-induced transcription of growth-inhibitory genes, despite the receptors being activated by $15dPGJ_2$, therefore indicating that the effects of $15dPGJ_2$ on IMR-32 cells occurred through PPARs.

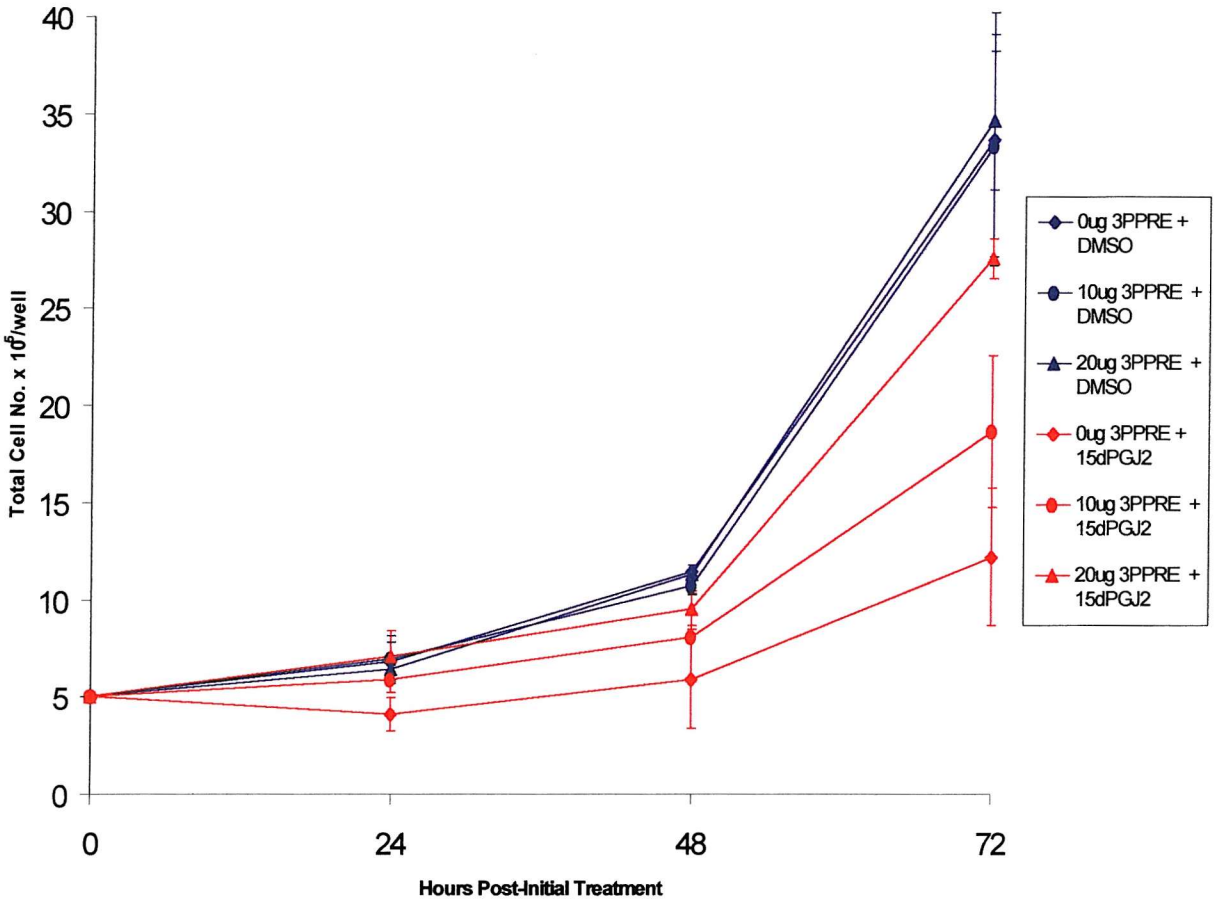

Figure 5.10 Decoy plasmids show that 15dPGJ2 acts through PPARs to inhibit IMR-32 cell growth. IMR-32 cells were transiently transfected with a reporter construct containing 3 consensus PPREs and were treated with DMSO or 5 μM 15dPGJ2 over 72 hours. Graphs represent two independent experiments with two samples per experiment. Transfections were normalised using a β-galactosidase vector.

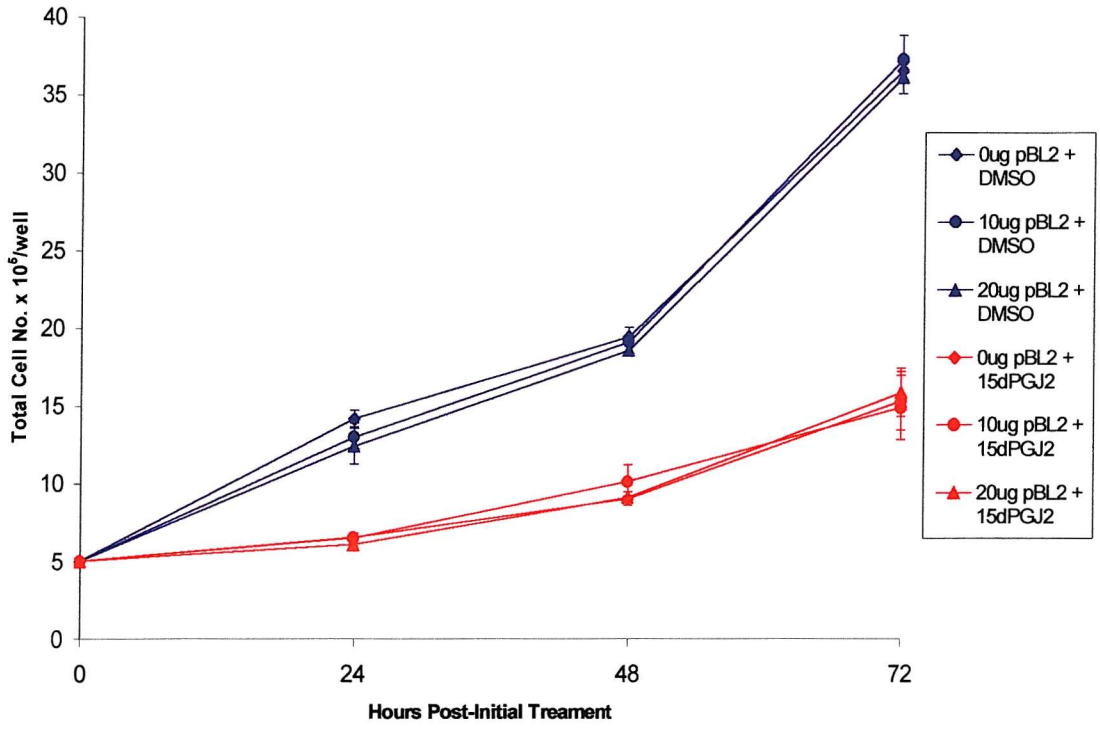

Figure 5.11 Control plasmids show that $15dPGJ_2$ acts through PPARs to inhibit IMR-32 cell growth. IMR-32 cells were transfected with 5 μg of a plasmid DNA lacking the decoy sequence (pBl_2) and the cells were treated with 5 μM $15dPGJ_2$. The effects on cell growth were measured by counting cell number for 72 hours. Graphs represent two independent experiments with two samples per experiment. Transfections were normalised using β-galactosidase.

5.2.6 *15-deoxy$\Delta^{12,14}$-prostglandin J_2 acts through PPARs to induce the death of IMR-32 cells*

The decoy method was also used to show that 15dPGJ$_2$-induced IMR-32 cell death through PPARs. IMR-32 cells were transfected with the decoy or control plasmids and treated with DMSO or 5 μM 15dPGJ$_2$, and cell viability was measured using the trypan blue exclusion assay. IMR-32 cells transfected with increasing amounts of decoy plasmid and treated with DMSO did not undergo cell death within 72 hours (Figure 5.12). 30 % of IMR-32 cells transfected with 0 μg decoy plasmid and 20 μg β-galactosidase and treated with 5 μM 15dPGJ$_2$ underwent cell death, whereas only 20 % of those cells transfected with 10 μg decoy plasmid and 10 μg β-galactosidase and treated 5 μM 15dPGJ$_2$ underwent cell death (Figure 5.12). IMR-32 cells transfected with 20 μg decoy plasmid and treated with 5 μM 15dPGJ$_2$, resulted in the death of less than 15 % of the cells (Figure 5.12).

IMR-32 cells were also transfected with 0, 10 or 20 μg of the control plasmid and a β-galactosidase vector was used to ensure equal amounts of DNA were transfected. The cells were treated with 5 μM 15dPGJ$_2$ and cell death was determined using the trypan blue assay. IMR-32 cells transfected with increasing amounts of the control plasmid and treated with DMSO remained almost 90 % viable throughout the experiment (Figure 5.13). However, 30 % of IMR-32 cells transfected with increasing amounts of control plasmid, even up to 20 μg, and treated with 5 μM 15dPGJ$_2$ underwent cell death within 72 hours (Figure 5.13). Thus confirming 15dPGJ$_2$ acts through PPARs to induce transcription of target genes, which may be involved in growth inhibition.

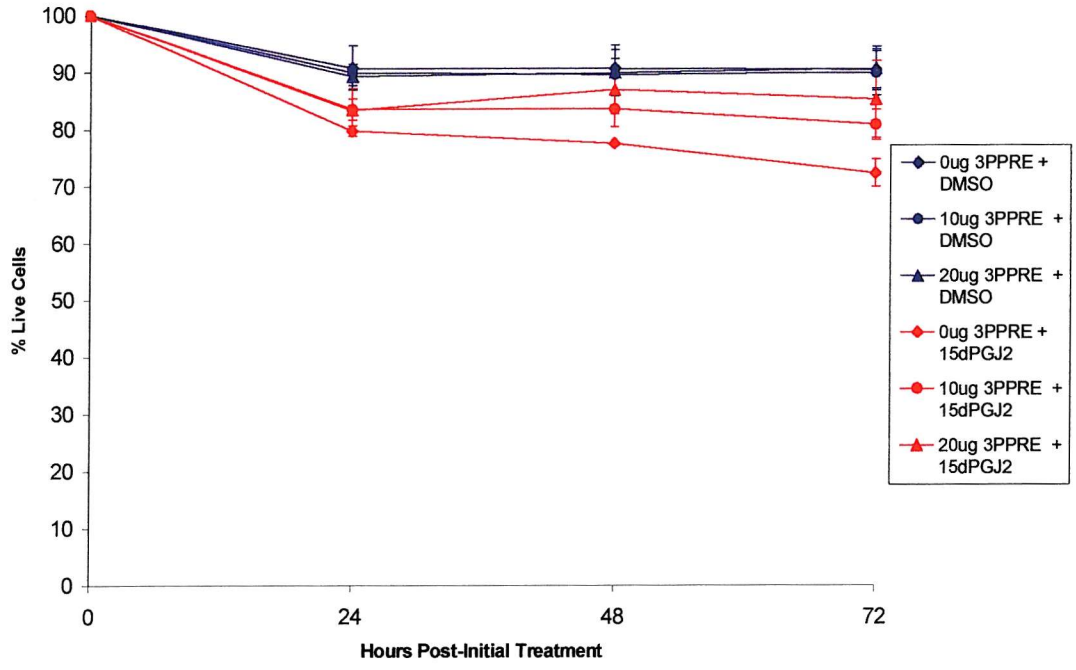

Figure 5.12 Decoy plasmids show that 15dPGJ$_2$ acts through PPARs to induce IMR-32 cell death. IMR-32 cells were transiently transfected with a reporter construct containing 3 consensus PPREs. The cells were treated with 5 μM 15dPGJ$_2$ and the effects on cell death measured by the trypan blue exclusion assay. The experiments were completed in duplicate with two samples per experiment and error bars represent errors of the mean.

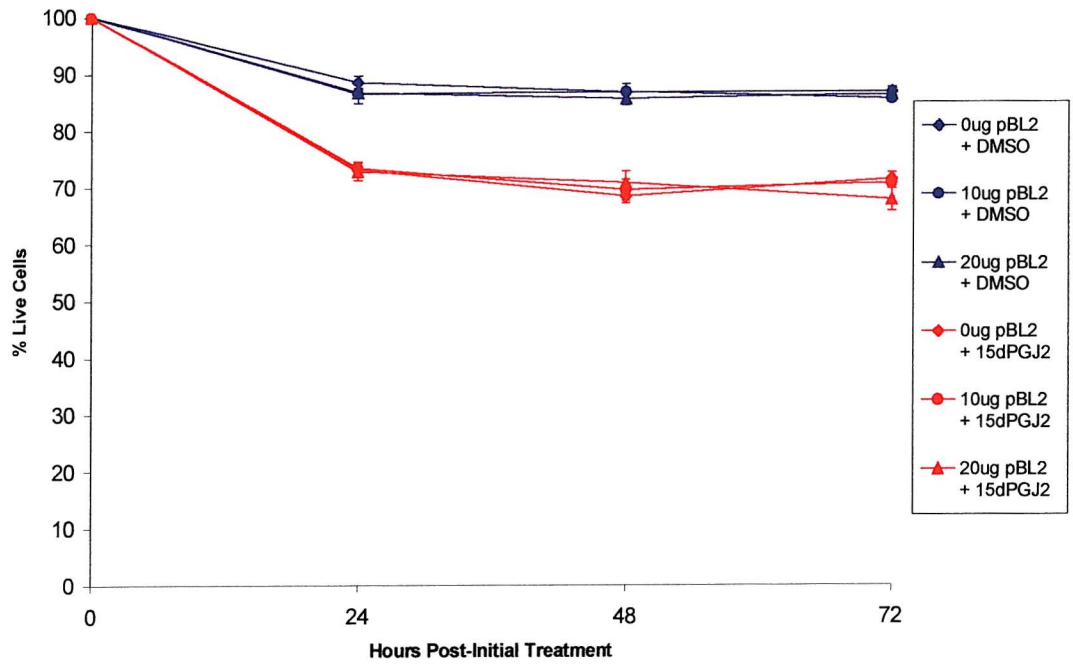

Figure 5.13 Control plasmids show that 15dPGJ$_2$ acts through PPARs to induce IMR-32 cell death. IMR-32 cells were transiently transfected with a plasmid DNA lacking the decoy sequence (pBl$_2$). The cells were treated with 5 μM 15dPGJ$_2$ and the effects on cell death measured by the trypan blue exclusion assay. The experiments were completed in duplicate with two samples per experiment and error bars represent errors of the mean.

5.3 *PPARγ dominant negative mutant – PAX8PPARγ1*

The activity of wild-type PPARγ can be abrogated using dominant negative PPARγ, which prevents activation of the wild-type receptor on treatment of cells with specific ligands of PPARγ. A dominant negative PPARγ protein has been identified in follicular thyroid cancer due to a chromosomal translocation, which forms an in-frame fusion of exons 1-7 and 9 of PAX8 to full-length PPARγ1 [344]. The dominant negative activity of PAX8PPARγ1 was confirmed by transfecting the cDNA for the mutant protein into U2OS cells alongside a reporter plasmid containing PPAR response elements [344]. PPARγ activation was induced by treatment of the cells with up to 500 nM rosiglitazone and reporter gene activity measured [344]. Reporter gene activity was increased in control cells transfected with PPARγ alone, but in cells transfected with PAX8PPARγ1, PPARγ ligands could not induce activation of PPARγ, even with 500 nM rosiglitazone and in fact activation of PPAR-induced transcription was completely abrogated [344]. No effects of the PAX8 portion of the protein were reported [344]. Therefore IMR-32 cells were stably transfected with the cDNA for PAX8PPARγ1 and the effects on the cells established.

5.3.1 *IMR-32 cells transfected with PAX8PPARγ1 gene stably express the PAX8PPARγ1 fusion protein*

To confirm expression of PAX8PPARγ1, total RNA was isolated from PAX8PPARγ1 transfected IMR-32 cells and vector controls. 1 μg RNA was reverse transcribed to cDNA, which was amplified by RT-PCR using a forward primer to PAX8 and a reverse primer to PPARγ, to produce a PCR product which would contain a unique sequence of part of the PAX8 gene fused to PPARγ1 (Figure 5.14). Expression of the mutant protein was confirmed using a vector control, pcDNA3.1+©, and by amplifying the PAX8PPARγ1 cDNA from the PAX8PPARγ1 vector alone.

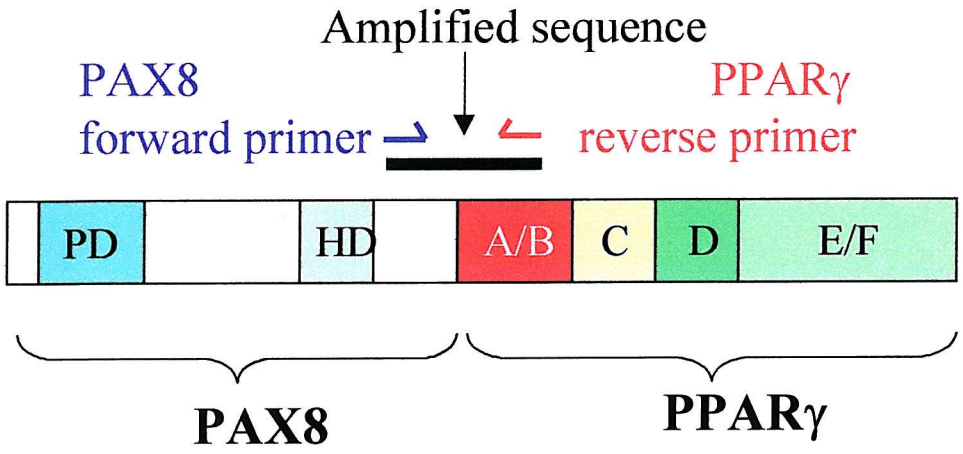

PD	PAX8 paired domain
HD	PAX8 homeodomain
A/B	PPARγ A/B domain
C	PPARγ DNA binding domain
D	PPARγ hinge region
E/F	PPARγ Ligand binding domain

Figure 5.14 The structure of the fusion protein, PAX8PPARγ1, showing RT-PCR primers and the range of the amplified sequence.

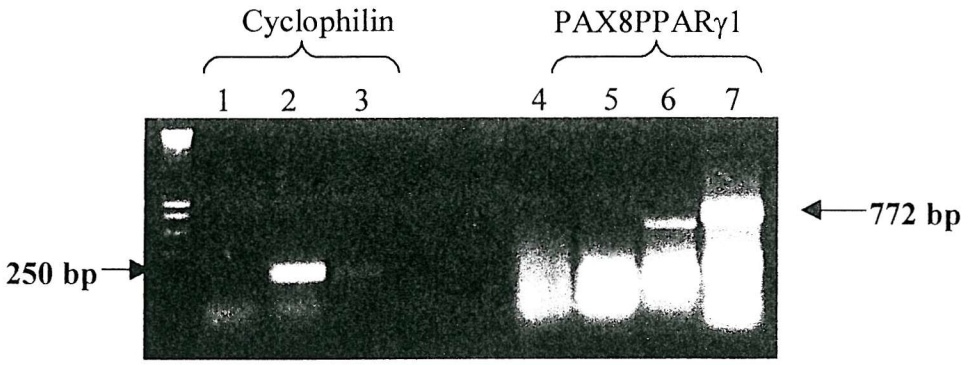

Lane 1	Negative control
Lane 2	IMR-32 cells - Vector control
Lane 3	IMR-32 cells – PAX8PPARγ1 clone
Lane 4	Negative control
Lane 5	IMR-32 cells - Vector control
Lane 6	IMR-32 – PAX8PPARγ1 clone
Lane 7	PAX8PPARγ1 cDNA plasmid

Figure 5.15 RT-PCR reactions showing expression of PAX8PPARγ1 dominant negative protein in IMR-32 cells. RNA was made from IMR-32 cells stably transfected with a plasmid containing the cDNA for PAX8PPARγ1 and reverse transcribed to cDNA. The cDNA was amplified at a unique sequence produced by the translocation of PAX8 to PPARγ1, using a forward primer for PAX8 and a reverse primer for PPARγ. The sequence was amplified for 50 cycles of denaturing at 94 °C for 40 seconds, annealing at 52 °C for 40 seconds and extension for 50 seconds at 72 °C. Control cells were stably transfected with pcDNA3.1+©alone. Cyclophilin primers were used control for amounts of cDNA used.

The RT-PCR reaction required a greater number of longer PCR cycles (see Materials and Methods) than used previously to amplified part of the PPARγ cDNA alone, as the product was much longer (772 base pairs compared to over 300 base pairs). The PCR product amplified was 772 base pairs in length, although expression levels were quite low (Figure 5.15). Several clones expressing PAX8PPARγ1 were produced (data not shown), however these have yet to be analysed.

5.3.2 *IMR-32 cells stably expressing PAX8PPARγ1 grow at a faster rate than normal IMR-32 cells and are resistant to 15dPGJ$_2$*

The effects of PAX8PPARγ1 expression on the growth of IMR-32 cells were determined, by measuring increases in cell number for 120 hours. Untreated vector control cells increased in number to 16 x 10^4 cells by 120 hours (Figure 5.16). However, untreated IMR-32 cells stably transfected with PAX8PPARγ1 grew at a faster rate with cell numbers reaching 36 x 10^4 cells, within the same experimental time (Figure 5.16). This proposes that expression of a dominant negative PPARγ within neuroblastoma cells provided the cells with a growth advantage compared to cells which did not express this protein.

IMR-32 cells expressing dominant negative PPARγ should in theory be resistant to activation by 15dPGJ$_2$, as the dominant negative protein prevents activation of the wild-type protein. To test this, vector control and PAX8PPARγ1 transfected IMR-32 cells were treated with 5 μM 15dPGJ$_2$ and the effect on cell growth determined. Vector control cells treated with DMSO grew throughout the experiment, whereas those treated with 5 μM 15dPGJ$_2$ hardly grew post-plating, with cell numbers only reaching 3.4 x 10^4 cells within 120 hours (Figure 5.17). IMR-32 cells transfected with PAX8PPARγ1 and treated with DMSO increased in number to 22 x 10^4 cells within 120 hours, showing that these cells had a growth advantage over control cells.

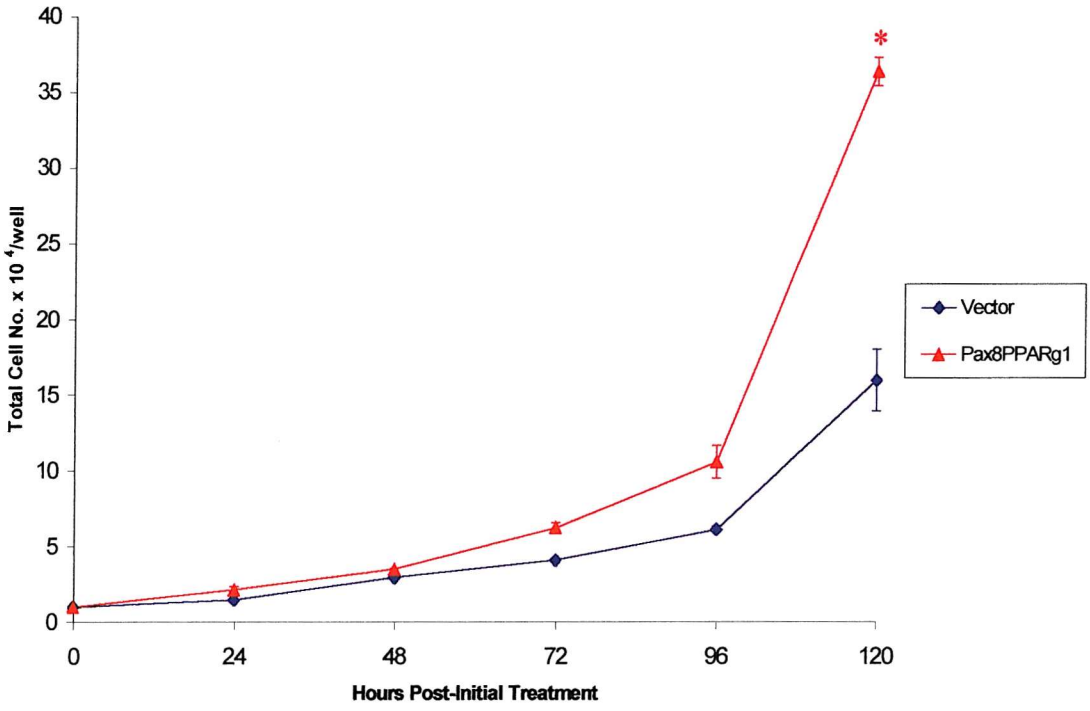

Figure 5.16 IMR-32 cells expressing the dominant negative PPARγ protein, PAX8PPARγ1, grow faster than vector controls. IMR-32 cells stably transfected with the dominant negative PAX8PPARγ1 fusion protein or vector control cells were plated out at 2 x 10^4 cells, left untreated and cell growth was measured by increases in cell number for 120 hours. The experiments were completed in duplicate and error bars are standard errors. Statistics were calculated using an ANOVA, which showed no significant difference in growth of PAX8PPARγ1 expressing cells throughout the experiment, but a t test showed a significant increase in cell number only after 120 hours, with a significance of $p < 0.05$ (*).

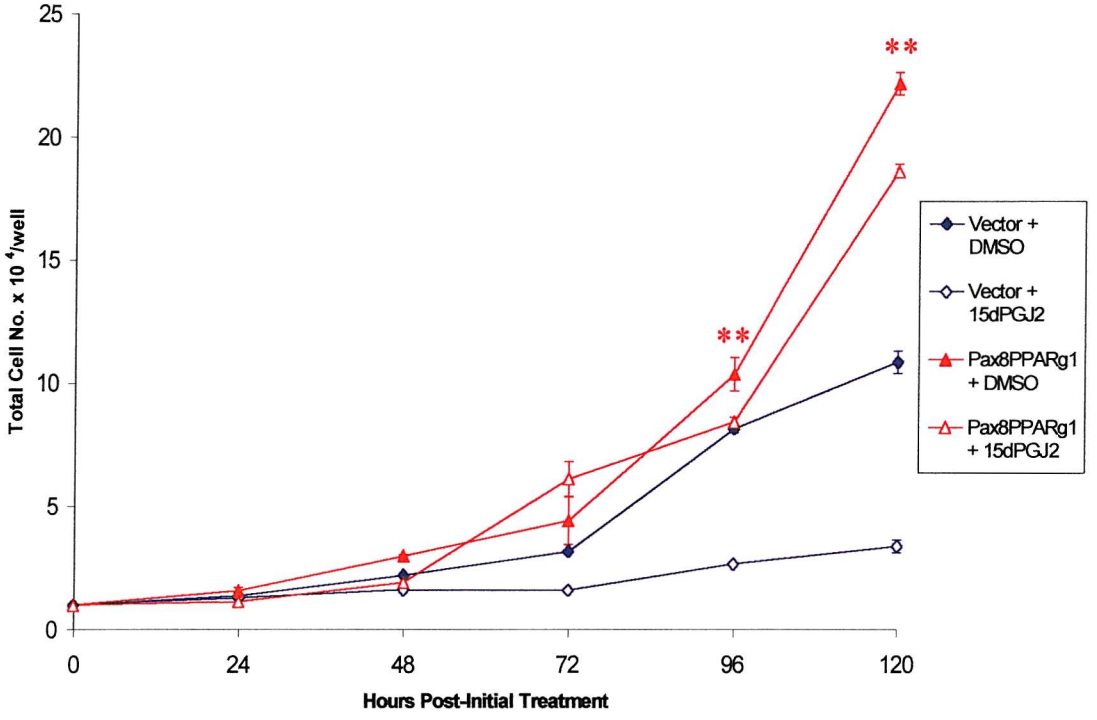

Figure 5.17 IMR-32 cells expressing PAX8PPARγ1 are resistant to the growth inhibitory effects of 15dPGJ$_2$. IMR-32 cells stably transfected with PAX8PPARγ1 and vector controls were treated with DMSO or 5 μM 15dPGJ$_2$ and the effect on cell growth determined by counting cell number over 120 hours. Two samples were counted per treatment per day and experiments were completed in duplicate and error bars represent s.e.m. Statistics were calculated using an ANOVA which showed a significant increase in growth rate of PAX8PPARγ1 expressing cells compared to controls throughout the experiment ($p<0.05$) and a student's t test revealed that after 96 hours only, the difference in growth was highly significant ($p<0.01$ **).

The growth of the PAX8PPARγ1-transfected IMR-32 cells was not inhibited by 5 μM $15dPGJ_2$ as the cells grew almost to the same level as those treated with DMSO (Figure 5.17), whereas growth of the control cells was almost completely inhibited. This shows that dominant negative PPARγ inhibited endogenous PPARγ within cells and prevented PPARγ ligands from inhibiting neuroblastoma cell growth *in vitro*.

5.3.4 *IMR-32 cells stably expressing the dominant negative PAX8PPARγ1 protein are resistant to $15dPGJ_2$ induced cell death*

IMR-32 cells expressing PAX8PPARγ1 were resistant to $15dPGJ_2$-induced growth inhibition and possibly $15dPGJ_2$-induced cell death. Therefore, vector controls and PAX8PPARγ1 expressing IMR-32 cells were treated with 5 μM $15dPGJ_2$ and cell viability measured using the trypan blue exclusion assay. Vector control cells treated with DMSO remained approximately 85 % viable throughout the experiment, whereas those treated with 5 μM $15dPGJ_2$ increasingly took up the trypan blue stain (Figure 5.18). This shows that more of the cell membranes had been compromised and only 70 % of cell remained viable after 120 hours of treatment (Figure 5.18). Like the vector-control cells treated with DMSO, most of the IMR-32 cells expressing PAX8PPARγ1 treated with DMSO survived, as there was little uptake of trypan blue (Figure 5.18). However, the IMR-32 cells expressing PAX8PPARγ1 treated with 5 μM $15dPGJ_2$ did not die at a similar rate to control cells and rates of cell death stayed similar to that of cells treated with DMSO (Figure 5.18). This shows that as well as preventing $15dPGJ_2$-induced growth inhibition, the dominant negative PPARγ also reduced cell death caused by this ligand.

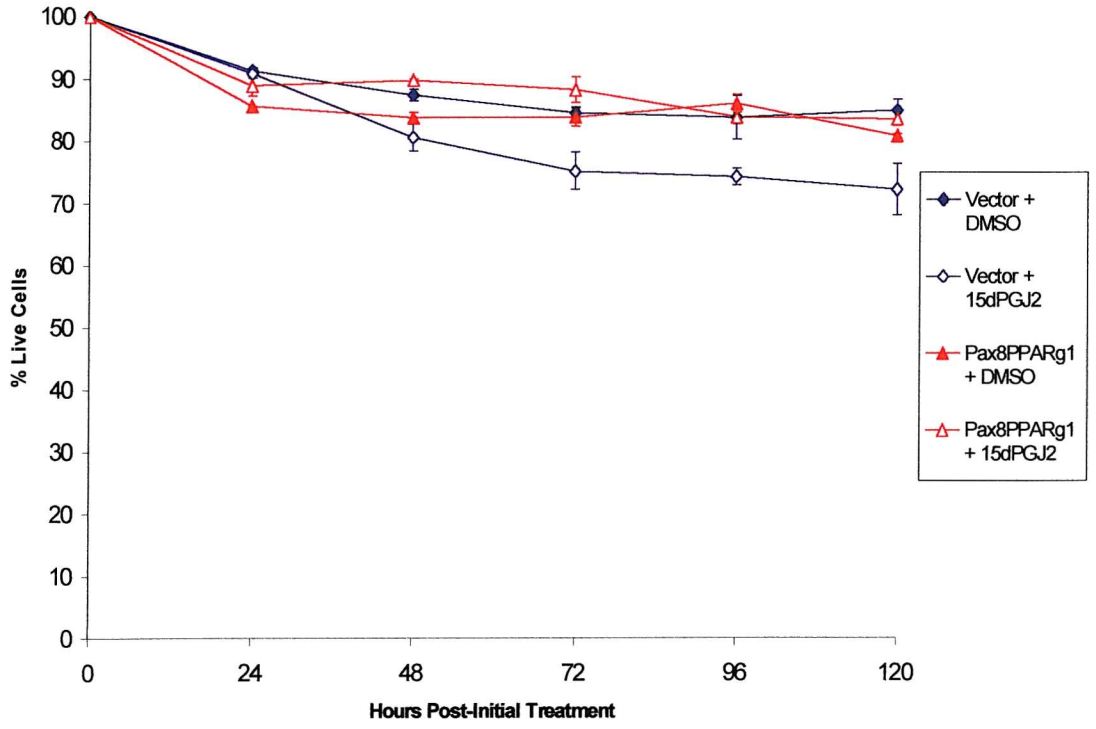

Figure 5.18 IMR-32 cells expressing PAX8PPARγ1 are resistant to cell death induced by $15dPGJ_2$. IMR-32 cells stably transfected with PAX8PPARγ1 and vector controls were treated with DMSO or 5 μM $15dPGJ_2$ and cell death measured by the trypan blue exclusion assay over 120 hours. Two samples were counted per treatment per day and experiments were completed in duplicate and error bars are standard errors. An ANOVA showed that PAX8PPARγ1 expressing cells were significantly resistant to $15dPGJ_2$-induced cell death compared to control cells throughout the experiment ($p<0.05$).

5.4 *Cellular Role of PPARγ*

5.4.1 *Increased expression of PPARγ in IMR-32 cells stably transfected with expression vectors for PPARγ1*

To assess the effects of increasing PPARγ expression in IMR-32 cells, cells were stably transfected with an expression vector containing the cDNA for PPARγ1 [141]. pLTRPoly and pcDNA3.1+© were used to control for amounts of DNA transfected into the cells, to provide transfected control cells with the selectable marker (neomycin resistance) and to control for the SV40 promoter. Transfected cells were cultured for 72 hours and then treated with G418 in fresh complete DMEM. Transfected cells were selected by treatment of cells with subsequent doses of 800 mM G418 in fresh medium, until clones were visible with the naked eye. Individual clones were "picked" using trypsin-EDTA and cultured as separate cell lines.

To determine which of the "picked" clones expressed increased levels of PPARγ1, total RNA was isolated from the transfected cells and 1 μg RNA was reverse transcribed to cDNA. The cDNA levels were normalised by amplifying the housekeeping gene, cyclophilin (Figure 5.19), and levels of PPARγ expression were determined by amplification using 35 cycles of RT-PCR and PPARγ-specific primers. Analysis of the PCR products from several of the clones showed that one of the clones transfected with PPARγ1, expressed higher levels of PPARγ than vector controls (Figure 5.19).

5.4.2 *IMR-32 cells stably expressing higher levels of PPARγ1 grow at a slower rate than normal IMR-32 cells*

Increasing the levels of PPARγ1 expression could affect the growth rates of IMR-32 cells *in vitro*, and therefore the PPARγ1 stably transfected cells were cultured alongside vector control cells.

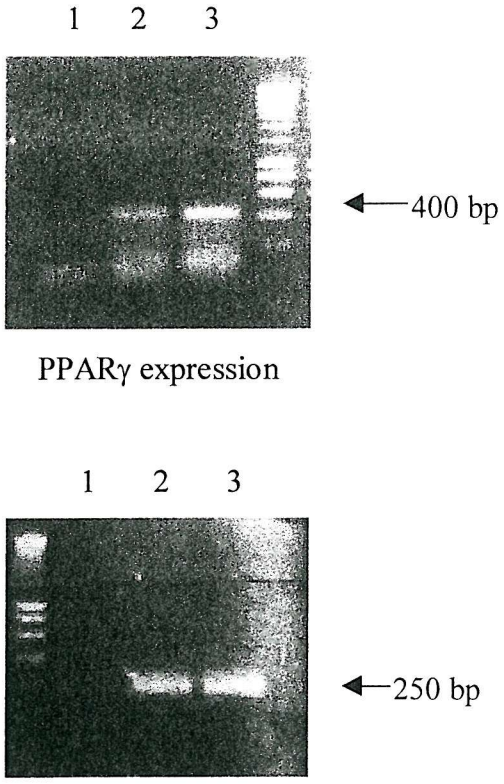

Lane 1	Negative control
Lane 2	IMR-32 cells transfected with control vector
Lane 3	IMR-32 cells transfected with PPARγ1 expression vector

Figure 5.19 IMR-32 cells stably transfected with cDNA encoding PPARγ1 express higher levels of PPARγ than controls. cDNA was made from total RNA from IMR-32 cells stably transfected with PPARγ1 cDNA or vector controls. The cDNA was amplified by RT-PCR using PPARγ-specific primers and cyclophilin primers were used control for amounts of cDNA used.

Proliferation rates were measured using the Biotrak™ cellular proliferation kit. The vector control IMR-32 cells proliferated throughout the 72-hour experiment, seen as increased labelling of cells with bromodeoxyuridine (Figure 5.20). However, untreated IMR-32 cells transfected with PPARγ1, proliferated at a much slower rate than control-treated cells and by 72 hours, proliferation rates for the control cells were nearly three times that of PPARγ1-transfected IMR-32 cells (Figure 5.20). This suggests that increasing the levels of PPARγ expression in neuroblastoma cells results in a decrease in cell proliferation.

5.4.3 *IMR-32 cells stably expressing high levels of PPARγ1 are less responsive to 15dPGJ$_2$ than vector control cells*

IMR-32 cells expressing increased levels of PPARγ1 grew slower than control cells and to investigate whether these cells respond differently to 15dPGJ$_2$, control cells and cells expressing increased PPARγ1 were treated with increasing concentrations of 15dPGJ$_2$ for 24, 48 or 72 hours. Cell proliferation was determined by measuring bromodeoxyuridine incorporation. The proliferation rates of vector control cells treated with increasing concentrations of 15dPGJ$_2$ for 24 hours were reduced, with only 50 % of cells treated with 10 μM 15dPGJ$_2$ proliferating, whereas concentrations of 1 μM and below had little effect on cellular proliferation (Figure 5.21a). At concentrations of 2.5 μM and below IMR-32 cells expressing increased levels of PPARγ1 grew similarly to controls, but at 5 μM and 7.5 μM, the cells actually proliferated to a greater extent that control cells, by around an extra 10-15 % (Figure 5.21a).

After 48 hours of treatment with increasing concentrations of 15dPGJ$_2$, vector control cells, proliferated slower than at 24 hours post-treatment, with 5 μM 15dPGJ$_2$ inducing over 50 % inhibition of proliferation and 10 μM 15dPGJ$_2$ inducing complete inhibition of IMR-32 cell proliferation (Figure 5.21b). This suggests that even at lower concentrations of 15dPGJ$_2$, longer exposure to the PPARγ ligand was more effective at inhibiting IMR-32 cell proliferation than at higher concentrations for a shorter time.

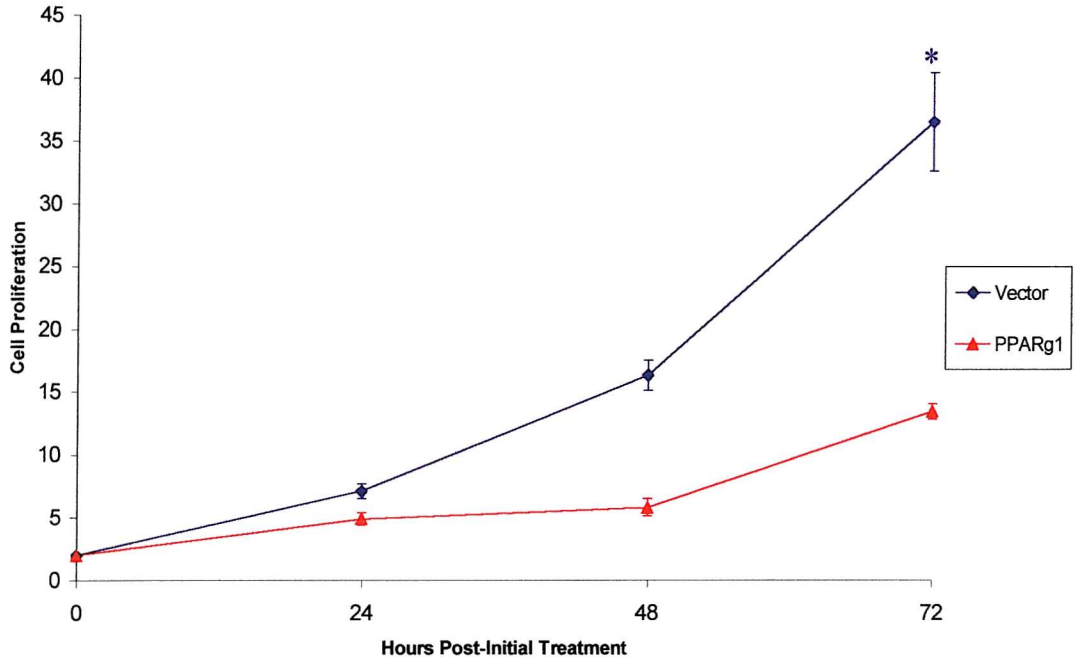

Figure 5.20 IMR-32 cells with increased expression of PPARγ proliferate slower than vector control cells. IMR-32 cells stably transfected with a plasmid containing the cDNA for PPARγ1 and vector control cells were plated out at 2 x 10^4 cells and cell proliferation measured as incorporation of bromodeoxyuridine for 120 hours in untreated cells. Two samples were counted per cell type per day and the experiments were completed in duplicate and errors shown as standard errors of the mean. Statistics were calculated using an ANOVA and showed no significant difference in growth rate throughout the experiment, but a t test revealed a significant difference in growth rate between control and PPARγ1-expressing cells at a significance of $p < 0.05$ (*), but only after 72 hours.

Figure 5.21 Dose response of $15dPGJ_2$ on IMR-32 cells with increased expression of PPARγ, shows that the cells are more resistant to $15dPGJ_2$. IMR-32 cells transfected with an expression vector containing the cDNA for PPARγ1 and vector control cells were treated with increasing doses of $15dPGJ_2$ and cellular proliferation measured as incorporation of bromodeoxyuridine after 24, 48 and 72 hours. IC_{50} values for $15dPGJ_2$ treatment of vector control IMR-32 cells are >10 μM at 24 hours, 4.4 μM at 48 hours and 3.8 μM at 72 hours. IC_{50} values for $15dPGJ_2$ treatment of IMR-32 cells with increased expression of PPARγ are 9.1 μM at 24 hours, 5.2 μM at 48 hours and 5.3 μM at 72 hours. The experiments were performed in duplicate with one sample per experiment.

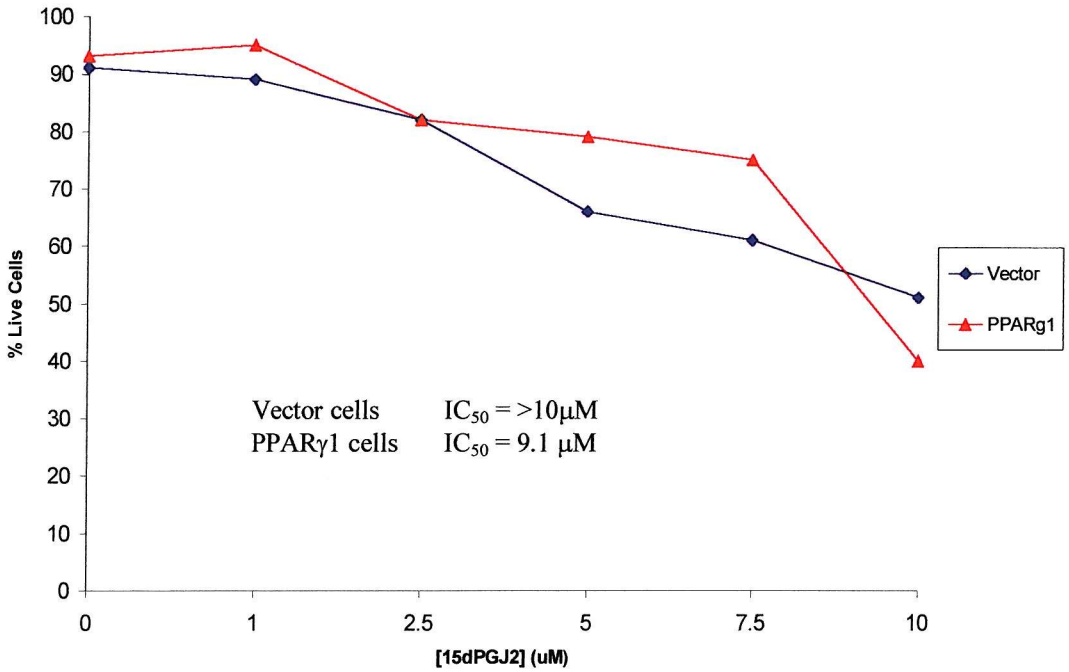

a 24 hours post-initial treatment

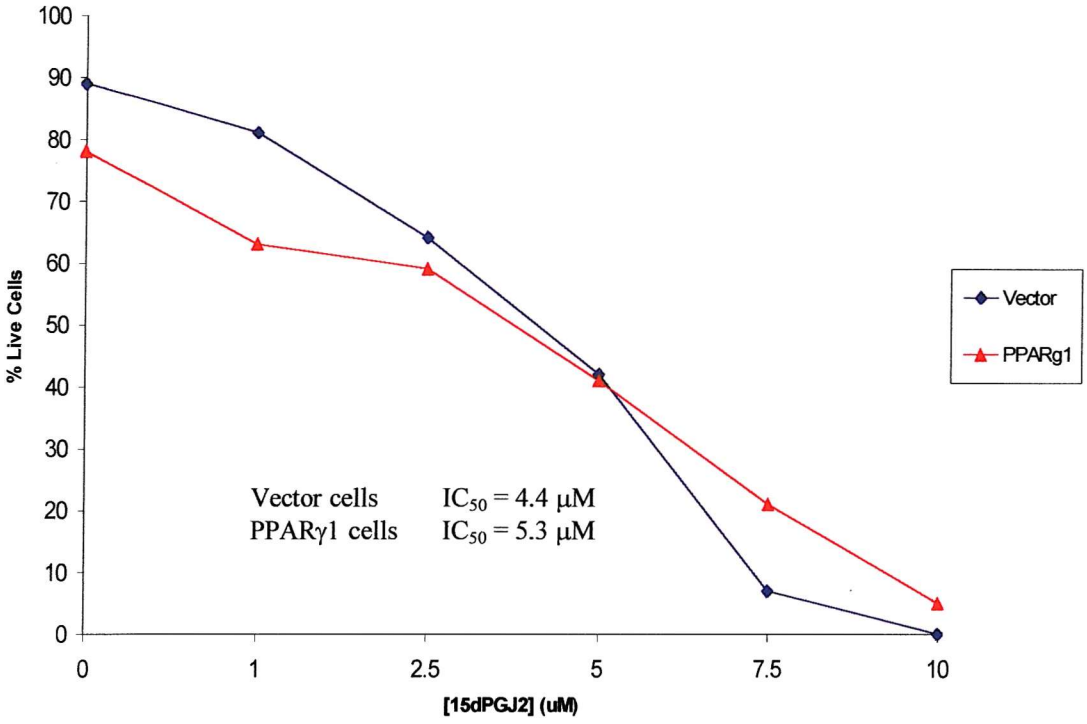

b 48 hours post-initial treatment

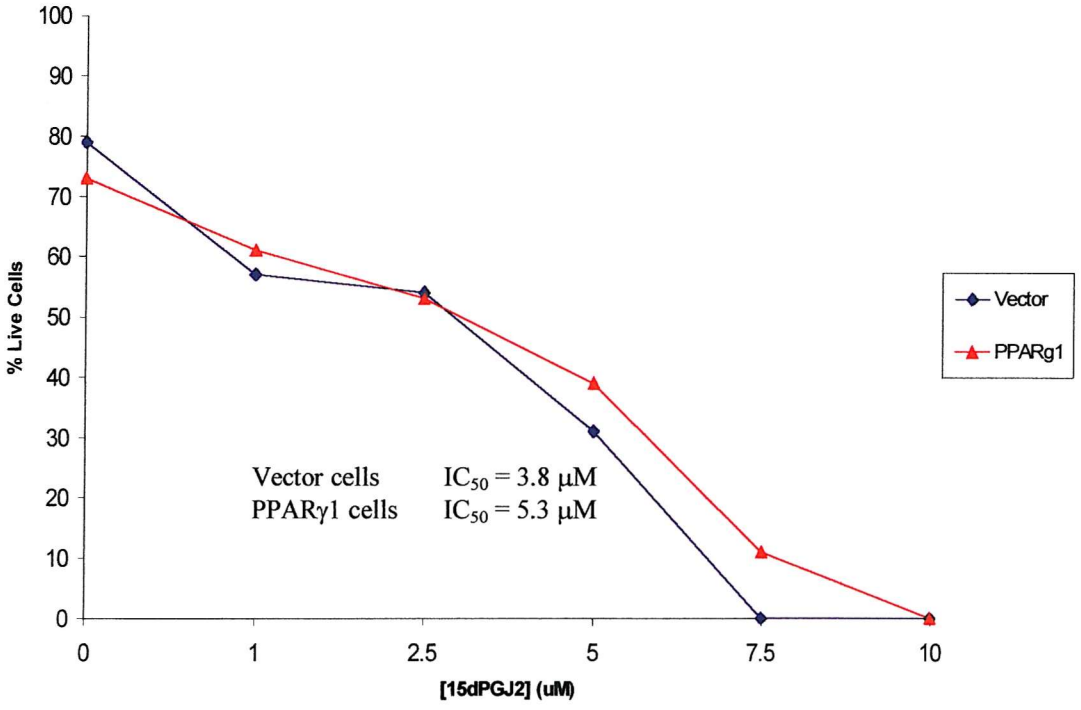

c 72 hours post-initial treatment

Likewise, the proliferation of PPARγ1-transfected IMR-32 cells was inhibited further after 48 hours of treatment, even at low concentrations of $15dPGJ_2$ compared to controls (Figure 5.21b). However, at much higher concentrations (7.5 μM and above), the PPARγ1-transfected cells proliferated at a faster rate than the vector control cells, suggesting that they were less responsive to high concentrations of $15dPGJ_2$.

After 72 hours of treatment, the proliferation of both the vector control-transfected and PPARγ1-transfected IMR-32 cells was inhibited by $15dPGJ_2$ to a greater extent that at previous time points (Figure 5.21c). This again suggested the inhibition of proliferation may be due more to the increased exposure to $15dPGJ_2$, than to the concentration of the ligand, although obviously concentration is also a factor in determining the level of inhibition. The inhibition of the proliferation of vector-control cells was around 50 % after 72 hours of treatment with 2.5 μM $15dPGJ_2$, whereas 7.5 μM $15dPGJ_2$ completely inhibited proliferation (Figure 5.21c). However, although 50 % inhibition of the PPARγ1-transfected IMR-32 cells was also achieved at 2.5 μM $15dPGJ_2$, total inhibition required 10 μM $15dPGJ_2$ (Figure 5.23). Unlike the control cells, only 90 % inhibition of cellular proliferation was achieved with 7.5 μM $15dPGJ_2$, suggesting that increased levels of PPARγ1 reduced the sensitivity of IMR-32 cells to the inhibitory effects of $15dPGJ_2$ at high concentrations.

5.5 *Potential downstream targets of activated PPARs*

5.5.1 *$15dPGJ_2$-induced growth inhibition does not involve MYC proteins*

cMYC and NMYC are two members of the MYC family of transcription factors, characterised by basic helix-loop-helix [475] and leucine zipper domains [476], which interact with other transcription factors to activate or repress transcription of genes [477, 478, 479]. MYC proteins activate transcription of genes when they are heterodimerised with Max [477, 478] and transcription is repressed when Max is heterodimerised with Mad [479]. MYC proteins regulate many cellular processes

including cell proliferation and apoptosis [480]. Aberrant regulation of cMYC is seen in many types of cancer including breast cancer and glioblastoma [481] and amplification of the cMYC gene is seen in non-small cell lung cancer [28]. At least one neuroblastoma cell line has amplification of the cMYC gene, instead of the NMYC gene [482]. NMYC is also aberrantly expressed in tumours, such as small cell lung carcinomas [483] and is commonly amplified in neuroblastoma, where it confers a growth advantage to cells [37] and has been correlated with rapid tumour progression [38]. NMYC amplification occurs in up to 40 % of advanced stage tumours and the presence of more than 10 copies correlates with poor prognosis [46].

cMYC expression correlates with neuronal differentiation [484, 485] and expression of NMYC decreases immediately preceding the differentiation of neuroblastoma cells induced by agents such as retinoic acid and ligands of PPARγ [342, 356]. Nuclear extracts of IMR-32 cells treated for 24 and 72 hours were resolved by SDS-PAGE and probed with an anti-cMYC or anti-NMYC antibody to determine the effects of $15dPGJ_2$-induced growth inhibition on MYC expression. No changes in cMYC expression were seen in control or $15dPGJ_2$ treated IMR-32 cells at either time point, however, different forms of cMYC were expressed at 24 and 72 hours (Figure 5.22). The different bands represent the expression of different forms of cMYC, cMYC1 and cMYC2 [486, 487]. Likewise there were no changes in NMYC expression in IMR-32 cells treated with $15dPGJ_2$ for 72 hours (Figure 5.23). This shows that $15dPGJ_2$-induced growth inhibition of IMR-32 cells did not occur through the same pathway as the growth arrest induced by retinoic acid.

There are several members of the MAD family, including MAD1, which is expressed in post-mitotic neurones and is up-regulated during cellular differentiation [488]. Mad proteins repress cMYC and antagonise its growth promoting functions, therefore in cells, which are arrested Mad1 expression may be elevated. Expression of MAD1 was studied in IMR-32 cells treated with $15dPGJ_2$ and Wy-14643, however MAD1 was not expressed at any time point, despite, expression being seen in serum starved ND7 cells, which express high levels of MAD (data not shown). This tallies with data showing no changes in the expression of MYC proteins in IMR-32 cells on treatment with $15dPGJ_2$.

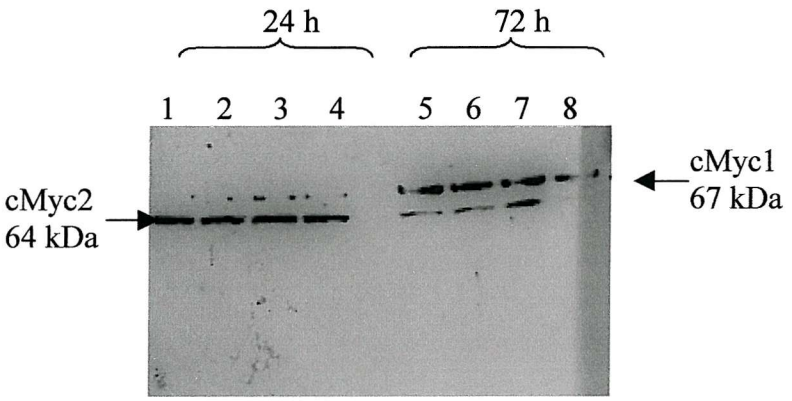

SDS-PAGE membrane

Lane 1 + 5	Untreated
Lane 2 + 6	DMSO
Lane 3 + 7	5 μM 15-deoxy$\Delta^{12,14}$-prostglandin J_2
Lane 4 + 8	5 μM Wy-14643

Figure 5.22 15dPGJ$_2$ does not down-regulate the expression of cMYC in IMR-32 cells. Nuclear extracts were made from IMR-32 cells treated with 5 μM 15dPGJ$_2$ or 5 μM Wy-14643 for 24 and 72 hours. The extracts were resolved by SDS-PAGE and cMYC levels determined by western blotting.

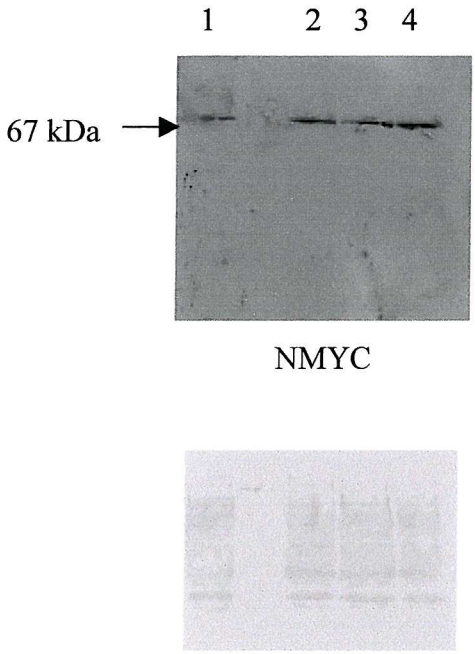

Lane 1	Untreated
Lane 2	DMSO
Lane 3	5 μM 15-deoxy$\Delta^{12,14}$-prostglandin J_2
Lane 4	5 μM Wy-14643

Figure 5.23 15dPGJ$_2$ does not down-regulate the expression of NMYC in IMR-32 cells. Nuclear extracts were made from IMR-32 cells treated with 5 μM 15dPGJ$_2$ or 5 μM Wy-14643 for 72 hours. The extracts were resolved by SDS-PAGE and the levels of NMYC were determined by western blotting.

5.5.2 *The paired box transcription factor, PAX3, is a downstream target of PPARγ*

PAX3 is a paired box transcription factor, which is expressed in undifferentiated immature neurones and is highly expressed in neural crest cells from which neuroblastomas derive [489, 490]. Mutations in *PAX3* result in the Splotch phenotype in mice [491] and Waardenburgs syndrome in humans [492], both of which have defects in the spinal column and melanocytes. PAX3 is also involved in alveolar rhabdomyosarcoma, an aggressive paediatric tumour, where PAX3 forms part of the PAX3/Forkhead (PAX3/FKHR) fusion gene, formed by a t(2;13)(q35;q14) translocation [493], which appears to bind to the same targets as PAX3, but it is a more potent transactivator [494]. PAX3 protein and PAX3 mRNA expression and DNA binding are reduced during the differentiation of neuroblastoma cells, corresponding with a slow cell cycle arrest and neurite output [495, 496]. As treatment of IMR-32 cells with 15dPGJ$_2$ results in a slow cell cycle arrest, the expression of PAX3 in 15dPGJ$_2$-treated IMR-32 cells was studied at 24 and 72 hours. Total RNA was isolated from IMR-32 cells treated with DMSO, 15dPGJ$_2$ or Wy-14643 and used to make cDNA. The cDNA was amplified using RT-PCR and PAX3 specific primers to determine whether any changes to PAX3 expression occurred. IMR-32 cells are undifferentiated cells of neural crest origin and therefore express high levels of PAX3 (Figure 5.24). No reduction in PAX3 expression was seen in IMR-32 cells treated with 15dPGJ$_2$ or Wy-14643 compared to controls at 24 hours. However, a reduction in PAX3 expression was seen at 72 hours in IMR-32 cells treated with 15dPGJ$_2$, and not in Wy-14643 or control-treated cells, coinciding with cell cycle arrest and a decline in cell growth.

5.5.3 *15dPGJ$_2$-induced growth inhibition does not involve p21$^{CIP1/SDI1/WAF1}$, but does induce translocation of p53*

p21$^{CIP1/SDI1/WAF1}$ is an inhibitor of cyclin dependent kinases (cdks), which binds to complexes of cdk2, cdk4 and cdk6 and blocks progression from G_1 phase of the cell cycle to S phase [497].

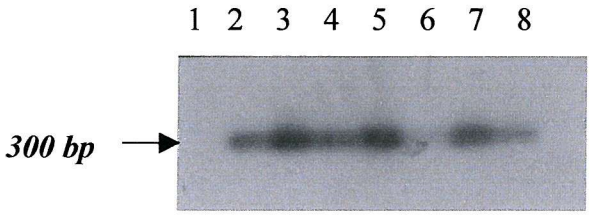

PAX3

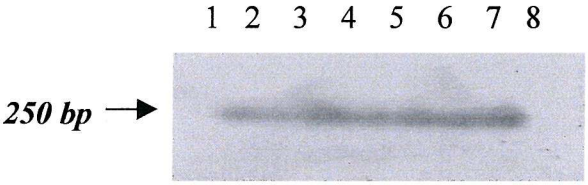

Cyclophilin

Lane 1	Negative control
Lane 2	Untreated
Lane 3	DMSO (24 hours)
Lane 4	DMSO (72 hours)
Lane 5	5 μM 15-deoxy$\Delta^{12,14}$-prostglandin J_2 (24 hours)
Lane 6	5 μM15-deoxy$\Delta^{12,14}$-prostglandin J_2 (72 hours)
Lane 7	5 μM Wy-14643 (24 hours)
Lane 8	5 μM Wy-14643 (72 hours)

Figure 5.24 15dPGJ_2 down-regulates PAX3 mRNA in IMR-32 cells after 72 hours of treatment. Total RNA was made from IMR-32 cells treated with ligands of PPARα and PPARγ. The RNA was reverse transcribed to cDNA and amplified by RT-PCR using PAX3-specific primers. Cyclophilin primers were used to amplify the cDNA and normalise levels of cDNA used.

$p21^{CIP1/SDI1/WAF1}$ is expressed in terminally differentiating cells and is required for the survival of neuroblastoma cells induced to differentiate by nerve growth factor [498]. $p21^{CIP1/SDI1/WAF1}$ is involved in p53-mediated G_2/M arrest of cells, which enter mitosis phase of the cell cycle with damaged DNA [499]. The involvement of $p21^{CIP1/SDI1/WAF1}$ in $15dPGJ_2$-induced growth arrest of IMR-32 cells was assessed by resolving nuclear extracts of cells treated with DMSO, 5 μM $15dPGJ_2$ or 5 μM Wy14643 by SDS-PAGE and probing with an anti-$p21^{CIP1/SDI1/WAF1}$ antibody. No changes in the expression of $p21^{CIP1/SDI1/WAF1}$ were observed in IMR-32 cells treated with 5 μM $15dPGJ_2$ (Figure 5.25), suggesting that in IMR-32 cells $15dPGJ_2$-induced growth arrest does not involve $p21^{CIP1/SDI1/WAF1}$. However, the $p21^{CIP1/SDI1/WAF1}$ antibody produced very weak bands and is not conclusive.

p53 is a key regulator of the cell cycle and it is the most commonly mutated protein occurring in human cancers. Despite this, some cancers including neuroblastoma, rarely have mutations in p53 [500], although it has been linked to multi-drug resistance during therapy for neuroblastoma [501]. The wild type p53 found in neuroblastoma has been suggested to be inactive due to cytoplasmic sequestration [502], or that it is in a conformation which cannot induce transcription [503]. It has also been suggested that p53 may be sequestered from the DNA within neuroblastoma cell nuclei and not be able to function properly (personal communication, Vince Kidd, St. Jude Children's Hospital, Memphis). The expression of p53 is related to an undifferentiated phenotype in neuroblastoma cells, as retinoic acid induced-differentiation results in a decrease in expression of p53 mRNA and protein [504]. p53 also induces G_2/M arrest as well as its main role as a checkpoint during progression to S phase of the cell cycle [499]. Therefore, to determine whether levels of p53 expression or location of the protein changed on treatment with $15dPGJ_2$, nuclear extracts of IMR-32 cells treated with DMSO or 5 μM $15dPGJ_2$ for 24 or 72 hours were resolved by SDS-PAGE and probed with a polyclonal anti-p53 antibody. p53 was not detected in nuclear extracts of IMR-32 cells treated 5 μM $15dPGJ_2$ for 24 hours, however, at 72 hours p53 was detected in the nuclei of IMR-32 cells treated with $15dPGJ_2$, but not in control-treated cells (Figure 5.26).

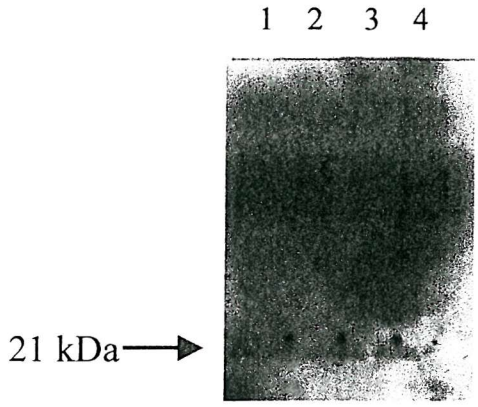

SDS-PAGE membrane

Lane 1	Untreated
Lane 2	DMSO
Lane 3	5 μM 15-deoxy$\Delta^{12,14}$-prostglandin J_2
Lane 4	5 μM Wy-14643

Figure 5.25 $15dPGJ_2$ does not alter the expression of $p21^{CIP1/SDI1/WAF1}$ in IMR-32 cells. IMR-32 cells were treated with 5 μM $15dPGJ_2$ or 5 μM Wy-14643 and nuclear extracts were made from the cells. The extracts were resolved by SDS-PAGE and analysed with an anti-$p21^{CIP1/SDI1/WAF1}$ antibody. However, the $p21^{CIP1/SDI1/WAF1}$ antibody produced very weak bands and is not conclusive.

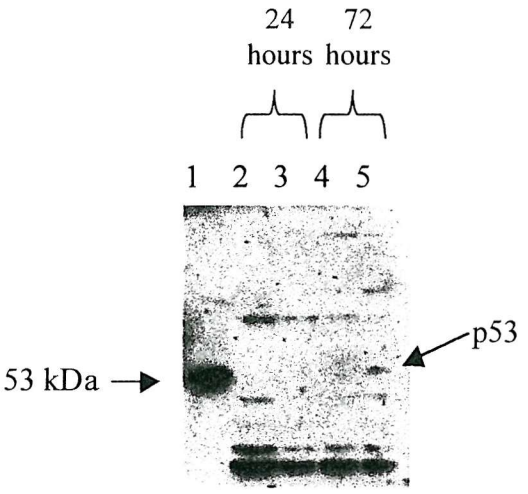

Lane 1	MCF-7 cells
Lane 2	IMR-32 cells + DMSO
Lane 3	IMR-32 cells + 15dPGJ$_2$
Lane 4	IMR-32 cells + DMSO
Lane 5	IMR-32 cells + 15dPGJ$_2$

Figure 5.26 15dPGJ$_2$ induces translocation of p53 to the nucleus of IMR-32 cells after 72 hours. Nuclear extracts were made from IMR-32 cells treated with 5 μM 15dPGJ$_2$ for 24 and 72 hours. The extracts were resolved by SDS-PAGE and western blotted with an anti-p53 antibody. Extracts of MCF-7 cells, a breast cancer cell line, were used as a positive control. p53 antibody and MCF-7 cells courtesy of Jeremy Blaydes, Southampton General Hospital.

This suggests that p53 may be a downstream target of PPARγ and sustained activation of the receptor with 15dPGJ$_2$ may result in p53 translocating to the nucleus and inhibiting the cell cycle at G_2/M.

5.5.4 *15dPGJ$_2$-induced growth inhibition of IMR-32 cells does not involve the tumour suppressor, PTEN*

PPARγ can regulate the tumour suppressor, phosphatase and tensin homologue deleted from chromosome 10 (PTEN) [505]. PTEN is also known as mutated in multiple advanced cancers (MMAC1) or transforming growth factor β regulated epithelial cell enriched phosphatase (TEP1) [506]. PTEN/MMAC1/TEP1 is one of the most frequently mutated genes in human cancer, second only to p53 [507], and it is also mutated in autosomal dominant diseases, which have a predisposition to developing cancer, such as Cowden disease [508]. PPARγ can bind to two response elements in the promoter of PTEN/MMAC1/TEP1 and activation of PPARγ by synthetic ligands such as rosiglitazone and pioglitazone have been shown to up-regulate PTEN/MMAC1/TEP1 expression in macrophages [505]. Activation of PPARγ by 1 μM rosiglitazone also up-regulates PTEN expression in Caco2 colorectal cancer cells and MCF-7 breast cancer cells, with a concurrent reduction in the proliferation of both cell types [505]. The up-regulation of PTEN by PPARγ correlates with decreased phosphatidylinositol 3-kinase (PI3K) activity measured by the reduced phosphorylation of protein kinase B (PKB). This is because PTEN/MMAC1/TEP1 catalyses the dephosphorylation of the D3 phosphate group from phosphatidylinositol 3,4,5-triphosphate (PIP_3) to form phosphatidylinositol 3,4-bisphosphate (PIP_2), whereas PI3K phosphorylates the D hydroxyl head group of PIP_2 to form PIP_3 (Figure 5.29) [507]. If PI3K activity is down-regulated, then there is no phosphorylation of PIP_2 to PIP_3 and without PIP_3 to target PKB for phosphorylation by kinases such as phosphatidylinositol 3,4,5-triphosphate-dependent protein kinase 1 (PDK1) [509], levels of phospho-PKB (P-PKB) decrease (Figure 5.27). The expression of P-PKB is reduced in macrophages and Caco2 cells on treatment with 1 μM rosiglitazone, due to an up-regulation in PTEN by activated PPARγ.

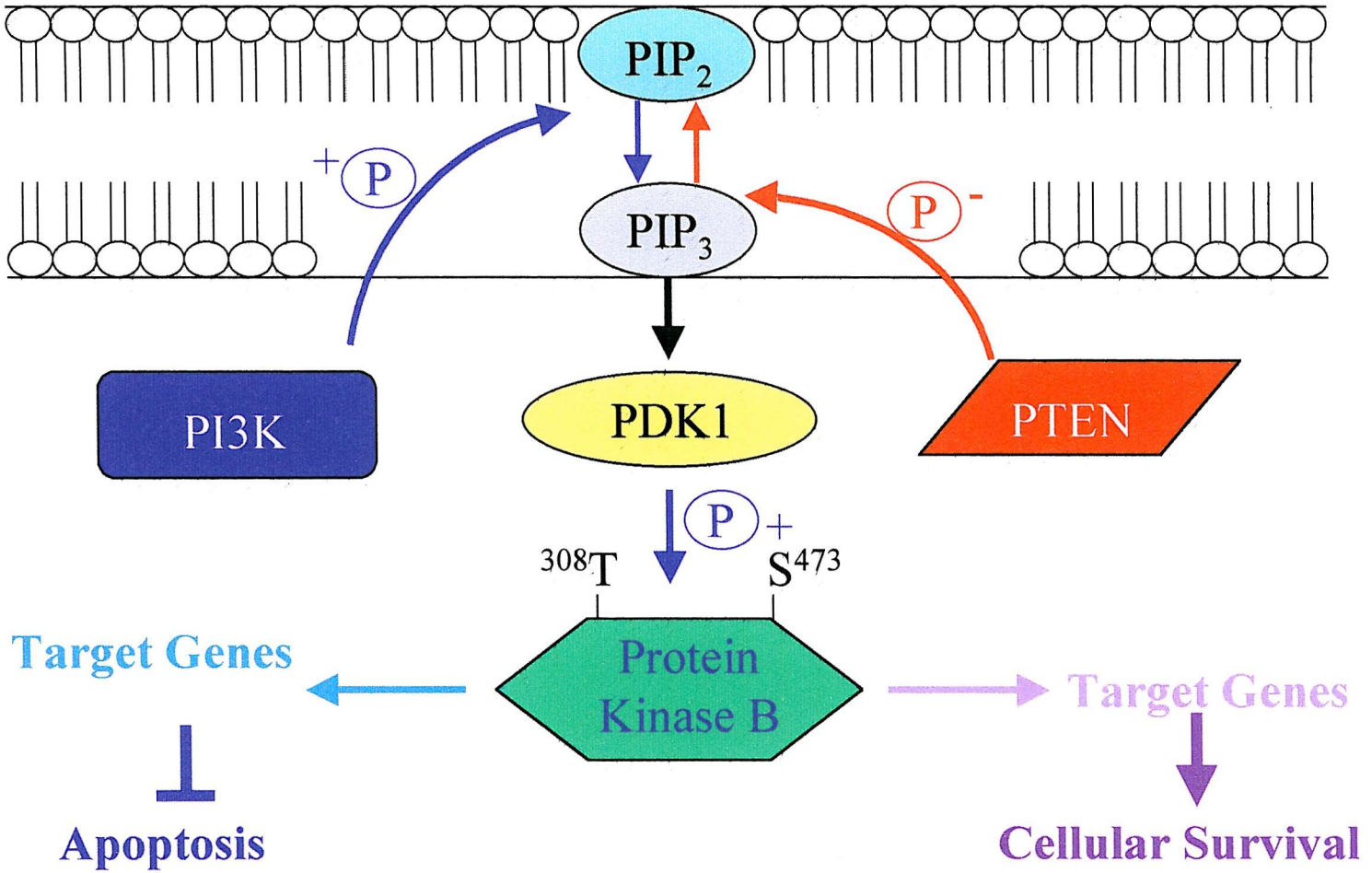

Figure 5.27 Scheme of the regulation of the phosphorylation state of protein kinase B.

PI3K	Phosphatidylinositol 3' kinase
PIP2	Phosphatidylinositol 3,4-bisphosphate
PIP3	Phosphatidylinositol 3,4,5-trisphosphate
PTEN	Phosphataseand tensin homologue deleted from chromosome 10
PDK1	Phosphatidylinositol3,4,5-trisphosphate-dependent protein kinase 1

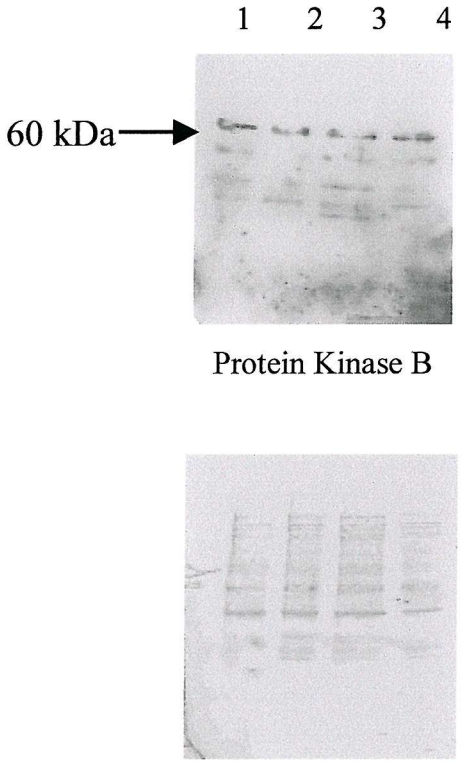

Lane 1	Untreated
Lane 2	DMSO
Lane 3	5 μM 15-deoxy$\Delta^{12,14}$-prostglandin J_2
Lane 4	5 μM Wy-14643

Figure 5.28 15dPGJ$_2$ does not inhibit IMR-32 cell growth through increasing the activity of the tumour suppressor, PTEN. IMR-32 cells were treated with 5 μM 15dPGJ$_2$ or 5 μM Wy-14643 and cytoplasmic extracts were made. The cytoplasmic extracts were resolved by SDS-PAGE and PTEN activity was measured by Western blotting with an anti-phospho-PKB antibody.

PKB is activated by phosphorylation and acts on downstream targets to promote cell survival and prevent apoptosis and therefore up-regulation of PTEN/MMAC1/TEP1 results in apoptosis, through inactivation of PKB.

To determine whether the $15dPGJ_2$-induced growth inhibition of IMR-32 cells was due to the up-regulation of PTEN/MMAC1/TEP1, treated cell extracts were analysed for a reduction in phospho-PKB (P-PKB) levels. Cytoplasmic extracts were resolved by SDS-PAGE and probed with an antibody specific to the $Serine^{473}$ phosphorylated form of PKB. No reduction in the level of P-PKB expression was seen in IMR-32 cells treated with 5 μM $15dPGJ_2$ or 5 μM Wy-14643 for 72 hours (Figure 5.28). This suggests that up-regulation of PTEN/MMAC1/TEP1 expression, was not the mechanism of action of activated PPARγ in IMR-32 cells.

5.6 *Discussion*

The expression of both PPARγ mRNA and protein has been shown to be down-regulated by treatment with its own ligands, suggesting that activation of PPARγ in adipocytes is auto-regulatory [279, 280]. Ligand-dependent degradation of the receptor protein is also seen in other members of the nuclear hormone receptor super-family, including oestrogen receptors (OER) [282], thyroid receptors (TRs) [510] and both retinoic acid receptors (RARs) [278] and retinoid X receptors (RXRs) [511]. This is interesting as PPARs have been shown to heterodimerise with RXRs [99] and there is thought to be cross-talk between the PPAR and OER [119, 120] and PPAR and TR pathways [227]. Unlike the effects seen in adipocytes on activation of PPARs, activation of RARs by retinoic acid results in an increase in mRNA expression, and a decrease in protein expression, due to the protein becoming ubiquitinated and targeted for destruction [278]. Vitamin D receptors (VDR), unlike other members of the nuclear receptor super-family, are not targeted for destruction after activation with vitamin D and the ligand actually elevates protein levels of VDR, by inhibition of ubiquitination [512]. However, ligands of PPARγ seemed to neither increase nor decrease the expression of PPARγ mRNA in IMR-32 cells (Figure 5.1).

Hauser *et al.*, [280] showed that in adipocytes PPARγ protein is degraded during normal turnover and post-activation with natural and synthetic ligands, through ubiquitination and destruction at the proteasome. PPARγ expression was reduced to 10 % of the expression seen in control cells by 24 hours, but within 72 hours, PPARγ expression had increased again to almost 80 % [279]. No changes in PPARγ protein expression were seen in IMR-32 cells treated with $15dPGJ_2$ or with Wy-14643 for 24 or 72 hours, therefore discounting the possibility of any ligand-dependent degradation of PPAR protein in these cells at these time points (Figure 5.2). Interestingly, PPARγ protein has been shown to be cleaved in SHSY5Y cells in response to treatment with 10 μM $15dPGJ_2$ to produce a fragment of approximately 25 kDa [362]. Rohn *et al.*, [362] suggest that the PPARγ protein was cleaved because PPARγ is a target of caspases, however, as $15dPGJ_2$ does not induce apoptosis in IMR-32 cells, this may explain why PPARγ remains intact in these cells. It is possible, however, that lengthy treatment of IMR-32 cells with $15dPGJ_2$ is required for degradation of PPARγ protein to occur. It has been shown that glucocorticoid receptors, another nuclear hormone receptor, require chronic treatment of cells with glucocorticoids, before the receptor becomes ubiquitinated [513]. However, in IMR-32 cells, regulation of PPARγ may occur through an alternative mechanism to auto-regulation and ubiquitination. Interestingly, Butler *et al.*, showed that treatment of prostate cancer cells with $15dPGJ_2$ resulted in no change in the levels of PPARγ1, but showed an increase in the expression of PPARγ2.

PPARs can also be regulated by co-activators and co-repressors [152], DNA binding and phosphorylation at serine[84] of PPARγ1 and serine[112] of PPARγ2 humans by mitogen-activated protein kinases (MAPK) such as extracellular signal regulated kinases (ERKs) [285, 288], c-Jun N-terminal kinase (JNK) or weakly by p38 [514]. Therefore, in IMR-32 cells these alternative regulatory pathways may be of more importance. Phosphorylation has been shown to be important in the regulation of nuclear hormone receptors and has also been shown to target progesterone [283] and retinoic acid receptors [278] for destruction. However, it is thought that phosphorylation of PPARγ acts to prevent its interaction with co-activators and accessory proteins [288]. This is because phosphorylation significantly inhibits

ligand-dependent and -independent transcriptional transactivation, but does not affect stability or DNA binding [288] or target the protein for destruction. In the future, it would be interesting to determine whether the activity of PPARγ within IMR-32 cells could be increased using inhibitors of MAP kinase, JNK or p38. Inhibitors of MAP kinase e.g. PD89059 have been shown to increase transcriptional activity of PPARγ and in combination with PPARγ ligands such as troglitazone induce further differentiation of breast cancer cells [290].

$15dPGJ_2$ effectively activates PPARγ, however, it is only able to weakly activate PPARα [167, 168]. $15dPGJ_2$ can bind to PPARγ and can compete with thiazolidinediones, which have been shown to bind directly to PPARγ [168]. It has been shown to effectively activate a reporter construct containing 3PPREs with activation being three times greater than that induced by the next most active metabolite, $\Delta^{12}PGJ_2$ [167]. The potent activator of PPARα, Wy-14643 has different effects on PPARγ. Kliewer *et al.*, showed that Wy-14643 was able to activate PPARγ, using expression and reporter plasmids [168], whereas Forman *et al.*, were unable to show activation of PPARγ by Wy-14643, using reporter constructs alone [167], despite both groups using the same cell line for their experiments. This maybe because of the different techniques used, and Forman *et al.*, may have shown an effect more indicative of the native response, as they were not introducing an expression vector. $15dPGJ_2$ and Wy-14643 both activated a CAT reporter construct containing three consensus PPREs upstream of a TK promoter in IMR-32 cells (Figure 5.3). $15dPGJ_2$ activated PPARs more effectively than Wy-14643, with reporter gene activity being increased 7 fold and 4 fold respectively. The reporter construct used in these experiments did not distinguish between activation of PPARα or PPARγ, however, as $15dPGJ_2$ has been shown only to weakly activate PPARα [167], the reporter gene activity may potentially be attributed to PPARγ, in the case of $15dPGJ_2$. However, as Wy-14643 has been shown to activate PPARγ by one group and by another not to activate PPARγ [167, 168], the effects seen with Wy-14643 could have been due to activation of either isoform or both together. Wy-14643 activates PPARα more effectively in rats and mice than in humans, which may explain some of the reasons why peroxisome proliferators

activate peroxisome proliferation and hepatocarcinogenesis in rats and mice, but not in humans [112, 113].

The activation of PPARγ in cancer cells has been shown to inhibit their growth [130, , 182, 241, 290] or activate programmed cell death [340, 341, 347, 357, 434, 515] in a wide variety of cancer cell types and animal models of cancer [242]. However, despite the appeal of a potential drug target protein, which can be activated by relatively low concentrations of natural and synthetic ligands, of which some have already entered successful clinical trials for diabetes, there should still be some caution in interpreting results. This is because both $15dPGJ_2$ and TZDs, notably troglitazone, have been shown to have PPARγ-independent effects on different cell types [190, 463]. These can involve the transcription factor, NFκB [190] and in the case of some osteosarcoma cells can actually involve other members of the nuclear hormone receptor super-family [466]. The PPARγ-independent effects of $15dPGJ_2$ are thought to be mediated through the reactive cyclopentenone ring of $15dPGJ_2$, and these reactive rings have also been shown to mediate the biological actions of prostaglandin A_1 and A_2 [192, 464]. Therefore the establishment of the role of PPARs in $15dPGJ_2$-induced growth inhibition in IMR-32 cells was necessary.

$15dPGJ_2$ is a metabolite of the PUFA, arachidonic acid, which has been shown to inhibit the growth of some cancer cells through changes to their membrane phospholipid composition [177]. To determine the effects of $15dPGJ_2$ on the composition of IMR-32 cell membrane phospholipids, phospholipid extracts were made from cells treated with $15dPGJ_2$ and Wy-14643 and analysed by ESI MS. No changes in the phosphatidylcholine (Figure 5.6), phosphatidylethanolamine (Figure 5.7) or acid phospholipid (Figure 5.8) species were seen in $15dPGJ_2$ or Wy-14643-treated cells, suggesting that the growth-inhibitory effects of $15dPGJ_2$ were not mediated through changes to the cellular membrane. This is unsurprising, as no reports of $15dPGJ_2$ affecting membrane phospholipids have been published and it is thought that it acts either through PPARγ or through other independent mechanisms. $15dPGJ_2$ has been shown to act independently of PPARγ in macrophages, by repressing gene expression through antagonism of transcription factors such as NFκB [190]. However, in IMR-32 cells, $15dPGJ_2$ did not act

independently of PPARγ through repression of NFκB, and in fact, it actually induced activation of NFκB-induced transcription (Figure 5.8). Interestingly, an increase in NFκB activity has also been seen in neuroblastoma cells induced to differentiate in the presence of retinoic acid [473] and bromodeoxyuridine [474].

Decoy plasmids to PPARs were able to reduce the growth inhibitory effects of the $15dPGJ_2$ on IMR-32 cells (Figure 5.10) and $15dPGJ_2$-induced cell death (Figure 5.12), showing that PPARs, possibly PPARγ, are involved in $15dPGJ_2$-induced growth arrest in these cells. A control plasmid lacking the 3PPRE sequence was unable to prevent $15dPGJ_2$ from inhibiting the growth of IMR-32 cells (Figure 5.11), or inducing cell death (Figure 5.13) showing that PPARs need to be "bound out" to prevent $15dPGJ_2$-induced growth inhibition. Decoy oligonucleotides have been successful in proving the involvement of PPARγ in endothelial cell apoptosis induced by $15dPGJ_2$ [183]. However, other methods have been used to inhibit PPARγ including antagonists of PPARγ, such as Bisphenol A diglycidyl ether (BADGE) [225, 516] and antisense oligonucleotides [505]. BADGE has been shown to be able to inhibit the differentiation of adipocytes and block the activation of PPARγ by rosiglitazone without any activation of the receptor itself in adipocytes and is reported to be a pure antagonist of PPARγ [516]. However, in the endothelial cell line, ECV304, BADGE has been shown to activate PPARγ, resulting in translocation of the receptor to the nucleus and cell death [225]. BADGE also induces apoptosis in tumour cells independently of PPARγ, in both caspase-dependent and caspase-independent manners [517]. Therefore, cautionary use of BADGE as an antagonist of PPARγ should be applied. New antagonists of PPARγ have also been developed by Glaxo Wellcome, including GW1929 [207, 342], and appear to be more successful than BADGE, however access to them is limited and they may be more widely used in the future.

Antisense oligonucleotides are complementary to the mRNA sequence of the protein of interest and bind to the transcribed RNA, thus preventing translation. This may occur through prevention of ribosome binding or progression along the mRNA or the formation of double-stranded RNA may stimulate the activity of the cellular nuclease ribonuclease-H, which degrades the RNA and prevents translation

of the protein [518]. Antisense oligonucleotides have been used to target PPARγ in macrophages, thus preventing its up-regulation by rosiglitazone [505]. This resulted in the down-regulation of PTEN and concurrent up-regulation in phospho-PKB [505]. The cells were prevented from undergoing apoptosis due to an increase in the levels of phospho-PKB, a survival factor, and a reduction in caspase 9 activity [505]. Unlike the decoy oligonucleotide method, this method was more specific for the γ isoform of PPAR, but the design of antisense probes can be more complicated, as the sequences must have high affinity, be specific and not form secondary structures, which would inhibit binding to the mRNA [518]. It can be difficult to design an oligonucleotide, which knocks out a large enough proportion of the protein for an effect to be seen (personal communication, Neil Jones, Institute of Cancer Research), as a small percentage of the protein can be sufficient to maintain function. The decoy sequence is shorter than that required for antisense, relieving problems of secondary structure and 15dPGJ$_2$ has been shown to potently activate PPARγ and only weakly activate PPARα. Therefore the decoy oligonucleotide method, which shows that 15dPGJ$_2$-activates PPARs in IMR-32 cells, is a suitable method.

Dominant negative PPARγs have been found in a number of diseases, including severe insulin resistance, diabetes and hypertension [329, 330] and more recently in follicular thyroid cancer [344]. A chromosomal translocation t(2;3)(q13;3p25) seen in follicular thyroid cancer results in the in-frame fusion of the genes of two transcription factors, PAX8 and PPARγ [344] (Figure 5.14). PAX8 is a paired box transcription factor, which is expressed during development in the thyroid and secretory system and also in the adult thyroid and in Wilm's tumour [519, 520]. The translocation results in the production of the PAX8PPARγ1 fusion protein, which contains the DNA binding domains of PAX8 and fused to domains A-F of PPARγ1, so that there is no transactivation domain of PAX8, which may result in alterations in PAX8 pathways [344]. Three alternative splice forms of PAX8 were found in the fusion proteins detected in the cells from patients with follicular thyroid cancer [344]. These variants were co-expressed, one contained exons 1 to 7 of PAX8, one contained exons 1 to 8 and one contained exons 1 to 7 plus exon 9 [344] and the fusion protein used in these studies contained the latter splice variant. The

functional domains of PAX8PPARγ1 are nearly identical to the respective PAX and nuclear receptor functional domains in the rhabdomyosarcoma oncoprotein, PAX3-Forkhead (PAX3-FKHR) [493]. However, unlike PAX8PPARγ1, PAX3-FKHR excessively activates transcription of target genes of wild-type PAX3, rather than acting in a dominant negative manner [493]. PAX8PPARγ1 also resembles the fusion proteins involved in acute promyelocytic leukaemia (PML), PML-RAR [521] and acute promyelocytic leukaemia zinc finger protein (PLZF)-RAR [522, 523], which act by antagonising the effects of retinoic acid receptors in the presence of retinoic acid and competing for retinoic acid response elements [521, 522, 523].

IMR-32 cells were stably transfected with a vector containing the cDNA for PAX8PPARγ1 to assess the effects of a dominant negative PPARγ on neuroblastoma cells. The IMR-32 cells expressing PAX8PPARγ1 (Figure 5.15) grew much faster than the vector control cells (Figure 5.16), possibly because the basal level of transcription, which would normally occur due to the presence of wild-type PPARγ was suppressed. Therefore, any "check" on the proliferation of these cells would be removed, thus allowing them to proliferate at a faster rate. The involvement of PAX8 in the increased growth of IMR-32 cells transfected with PAX8PPARγ1 cannot be discounted, however, as it is thought that PAX genes may be involved in growth regulation [524]. PAX8 is also involved in the proliferation of thyroid cell proliferation induced by thyroid-stimulating hormone [524] and is known to transactivate the Wilm's tumour gene and modulate its expression [525, 526]. Therefore without further experimental data we cannot be sure that the effects of PAX8PPARγ1 on IMR-32 cells are solely due to the dominant negative effects of PPARγ1. It would also be interesting to determine whether other dominant negative PPARγ proteins, such as truncated PPARγ, had similar effects in IMR-32 cells, which would not be complicated by the PAX8 element.

Dominant negative PPARγ proteins have been shown to inhibit transcription induced by ligands of PPARγ, such as TZDs, but by different mechanisms [222, 328, 329, 330, 344]. Mutations in helix 12 of PPARγ destabilise the helix, which mediates transactivation, resulting in a protein which not only cannot recruit co-activators, but recruits co-repressors more avidly than the wild-type protein and exhibits

delayed ligand-dependent co-repressor release [329, 330]. Other dominant negative PPARγs have impaired ligand binding and abrogate wild-type receptor activity in a dose-responsive manner, such as the PPARγ lacking 5 carboxyl-terminal amino acids [222]. Both the wild type and the 5 residue C-terminally truncated protein heterodimerised with RXR and bound to PPREs, therefore it was thought that this dominant negative protein competed with the wild type for RXR and binding to PPRE [222]. Likewise a dominant negative PPARγ lacking 16 C-terminal amino acids also had impaired ligand binding, but retained its capacity to bind to PPREs, therefore competing with the wild-type for binding to PPREs and inhibited PPARγ-mediated adipogenesis [328].

Aside from follicular thyroid cancer, no other cancers have been shown to involve dominant negative activity of PPARγ, however, loss-of-function mutations have been observed in colon cancer [352]. Therefore, the effects of introducing a PPARγ dominant negative protein into neuroblastoma cells can only be speculated. It is expected that the levels of basal transcription would decrease and that the effects of ligands of PPARγ would be ineffective at inhibiting the growth of IMR-32 cells stably expressing this mutant protein. Indeed, treatment of IMR-32 cells transfected with a vector control with 5 μM $15dPGJ_2$ resulted in inhibition of cell growth and an increase in cell death. However, IMR-32 cells stably transfected with PAX8PPARγ1 were resistant to the effects of 5 μM $15dPGJ_2$ and continued to grow at a faster rate than control cells and almost equivalent to that of IMR-32 cells transfected PAX8PPARγ1 and treated with DMSO alone (Figure 5.17). No obvious morphological changes to the IMR-32 cells expressing PAX8PPARγ1 were evident. This shows that PAX8PPARγ1 is able to abrogate the activation of wild-type PPARγ and prevent the transcription of PPARγ target genes, which would result in inhibition of cell growth. It also shows that the effects of $15dPGJ_2$ are mediated through PPARγ, as the presence of the dominant negative PPARγ is able to prevent $15dPGJ_2$-induced effects on IMR-32 cells.

PPARγ is expressed at high levels in several cancer cell lines and primary tumours, including neuroblastoma [342]. To determine the effects of increasing PPARγ expression within IMR-32 cells, the cells were transfected with an expression

vector containing the cDNA for PPARγ1 [141]. The untreated cells expressing increased levels of PPARγ grew at a slower rate than untreated control cells over 72 hours (Figure 5.20). This correlates with the suggestion that early stage neuroblastomas, which may be less aggressive and grow slower than more primitive neuroblasts, express higher levels of PPARγ [342]. Neuroblasts expressing higher levels of PPARγ have been shown to be more mature, with evidence of ganglionic differentiation [342], and therefore increasing the expression of PPARγ within IMR-32 cells may alter the phenotype of the cells from being fast growing and malignant, to more differentiated and less malignant. Neuroblastoma is related to ganglioneuroblastoma, which is characterised by more areas of cellular maturation and ganglioneuromas, which are considered to be further differentiated [1]. These three tumours represent the spectrum of histology seen in cases of "neuroblastoma" with the more primitive neuroblastomas representing aggressive disease and ganglioneuromas representing the fully differentiated, benign masses and ganglioneuroblastomas possessing characteristics of each of these extremes [3]. However no morphological changes to IMR-32 cells expressing increased levels of PPARγ1 were seen.

IMR-32 cells expressing increased levels of PPARγ remained more viable when exposed to higher concentrations of $15dPGJ_2$, than vector controls cells (Figure 5.21). This was apparent only after 48 hours of treatment, at concentrations of 5 μM $15dPGJ_2$ and above, whereas at low concentrations of $15dPGJ_2$ (2.5 μM and below), there was no difference in the sensitivity between control and PPARγ1 expressing cells. Increased levels of PPARγ expressed in IMR-32 cells may have diluted the effect of higher concentrations of $15dPGJ_2$, as the ligand could bind to a greater number of receptors, but may have been limited by the number of binding site on the DNA that the activated receptors may bind to. The availability of co-activators and access to the heterodimeric partners of PPARγ may be limiting and also the cells may require a certain proportion of the PPARs to be activated before they undergo autophagic cell death.

In conclusion, expression of normal levels of functional PPARγ are required to maintain the normal state of the cell. This is shown by the fact that dominant

negative PPARγ induces severe insulin resistance, diabetes, hypertension [329, 330] and cancer [344] and that loss-of-function mutations in PPARγ also result in the development of colon cancer [352]. Variants of PPARγ are also over-represented in endometrial cancer and under-represented in renal cell carcinoma [345]. Therefore, further studies on the expression and function of PPARs are required to forward research into the normal cell, cancer and other diseases, such as diabetes.

Ultimately knocking out the PPARγ gene would provide further insight into its function. Although PPARγ null cells are not viable [144], heterozygous PPARγ knock-out cells have a phenotype intermediate to that of null and wild-type cells and would assist research into PPARγ function [145, 146]. It may also be possible to create conditional mutants of PPARγ, which would allow PPARγ to be switched on or off under certain conditions. Over-expression of the receptors could also be studied using inducible systems such as the Tet-On™ and Tet-Off™ gene expression system (Clontech Laboratories, Basingstoke, UK) to allow regulation of the expression of the protein by adding an inducer, doxycycline to the cells, or by having the inducer absent. These systems use a chimeric transactivator to activate transcription of the gene of interest from a silent promoter. The PPARγ protein could also be linked to the oestrogen receptor and its expression regulated by the addition of tamoxifen to the cells. These systems would allow a greater expression of the protein compared to the expression achieved in these experiments. This is because although the SV40 promoter is a fairly strong promoter, another stronger promoter, such as CMV could be used.

Prior to neuronal differentiation and exit from the cell cycle, MYC proteins are down-regulated in neuroblastoma cells, which have been treated with PPARγ ligands [207, 342]. However, peroxisome proliferators, which activate the α isoform of PPARs have actually been shown to induce oncogenes including cMYC and their ability to induce these genes correlates with tumour-promoting potential [165, 294]. No changes in the levels of expression of either cMYC (Figure 5.22) or NMYC (Figure 5.23) were seen in IMR-32 cells treated with $15dPGJ_2$ indicating that the cells were not differentiating. This contrasts the effects of $15dPGJ_2$ seen in Lan-5 neuroblastoma cells, which differentiate following down-regulation of NMYC [342].

These cells are, like IMR-32 cells, NMYC amplified, but do differ in other respects including their response to retinoic acid, as Lan-5 cells extend their neurites and differentiate, whereas IMR-32 cells undergo cellular enlargement and vacuolisation without neurite formation [77].

Interestingly, despite there being no differences in cMYC expression between treated and control IMR-32 cells, the type of cMYC changed between 24 and 72 hours post-plating of the cells and may reflect different regulation by cMYC as the cells become established on the tissue culture plastic. This may suggest that there was some deprivation of methionine or high cell density in the cell cultures, which have been shown to promote translation of cMYC1 in preference to cMYC2, which is translated from the AUG codon [527, 528]. PPARγ has been shown to down-regulate cMYC through interactions with the transcription factor TCF-4 in leukaemia cells [469]. One hour after treatment with troglitazone, DNA binding of TCF-4 was completely abrogated and within 12 hours, the expression of both cMYC mRNA and cMYC protein was down-regulated [469]. However, these cells, unlike IMR-32 cells, rapidly underwent apoptosis following treatment with either $15dPGJ_2$ or troglitazone with activation of caspase 3 within 24 hours [469]. Therefore, activated PPARγ is having a different effect on the leukaemia cells than on the IMR-32 cells. MAD1 is expressed in post-mitotic neurones and Mad proteins have been shown to repress cMYC and antagonise its growth promoting functions [488]. Therefore in cells, which are arrested Mad1 expression may be elevated, and MYC proteins down-regulated. However, like cMYC and NMYC, there were no changes on Mad1 expression when IMR-32 cells were treated with $15dPGJ_2$, and this would be expected as no evidence of arrest at G_1 has been seen in these cells.

PAX3 is a paired box transcription factor, which is expressed in undifferentiated immature neurones and is highly expressed in neuroblastoma cells [489, 490]. PAX3 protein and PAX3 mRNA expression and DNA binding are decreased on induction of differentiation of neuroblastoma cells, corresponding with a slow cell cycle arrest and changes to the cellular morphology, such as neurite output [495, 496]. A similar slow cell cycle arrest, but without neurite output, was seen in IMR-32 cells with $15dPGJ_2$ and this corresponds with a reduction in expression of PAX3 mRNA,

as both occurred at 72 hours but not 24 hours post-initial treatment. This decrease in PAX3 expression at 72 hours (Figure 5.24), suggests that PAX3 is not a direct target of PPARγ, but that that it may be down-regulated as IMR-32 cells cease growing and is just a downstream effect of growth arrest in these cells. This is in contrast to the results seen in the ND7 neuroblastoma cell line, which is a hybrid of a mouse neuroblastoma cell fused to a rat dorsal root ganglion cell [529]. In these cells, a decrease in PAX3 expression led to the cells extending their neurites [496], whereas IMR-32 cells retracted their neurites and rounded up. The changes in PAX3 expression in ND7 cells also occurred very early, within one hour post-transfection with PAX3 antisense oligonucleotides, resulting in reduced PAX3 binding to DNA [496], whereas in IMR-32 cells the decreased expression of PAX3 was only seen later. Unlike in the IMR-32 cells, the effects mentioned above in ND7 cells do not involve PPARγ, although 15dPGJ$_2$ does reduce the expression of *PAX3* mRNA within 24 hours in this cell line (data not shown) and this may reflect differences already noted between human and rodent PPARs [309, 134]. No other reports of PPARγ interacting with members of the PAX family of transcription factors have been published, except one paper suggesting an interaction between PPARγ and PAX6 [530]. PPARγ inhibits transcription of the glucagon gene through the inhibition of PAX6 transcriptional activity, in a ligand-dependent, but not DNA-binding dependent manner [530]. Therefore PAX6 may be a novel target of PPARγ, however, these results relate to the anti-diabetic effects of activated PPARγ [312], and do not result in growth arrest of the pancreatic islet α cells, that this effect was seen in.

p21$^{CIP1/SDI1/WAF1}$ is thought to be involved in p53-mediated G_2/M arrest of cells [499], however, it is not involved in the arrest seen in IMR-32 cells treated with 15dPGJ$_2$ (Figure 5.25). In contrast, bladder cancer cells treated with 10 μM troglitazone underwent growth arrest at G_1 and differentiation associated with increases in both p21$^{CIP1/SDI1/WAF1}$ mRNA and protein levels [434]. p53 is able to induce G_2/M arrest by down-regulation of the cdc2 and topoisomerase II genes [499]. No p53 was detected in the nuclei of IMR-32 cells treated with 15dPGJ$_2$ within 24 hours of treatment, however, after 72 hours treatment, p53 was detected in the IMR-32 cell nuclei (Figure 5.26). This suggests that prolonged treatment of IMR-32 cells with

15dPGJ$_2$ results in translocation of p53 to the nucleus and that p53 may be involved in the G_2/M arrest in these cells induced by 15dPGJ$_2$.

The tumour suppressor PTEN/MMAC1/TEP1 contains two response elements for PPARγ in the sequence directly upstream of the gene and activation of PPARγ by rosiglitazone induces increased expression of PTEN/MMAC1/TEP1 in colorectal cancer and breast cancer cells, correlating with reduced proliferation of these cells [505]. Increases in PTEN expression can be measured as a reduction in the phosphorylation of PKB, due to reduced activity of phosphatidylinositol 3,4,5-trisphosphate (PIP_3) (Figure 5.27). Treatment of IMR-32 cells with 15dPGJ$_2$ activated PPARs, but there was no up-regulation of PTEN/MMAC1/TEP1, as there was no reduction in the expression of phospho-PKB (Figure 5.28). Activated PPARγ did not seem to regulate PTEN in IMR-32 cells, possibly because 15dPGJ$_2$ did not stimulate PPARγ to bind to these elements. The effect of activated PPARγ regulating PTEN expression was also seen in macrophages [505], which express PPARγ1 and PPARγ2 transcripts and protein, as well as the transcript PPARγ3 [142]. This may indicate a different regulation of PPARγ in these cells involving PTEN, which may not occur in IMR-32 cells, or it may be simply a cell-specific effect. Also, interestingly, although PTEN/MMAC1/TEP1 is commonly mutated in cancers [507], second only to p53, coding mutations of PTEN/MMAC1/TEP1 are infrequently involved in the oncogenesis of neuroblastoma [531].

Importantly, PPARs have been shown to be involved in the growth arrest mediated by 15dPGJ$_2$ in IMR-32 cells and therefore this protein can be targeted with other more potent activators to try and improve on it effects on IMR-32 cells. However, another way to look at this would be to establish the target proteins of activated PPARγ and use these as potential therapies for neuroblastoma. The problem of identifying the PPARγ target genes involved in growth arrest could be tackled using methods such a microarrays to determine the many changes to gene expression, which must occur on treatment of the cells with 15dPGJ$_2$. IMR-32 cells could be treated with DMSO or 15dPGJ$_2$ and protein synthesis blocked by cycloheximide and the mRNA isolated from the cells could be radiolabelled and

hybridised to a microarray, so that only the genes directly up-regulated or down-regulated by the activated PPARγ could be determined.

Synthetic ligands for PPARγ have already reached the clinical trial stage for the treatment of diabetes and have been shown to have few side effects. However, Troglitazone, which is marketed as Rezulin™, has been shown to cause hepatic dysfunction and liver failure [532] and an anti-diabetic drug as a treatment for neuroblastoma may not be suitable for use in the young children that neuroblastoma affects. It should also be noted that activation of PPARγ in mouse models of colon cancer has been shown to increase the formation of colon polyps [350, 351]. However, this effect has not been seen in humans, except in a cyclo-oxygenase depleted colorectal cancer cell line, but these effects may be independent of PPARγ [188]. Therefore, activation of PPARγ still has potential in the treatment of neuroblastoma, but requires more detailed studies on its functions and effects *in vivo* before it can go further.

Chapter 6

Under Delipidated Conditions PUFAs and 15dPGJ$_2$ Induce Apoptosis in IMR-32 Cells *In Vitro*

6.1 *Introduction*

Foetal calf serum used in tissue culture contains mitogenic factors within the lipid fraction, which may alter cell growth and the effects of treatments on cells [533, 534]. This lipid fraction can be removed from serum by delipidation, which removes lipids without significantly denaturing serum proteins [404, 535]. Components within this lipid fraction include lysophosphatidic acid (LPA) and sphingosine-1-phosphate (personal communication, Hunt and Neale, Southampton General Hospital) [533, 534, 536], which have been shown to have mitogenic effects on neuroblastoma cells *in vitro* [537, 538]. LPA acts through Edg2 and Edg4 receptors [539, 540] and it is thought that albumin-bound LPA is responsible for the biological activity of heat-stable whole serum [536]. LPA is able to reverse the differentiation phenotype of neuroblastoma cells, including withdrawal of neurites [537, 538]. Sphingosine-1-phosphate (S1P) induces neurite retraction and cell rounding in the neuroblastoma cell line N1E-115 [541] and also in PC12 cells, where neurite retraction correlates with apoptosis of these cells [542, 543]. S1P-induced neurite retraction is mediated through the G-protein coupled receptor, H218 [542], but other functions of S1P occur through another related receptor, Edg-1 [544]. S1P has been shown to suppress apoptosis [545] and the presence of S1P and LPA within the serum may influence the growth of neuroblastoma cells *in vitro* [537, 538]. LPA and S1P may prevent neuroblastoma cells from undergoing apoptosis or suppress the differentiated phenotype of neuroblastoma cells, despite the cells being treated with agents which would induce these processes. Polyunsaturated fatty acids (PUFAs) inhibit growth of some cancer cell lines and can also induce apoptosis in colon cancer cells and leukaemia cells [177, 409]. However, PUFAs only had marginal effects on IMR-32 cells and it is possible that factors within the serum could be preventing the fatty acids from having more effects on the neuroblastoma cells. Likewise, 15-deoxy$\Delta^{12,14}$-prostglandin J_2 ($15dPGJ_2$) has been shown to induce apoptosis in SHSY5Y neuroblastoma cells [362] and differentiation in Lan-5 neuroblastoma cells [207, 342]. However, IMR-32 cells undergo autophagy on treatment with this PPARγ ligand, but by removing mitogenic lipids from the tissue

culture medium, it is possible that $15dPGJ_2$ may have different effects on the IMR-32 cells and may indeed induce differentiation or apoptosis.

6.2 *The effects of fatty acid supplementation on neuroblastoma cell under delipidated conditions*

6.2.1 *PUFAs in the presence of delipidated serum are potent inhibitors of IMR-32 cell growth*

IMR-32 cells were grown in complete or delipidated sera together with 30 μM AA, DHA or OA and the effect on IMR-32 cell growth assessed over 72 hours. Control or HBSS-treated IMR-32 cells grew consistently throughout the experiments in normal conditions, but when the control-treated cells were grown under delipidated conditions, little or no cell growth was observed during the experiment and cell number remained around 1.5×10^4 cells (Figure 6.1). When the IMR-32 cells were grown in the presence of AA or DHA in complete media, cell growth was reduced after 72 hours compared to untreated or HBSS treated cells. However, when AA or DHA were added to IMR-32 cells in delipidated medium, cell growth dramatically decreased and at 48 hours little cell growth was observed (Figure 6.1).

6.2.2 *PUFA supplementation in delipidated medium results in the death of IMR-32 cells*

Both AA and DHA inhibited IMR-32 cell growth in delipidated media, and this could have been due to the onset of differentiation or cell death. Human neuroblastoma cells grown under delipidated conditions did not grow, with numbers of control cells throughout experiment being similar to that of that initially plated out (1.6×10^4 cells) and therefore the growth of the control cells was arrested. Large numbers of IMR-32 cells grown in delipidated medium and treated with PUFAs appeared to detach from the tissue culture plastic, suggesting that the cells were dying. Cell death was measured by the uptake of the polar dye trypan blue, which is excluded by live cells.

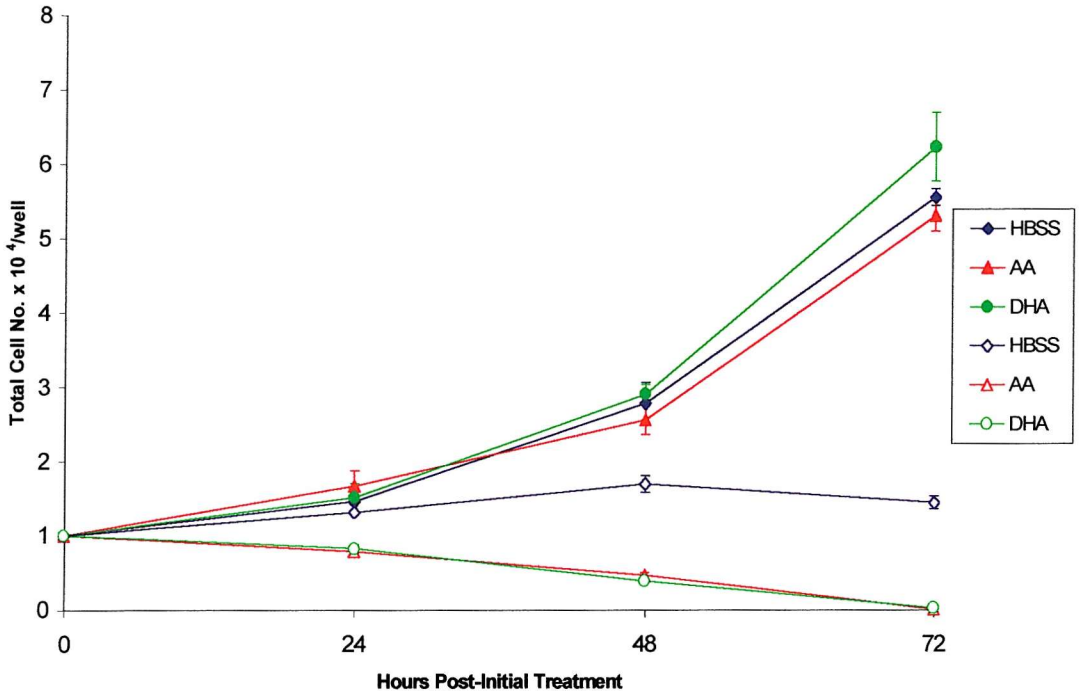

Normal medium	Solid symbols
Delipidated medium	Open symbols

Figure 6.1 PUFAs effectively inhibit the growth of IMR-32 cells under delipidated conditions. IMR-32 cells were cultured under normal and delipidated conditions, supplemented with 30 μM PUFAs. The treatments, but not the medium were replaced daily and increases in cell number measured. Two samples were counted per treatment per day and experiments were completed in duplicate and error bars represent standard errors of the mean. Statistics were calculated using an ANOVA and showed that both arachidonic acid and docosahexaenoic acid significantly inhibited cell growth under delipidated conditions compared to under complete conditions at a significance of $p<0.05$.

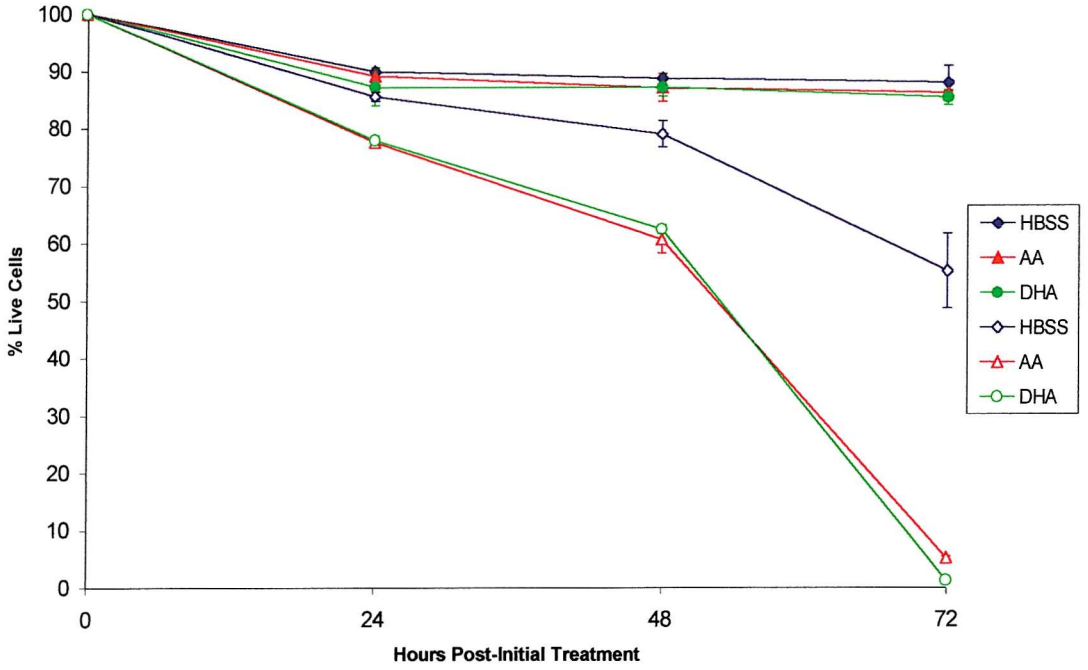

Normal medium	Solid symbols
Delipidated medium	Open symbols

Figure 6.2 PUFAs effectively induce death of IMR-32 cells under delipidated conditions. IMR-32 cells per well were plated out and treated with 30 μM PUFAs under normal and delipidated conditions, and the proportion of dead cells measured by the trypan blue exclusion assay. Two samples were counted per treatment per day and experiments were completed in duplicate and error bars represent standard errors of the mean. Statistics were calculated using an ANOVA and showed that under delipidated conditions compared to normal conditions, arachidonic acid and docosahexaenoic acid significantly induce cell death at $p < 0.05$.

Little trypan blue staining was found in control cells or cells treated with AA or DHA grown in complete medium. In contrast, in control cells grown in delipidated media, a small percentage of cells stained with trypan blue by 48 hours (Figure 6.2). However, by 72 hours, the PUFA-treated cells cultured in delipidated media, had extensive uptake of the dye, indicating that AA and DHA in delipidated media, were inhibiting cell growth through the induction of cell death (Figure 6.2).

6.2.3 *A combination of treatment with PUFAs and delipidated medium induces apoptosis in IMR-32 cells*

The cell death induced by the fatty acids in delipidated medium could have been due to autophagic cell death or apoptosis. One molecular hallmark of apoptosis is DNA degradation resulting in the formation of a laddered pattern of DNA consisting of multiples of 180 base pairs, where a caspase-dependent DNAse cleaves the DNA of apoptotic cells between the histones [359, 360]. DNA was therefore extracted from cells treated with AA, DHA and OA after 24, 48 and 72 hours and analysed by gel electrophoresis. No DNA fragmentation occurred in untreated cells grown in complete or delipidated media or in fatty acid treated cells grown in complete media (Figure 6.3 and data not shown). However, when IMR-32 cells were treated with AA or DHA in delipidated media, DNA laddering was observed at 48 hours, indicating that these cells were undergoing cell death via an apoptotic pathway (Figure 6.3). Little degradation was seen with cell treated with oleic acid (Figure 6.3).

Poly ADP ribose polymerase (PARP) cleavage was also used to determine whether apoptosis was occurring as some cells have been shown to undergo apoptosis without the presence of DNA fragmentation [423, 546], including IMR-32 cells treated with staurosporine [436]. PARP is cleaved by caspases during apoptosis from a 116 kDa protein, into two fragments of 85 kDa and 24 kDa [424, 425]. The larger, 85 kDa, fragment is able to bind to DNA and prevents access to DNA repair enzymes, thus allowing apoptosis to continue [424, 425]. No evidence of PARP cleavage was seen in control or fatty acid treated cells grown in complete media (data not shown). However, when IMR-32 cells were grown in delipidated media, a small amount of PARP cleavage was detectable.

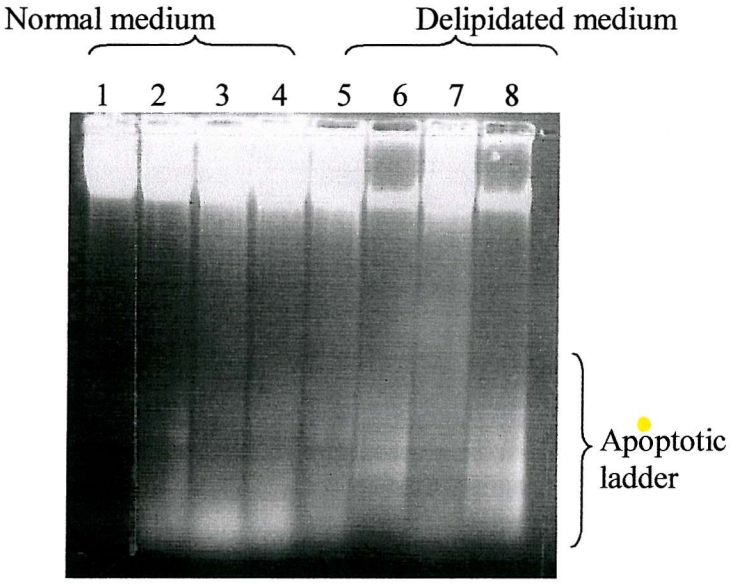

Lane 1 + 5 IMR-32 cells – HBSS

Lane 2 + 6 IMR-32 cells – Arachidonic acid

Lane 3 + 7 IMR-32 cells – Oleic acid

Lane 4 +8 IMR-32 cells – Docosahexaenoic acid

Figure 6.3 PUFAs induce fragmentation of IMR-32 cell DNA under delipidated conditions. IMR-32 cells were treated with 30 μM PUFAs under normal and delipidated conditions for 48 hours. DNA from the cells was isolated and was electrophoresed on a 1 % agarose gel. This was to determine whether DNA fragmentation and therefore apoptosis, was occurring. The DNA was visualised by UV illumination.

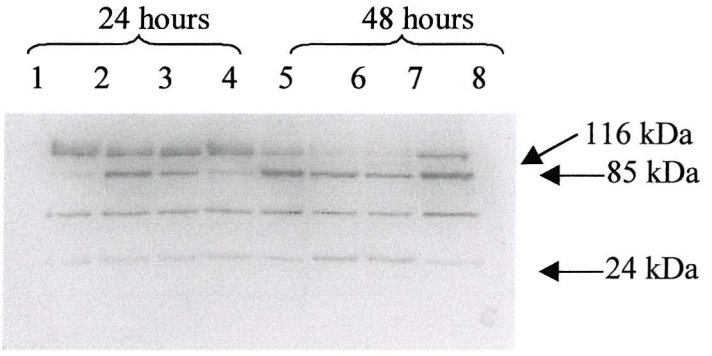

Poly-ADP ribose polymerase (PARP)

SDS-PAGE membrane

Lane 1 +5	IMR-32 cells – HBSS
Lane 2+ 6	IMR-32 cells – Arachidonic acid
Lane 3 + 7	IMR-32 cells – Docosahexaenoic acid
Lane 4 +8	IMR-32 cells – Oleic acid

Figure 6.4 PUFAs induce cleavage of poly-ADP ribose polymerase (PARP) under delipidated conditions. Nuclear extracts of IMR-32 cells treated with 30 μM PUFAs under delipidated conditions were resolved by SDS-PAGE. Full-length PARP (116 kDa) and the cleavage products of PARP (85 kDa and 24 kDa) were detected by western blotting.

PARP cleavage may be a more sensitive assay than DNA fragmentation, as it suggests that a small percentage of cells in delipidated media are undergoing apoptosis, which cannot be detected by DNA fragmentation. In IMR-32 cells treated with fatty acids under delipidated conditions, full-length PARP was completely cleaved and the production of cleavage fragments were observed (Figure 6.4).

6.3 *The effect of PPAR ligands on IMR-32 cells grown under delipidated conditions*

6.3.1 *15dPGJ$_2$ further inhibits the growth of IMR-32 cells grown under delipidated conditions*

The removal of mitogenic lipids from serum altered the effects of fatty acids on IMR-32 cells, and therefore it was investigated whether delipidation of serum also altered the effects of 15-deoxy$\Delta^{12,14}$-prostglandin J_2 (15dPGJ$_2$) on IMR-32 cells. The cells were cultured under delipidated conditions and treated with DMSO, 5 μM 15dPGJ$_2$, 5 μM Wy-14643 or left untreated and cell number counted daily. Control cells grown under delipidated conditions hardly grew during the experimental time (Figure 6.5). The cells treated with 15dPGJ$_2$ and grown under normal conditions, as previously described did not increase in number within 72 hours, however, those treated with 15dPGJ$_2$ and grown under delipidated conditions actually decreased in number within 48 hours from initial numbers of cells plated out (Figure 6.5). The delipidated medium enhanced the inhibitory effects of 15dPGJ$_2$ on the growth of IMR-32 cells therefore a component of the normal serum may have prevented 15dPGJ$_2$ from having the same effect under normal conditions. The PPARα ligand, Wy-14643 did not inhibit growth of IMR-32 cells compared to controls in either complete or delipidated medium (Figure 6.6). The effects of the delipidated medium alone were seen within 48 hours, but addition of Wy-14643 did not increase inhibition of IMR-32 cell growth under normal or delipidated conditions.

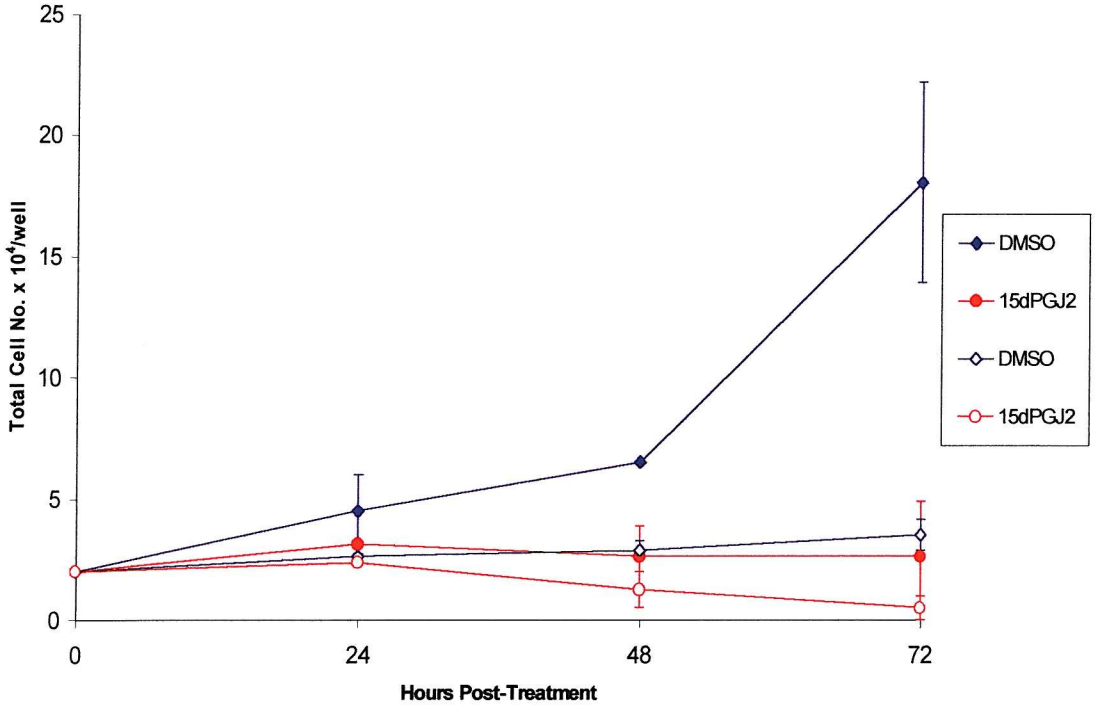

Normal medium	Solid symbols
Delipidated medium	Open symbols

Figure 6.5 $15dPGJ_2$ is more effective at inhibiting the growth of IMR-32 cells under delipidated conditions than under normal conditions. IMR-32 cells were cultured under normal and delipidated conditions and treated with 5 μM $15dPGJ_2$ daily without a change of medium and cell growth assessed over 120 hours. Two samples were counted per treatment per day and two independent experiments were completed. Statistics were calculated using an ANOVA, which showed that under delipidated conditions, $15dPGJ_2$ significantly inhibited cell growth compared to under normal conditions at a significance of $p < 0.05$.

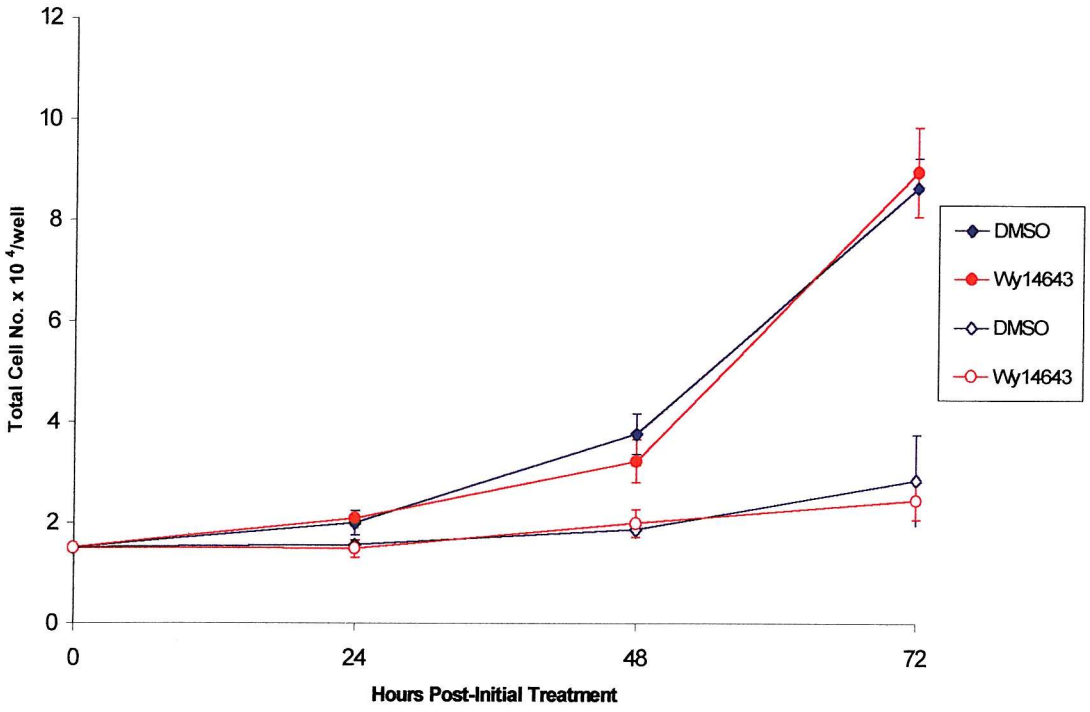

Normal medium	Solid symbols
Delipidated medium	Open symbols

Figure 6.6 Wy-14643 does not inhibit IMR-32 cell growth under delipidated conditions. IMR-32 cells were plated out at 2 x 10^4 cells and grown in normal or delipidated medium and treated with 5 μM Wy-14643. Cell number was counted daily for 120 hours to establish cell growth. Two samples were counted per treatment per day and experiments were completed in duplicate.

6.3.2 *15dPGJ$_2$ further induces the death of IMR-32 cells grown under delipidated conditions*

The trypan blue exclusion assay was used to determine if IMR-32 cells grown under delipidated conditions and treated with 15dPGJ$_2$ died in increasing numbers. At 24 hours, there was no increase in trypan blue uptake in the cells in delipidated medium, compared to normal conditions. However, from 48 hours there was a 20 % increase in the number of cells and by 72 hours there was a 35 % increase in trypan blue stained cells (Figure 6.7). This shows that removal of the lipid fraction reduces the survival of untreated and control treated IMR-32 cells and may induce the cells to die.

Supplementation of IMR-32 cells with 15dPGJ$_2$ under delipidated conditions increased the levels of cell death compared to those cells treated with 15dPGJ$_2$ in normal medium. In normal medium only 33 % of the cells were viable after 72 hours of treatment with 15dPGJ$_2$, however under delipidated conditions only 3 % of the cells were viable (Figure 6.7). This effect was not synergistic, but there was an additive effect of a combination of 15dPGJ$_2$ and delipidation of medium. However, IMR-32 cells treated with Wy-14643 did not undergo cell death at any rate above that of controls (Figure 6.8). In delipidated medium, however, there was a slight increase in IMR-32 cell death from control treatments from 48 hours (Figure 6.8). This effect was less at 72 hours, when the effect of the delipidated medium alone caused cell death, compared to cells grown in complete medium.

6.3.3 *Delipidated foetal calf serum induces apoptosis of IMR-32 cells when combined with PPARγ, but not PPARα ligands*

IMR-32 cells grown in delipidated medium and treated with 5 μM 15dPGJ$_2$ underwent further cell death than the cells grown under normal conditions and treated with 15dPGJ$_2$. This effect could have been due to more cells undergoing growth arrest and autophagy, or apoptosis. To determine whether the cells were apoptosing, several apoptotic assays were employed.

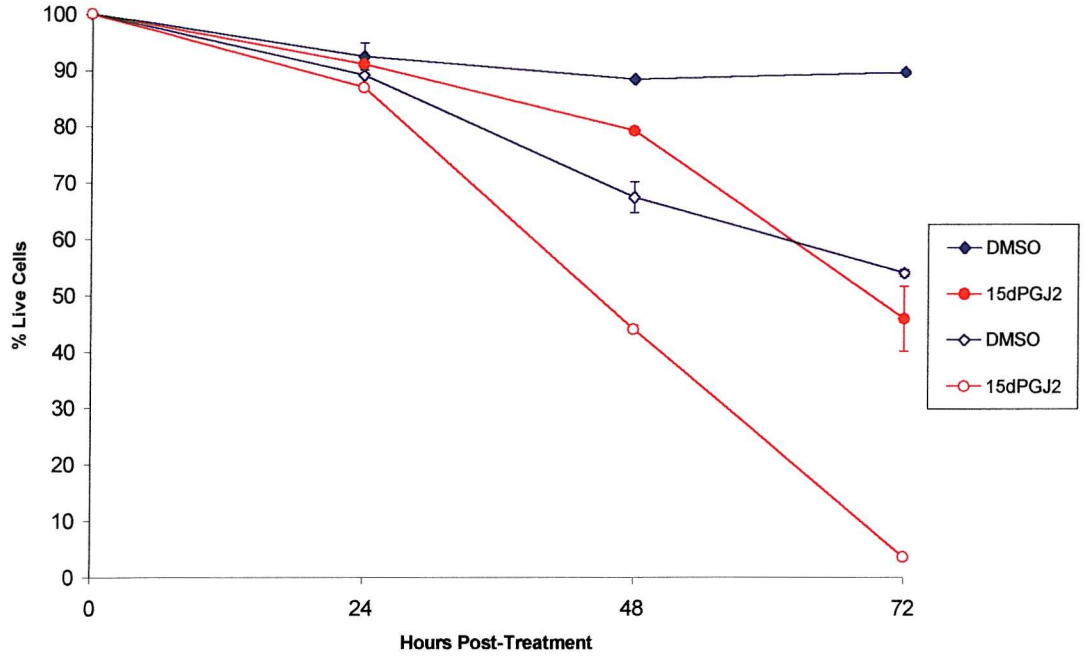

Normal medium Solid symbols

Delipidated medium Open symbols

Figure 6.7 $15dPGJ_2$ is more effective at inducing the death of IMR-32 cells under delipidated conditions, than under normal conditions. IMR-32 cells were plated out and treated with DMSO or $15dPGJ_2$ under normal or delipidated conditions. The proportion of live and dead cells were determined using the trypan blue exclusion assay. Two samples were counted per treatment per day and the experiment was performed in duplicate and error bars represent s.e.m. Statistics were calculated using an ANOVA and showed that under delipidated conditions, $15dPGJ_2$ significantly induced cell death compared to under normal conditions, throughout the experiment, at a significance of $p < 0.05$.

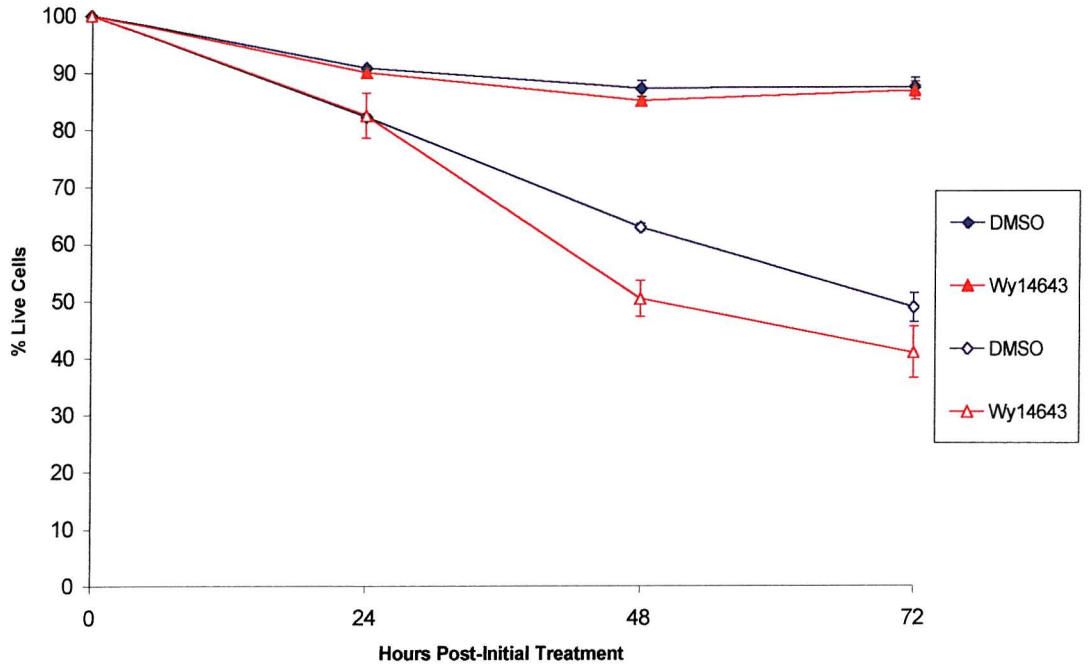

Normal medium	Solid symbols
Delipidated medium	Open symbols

Figure 6.8 Wy-14643 does not induce the death of IMR-32 cells grown under delipidated conditions. IMR-32 cells were grown under normal conditions or delipidated conditions and treated with 5 μM Wy-14643. The proportion of live and dead cells were determined using the trypan blue exclusion assay. This graph represents duplicate experiments with two samples per experiment and the errors are s.e.m.

Total DNA was isolated from IMR-32 cells treated with DMSO, 5 μM $15dPGJ_2$ or 5 μM Wy-14643 and grown either under delipidated or normal conditions and electrophoresed to look for the presence of an apoptotic DNA ladder. IMR-32 cells treated with $15dPGJ_2$ in delipidated medium underwent apoptosis, seen as a pronounced ladder on the gel (Figure 6.9). However, control treated cells grown under delipidated conditions also died in greater numbers than control cells in normal conditions (Figure 6.7), therefore, they may have also been apoptosing, but DNA fragmentation may not be able to detect a lower level of apoptosis. IMR-32 cells treated with Wy-14643 did not undergo a greater degree of cell death than control cells under the same conditions and in accordance with this, no apoptotic ladder was seen on an agarose gel, when the DNA from these cells was electrophoresed (Figure 6.10). However, IMR-32 cells can undergo DNA fragmentation, as seen by cells treated with 20 μg/ml betulinic acid for 24 hours (Figure 6.10).

To confirm that IMR-32 cells treated with $15dPGJ_2$, but not Wy-14643, underwent apoptosis under delipidated conditions, cleavage of the caspase substrate, poly-ADP ribose polymerase (PARP) was also measured. This is because the DNA fragmentation method did not show any apoptosis in control-treated and untreated IMR-32 cells, and yet the cells were dying compared to controls under normal conditions and the assay may not have been sensitive enough to detect a lower level of apoptosis. Nuclear extracts of treated and untreated IMR-32 cells grown under normal and delipidated conditions were resolved by SDS-PAGE and full-length and cleaved PARP was detected using an antibody, which detects both forms of PARP (Upstate Biotechnology, Buckinghamshire, UK). No cleavage of PARP was seen in control-treated and treated IMR-32 cells grown under normal conditions, however some cleavage of PARP was seen in control and Wy-14643-treated IMR-32 cells after 48 hours growth under delipidated conditions (Figure 6.11). This explains the increase in cell death under delipidated conditions compared to that seen under normal conditions, but it may only involve a proportion of cells and this may explain why no apoptosis was detected by DNA fragmentation.

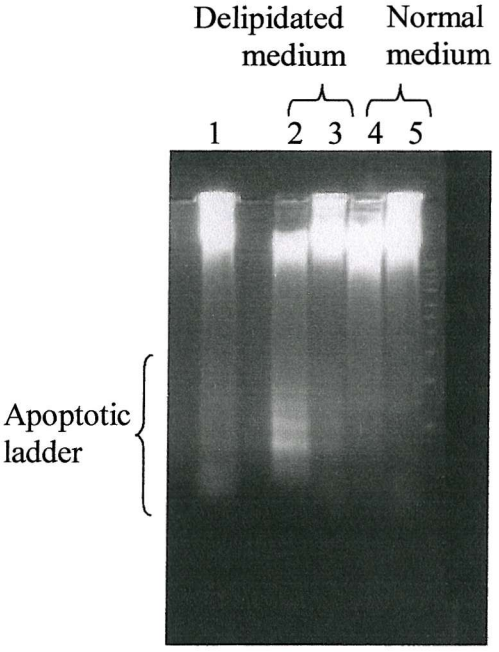

Lane 1	Betulinic acid (20 μg/ml)) (24 hours)
Lane 2	5 μM $15dPGJ_2$
Lane 3	DMSO
Lane 4	5 μM $15dPGJ_2$
Lane 5	DMSO

Figure 6.9 $15dPGJ_2$ induces DNA fragmentation and therefore apoptosis of IMR-32 cells under delipidated conditions. IMR-32 cells were treated with DMSO or 5 μM $15dPGJ_2$ under normal and delipidated conditions and after 48 hours, the DNA was electrophoresed to detect any fragmentation of DNA and therefore apoptosis.

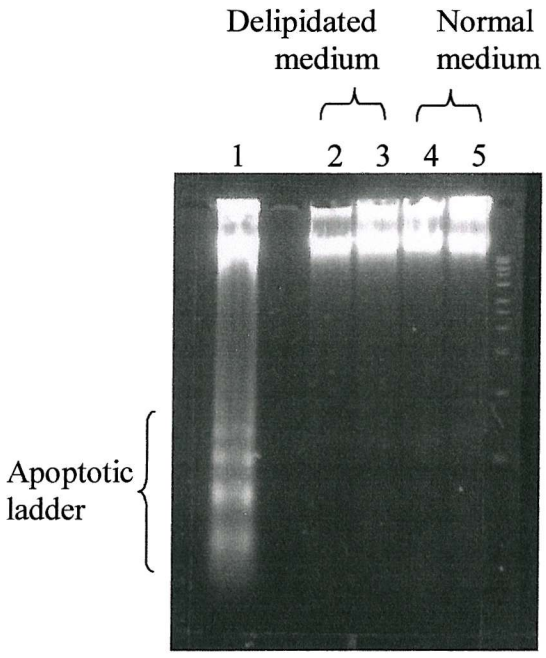

Lane 1	Betulinic acid (20 μg/ml) (24 hours)
Lane 2	5 μM Wy-14643
Lane 3	DMSO
Lane 4	5 μM Wy-14643
Lane 5	DMSO

Figure 6.10 Wy-14643 does not induce DNA fragmentation in IMR-32 cells under delipidated conditions. IMR-32 cells were treated with 5 μM Wy-14643 under normal and delipidated conditions and after 48 hours, the DNA from the cells was electrophoresed to detect any fragmentation of DNA and therefore apoptosis.

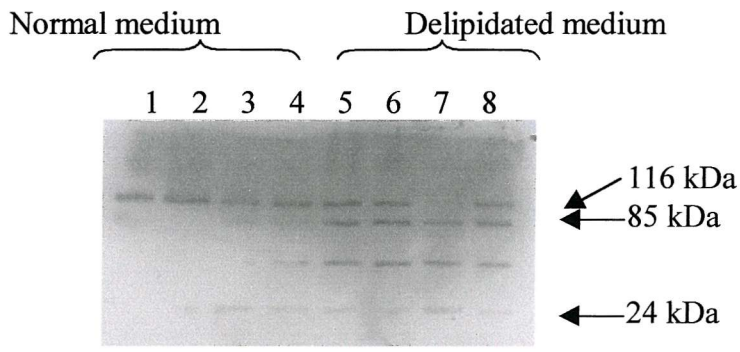

Poly-ADP ribose polymerase (PARP)

SDS-PAGE membrane

Lane 1 +5	IMR-32 cells – Untreated
Lane 2 + 6	IMR-32 cells – DMSO
Lane 3 +7	IMR-32 cells – 15-deoxy$\Delta^{12,14}$-prostglandin J_2
Lane 4 +8	IMR-32 cells – Wy-14643

Figure 6.11 15dPGJ$_2$ induces complete cleavage of the full-length poly-ADP ribose polymerase (PARP) under delipidated conditions. IMR-32 cells treated with 5 μM 15dPGJ$_2$ or Wy-14643 under normal or delipidated conditions and nuclear extracts made after 48 hours. Full-length and cleaved PARP was detected by resolving the nuclear extracts by SDS-PAGE and western blotting.

IMR-32 cells treated with 15dPGJ$_2$ under delipidated conditions undergo apoptosis with the compete degradation of full-length PARP (Figure 6.11). Although there was not a large increase in the 85 kDa cleavage product of PARP, the smaller fragment may not detected by this antibody and may have shown an increase in amount or the cleavage products of PARP may have also been degraded during apoptosis. This shows that the IMR-32 cells were undergoing a higher degree of apoptotic cell death than controls under delipidated conditions (Figure 6.11).

6.4 *The effects of delipidation of serum on neuroblastoma cells in vitro are due to the removal of sphingosine-1-phophate and not lysophosphatidic acid*

6.4.1 *Supplementation of delipidated medium with lysophosphatidic acid has no effect on growth of IMR-32 cells*

As previously described, lysophosphatidic acid (LPA) is a component of the mitogenic lipid fraction, which is removed on delipidation of serum and it has effects on neuroblastoma cell *in vitro* [537, 538]. Therefore to determine whether the effects of delipidated serum are solely due to the removal of LPA, LPA was added back to the serum and cell growth compared to that under delipidated conditions. 5 μM oleoyl-LPA was used as there are several different types of LPA within serum and oleoyl-LPA is the most abundant [547] (personal communication, Alan Hunt, Southampton General Hospital and Figure 6.12). Supplementation of the delipidated tissue culture medium with 5 μM oleoyl-LPA had little effect on the growth of IMR-32 cells. DMSO-treated IMR-32 cells actually grew even slower when oleoyl-LPA was added to the culture medium, than under delipidated conditions alone (Figure 6.13). There was also no difference between cells treated with 15dPGJ$_2$ grown under delipidated conditions, or under the same conditions with a supplement of oleoyl-LPA (Figure 6.13). This suggests that either another component of the mitogenic lipid fraction is more important or more than one component is required to be added back to the serum.

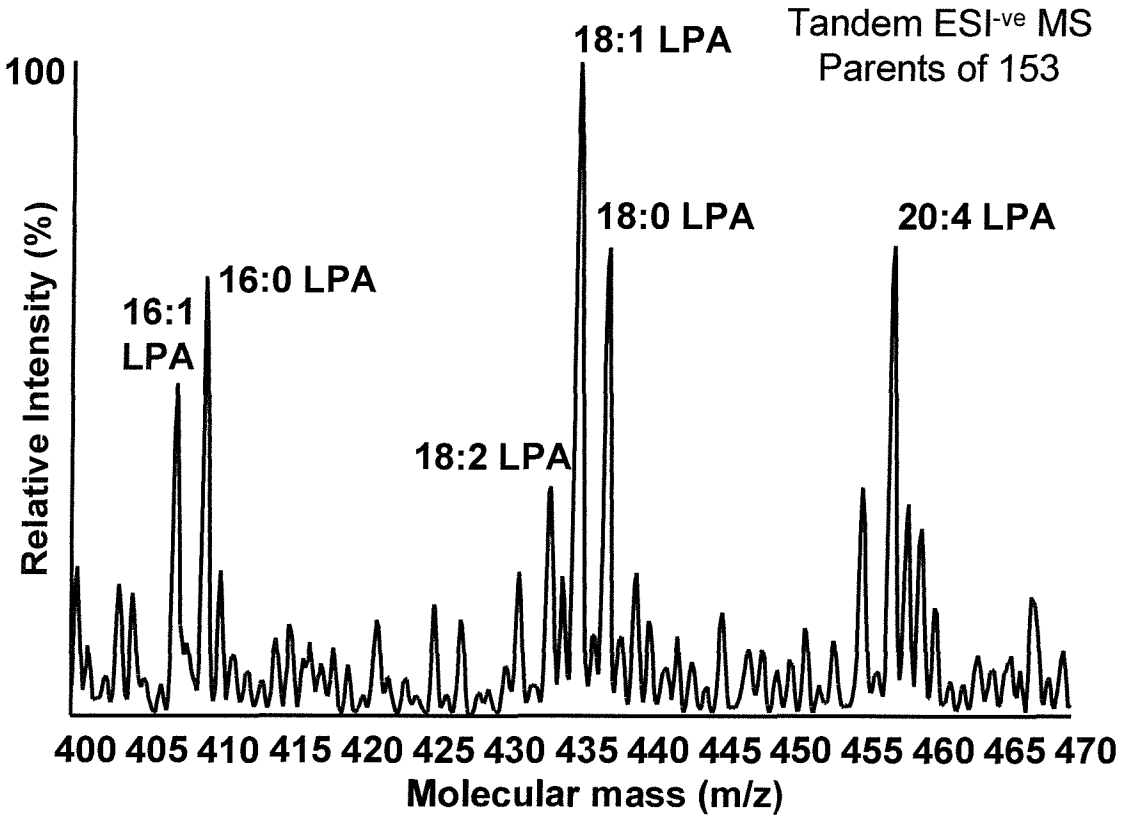

Figure 6.12 Molecular species of lysophosphatidic acid (LPA) found within foetal calf serum used for tissue culture of neuroblastoma cells used in all experiments. Courtesy of Alan Hunt, Southampton General Hospital.

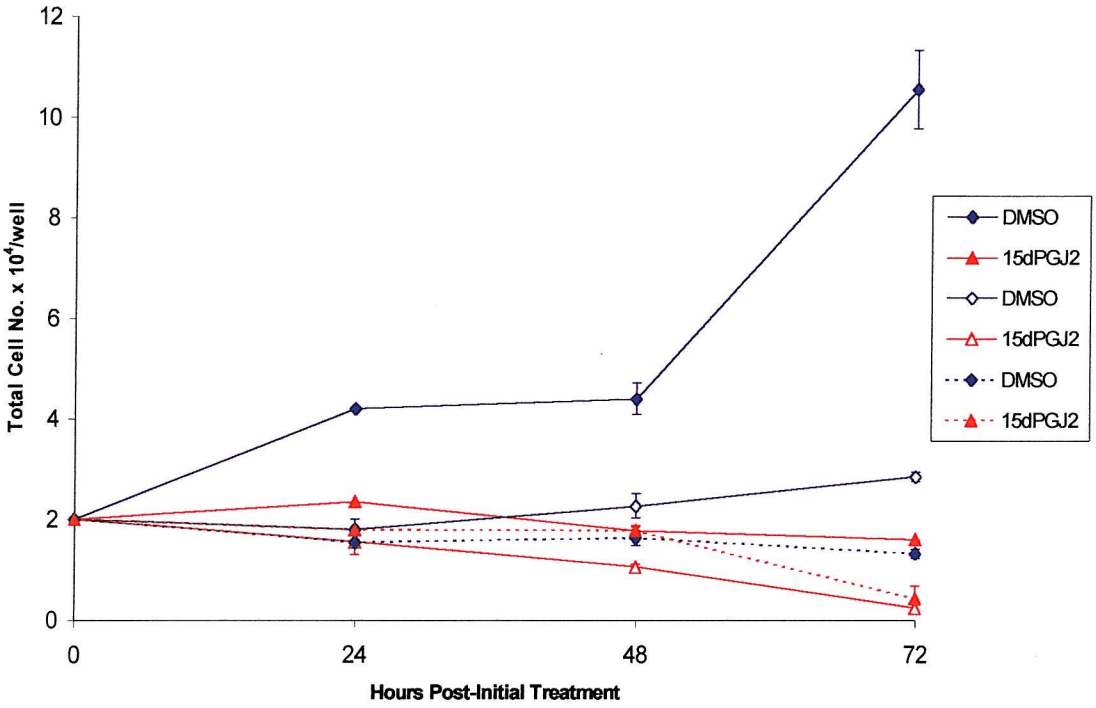

Normal medium	Solid line + closed symbol
Delipidated medium	Solid line + open symbol
Delipidated medium + oleoyl-LPA	Dashed line + closed symbol

Figure 6.13 Supplementation of delipidated medium with oleoyl-LPA does not prevent inhibition of IMR-32 cell growth induced by 15dPGJ$_2$ and delipidated medium. IMR-32 cells were treated with 5 μM 15dPGJ$_2$ under normal and delipidated conditions and under delipidated conditions supplemented with 5 μM oleoyl-lysophosphatidic acid (LPA). Cell growth was measured as increases in cell number for 120 hours. Two samples were counted per treatment per day and experiments were completed in duplicate and error bars represent standard errors.

6.4.2 *Supplementation of delipidated medium with LPA does not prevent the death of IMR-32 cells treated with 15dPGJ$_2$*

To determine whether supplementation of delipidated medium with 5 μM oleoyl-LPA had any effect on the death of IMR-32 cells caused by growing them in delipidated medium, proportion of dead cells was measured using the trypan blue exclusion assay. As with the cell growth experiment, the addition of oleoyl-LPA increased the amount of cell death in DMSO-treated cells, but had no effect on the levels of cell death seen in cells treated with 15dPGJ$_2$ (Figure 6.14). However, the cell death induced by a combination of 15dPGJ$_2$ and delipidated medium is less in this experiment than in previous experiments, but the effects seen are similar compared to controls.

6.4.3 *Sphingosine-1-phosphate reverses the effects of delipidated medium and 15dPGJ$_2$ on IMR-32 cell growth*

Like LPA, sphingosine-1-phosphate (S1P) is a component of the lipid fraction of serum, which has been shown to affect the growth of neuroblastoma cells *in vitro*. To determine whether removal of S1P during delipidation of serum resulted in the increased effects of 15dPGJ$_2$ on IMR-32 cells, S1P was added back to the tissue culture medium and the effects on cell growth were investigated. Control cells grown under delipidated conditions did not grow and IMR-32 cells treated with 15dPGJ$_2$ under these conditions did not survive (Figure 6.15). When normal tissue culture medium was supplemented with 5 μM S1P, 15dPGJ$_2$ did not inhibit the growth of IMR-32 cells as much as that seen under normal tissue culture conditions alone and the cells did marginally grow (Figure 6.15). However, when S1P was added to cells treated with 15dPGJ$_2$ and grown under delipidated conditions, it dramatically reversed the growth inhibition induced by 15dPGJ$_2$ together with the delipidated serum and the cells actually increased in number to a greater degree than control cells (Figure 6.15). The addition of S1P to the delipidated tissue culture medium actually allowed the 15dPGJ$_2$-treated cells to grow tenfold compared to those grown under delipidated conditions alone (Figure 6.15).

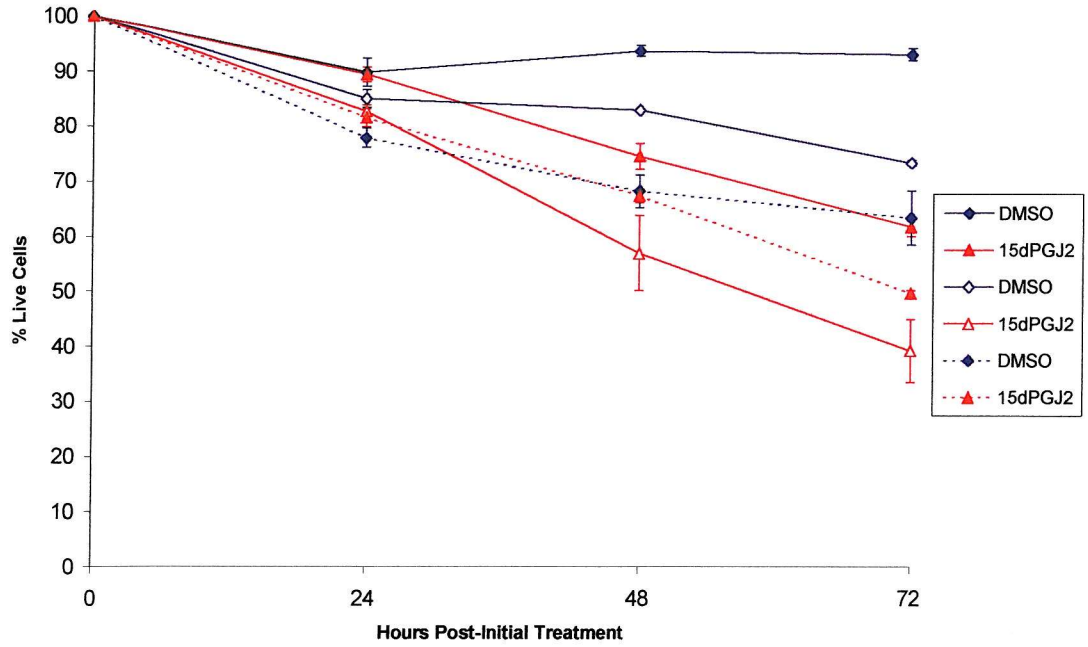

Normal medium	Solid line + closed symbol
Delipidated medium	Solid line + open symbol
Delipidated medium + oleoyl-LPA	Dashed line + closed symbol

Figure 6.14 Supplementation of delipidated medium with oleoyl-LPA does not prevent death of IMR-32 cells induced by 15dPGJ$_2$. IMR-32 cells were cultured under normal and delipidated conditions and in delipidated medium supplemented with 5 μM oleoyl-LPA and were treated with 5 μM 15dPGJ$_2$. The proportion of live and dead cells were established using the trypan blue exclusion assay. Two samples were counted per treatment per day and experiments were completed in duplicate and errors shown as s.e.m.

This indicates that the effects of delipidation were either solely or mainly due to the removal of S1P from the serum.

6.4.4 *Sphingosine-1-Phosphate prevents cell death induced by 15dPGJ$_2$ in IMR-32 cells under delipidated conditions*

IMR-32 cells grown under delipidated conditions and treated with 15dPGJ$_2$ underwent a high level of cell death measured by trypan blue uptake. If S1P was able to prevent 15dPGJ$_2$ from having growth inhibitory effects under delipidated conditions, then it may have been preventing IMR-32 cell death. In order to investigate this, IMR-32 cells were treated under delipidated conditions with or without supplementation with S1P and trypan blue uptake was measured. A low level of trypan blue uptake and therefore cell death was seen in the control-treated IMR-32 cells under normal and delipidated conditions (Figure 6.16). Cells treated with 5 μM 15dPGJ$_2$ under normal conditions increasingly took up trypan blue with almost 50 % of cells dying at 72 hours (Figure 6.16). However, addition of 5 μM S1P under normal conditions reduced the rate of cell death, by 20 %, as only approximately 30 % of cells treated in this way were dying (Figure 6.16). Under delipidated conditions 15dPGJ$_2$ induced 80 % of cells to die, but supplementation of 5 μM S1P reduced the rate of cell death to only 25 % (Figure 6.16). This shows that S1P within tissue culture medium was able to suppress cell death and that if it is removed, agents such as 15dPGJ$_2$ can have greater affects on cells, such as neuroblastoma cells.

6.5 *Discussion*

The different responses of cancer cells *in vitro* to ligands of PPARs including polyunsaturated fatty acids and 15dPGJ$_2$ may be due to cell-type specific responses, or they may reflect the different culture conditions of the cells. Foetal calf serum has been shown to contain mitogens within its lipid fraction, including lysophosphatidic acid and sphingosine-1-phopsphate [533, 534, 536]. Both LPA and S1P have been shown to affect the growth of neuroblastoma cells.

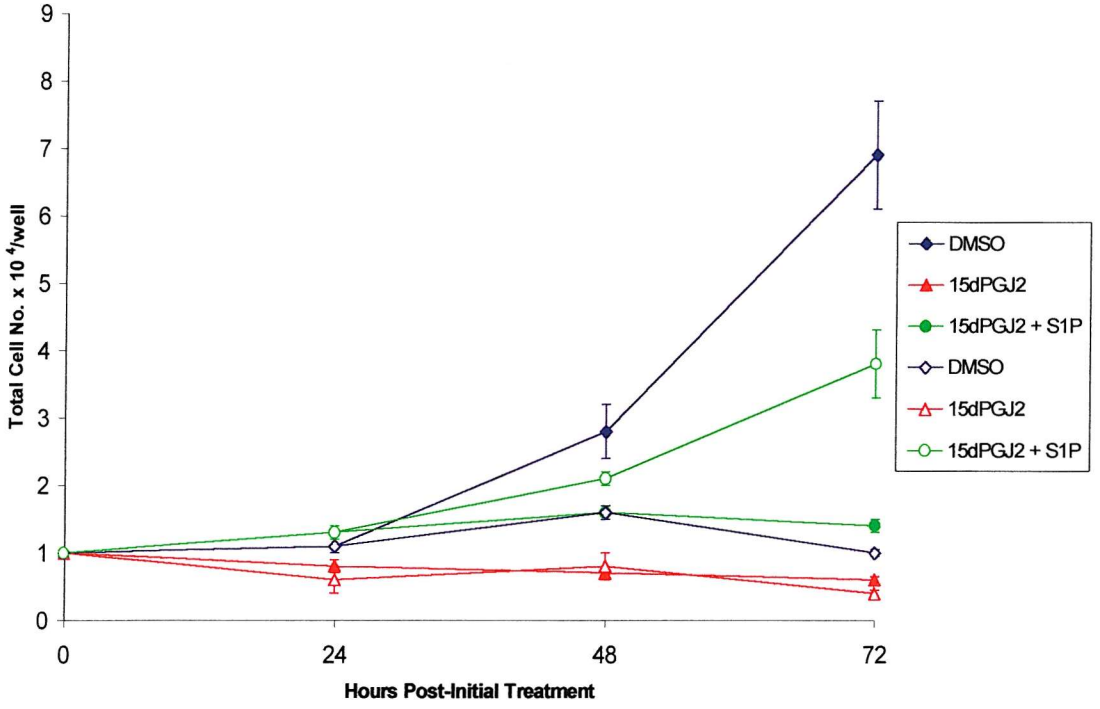

Normal medium	Solid line + closed symbol
Delipidated medium	Solid line + open symbol

Figure 6.15 Supplementation of delipidated medium with S1P prevents $15dPGJ_2$-induced growth inhibition of IMR-32 cells. IMR-32 cells were grown under delipidated conditions supplemented with 5 μM sphingosine-1-phosphate (S1P) and treated with $15dPGJ_2$. Cell growth was measured by increases in cell number for 120 hours. Two samples were counted per treatment per day and the experiments were performed in duplicate. Error bars represent standard errors. Statistics were calculated using an ANOVA, which showed that S1P significantly prevented $15dPGJ_2$-induced cell death under delipidated conditions at a significance of $p < 0.01$.

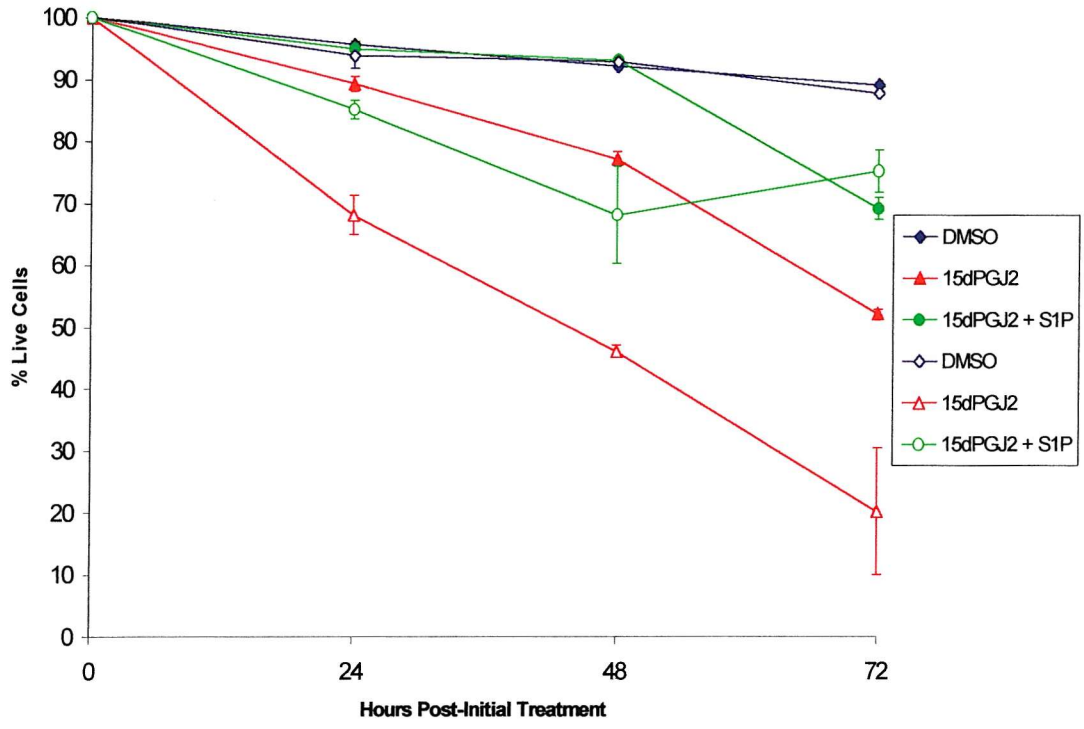

Normal medium	Solid line + closed symbol
Delipidated medium	Solid line + open symbol

Figure 6.16 Supplementation of delipidated medium with S1P prevents the death of IMR-32 cells induced by 15dPGJ$_2$. IMR-32 cells were cultured under normal and delipidated conditions and delipidated conditions supplemented with 5 μM sphingosine-1-phosphate (S1P) and treated with 15dPGJ$_2$. Cell death measured using the trypan blue exclusion assay. Two samples were counted per treatment per day and experiments were completed in duplicate. Errors represented as standard errors of the mean. Statistics were calculated using an ANOVA and showed that S1P significantly prevents 15dPGJ$_2$-induced cell death under delipidated conditions at a significance of $p < 0.05$.

Lysophosphatidic acid (LPA) is a normal constituent of serum released by activated platelets during coagulation [548, 549], which binds albumin [548] and has also been implicated as a signalling molecule [536]. It is also thought that albumin-bound LPA is responsible for the biological activity of heat-stable whole serum [536]. LPA, which acts through Edg2 and Edg4 receptors, has be shown to be able to reverse the differentiation of C1300 murine neuroblastoma cells, resulting in neurite retraction and rounding of the cell body [537] and a similar effect, although to a lesser extent was seen in PC12 cells [548]. LPA has also been shown to be important in normal neural development, mediating survival of Schwann cells [550] and oligodendrocytes [551].

Sphingosine-1-phosphate is a sphingolipid metabolite, which is thought to be a lipid signalling molecule [534]. It acts through several G protein coupled receptors [542, 544], which are related to the Edg receptors Edg-2 and Edg-4, through which LPA acts [539, 540]. Like LPA, S1P also induces neurite retraction and cell rounding in both PC12 cells [543, 548] and in a mouse neuroblastoma cell line, N1E-115 [541]. This cell rounding correlated with apoptosis and may be due to a loss of cellular attachment [541, 543]. S1P-induced neurite retraction is mediated through the G-protein coupled receptor, H218 [542], but other functions of S1P, such as activation of MAPKs occur through another related receptor, Edg-1 [544]. S1P is mitogenic in a diverse range of cell types including, fibroblasts [552] and airway smooth muscle cells [553]. It is increased within cells in response to stimuli such as nerve growth factor and is thought to regulate both cell proliferation and calcium homeostasis, as micro-injected S1P mobilises calcium from internal sources [554].

To determine whether LPA and S1P in the lipid fraction were able to prevent apoptosis or further inhibition of cell growth induced by ligands of PPARs, IMR-32 cells were grown in culture medium containing FCS which had been delipidated in a modification of the method of Cham and Knowles [404]. Any changes to cell growth should be due to the removal of lipids and not due to the removal of growth factors, such as platelet derived growth factor, as the technique used is not thought to remove any of the protein fraction of the serum [535]. IMR-32 cells were initially

allowed to attach in medium containing complete FCS, as they failed to initially attach in medium containing delipidated serum (personal observation). These cells did not die, but re-attached on addition of tissue culture medium containing lipids (personal communication, Hunt and Neale, Southampton General Hospital). LPA has been shown to be involved in cell attachment, through rearrangement of the actin cytoskeleton and this can be mimicked by the micro-injection of activated Rho, a Ras-related GTP-binding protein that regulates actin assembly via an unknown mechanism [555, 556]. Removed of LPA from the serum, may prevent initial cell attachment, but once cells are attached they can grow under delipidated conditions for up to 72 hours before the cells start to detach again. This delay in detachment of the cells may be due to slow actin rearrangements from their attached state to an attached state, but lacking LPA. The detachment may be due to a lack of growth factors in the culture medium, as in these experiments, the medium was not replaced daily. This was done as the cells were only weakly attached, possibly due to the actin rearrangements because of a lack of LPA, and tended to slough off with a change of medium (personal observation).

Control-treated IMR-32 cells have been shown to morphologically differentiate under delipidated conditions, with the output of neurites (personal communication, Alan Hunt, Southampton General Hospital) and a concurrent reduction in growth rates (Figure 6.1). The morphological differentiation of the IMR-32 cells was consistent with previous experiments, which used the mouse neuroblastoma cell line, NB2-A, although, the reduction in growth rate was not observed with NB2-A cells [557]. Interestingly, the addition of 30 μM of the fatty acids AA or DHA to IMR-32 cells in delipidated media led to a decrease in the number of cells with neurite outgrowths (personal communication, Alan Hunt, Southampton General Hospital), suggesting that fatty acids suppress the morphological differentiation of the cells in delipidated serum. Monard *et al.*, [557] also observed that oleic acid inhibited neurite outgrowth in NB2A neuroblastoma cells grown in delipidated serum. Erucic acid, in contrast to its *cis*-isomer, oleic acid, did not inhibit neurite outgrowth [557]. Similarly, they found that short chain fatty acids such as butyric, caproic and lauric acid also had no inhibitory effect [557]. PUFAs also massively inhibited the growth of IMR-32 cells under delipidated conditions (Figure 6.1) and

this suggests that under normal conditions, PUFA-treatment of IMR-32 cells resulted in growth inhibition, but when a mitogenic lipid component, possibly either LPA or S1P, was removed, other processes occurred.

Other processes which may be suppressed by mitogenic lipid components include cell death. Neuroblastoma cells grown in serum-free conditions, undergo growth arrest at G_1 and eventually underwent apoptosis [416] and this can be reversed by the replacement of serum onto these cells, which may involve LPA, S1P or both. Interestingly, S1P has been shown to suppress apoptosis [545], suggesting that the absence of S1P, fatty acids can induce apoptosis, whereas in the presence of S1P, fatty acids may only be able to inhibit cell growth. IMR-32 cells grown under delipidated conditions underwent a small amount of cell death (Figure 6.2), measured by trypan blue uptake, compared to those grown under normal conditions, after 24 hours treatment, when they grew to a similar level. This cell death occurred via an apoptotic pathway, which can be detected by Western blotting for cleavage of the caspase target protein, PARP. Apoptosis occurred before 48 hours post-treatment, but could not be detected by DNA fragmentation or propidium iodide, possibly because these assays are less sensitive methods, than detecting PARP cleavage.

On supplementation with PUFAs under delipidated conditions, IMR-32 cells underwent rapid cell death within 48 hours (Figure 6.2). Most cells took up trypan blue within 24 hours, by 48 hours, apoptosis was detected and by 72 hours, all of the IMR-32 cells treated with AA or DHA under delipidated conditions took up trypan blue, compared no cell death seen in those cells treated under normal conditions (Figure 6.2). At 24 hours post-initial treatment some cleavage of PARP was observed in the PUFA-treated cells, with some full-length PARP still present, this may have represented an early in the apoptotic pathway, as DNA fragmentation was not detected at this time point. By 48 hours, post-initial treatment, DNA laddering (Figure 6.3) and complete cleavage of full-length PARP in cells treated with AA and DHA (Figure 6.4) were observed. Few cells were actually observed with condensed or fragmented nuclei and this may be because this step directly precedes detachment from the coverslip or that the washes involved in the staining

procedure removed all the cells, which were not strongly attached, because they were degrading. These data together suggest that one of the mitogenic factors removed on FCS delipidation is able to suppress cell apoptosis. Interestingly, fibroblasts grown in delipidated serum and treated with retinoic acid undergo apoptosis, whereas those grown under normal conditions did not apoptose [558]. Similarly, it has been shown that the murine neuroblastoma cell line, N1E-115, underwent apoptosis when deprived of serum, but not in culture medium containing serum [541]. This indicates that a serum component is able to inhibit apoptosis and promote cellular survival and may be part of the lipid component of serum, such as LPA or S1P. Interestingly, another component of the mitogenic lipid fraction of serum, sphingomyelin, has been shown to down-regulate the expression of both PPARγ transcripts and protein in fibroblasts [559]. Therefore, removal of lipids from serum may result in increased expression of PPARγ and on treatment with PPAR activators, such as PUFAs, IMR-32 cells underwent apoptosis, whereas under normal conditions, they only underwent growth inhibition, due to lower levels of PPARγ.

The apoptosis observed in IMR-32 cells treated with 30 μM fatty acids and grown under delipidated conditions occurred through cell cycle arrest, detachment and cell death. Epithelial cells, which become detached from the extracellular matrix undergo a detachment-dependent programmed cell death known as anoikis, which is thought prevent reattachment of cells in other inappropriate locations [560]. This process involves integrins which interact with growth factor receptors and input is required from both integrins and these receptors for progression through G_1 of the cell cycle [561]. Altered expression of integrins has been observed in many human tumours [562] and it is thought that this altered signalling may contribute to the malignant phenotype of cancer cells, by promoting anchorage-independent growth [562, 561]. It has long been known that cancer cells are able to undergo anchorage-independent growth and this is one of the feature that distinguishes between benign and malignant tumours [563, 564] and neuroblastoma cells are highly malignant cells. LPA has been shown to be involved in cell attachment, involving the actin cytoskeleton [556] and when it is removed from the tissue culture medium, this may prevent initial cellular attachment, but would not induce cell death. Indeed the

neurite retraction seen in neuroblastoma cells treated with LPA is driven by contraction of the cytoskeleton rather than a loss of adhesion to the substratum [537]. Therefore, the cell death seen in IMR-32 cells treated with fatty acids and grown under delipidated conditions may have involved cell cycle arrest and subsequent apoptosis, but the cell death was not due to the actual detachment of the cells.

Similarly to the IMR-32 cells treated with fatty acids under delipidated conditions, those treated with $15dPGJ_2$ also underwent a greater degree of growth inhibition (Figure 6.5) and cell death (Figure 6.7) than controls and also underwent apoptosis. However, the effects seen with the fatty acids were more rapid with cell death occurring in more than 85 % of IMR-32 cells treated with AA or DHA under delipidated conditions within 24 hours compared to only 13 % of cells treated with $15dPGJ_2$ (Figures 6.2 and 6.7). Within 48 hours all the cells treated with fatty acids under delipidated conditions were dead (Figure 6.2), however, 43 % of the cells treated with $15dPGJ_2$ remained viable and it took until 72 hours for the cells to almost completely die (Figure 6.7). The delay in effect of $15dPGJ_2$ is of a similar time to that seen under normal conditions and may require a similar level of activation of PPARγ. However, no response was seen with the fatty acids under normal conditions and yet a rapid induction of cell death was achieved under delipidated conditions. This may indicate that the mitogenic lipids in FCS inhibited the effects of the fatty acids to a greater degree or that the apoptosis induced by the fatty acids occurred via a different mechanism to that induced by $15dPGJ_2$ and may not involve PPARs.

Fatty acids and $15dPGJ_2$ both induced DNA fragmentation in IMR-32 cells within 48 hours of growth under delipidated conditions (Figures 6.3 and 6.9). However, the DNA from the cells treated with fatty acids was almost completely degraded within 48 hours, whereas the DNA from cells treated with $15dPGJ_2$ was degraded but not to the same extent. This may have been due to different amounts of DNA being loaded onto the gel, but as the same number of cells were plated out for each experiment, it reflects the efficacy of the fatty acids at inducing apoptosis compared to that induced by $15dPGJ_2$. Fatty acids and $15dPGJ_2$ induced apoptosis in IMR-32 cells grown under delipidated conditions and both treatments resulted in the

complete loss of full-length PARP from IMR-32 cells. This was seen at 48 hours in both fatty acid treated (Figure 6.4) and $15dPGJ_2$-treated (Figure 6.11) cells, although some cleavage of PARP was seen within 24 hours with the fatty acid treated cells, reflecting the more rapid induction of cell death in the fatty acid treated cells. Levels of 85 kDa cleavage fragment of PARP were high in fatty acid-treated IMR-32 cells at 24 hours, but not seen at all with $15dPGJ_2$-treatment within 24 hours under delipidated conditions. Some cleavage of PARP was also seen in the Wy-14643-treated IMR-32 cells (Figure 11), but to a similar level to that cleaved in the DMSO-treated cells and this corresponds to data showing that it did not increase cell death from controls under normal or delipidated conditions (Figures 6.6 and 6.8), or cause DNA fragmentation (Figure 6.10).

Interestingly, another component of the mitogenic lipid fraction of serum, sphingomyelin, has been shown to down-regulate the expression of both PPARγ transcripts and protein in fibroblasts [559] and the expression of PPARγ in neuroblastoma cells has been shown to be altered in the presence or absence of lipid components [343]. Therefore, removal of lipids from serum may result in increased expression of PPARγ and on treatment with ligands of PPARγ IMR-32 cells may undergo apoptosis, whereas under normal conditions, they would only undergo growth inhibition, due to lower levels of PPARγ. This may also explain why fatty acids, which activate both PPARα and PPARγ induce apoptosis in IMR-32 cells grown under delipidated conditions, whereas Wy-14643, which is a potent activator of the α isoform of PPAR is unable to induce apoptosis in IMR-32 cells grown in delipidated medium. Wy-14643 does however, reverse the effects of delipidated serum on 3T3-L1 preadipocytes, which under delipidated conditions exhibit a proliferative and elongated phenotype, however Wy-14643 causes them to differentiate [558]. 3T3-L1 preadipocytes are also more susceptible to cell death induced by 9-*cis* retinoic acid under delipidated conditions, than under normal conditions, suggesting that it may not only be $15dPGJ_2$–induced cell death which is suppressed by lipid components of the FCS, but also cell death induced by other compounds [558].

Oleoyl-LPA is not the component of foetal calf serum, which is required for normal growth of IMR-32 cells *in vitro*. However, it may be required for attachment of the cells to the tissue culture plastic through its interaction with the actin cytoskeleton. Replacement of LPA into delipidated foetal calf serum did not reverse the growth-inhibitory effects of the FCS on IMR-32 cells, as the cells grew similarly to that of cells grown in delipidated medium alone (Figure 6.13). It was also not able to prevent the cell death of control IMR-32 cells under delipidated conditions or reduce the apoptosis seen when IMR-32 cells were treated with $15dPGJ_2$ under delipidated conditions (Figure 6.14). In contrast, LPA is a survival factor required for the survival of neonatal Schwann cells *in vitro* [550] and is also involved in the differentiation and survival of oligodendrocytes [551]. This indicates and important role for LPA in the survival of cells in both the central nervous system and peripheral nervous system, but possibly not the sympathetic nervous system. In Schwann cells, LPA promotes cellular survival by the accumulation of phosphorylated (active) protein kinase B (PKB), via phosphatidylinositol 3-kinase (PI3K)-dependent pathway [550]. The active PKB suppresses apoptosis and promotes survival of the Schwann cells [550]. However, removal of LPA did not affect IMR-32 cells and therefore another serum component may be able to do this or a combination of LPA and other components may be required.

S1P has been shown to suppress apoptosis [545], suggesting that the absence of S1P, $15dPGJ_2$ can induce apoptosis. It has been suggested that autophagy and apoptosis are overlapping forms of programmed cell death [367] and also that cells which are undergoing autophagy have a greater tendency to apoptose [368]. Therefore, $15dPGJ_2$ treatment of IMR-32 cells may only be able to induce autophagy in the presence of S1P, but when the mitogen is removed, then the cells can die via the apoptotic pathway. Treatment of IMR-32 cells with 5 μM $15dPGJ_2$ inhibited cell growth induced cell death under normal conditions. When S1P was added to normal medium, it prevented $15dPGJ_2$ from inducing growth inhibition (Figure 6.15) and death of some of the cells (Figure 6.16), suggesting that as well as suppressing apoptosis, S1P may be able to suppress autophagic cell death. Under delipidated conditions S1P further prevented $15dPGJ_2$ from inducing death of IMR-32 cells and even improved cell survival above that of control-treated cells under

delipidated conditions alone (Figures 6.15 and 6.1.6). Therefore, S1P was the main component of serum responsible for suppressed the effects of $15dPGJ_2$ and probably fatty acids on IMR-32 cells. It suppresses apoptosis, which can be induced in IMR-32 cells under delipidated conditions. In the case of $15dPGJ_2$ treatment, the cells may have become programmed to die, but the presence of S1P prevented apoptosis and the cells therefore use an alternative form of programmed cell death to die. In contrast to the effects in IMR-32 cells and to those using LPA, S1P was unable to promote the survival of neonatal Schwann cells *in vitro*.

It would be interesting to determine whether LPA or S1P supplementation was able to reverse the effects of a combination of PUFAs and delipidated serum on IMR-32 cells. It would also be interesting to try to specifically inhibit S1P within serum, to determine whether this also allows PUFAs and $15dPGJ_2$ to induce apoptosis of IMR-32 cells. This could be done by blocking S1P receptors with antibodies or antagonising them with pharmacological agents. Research into the mechanism by which S1P suppresses apoptosis induced by PUFAs and $15dPGJ_2$, would show if S1P directly interacted with PPARγ or one of its target genes, thus preventing apoptosis and pushing the cells down an autophagic cell death pathway instead. S1P suppresses apoptosis caused by accumulation of ceramides produced by the breakdown of sphingomyelin during cell death [565]. Therefore activation of PPARs by PUFAs and $15dPGJ_2$ may result in the accumulation of ceramides. It would also be exciting to see whether other mitogenic lipids removed on delipidation of serum are involved in inhibiting apoptosis on treatment with PUFAs and $15dPGJ_2$, especially sphingomyelin, which has been shown to down-regulate the expression of both PPARγ transcripts and protein in fibroblasts [559].

The mitogenic factors present within FCS should be considered when analysing the response of cells to treatments *in vitro*. S1P is able to suppress apoptosis and LPA is able to reverse the differentiation of neuroblastoma cells, amongst other cellular effects. The removal of sphinogsine-1-phosphate massively altered the response of the human neuroblastoma cell line, IMR-32 to fatty acid supplementation and treatment with $15dPGJ_2$. Therefore, when evaluating the efficacy of inhibitors of cancer cell growth, the culture medium should be considered and perhaps

treatments of cancer cells should incorporate inhibitors of the mitogenic lipid signalling pathways. These could include inhibitors of S1P receptors or by targeting components downstream of S1P.

Chapter 7

Discussion

Discussion

Since the discovery just over a decade ago [107], of the receptor which is activated by peroxisome proliferators and induces peroxisome proliferation in rodents, the field of research into PPARs has expanded many fold. Activation of the γ isoform of PPAR inhibits cancer cell growth and this has lead to research into PPARγ ligands as potential therapies for the treatment of cancers [312]. This includes neuroblastoma, an aggressive childhood cancer, which can spontaneously differentiate without any treatment [1, 3]. The main aim of my project was to use ligands of PPARγ to inhibit the growth of neuroblastoma cells and to determine the mechanism of action of PPARγ and its target genes.

Fatty acids can inhibit the growth of some cancer cell types [405, 408, 177], however, they had little effect on the growth of IMR-32 cells *in vitro*. Possible mechanisms whereby fatty acids can inhibit cell growth include changes to the phospholipid composition of cancer cell membranes [177, 176] or through activation of PPAR-induced transcription [175]. PUFAs effectively altered the composition of IMR-32 cell membranes, but there was no correlation between growth inhibition and activation of PPARγ. DHA had the greatest effect on cell growth and membrane phospholipid composition, but was one of the least effective PUFAs at activating PPARs. This strongly suggests that any effects on the cells were mediated through changes to the cell membrane and not through PPARs. Fatty acids may not be a suitable treatment for neuroblastoma as they have limited effects on cell growth. However, the evidence that PUFAs effectively induced growth inhibition and apoptosis in IMR-32 cells under delipidated conditions, suggests that the cellular environment plays a role in the response of neuroblastoma cells to PPAR ligands. In the presence of lipid mitogens in normal serum, PUFAs may not be able to activate PPARγ and/or induce apoptosis, and as a result are incorporated into the membranes instead.

This project has concentrated on PPARα and PPARγ, as at the start, little was known about the function of β isoform, its ligands or its use in inhibiting the growth of cancer cells. The neuroblastoma cell lines IMR-32 and Kelly, both

expressed PPARα and PPARγ, whereas Han *et al.*, [342] showed that the neuroblastoma cell line, Lan-5 expressed PPARβ and PPARγ, but not PPARα. Changing the level of expression of PPARγ in IMR-32 cells altered their growth characteristics. Those cells induced to express higher levels of PPARγ1 grew slower than normal cells, possibly through increasing the level of basal transcription of PPARγ target genes, whereas those induced to express dominant negative PPARγ1 proliferated at a much increased rate, possibly through reducing basal transcription rates. These results indicate that the levels of PPARγ expression in cancer cells are important and should be considered if PPARγ is to be used as a drug target.

Prostaglandins are thought to be more potent inducers of growth inhibition of cancer cells than PUFAs. 15-deoxy$\Delta^{12,14}$-prostglandin J_2 effectively inhibited IMR-32 cell growth and induced arrest at G_2/M of the cell cycle. However the ligand of PPARα, Wy-14643, did not have any effect on the cells. This agrees with published data showing that activation of PPARγ, but not PPARα [312, 309] is important in inhibiting the growth of cancer cells. IMR-32 cells underwent cell death requiring *de novo* protein synthesis, but did not exhibit any features of apoptosis, or necrosis. This is important, as necrotic cells lyse as they die and release cellular contents, invoking an inflammatory response, which would not be a suitable side effect for a cancer therapy. IMR-32 cells treated with 15dPGJ$_2$ died by autophagy and is one of only 3 cancer cell lines so far shown to undergo autophagy in response to ligands of PPARγ and the only neuroblastoma cell line to do so. As autophagy is a programmed cell death, requiring *de novo* protein synthesis, it would be a suitable response for a treatment for cancer, indicating that activation of PPARγ could be used to treat neuroblastoma.

Other neuroblastoma cell lines have been shown respond differently to ligands of PPARγ, including Lan-5 cells, which differentiate in response to 15dPGJ$_2$ and phenylacetate [342, 207], SHSY5Y cells, which undergo 15dPGJ$_2$-induced apoptosis [362] and Kelly cells, whose growth is inhibited by 15dPGJ$_2$, but by as yet an unidentified mechanism. However, it is worth noting that only the effects of the phenylacetate on Lan-5 cells were shown to be dependent on PPARγ [207].

Subsequent work on this project in the laboratory has shown that neuroblastoma cell lines do respond very differently to $15dPGJ_2$ and this may also relate to the levels of PPARγ expression (personal communication, Dr. Lillycrop, Southampton University). Importantly, one cell line, SKNSH, proliferated in response to low levels of $15dPGJ_2$, underwent growth arrest in response to 5 μM $15dPGJ_2$ and underwent cell death in response to higher levels of $15dPGJ_2$ (personal communication, Dr. Lillycrop, Southampton University). This mirrors the effects seen in breast cancer cells treated with $15dPGJ_2$ and TZDs by Clay *et al.*, [432] and is important if ligands of PPARγ are to be used as therapies. This is because levels of PPARγ expression and activation would need to be sufficient to induce growth inhibition rather than proliferation. Therefore, it is proposed that very low level activation of PPARγ leads to proliferation of cancer cells, low level activation leads to some growth arrest followed by cell death, whereas higher activation leads to severe growth arrest and autophagy and very high activation results in apoptosis. Certainly in IMR-32 cells treated with $15dPGJ_2$, growth arrest appears to be a primary event and cell death a secondary event, also in Kelly cells treated with $15dPGJ_2$, the level of cell death is very small compared to the growth inhibition, therefore in both cell lines growth arrest may be more important.

$15dPGJ_2$ inhibited neuroblastoma cell growth to a greater extent than fatty acids, but activated PPAR-induced transcription less than fatty acids. This could mean that very high activation of PPARγ is not necessarily required to inhibit cell growth and also that fatty acids could be very weak activators of the γ isoform. $15dPGJ_2$ specifically inhibited IMR-32 cell growth through PPARs, presumably PPARγ and 20 μg of the decoy oligonucleotide to PPARs was sufficient to completely inhibit activation of PPARs by $15dPGJ_2$. $15dPGJ_2$ can act independently of PPARs through antagonism of NFκB [190], however in IMR-32 cells, $15dPGJ_2$ actually activated NFκB-induced transcription. Unlike PUFAs, $15dPGJ_2$ did not alter the composition of IMR-32 cell membrane phospholipids and therefore seems to exclusively act through PPARs. These data are important, as it needed to be established that PPARγ is involved in $15dPGJ_2$-induced growth inhibition, so that its potential as a therapeutic target can be determined.

As well as altering the growth characteristics of IMR-32 cells, changing the levels of PPARγ made the cells more resistant $15dPGJ_2$. Cells expressing increased levels of PPARγ were resistant to higher levels of $15dPGJ_2$, possibly because a certain proportion of receptors may have needed to be activated to inhibit IMR-32 cell growth. The availability of co-activators, retinoid X receptors and binding sites may also have been limiting. Remarkably, IMR-32 cells with either increased expression of PPARγ or decreased activity of PPARγ were resistant to $15dPGJ_2$. In the case of the dominant negative PPARγ, which abrogated wild-type PPARγ function, this may have been because $15dPGJ_2$ could not activate PPARγ-induced transcription of target genes involved in the inhibition of cell growth. Interestingly, non-functional PPARγ has been associated with the development of colon cancer [352] and variants of PPARγ are also represented differently in other cancers [345, 566]. Therefore, functional PPARγ is required for normal cell growth and treatment with PPARγ ligands, would not be suitable in cancer cells lacking functional PPARγ.

The target genes of PPARγ and its role in signalling pathways also require further investigation. $15dPGJ_2$-induced growth inhibition of IMR-32 cells coincided with nuclear translocation of p53 and down-regulation of PAX3. However, other down-stream targets of PPARγ remain unidentified. Establishing the target genes of PPARγ could be achieved by treating IMR-32 cells with $15dPGJ_2$ and cycloheximide to block protein synthesis and therefore only genes whose expression is directly affected by $15dPGJ_2$ treatment could be established using cDNA arrays. Obviously, this would need to be repeated at various concentrations of $15dPGJ_2$ and time points to establish both early and late target genes transcribed on activation of PPARγ. Interestingly, only a few proteins have been shown to be specifically involved in autophagy in human cells, one of which is a Bcl-2 interacting protein, called beclin-1 [567, 568, 569] and others include homologues of *Saccharomyces cerevisiae* proteins of the Apg family [570, 571, 450, 572], which are involved in autophagy and vacuolar protein sorting. The role of activated PPARγ in regulating the expression or function of genes involved in autophagy would allow part of its mechanism of action to be determined and may also provide information on other potential downstream targets for cancer therapies.

Similar to the effects seen with PUFAs, $15dPGJ_2$ treatment induced IMR-32 cells to apoptose under delipidated conditions and therefore mitogens within the serum used for tissue culture can influence cellular responses to PPAR ligands [533, 536, 534]. This effect occurred along a similar time scale to the autophagic cell death induced under normal conditions, but more cells were induced to die, suggesting that activation of PPARγ was more effective under delipidated conditions. LPA and S1P can be removed from the serum by delipidation [404, 535] and both reverse the differentiation of neuroblastoma cells [537, 538, 541] and S1P suppresses apoptosis [542, 543]. Supplementation of the delipidated serum with LPA had no affect on the growth of IMR-32 cells treated with $15dPGJ_2$ and this may be because it has not been shown to suppress apoptosis. However, addition of S1P reduced the levels of growth inhibition and cell death induced by a combination of $15dPGJ_2$ and delipidated tissue culture conditions. It is not known whether S1P supplementation is able to prevent apoptosis induced by $15dPGJ_2$ under these conditions, although this could easily be measured.

Interestingly, S1P is reported to activate extracellular signal regulated kinase-1 ERK-1 and ERK-2 [573], but not JNK [553]. This is important as MAP kinases such as ERK-1 and ERK-2 can phosphorylate both PPARγ1 and PPARγ2 and reduce their activity [285, 288]. Therefore it is proposed that under normal conditions, S1P activates ERK-1 and ERK-2, which phosphorylates PPARγ, thereby reducing its activity and when PPARγ is activated by $15dPGJ_2$, the level of activation is only sufficient to induce the cells to undergo autophagic cell death. Subsequent work in the laboratory has shown that in IMR-32 cells, ERK-1 and ERK-2 activity is higher under normal conditions than under delipidated conditions, and that supplementation of delipidated medium with S1P increases expression of MAPK (personal communication, Dr. Lillycrop, Southampton University). Therefore, under delipidated conditions, there is no S1P to activate MAP kinases, so PPARγ remains in a non-phosphorylated state and has higher activity. On treatment of IMR-32 cells with $15dPGJ_2$, PPARγ activity is sufficient to induce the cells to undergo apoptotic cell death instead. It is also possible that $15dPGJ_2$ activates PPARγ, resulting in membrane depolarisation of mitochondria, as autophagy occurs if a few mitochondria are involved, but if more are involved then apoptosis occurs

[445]. Under normal conditions, S1P (via MAPKs) may reduce PPARγ activity, so that it only induces a few mitochondria to depolarise, whereas under delipidated conditions the higher activity of PPARγ may induce more mitochondria to depolarise and therefore result in apoptotic cell death. As S1P activates MAP kinases via the Edg-1 receptor, this receptor could be antagonised in conjunction with treatment of IMR-32 cells with $15dPGJ_2$, to determine whether this was a more effective method for inducing growth inhibition or cell death. Similarly, inhibitors of MAP kinases and $15dPGJ_2$ could also be used as a therapy for neuroblastoma.

The activation of PPARγ has a great deal of potential in the treatment of cancer, however, before ligands of this receptor can have therapeutic potential we need to expand our knowledge of the receptor, its mechanism of action, its regulation and its target genes. These areas of research also need to be explored in many more cell types, as the receptors seem to act differently in different cells and even between cell lines from the same cancer. Research into the levels of PPARγ in cells and altering these levels of expression may help us to understand the role of these receptors in normal and malignant cells. It may also help us to elucidate the role of PPARγ in signalling pathways. The regulation of PPARγ by MAPK should also be further studied as PPARγ ligands could be combined with inhibitors of MAPK or the S1P receptor, Edg-1, to enhance PPARγ activity within cancer cells and possibly provide a more potent anti-cancer treatment.

It is also important to confirm that any effects are PPARγ-dependent and that we can activate PPARγ to specifically inhibit the growth of cancer cells and not have toxic affects in normal cells. Activation of PPARγ with thiazolidinediones has been used in clinical trials as a treatment for diabetes, however treating patients with neuroblastoma with TZDs may not be suitable. This is because the patients are small children and treating patients without diabetes with drugs that will alter the storage of lipids and cause the differentiation of adipocytes could cause further complications. Therefore, treatment with such ligands may require targeting the cancer cells directly or activating the receptor so that it only has growth inhibitory effects, possibly using synthetic ligands, or by using the natural ligand of PPARγ,

15-deoxy$\Delta^{12,14}$-prostglandin J_2. Research into PPARγ is gradually opening up new avenues for treating cancers and may in the future prove to be a success in the treatment of patients and not just as a laboratory tool.

References

1.Brodeur GM. Neuroblastoma and other peripheral neuroectodermal tumours. In: Fernbach DJ, Vietti TJ, editors. *Clinical Paediatric Oncology*. St. Louis: Mosby 1991: 437-464.

2.Niethammer D, Handgretinger R. Clinical strategies for the treatment of neuroblastoma. *Eur J Cancer* 1995; **31A:** 568-571.

3.Brodeur GM, Castleberry RP. Neuroblastoma. In: Rizzo PA, Poplack DG, editors. *Principles and Practice of Paediatric Oncology*. Philadelphia: JB Lippincott Company 1993: 739-767.

4.Young JL, Ries LG, Silverberg E, Horm JW, Miller RW. Cancer incidence, survival, and mortality for children younger than age 15 years. *Cancer* 1986; **58:** 598-602.

5.Gurney JG, Severson RK, Davis S, Robison LL. Incidence of cancer in children in the United States. Sex-, race-, and 1-year age-specific rates by histologic type. *Cancer* 1995; **75:** 2186-2195.

6.Miller RW, Young JL, Novakovic B. Childhood cancer. *Cancer* 1995; **75:** 395-405.

7.Lemire RJ, Loeser JD, Leech RW, Alvord Jnr. EC. *Congenital tumours of the nervous system.* Hagerstown: Harper and Row 1975.

8.Voute PA. *Neuroblastoma*. St. Louis: CV Mosby Company 1984.

9.Altman AJ, Schwartz AD. *Malignant diseases of infancy, childhood and adolescence.* London: W. B. Saunders Company 1978.

10. Schofield D, Cotran RS. Disease of childhood and infancy. Philadelphia: W. B. Saunders Company 1999.

11. Castleberry RP. Neuroblastoma. *Eur J Cancer* 1997; **33:** 1430-1437.

12. Russell DS, Rubenstein LJ. *Tumours of peripheral neuroblasts and ganglion cells.* Baltimore: Wilkins and Wilkins 1989.

13. Turkel SB, Itabashi HH. The natural history of neuroblastic cells in the foetal adrenal gland. *Am J Pathol* 1975; **76:** 225.

14. Ikeda Y, Lister J, Bouton M, Buyukpamukcu M. Congenital neuroblastoma, neuroblastoma *in situ* and normal foetal development of the adrenal. *J Paediatr Surg* 1981; **16.**

15. Brodeur GM, Seeger RC, Barrett A *et al.* International criteria for diagnosis, staging, and response to treatment in patients with neuroblastoma. *J Clin Oncol* 1988; **6:** 1874-1881.

16. Shimada H, Chatten J, Newton WA *et al.* Histopathologic prognostic factors in neuroblastic tumours: definition of subtypes of ganglioneuroblastoma and an age-linked classification of neuroblastomas. *J Natl Cancer Inst* 1984; **73:** 405-416.

17. Shimada H, Ambros IM, Dehner LP, Hata J, Joshi VV, Roald B. Terminology and morphologic criteria of neuroblastic tumours: recommendations by the International Neuroblastoma Pathology Committee. *Cancer* 1999; **86:** 349-363.

18. Shimada H, Ambros IM, Dehner LP *et al.* The International Neuroblastoma Pathology Classification (the Shimada system). *Cancer* 1999; **86:** 364-372.

19. Cotterill SJ, Pearson AD, Pritchard J *et al.* Clinical prognostic factors in 1277 patients with neuroblastoma: Results of the European Neuroblastoma Study Group 'Survey' 1982-1992. *Eur J Cancer* 2000; **36:** 901-908.

20. Hughes M, Marsden HB, Palmer MK. Histological patterns of neuroblastoma related to prognosis and clinical staging. *Cancer* 1974; **34:** 1706.

21. Borrello MG, Bongarzone I, Pierotti MA *et al. trk* and *ret* proto-oncogene expression in human neuroblastoma specimens: high frequency of *trk* expression in non-advanced stages. *Int J Cancer* 1993; **54:** 540-545.

22. Kogner P, Barbany G, Dominici C, Castello MA, Raschella G, Persson H. Co-expression of messenger RNA for *TRK* proto-oncogene and low affinity nerve growth factor receptor in neuroblastoma with favourable prognosis. *Cancer Res* 1993; **53:** 2044-2050.

23. Loeb D, Martin-Zanaca D, Chao M, Parada L, Greene L. The *TRK* proto-oncogene rescues NGF responsiveness in mutant NGF-non-responsive PC12 cell lines. *Cell* 1991; **66:** 961-966.

24. Zeltzer PM, Marangos PJ, Parma AM *et al.* Raised neurone-specific enolase in serum of children with metastatic neuroblastoma. A report from the Children's Cancer Study Group. *Lancet* 1983; **2:** 361-363.

25. Fitzgibbon MC, Tormey WP. Paediatric reference ranges for urinary catecholamines/metabolites and their relevance in neuroblastoma diagnosis. *Ann Clin Biochem* 1994; **31 (Pt 1):** 1-11.

26. Hann HWL, Stahlhut MW, Evans AE. Serum ferritin as a prognostic indicator in neuroblastoma: Biological effects of iso-ferritins. *Prog Clin Biol Res* 1985; **175:** 331.

27. Tsuchida Y, Honna T, Iwanaka T *et al.* Serial determination of serum neurone-specific enolase in patients with neuroblastoma and other paediatric tumours. *J Pediatr Surg* 1987; **22:** 419-424.

28. Schwab M, Alitalo K, Klempnauer KH *et al.* Amplified DNA with limited homology to MYC cellular oncogene is shared by human neuroblastoma cell lines and a neuroblastoma tumour. *Nature* 1983; **305:** 245-248.

29. Schwab M, Varmus HE, Bishop JM. Human NMYC gene contributes to neoplastic transformation of mammalian cells in culture. *Nature* 1985; **316:** 160-162.

30. Christiansen H, Schestag J, Christiansen NM, Grzeschik KH, Lampert F. Clinical impact of chromosome 1 aberrations in neuroblastoma: A metaphase and interphase cytogenetic study. *Genes Chromosomes Cancer* 1992; **5:** 141-149.

31. Strehl S, Ambros PF. Fluorescence *in situ* hybridisation combined with immunohistochemistry for highly sensitive detection of chromosome 1 aberrations in neuroblastoma. *Cytogenet Cell Genet* 1993; **63:** 24-28.

32. Lastowska M, Cotterill S, Pearson AD *et al.* Gain of chromosome arm 17q predicts unfavourable outcome in neuroblastoma patients. U.K. Children's Cancer Study Group and the U.K. Cancer Cytogenetics Group. *Eur J Cancer* 1997; **33:** 1627-1633.

33. Lastowska M, Roberts P, Pearson AD, Lewis I, Wolstenholme J, Bown N. Promiscuous translocations of chromosome arm 17q in human neuroblastomas. *Genes Chromosomes Cancer* 1997; **19:** 143-149.

34. Plantaz D, Mohapatra G, Matthay KK, Pellarin M, Seeger RC, Feuerstein BG. Gain of chromosome 17 is the most frequent abnormality detected in neuroblastoma by comparative genomic hybridisation. *Am J Pathol* 1997; **150:** 81-89.

35. Thorner PS, Squire JA. Molecular genetics in the diagnosis and prognosis of solid paediatric tumours. *Pediatr Dev Pathol* 1998; **1:** 337-365.

36. Look AT, Hayes FA, Shuster JJ *et al.* Clinical relevance of tumour cell ploidy and NMYC gene amplification in childhood neuroblastoma: A Paediatric Oncology Group study. *J Clin Oncol* 1991; **9:** 581-591.

37. Schwab M, Ellison J, Busch M, Rosenau W, Varmus HE, Bishop JM. Enhanced expression of the human gene NMYC consequent to amplification of DNA may contribute to malignant progression of neuroblastoma. *Proc Natl Acad Sci U S A* 1984; **81:** 4940-4944.

38. Seeger RC, Brodeur GM, Sather H *et al.* Association of multiple copies of the NMYC oncogene with rapid progression of neuroblastomas. *N Engl J Med* 1985; **313:** 1111-1116.

39. Amler LC, Schwab M. Amplified NMYC in human neuroblastoma cells is often arranged as clustered tandem repeats of differently recombined DNA. *Mol Cell Biol* 1989; **9:** 4903-4913.

40. Brodeur GM, Sekhon G, Goldstein MN. Chromosomal aberrations in human neuroblastomas. *Cancer* 1977; **40:** 2256-2263.

41. Balaban-Malenbaum G, Gilbert F. Relationship between homogeneously staining regions and double minute chromosomes in human neuroblastoma cell lines. *Prog Cancer Res Therap* 1980; **12:** 97.

42. Biedler JL. Human neuroblastoma cytogenetics: Search for significance of homogeneously staining regions and double minute chromosomes. *Prog Cancer Res Therap* 1980; **12:** 81.

43. Brodeur GM, Green AA, Hayes FA, Williams KJ, Williams DL, Tsiatis AA. Cytogenetic features of human neuroblastomas and cell lines. *Cancer Res* 1981; **41:** 4678-4686.

44. Manohar CF, Salwen HR, Brodeur GM, Cohn SL. Co-amplification and concomitant high levels of expression of a DEAD box gene with MYCN in human neuroblastoma. *Genes Chromosomes Cancer* 1995; **14:** 196-203.

45. Squire JA, Thorner PS, Weitzman S *et al.* Co-amplification of MYCN and a DEAD box gene (DDX1) in primary neuroblastoma. *Oncogene* 1995; **10:** 1417-1422.

46. Brodeur GM, Fong CT. Molecular biology and genetics of human neuroblastoma. *Cancer Genet Cytogenet* 1989; **41:** 153-174.

47. Brodeur GM. *Molecular biology and genetics of human neuroblastoma.* Boca Raton: CRC Press 1990.

48. Gilbert F, Feder M, Balaban G *et al.* Human neuroblastomas and abnormalities of chromosomes 1 and 17. *Cancer Res* 1984; **44:** 5444-5449.

49. Hayashi Y, Hanada R, Yamamoto K, Bessho F. Chromosome findings and prognosis in neuroblastoma. *Cancer Genet Cytogenet* 1987; **29:** 175-177.

50. Hayashi Y, Kanda N, Inaba T *et al.* Cytogenetic findings and prognosis in neuroblastoma with emphasis on marker chromosome 1. *Cancer* 1989; **63:** 126-132.

51. Weith A, Martinsson T, Cziepluch C *et al.* Neuroblastoma consensus deletion maps to 1p36.1-2. *Genes Chromosomes Cancer* 1989; **1:** 159-166.

52. Maris JM, White PS, Beltinger CP *et al.* Significance of chromosome 1p loss of heterozygosity in neuroblastoma. *Cancer Res* 1995; **55:** 4664-4669.

53. Caron H. Allelic loss of chromosome 1 and additional chromosome 17 material are both unfavourable prognostic markers in neuroblastoma. *Med Pediatr Oncol* 1995; **24:** 215-221.

54. Caron H, van Sluis P, de Kraker J *et al.* Allelic loss of chromosome 1p as a predictor of unfavourable outcome in patients with neuroblastoma. *N Engl J Med* 1996; **334:** 225-230.

55. Fong CT, Dracopoli NC, White PS *et al.* Loss of heterozygosity for the short arm of chromosome 1 in human neuroblastomas: correlation with N-myc amplification. *Proc Natl Acad Sci U S A* 1989; **86:** 3753-3757.

56. Kaghad M, Bonnet H, Yang A *et al.* Monoallelically expressed gene related to p53 at 1p36, a region frequently deleted in neuroblastoma and other human cancers. *Cell* 1997; **90:** 809-819.

57.Jost CA, Marin MC, Kaelin WG. p73 is a simian [correction of human] p53-related protein that can induce apoptosis. *Nature* 1997; **389:** 191-194.

58. Plantaz D, Mohapatra G, Matthay K *et al.* Genetic gains and losses in neuroblastoma. *Eur J Cancer* 1997; **33**, 2137.

59. Corvi R, Savelyeva L, Breit S *et al.* Non-syntenic amplification of MDM2 and MYCN in human neuroblastoma. *Oncogene* 1995; **10:** 1081-1086.

60.Takita J, Hayashi Y, Kohno T *et al.* Allelotype of neuroblastoma. *Oncogene* 1995; **11:** 1829-1834.

61.Takita J, Hayashi Y, Kohno T *et al.* Deletion map of chromosome 9 and p16 (CDKN2A) gene alterations in neuroblastoma. *Cancer Res* 1997; **57:** 907-912.

62.Weichselbaum RR, Epstein J, Little JB, Kornblith PL. *In vitro* cellular radiosensitivity of human malignant tumours. *Eur J Cancer* 1976; **12:** 47-51.

63.D'Angio GJ, Evans AE, Koop CE. Special pattern of widespread neuroblastoma with a favourable prognosis. *Lancet* 1971; **1:** 1046-1049.

64.Evans AE, Chatten J, D'Angio GJ, Gerson JM, Robinson J, Schnaufer L. A review of 17 IV-S neuroblastoma patients at the Children's Hospital of Philadelphia. *Cancer* 1980; **45:** 833-839.

65.Evans AE, Baum E, Chard R. Do infants with Stage IV-S neuroblastoma need treatment? *Arch Dis Child* 1981; **56:** 271-274.

66.Nickerson HJ, Nesbit ME, Grosfeld JL, Baehner RL, Sather H, Hammond D. Comparison of Stage IV and IV-S neuroblastoma in the first year of life. *Med Pediatr Oncol* 1985; **13:** 261-268.

67.Knudson Jnr. AG, Meadows AT. Regression of neuroblastoma IV-S: A genetic hypothesis. *N Engl J Med* 1989; **302:** 1254-1256.

68.Haas D, Ablin AR, Miller C, Zoger S, Matthay KK. Complete pathologic maturation and regression of Stage IVS neuroblastoma without treatment. *Cancer* 1988; **62:** 818-825.

69.Pritchard J, Hickman JA. Why does Stage IV-S neuroblastoma regress spontaneously? *Lancet* 1994; **344:** 869-870.

70.Hellstrom IE, Hellstrom KE, Pierce GE, Bill AH. Demonstration of cell-bound and humoral immunity against neuroblastoma cells. *Proc Natl Acad Sci U S A* 1968; **60:** 1231-1238.

71.Rangecroft L, Lauder I, Wagget J. Spontaneous maturation of Stage IV-S neuroblastoma. *Arch Dis Child* 1978; **53:** 815-817.

72.Lynch RG. Differentiation and cancer: The conditional autonomy of phenotype. *Proc Natl Acad Sci U S A* 1995; **92:** 647-648.

73.Pierce GB. Teratocarcinomas. *Canadian Cancer Conference* 1961; **4:** 119-137.

74.Warrell RP, Frankel SR, Miller WH *et al.* Differentiation therapy of acute promyelocytic leukaemia with tretinoin (all-*trans* retinoic acid). *N Engl J Med* 1991; **324:** 1385-1393.

75.Degos L, Dombret H, Chomienne C *et al.* All-*trans* retinoic acid as a differentiating agent in the treatment of acute promyelocytic leukaemia. *Blood* 1995; **85:** 2643-2653.

76.Påhlman S, Ruusala AI, Abrahamsson L, Mattsson ME, Esscher T. Retinoic acid-induced differentiation of cultured human neuroblastoma cells: A comparison with phorbol ester-induced differentiation. *Cell Differ* 1984; **14:** 135-144.

77.Sidell N, Altman A, Haussler MR, Seeger RC. Effects of retinoic acid (RA) on the growth and phenotypic expression of several human neuroblastoma cell lines. *Exp Cell Res* 1983; **148:** 21-30.

78.Lovat PE, Irving H, Annicchiarico-Petruzzelli M *et al.* Retinoids in neuroblastoma therapy: distinct biological properties of 9-*cis*- and all-*trans*-retinoic acid. *Eur J Cancer* 1997; **33:** 2075-2080.

79.Helson L. Chemotherapy of neuroblastoma. *Clin Bull* 1975; **5:** 47-50.

80.Nitschke R, Cangir A, Crist W, Berry DH. Intensive chemotherapy for metastatic neuroblastoma: A Southwest Oncology Group study. *Med Pediatr Oncol* 1980; **8:** 281-288.

81.Raaf JH, Cangir A, Luna M. Induction of neuroblastoma maturation by a new chemotherapy protocol. *Med Pediatr Oncol* 1982; **10:** 275-282.

82.Finklestein JZ, Krailo MD, Lenarsky C *et al.* 13-*cis* retinoic acid (NSC 122758) in the treatment of children with metastatic neuroblastoma unresponsive to conventional chemotherapy: Report from the Children's Cancer Study Group. *Med Pediatr Oncol* 1992; **20:** 307-311.

83.Smith MA, Adamson PC, Balis FM *et al.* Phase I and pharmacokinetic evaluation of all-*trans* retinoic acid in paediatric patients with cancer. *J Clin Oncol* 1992; **10:** 1666-1673.

84.Villablanca JG, Khan AA, Avramis VI *et al.* Phase I trial of 13-*cis* retinoic acid in children with neuroblastoma following bone marrow transplantation. *J Clin Oncol* 1995; **13:** 894-901.

85.Giguere V, Ong ES, Segui P, Evans RM. Identification of a receptor for the morphogen retinoic acid. *Nature* 1987; **330:** 624-629.

86.Petkovich M, Brand NJ, Krust A, Chambon P. A human retinoic acid receptor which belongs to the family of nuclear receptors. *Nature* 1987; **330:** 444-450.

87.Heyman RA, Mangelsdorf DJ, Dyck JA *et al.* 9-*cis* retinoic acid is a high affinity ligand for the retinoid X receptor. *Cell* 1992; **68:** 397-406.

88.Mangelsdorf DJ, Borgmeyer U, Heyman RA *et al.* Characterisation of three RXR genes that mediate the action of 9-*cis* retinoic acid. *Genes Dev* 1992; **6:** 329-344.

89.Petkovich PM, Heersche JN, Tinker DO, Jones G. Retinoic acid stimulates 1,25-dihydroxyvitamin D3 binding in rat osteosarcoma cells. *J Biol Chem* 1984; **259:** 8274-8280.

90. Webster NJ, Green S, Jin JR, Chambon P. The hormone-binding domains of the oestrogen and glucocorticoid receptors contain an inducible transcription activation function. *Cell* 1988; **54:** 199-207.

91. Kumar V, Chambon P. The oestrogen receptor binds tightly to its responsive element as a ligand-induced homodimer. *Cell* 1988; **55:** 145-156.

92. Thompson CC, Weinberger C, Lebo R, Evans RM. Identification of a novel thyroid hormone receptor expressed in the mammalian central nervous system. *Science* 1987; **237:** 1610-1614.

93. Dreyer C, Krey G, Keller H, Givel F, Helftenbein G, Wahli W. Control of the peroxisomal β-oxidation pathway by a novel family of nuclear hormone receptors. *Cell* 1992; **68:** 879-887.

94. Willy PJ, Umesono K, Ong ES, Evans RM, Heyman RA, Mangelsdorf DJ. LXR, a nuclear receptor that defines a distinct retinoid response pathway. *Genes Dev* 1995; **9:** 1033-1045.

95. Forman BM, Samuels HH. Dimerisation among nuclear hormone receptors. *New Biol* 1990; **2:** 587-594.

96. Forman BM, Samuels HH. Interactions among a subfamily of nuclear hormone receptors: the regulatory zipper model. *Mol Endocrinol* 1990; **4:** 1293-1301.

97. Yu VC, Delsert C, Andersen B *et al.* RXRβ: a coregulator that enhances binding of retinoic acid, thyroid hormone, and vitamin D receptors to their cognate response elements. *Cell* 1991; **67:** 1251-1266.

98. Kliewer SA, Umesono K, Mangelsdorf DJ, Evans RM. Retinoid X receptor interacts with nuclear receptors in retinoic acid, thyroid hormone and vitamin D3 signalling. *Nature* 1992; **355:** 446-449.

99. Kliewer SA, Umesono K, Noonan DJ, Heyman RA, Evans RM. Convergence of 9-*cis* retinoic acid and peroxisome proliferator signalling pathways

through heterodimer formation of their receptors. *Nature* 1992; **358:** 771-774.

100. Leid M, Kastner P, Chambon P. Multiplicity generates diversity in the retinoic acid signalling pathways. *Trends Biochem Sci* 1992; **17:** 427-433.

101. Zhang XK, Hoffmann B, Tran PB, Graupner G, Pfahl M. Retinoid X receptor is an auxiliary protein for thyroid hormone and retinoic acid receptors. *Nature* 1992; **355:** 441-446.

102. Bugge TH, Pohl J, Lonnoy O, Stunnenberg HG. RXRα, a promiscuous partner of retinoic acid and thyroid hormone receptors. *EMBO J* 1992; **11:** 1409-1418.

103. Bardot O, Aldridge TC, Latruffe N, Green S. PPAR-RXR heterodimer activates a peroxisome proliferator response element upstream of the bi-functional enzyme gene. *Biochem Biophys Res Commun* 1993; **192:** 37-45.

104. Evans RM. The steroid and thyroid hormone receptor superfamily. *Science* 1988; **240:** 889-895.

105. Green S, Chambon P. Nuclear receptors enhance our understanding of transcription regulation. *Trends Genet* 1988; **4:** 309-314.

106. Dreyer C, Keller H, Mahfoudi A, Laudet V, Krey G, Wahli W. Positive regulation of the peroxisomal β-oxidation pathway by fatty acids through activation of PPARs. *Biol Cell* 1993; **77:** 67-76.

107. Issemann I, Green S. Activation of a member of the steroid hormone receptor superfamily by peroxisome proliferators. *Nature* 1990; **347:** 645-650.

108. Schmidt A, Endo N, Rutledge SJ, Vogel R, Shinar D, Rodan GA. Identification of a new member of the steroid hormone receptor superfamily that is activated by a peroxisome proliferator and fatty acids. *Mol Endocrinol* 1992; **6:** 1634-1641.

109. Zhu Y, Alvares K, Huang Q, Rao MS, Reddy JK. Cloning of a new member of the PPAR gene family from mouse liver. *J Biol Chem* 1993; **268:** 26817-26820.

110. Tontonoz P, Hu E, Spiegelman BM. Stimulation of adipogenesis in fibroblasts by PPARγ2, a lipid-activated transcription factor. *Cell* 1994; **79:** 1147-1156.

111. Chen F, Law SW, Malley BW. Identification of two mPPAR related receptors and evidence for the existence of five subfamily members. *Biochem Biophys Res Commun* 1993; **196:** 671-677.

112. Popp JA, Cattley RC. *Peroxisome proliferators as initiators and promoters of rodent hepatocarcinogenesis.* London: Taylor and Francis 1993.

113. Ashby J, Brady A, Elcombe CR *et al.* Mechanistically-based human hazard assessment of peroxisome proliferator-induced hepatocarcinogenesis. *Hum Exp Toxicol* 1994; **13 Suppl 2:** S1-117.

114. Kliewer SA, Forman BM, Blumberg B *et al.* Differential expression and activation of a family of murine PPARs. *Proc Natl Acad Sci U S A* 1994; **91:** 7355-7359.

115. Sher T, Yi HF, McBride OW, Gonzalez FJ. cDNA cloning, chromosomal mapping, and functional characterisation of the human PPAR. *Biochemistry* 1993; **32:** 5598-5604.

116. Gottlicher M, Widmark E, Li Q, Gustafsson JA. Fatty acids activate a chimaera of the clofibric acid-activated receptor and the glucocorticoid receptor. *Proc Natl Acad Sci U S A* 1992; **89:** 4653-4657.

117. Fajas L, Auboeuf D, Raspe E *et al.* The organisation, promoter analysis, and expression of the human PPARγ gene. *J Biol Chem* 1997; **272:** 18779-18789.

118. Krey G, Keller H, Mahfoudi A *et al. Xenopus* PPARs: genomic organisation, response element recognition, heterodimer formation with

RXR and activation by fatty acids. *J Steroid Biochem Mol Biol* 1993; **47:** 65-73.

119. Ma H, Tam QT, Kolattukudy PE. PPARγ1 as a major PPAR in a tissue in which oestrogen induces peroxisome proliferation. *FEBS Lett* 1998; **434:** 394-400.

120. Ma H, Sprecher HW, Kolattukudy PE. Oestrogen-induced production of a PPAR ligand in a PPARγ-expressing tissue. *J Biol Chem* 1998; **273:** 30131-30138.

121. Diot C, Douaire M. Characterisation of a cDNA sequence encoding the PPARα in the chicken. *Poult Sci* 1999; **78:** 1198-1202.

122. Tugwood JD, Holden PR, James NH, Prince RA, Roberts RA. A PPARα cDNA cloned from guinea-pig liver encodes a protein with similar properties to the mouse PPARα: Implications for species differences in responses to peroxisome proliferators. *Arch Toxicol* 1998; **72:** 169-177.

123. Mano H, Kimura C, Fujisawa Y *et al.* Cloning and function of rabbit PPARδ/β in mature osteoclasts. *J Biol Chem* 2000; **275:** 8126-8132.

124. Houseknecht KL, Bidwell CA, Portocarrero CP, Spurlock ME. Expression and cDNA cloning of porcine PPARγ. *Gene* 1998; **225:** 89-96.

125. Aperlo C, Pognonec P, Saladin R, Auwerx J, Boulukos KE. cDNA cloning and characterisation of the transcriptional activities of the hamster PPAR, haPPARγ. *Gene* 1995; **162:** 297-302.

126. Sundvold H, Brzozowska A, Lien S. Characterisation of bovine PPARγ1 and γ2: Genetic mapping and differential expression of the two isoforms. *Biochem Biophys Res Commun* 1997; **239:** 857-861.

127. Hotta K, Gustafson TA, Yoshioka S, Ortmeyer HK, Bodkin NL, Hansen BC. Relationships of PPARγ1 and PPARγ2 mRNA levels to obesity, diabetes and hyperinsulinaemia in Rhesus monkeys. *Int J Obes Relat Metab Disord* 1998; **22:** 1000-1010.

128. Andersen O, Eijsink VG, Thomassen M. Multiple variants of the PPARγ are expressed in the liver of Atlantic salmon (*Salmo salar*). *Gene* 2000; **255:** 411-418.

129. Braissant O, Foufelle F, Scotto C, Dauca M, Wahli W. Differential expression of PPARs: tissue distribution of PPAR-α, -β, and -γ in the adult rat. *Endocrinology* 1996; **137:** 354-366.

130. Kubota T, Koshizuka K, Williamson EA *et al.* Ligand for PPARγ (troglitazone) has potent anti-tumour effect against human prostate cancer both *in vitro* and *in vivo*. *Cancer Res* 1998; **58:** 3344-3352.

131. Sapone A, Peters JM, Sakai S *et al.* The human PPARα gene: Identification and functional characterisation of two natural allelic variants. *Pharmacogenetics* 2000; **10:** 321-333.

132. Mukherjee R, Jow L, Croston GE, Paterniti JR. Identification, characterisation, and tissue distribution of human PPAR isoforms PPARγ2 versus PPARγ1 and activation with retinoid X receptor agonists and antagonists. *J Biol Chem* 1997; **272:** 8071-8076.

133. Schoonjans K, Martin G, Staels B, Auwerx J. PPARs, orphans with ligands and functions. *Curr Opin Lipidol* 1997; **8:** 159-166.

134. Lee SS, Pineau T, Drago J *et al.* Targeted disruption of the α isoform of the PPAR gene in mice results in abolishment of the pleiotropic effects of peroxisome proliferators. *Mol Cell Biol* 1995; **15:** 3012-3022.

135. Skogsberg J, Kannisto K, Roshani L *et al.* Characterisation of the human PPARδ gene and its expression. *Int J Mol Med* 2000; **6:** 73-81.

136. Jow L, Mukherjee R. The human PPAR subtype NUC1 represses the activation of hPPARα and thyroid hormone receptors. *J Biol Chem* 1995; **270:** 3836-3840.

137. Basu-Modak S, Braissant O, Escher P, Desvergne B, Honegger P, Wahli W. PPARβ regulates acyl-CoA synthetase 2 in re-aggregated rat brain cell cultures. *J Biol Chem* 1999; **274:** 35881-35888.

138. Lim H, Dey SK. PPARδ functions as a prostacyclin receptor in blastocyst implantation. *Trends Endocrinol Metab* 1999; **11:** 137-142.

139. Beamer BA, Negri C, Yen CJ *et al.* Chromosomal localisation and partial genomic structure of the human PPARγ gene. *Biochem Biophys Res Commun* 1997; **233:** 756-759.

140. Greene ME, Blumberg B, McBride OW *et al.* Isolation of the human PPARγ cDNA: expression in haematopoietic cells and chromosomal mapping. *Gene Expr* 1995; **4:** 281-299.

141. Elbrecht A, Chen Y, Cullinan CA *et al.* Molecular cloning, expression and characterisation of human PPARs γ1 and γ2. *Biochem Biophys Res Commun* 1996; **224:** 431-437.

142. Fajas L, Fruchart JC, Auwerx J. PPARγ3 mRNA: a distinct PPARγ mRNA subtype transcribed from an independent promoter. *FEBS Lett* 1998; **438:** 55-60.

143. Sundvold H, Lien S. Identification of a novel PPARγ promoter in man and transactivation by the nuclear receptor RORα1. *Biochem Biophys Res Commun* 2001; **287:** 383-390.

144. Barak Y, Nelson MC, Ong ES *et al.* PPARγ is required for placental, cardiac, and adipose tissue development. *Mol Cell* 1999; **4:** 585-595.

145. Kubota N, Terauchi Y, Miki H *et al.* PPARγ mediates high-fat diet-induced adipocyte hypertrophy and insulin resistance. *Mol Cell* 1999; **4:** 597-609.

146. Rosen ED, Sarraf P, Troy AE *et al.* PPARγ is required for the differentiation of adipose tissue *in vivo* and *in vitro*. *Mol Cell* 1999; **4:** 611-617.

147. Giguere V, Hollenberg SM, Rosenfeld MG, Evans RM. Functional domains of the human glucocorticoid receptor. *Cell* 1986; **46:** 645-652.

148. Hollenberg SM, Evans RM. Multiple and co-operative trans-activation domains of the human glucocorticoid receptor. *Cell* 1988; **55:** 899-906.

149. Wahli W, Martinez E. Superfamily of steroid nuclear receptors: positive and negative regulators of gene expression. *FASEB J* 1991; **5:** 2243-2249.

150. Luisi BF, Xu WX, Otwinowski Z, Freedman LP, Yamamoto KR, Sigler PB. Crystallographic analysis of the interaction of the glucocorticoid receptor with DNA. *Nature* 1991; **352:** 497-505.

151. Schwabe JW, Chapman L, Finch JT, Rhodes D. The crystal structure of the oestrogen receptor DNA-binding domain bound to DNA: how receptors discriminate between their response elements. *Cell* 1993; **75:** 567-578.

152. Schoonjans K, Staels B, Auwerx J. The PPARs and their effects on lipid metabolism and adipocyte differentiation. *Biochim Biophys Acta* 1996; **1302:** 93-109.

153. Nolte RT, Wisely GB, Westin S *et al.* Ligand binding and co-activator assembly of the PPARγ. *Nature* 1998; **395:** 137-143.

154. Bourguet W, Ruff M, Chambon P, Gronemeyer H, Moras D. Crystal structure of the ligand-binding domain of the human nuclear receptor RXRα. *Nature* 1995; **375:** 377-382.

155. Renaud JP, Rochel N, Ruff M *et al.* Crystal structure of the RARγ ligand-binding domain bound to all-*trans* retinoic acid. *Nature* 1995; **378:** 681-689.

156. Wagner RL, Apriletti JW, McGrath ME, West BL, Baxter JD, Fletterick RJ. A structural role for hormone in the thyroid hormone receptor. *Nature* 1995; **378:** 690-697.

157. Xu HE, Lambert MH, Montana VG *et al.* Molecular recognition of fatty acids by PPARs. *Mol Cell* 1999; **3:** 397-403.

158. Barettino D, Vivanco-Ruiz MM, Stunnenberg HG. Characterisation of the ligand-dependent transactivation domain of thyroid hormone receptor. *EMBO J* 1994; **13:** 3039-3049.

159. Danielian PS, White R, Lees JA, Parker MG. Identification of a conserved region required for hormone dependent transcriptional activation by steroid hormone receptors. *EMBO J* 1992; **11:** 1025-1033.

160. Nagpal S, Saunders M, Kastner P, Durand B, Nakshatri H, Chambon P. Promoter context- and response element-dependent specificity of the transcriptional activation and modulating functions of retinoic acid receptors. *Cell* 1992; **70:** 1007-1019.

161. Pierrat B, Heery DM, Chambon P, Losson R. A highly conserved region in the hormone-binding domain of the human oestrogen receptor functions as an efficient transactivation domain in yeast. *Gene* 1994; **143:** 193-200.

162. Green S. PPAR: a mediator of peroxisome proliferator action. *Mutat Res* 1995; **333:** 101-109.

163. Krey G, Braissant O, Horset F *et al.* Fatty acids, eicosanoids, and hypolipidaemic agents identified as ligands of PPARs by coactivator-dependent receptor ligand assay. *Mol Endocrinol* 1997; **11:** 779-791.

164. Forman BM, Chen J, Evans RM. Hypolipidaemic drugs, polyunsaturated fatty acids, and eicosanoids are ligands for PPAR α and δ. *Proc Natl Acad Sci U S A* 1997; **94:** 4312-4317.

165. Ledwith BJ, Johnson TE, Wagner LK *et al.* Growth regulation by peroxisome proliferators: opposing activities in early and late G_1. *Cancer Res* 1996; **56:** 3257-3264.

166. Kliewer SA, Sundseth SS, Jones SA *et al.* Fatty acids and eicosanoids regulate gene expression through direct interactions with PPARs α and γ. *Proc Natl Acad Sci U S A* 1997; **94:** 4318-4323.

167. Forman BM, Tontonoz P, Chen J, Brun RP, Spiegelman BM, Evans RM. 15-deoxy-$\Delta^{12,14}$-prostaglandin J_2 is a ligand for the adipocyte determination factor PPARγ. *Cell* 1995; **83:** 803-812.

168. Kliewer SA, Lenhard JM, Willson TM, Patel I, Morris DC, Lehmann JM. A prostaglandin J_2 metabolite binds PPARγ and promotes adipocyte differentiation. *Cell* 1995; **83:** 813-819.

169. Lehmann JM, Lenhard JM, Oliver BB, Ringold GM, Kliewer SA. PPARs α and γ are activated by indomethacin and other non-steroidal anti-inflammatory drugs. *J Biol Chem* 1997; **272:** 3406-3410.

170. Alberts B, Bray D, Lewis J, Raff M, Roberts K, Watson JD. *Molecular biology of the cell.* New York: Garland Publishing Incorporated 1994.

171. Vamecq J, Latruffe N. Medical significance of peroxisome proliferator-activated receptors. *Lancet* 1999; **354:** 141-148.

172. Keller H, Dreyer C, Medin J, Mahfoudi A, Ozato K, Wahli W. Fatty acids and retinoids control lipid metabolism through activation of PPAR-RXR heterodimers. *Proc Natl Acad Sci U S A* 1993; **90:** 2160-2164.

173. Gulick T, Cresci S, Caira T, Moore DD, Kelly DP. The PPAR regulates mitochondrial fatty acid oxidative enzyme gene expression. *Proc Natl Acad Sci U S A* 1994; **91:** 11012-11016.

174. Wahli W, Devchand PR, IJpenberg A, Desvergne B. Fatty acids, eicosanoids, and hypolipidaemic agents regulate gene expression through direct binding to PPARs. *Adv Exp Med Biol* 1999; **447:** 199-209.

175. Burdge GC, Rodway HA, Kohler JA, Lillycrop KA. Effect of fatty acid supplementation on growth and differentiation of human IMR-32 neuroblastoma cells *in vitro*. *J Cell Biochem* 2000; **80:** 266-273.

176. Rose DP, Connolly JM, Rayburn J, Coleman M. Influence of diets containing eicosapentaenoic or docosahexaenoic acid on growth and

metastasis of breast cancer cells in nude mice. *J Natl Cancer Inst* 1995; **87:** 587-592.

177. Ligo M, Nakagawa T, Ishikawa C *et al.* Inhibitory effects of docosahexaenoic acid on colon carcinoma 26 metastasis to the lung. *Br J Cancer* 1997; **75:** 650-655.

178. Crawford MA, Costeloe K, Ghebremeskel K, Phylactos A, Skirvin L, Stacey F. Are deficits of arachidonic and docosahexaenoic acids responsible for the neural and vascular complications of pre-term babies? *Am J Clin Nutr* 1997; **66:** 1032S-1041S.

179. Fitzpatrick FA, Wynalda MA. Albumin-catalysed metabolism of prostaglandin D_2. Identification of products formed *in vitro*. *J Biol Chem* 1983; **258:** 11713-11718.

180. Kikawa Y, Narumiya S, Fukushima M, Wakatsuka H, Hayaishi O. 9-Deoxy-Δ^{9},$\Delta^{12\text{-}13,14}$-dihydroprostaglandin D_2, a metabolite of prostaglandin D_2 formed in human plasma. *Proc Natl Acad Sci U S A* 1984; **81:** 1317-1321.

181. Hirata Y, Hayashi H, Ito S *et al.* Occurrence of 9-deoxyΔ^{9},$\Delta^{12\text{-}13,14}$-dihydroprostaglandin D_2 in human urine. *J Biol Chem* 1988; **263:** 16619-16625.

182. Sarraf P, Mueller E, Jones D *et al.* Differentiation and reversal of malignant changes in colon cancer through PPARγ. *Nat Med* 1998; **4:** 1046-1052.

183. Bishop-Bailey D, Hla T. Endothelial cell apoptosis induced by the PPARγ ligand 15-deoxy-$\Delta^{12,14}$-prostaglandin J_2. *J Biol Chem* 1999; **274:** 17042-17048.

184. Narumiya S, Fukushima M. Site and mechanism of growth inhibition by prostaglandins. I. Active transport and intracellular accumulation of cyclopentenone prostaglandins, a reaction leading to growth inhibition. *J Pharmacol Exp Ther* 1986; **239:** 500-505.

185. Narumiya S, Ohno K, Fujiwara M, Fukushima M. Site and mechanism of growth inhibition by prostaglandins. II. Temperature-dependent transfer of a cyclopentenone prostaglandin to nuclei. *J Pharmacol Exp Ther* 1986; **239:** 506-511.

186. Narumiya S, Ohno K, Fukushima M, Fujiwara M. Site and mechanism of growth inhibition by prostaglandins. III. Distribution and binding of prostaglandin A_2 and Δ^{12}-prostaglandin J_2 in nuclei. *J Pharmacol Exp Ther* 1987; **242:** 306-311.

187. Thevenon C, Guichardant M, Lagarde M. Gas chromatographic-mass spectrometric measurement of 15 deoxy-$\Delta^{12,14}$ prostaglandin J_2, the PPARγ ligand, in urine. *Clin Chem* 2001; **47:** 768-770.

188. Chinery R, Coffey RJ, Graves-Deal R *et al.* Prostaglandin J_2 and 15-deoxy-$\Delta^{12,14}$ prostaglandin J_2 induce proliferation of cyclo-oxygenase-depleted colorectal cancer cells. *Cancer Res* 1999; **59:** 2739-2746.

189. Maxey KM, Hessler E, MacDonald J, Hitchingham L. The nature and composition of 15-deoxy-$\Delta^{12,14}$prostaglandin J_2. *Prostaglandins Other Lipid Mediat* 2000; **62:** 15-21.

190. Straus DS, Pascual G, Li M *et al.* 15-deoxy-$\Delta^{12,14}$-prostaglandin J_2 inhibits multiple steps in the NFκB signalling pathway. *Proc Natl Acad Sci U S A* 2000; **97:** 4844-4849.

191. Liou HC, Baltimore D. Regulation of the NF- κB/rel transcription factor and IκB inhibitor system. *Curr Opin Cell Biol* 1993; **5:** 477-487.

192. Bui T, Straus DS. Effects of cyclopentenone prostaglandins and related compounds on insulin-like growth factor-I and Waf1 gene expression. *Biochim Biophys Acta* 1998; **1397:** 31-42.

193. Satoh T, Furuta K, Suzuki M, Watanabe Y. Prostaglandin J_2 and its metabolites promote neurite outgrowth induced by nerve growth factor in PC12 cells. *Biochem Biophys Res Commun* 1999; **258:** 50-53.

194. Davies SS, Pontsler AV, Marathe GK *et al.* Oxidised alkyl phospholipids are specific, high affinity PPARγ ligands and agonists. *J Biol Chem* 2001; **276:** 16015-16023.

195. Lehmann JM, Moore LB, Smith-Oliver TA, Wilkison WO, Willson TM, Kliewer SA. An anti-diabetic thiazolidinedione is a high affinity ligand for PPARγ. *J Biol Chem* 1995; **270:** 12953-12956.

196. Sohda T, Mizuno K, Tawada H, Sugiyama Y, Fujita T, Kawamatsu Y. Studies on anti-diabetic agents. I. Synthesis of 5-[4-(2-methyl-2-phenylpropoxy)-benzyl]thiazolidine-2,4-dione (AL-321) and related compounds. *Chem Pharm Bull (Tokyo)* 1982; **30:** 3563-3573.

197. Sohda T, Mizuno K, Imamiya E, Sugiyama Y, Fujita T, Kawamatsu Y. Studies on anti-diabetic agents. II. Synthesis of 5-[4-(1-methylcyclohexylmethoxy)-benzyl]thiazolidine-2,4-dione (ADD-3878) and its derivatives. *Chem Pharm Bull (Tokyo)* 1982; **30:** 3580-3600.

198. Hulin B, McCarthy PA, Gibbs ME. The glitazone family of anti-diabetic agents. *Curr Pharm Des* 1996; **2:** 85-102.

199. Harris PK, Kletzien RF. Localisation of a pioglitazone response element in the adipocyte fatty acid-binding protein gene. *Mol Pharmacol* 1994; **45:** 439-445.

200. Ibrahimi A, Teboul L, Gaillard D *et al.* Evidence for a common mechanism of action for fatty acids and thiazolidinedione anti-diabetic agents on gene expression in pre-adipose cells. *Mol Pharmacol* 1994; **46:** 1070-1076.

201. Schoonjans K, Auwerx J. Thiazolidinediones: An update. *Lancet* 2000; **355:** 1008-1010.

202. Watkins PB, Whitcomb RW. Hepatic dysfunction associated with troglitazone. *N Engl J Med* 1998; **338:** 916-917.

203. Wang M, Wise SC, Leff T, Su TZ. Troglitazone, an anti-diabetic agent, inhibits cholesterol biosynthesis through a mechanism independent of PPARγ. *Diabetes* 1999; **48:** 254-260.

204. Chawla A, Schwarz EJ, Dimaculangan DD, Lazar MA. PPARγ: adipose-predominant expression and induction early in adipocyte differentiation. *Endocrinology* 1994; **135:** 798-800.

205. Tontonoz P, Hu E, Graves RA, Budavari AI, Spiegelman BM. mPPARγ2: tissue-specific regulator of an adipocyte enhancer. *Genes Dev* 1994; **8:** 1224-1234.

206. Pineau T, Hudgins WR, Liu L *et al.* Activation of a human PPAR by the anti-tumour agent phenylacetate and its analogues. *Biochem Pharmacol* 1996; **52:** 659-667.

207. Han SW, Wada RK, Sidell N. Differentiation of human neuroblastoma by phenylacetate is mediated by PPARγ. *Cancer Res* 2001; **61:** 3998-4002.

208. Heinzel T, Lavinsky RM, Mullen TM *et al.* A complex containing N-CoR, mSin3 and histone deacetylase mediates transcriptional repression. *Nature* 1997; **387:** 43-48.

209. Nagy L, Kao HY, Chakravarti D *et al.* Nuclear receptor repression mediated by a complex containing SMRT, mSin3A, and histone deacetylase. *Cell* 1997; **89:** 373-380.

210. Laherty CD, Yang WM, Sun JM, Davie JR, Seto E, Eisenman RN. Histone deacetylases associated with the mSin3 co-repressor mediate MAD transcriptional repression. *Cell* 1997; **89:** 349-356.

211. Alland L, Muhle R, Hou H *et al.* Role for N-CoR and histone deacetylase in Sin3-mediated transcriptional repression. *Nature* 1997; **387:** 49-55.

212. Zhang Y, Iratni R, Erdjument-Bromage H, Tempst P, Reinberg D. Histone deacetylases and SAP18, a novel polypeptide, are components of a human Sin3 complex. *Cell* 1997; **89:** 357-364.

213. Hassig CA, Fleischer TC, Billin AN, Schreiber SL, Ayer DE. Histone deacetylase activity is required for full transcriptional repression by mSin3A. *Cell* 1997; **89:** 341-347.

214. Torchia J, Glass C, Rosenfeld MG. Co-activators and co-repressors in the integration of transcriptional responses. *Curr Opin Cell Biol* 1998; **10:** 373-383.

215. Schulman IG, Shao G, Heyman RA. Transactivation by RXR-PPARγ heterodimers: intermolecular synergy requires only the PPARγ hormone-dependent activation function. *Mol Cell Biol* 1998; **18:** 3483-3494.

216. Fritsch M, Leary CM, Furlow JD *et al.* A ligand-induced conformational change in the oestrogen receptor is localised in the steroid binding domain. *Biochemistry* 1992; **31:** 5303-5311.

217. Elbrecht A, Chen Y, Adams A *et al.* L-764406 is a partial agonist of human PPARγ. The role of Cys^{313} in ligand binding. *J Biol Chem* 1999; **274:** 7913-7922.

218. Johnson BA, Wilson EM, Li Y, Moller DE, Smith RG, Zhou G. Ligand-induced stabilisation of PPARγ monitored by NMR spectroscopy: Implications for nuclear receptor activation. *J Mol Biol* 2000; **298:** 187-194.

219. Ribeiro RCJ, Kushner PJ, Baxter JD. The nuclear hormone receptor gene superfamily. *Annu Rev Med* 1995; **46:** 443-453.

220. Kainu T, Wikstrom K, Gustafsson JA, Pielto-Huikko M. Localisation of the PPAR in the brain. *Neuroreport* 1994; **5:** 2481-2485.

221. Gervois P, Torra IP, Chinetti G *et al.* A truncated human PPARα splice variant with dominant negative activity. *Mol Endocrinol* 1999; **13:** 1535-1539.

222. Berger J, Patel HV, Woods J *et al.* A PPARγ mutant serves as a dominant negative inhibitor of PPAR signalling and is localised in the nucleus. *Mol Cell Endocrinol* 2000; **162:** 57-67.

223. Chattopadhyay N, Singh DP, Heese O *et al.* Expression of PPARs in astrocytic cells: PPAR agonist as inducers of apoptosis. *J Neurosci* 2000; **61:** 67-74.

224. Jiang WG, Redfern A, Bryce RP, Mansel RE. PPARγ mediates the action of γ-linolenic acid in breast cancer cells. *Prostaglandins Leukot Essent Fatty Acids* 2000; **62:** 119-127.

225. Bishop-Bailey D, Hla T, Warner TD. Bisphenol A diglycidyl ether (BADGE) is a PPARγ agonist in an ECV304 cell line. *Br J Pharmacol* 2000; **131:** 651-654.

226. Miyata KS, McCaw SE, Patel HV, Rachubinski RA, Capone JP. The orphan nuclear hormone receptor LXRα interacts with the PPAR and inhibits peroxisome proliferator signalling. *J Biol Chem* 1996; **271:** 9189-9192.

227. Juge-Aubry CE, Gorla-Bajszczak A, Pernin A *et al.* PPAR mediates cross-talk with thyroid hormone receptor by competition for retinoid X receptor. Possible role of a leucine zipper-like heptad repeat. *J Biol Chem* 1995; **270:** 18117-18122.

228. Hunter J, Kassam A, Winrow CJ, Rachubinski RA, Capone JP. Crosstalk between the thyroid hormone and PPARs in regulating peroxisome proliferator-responsive genes. *Mol Cell Endocrinol* 1996; **116:** 213-221.

229. Castelein H, Declercq PE, Baes M. DNA binding preferences of PPARα/RXRα heterodimers. *Biochem Biophys Res Commun* 1997; **233:** 91-95.

230. Gampe RT, Montana VG, Lambert MH *et al.* Asymmetry in the PPARγ/RXRα crystal structure reveals the molecular basis of heterodimerisation among nuclear receptors. *Mol Cell* 2000; **5:** 545-555.

231. Mangelsdorf DJ, Evans RM. The RXR heterodimers and orphan receptors. *Cell* 1995; **83:** 841-850.

232. Di Renzo J, Soderstrom M, Kurokawa R *et al.* PPARs and RARs differentially control the interactions of RXR heterodimers with ligands, co-activators and co-repressors. *Mol Cell Biol* 1997; **17:** 2166-2176.

233. Tugwood JD, Issemann I, Anderson RG, Bundell KR, McPheat WL, Green S. The mouse PPAR recognises a response element in the 5' flanking sequence of the rat acyl CoA oxidase gene. *EMBO J* 1992; **11:** 433-439.

234. Nakshatri H, Bhat-Nakshatri P. Multiple parameters determine the specificity of transcriptional response by nuclear receptors HNF-4, ARP-1, PPAR, RAR and RXR through common response elements. *Nucleic Acids Res* 1998; **26:** 2491-2499.

235. Metzger S, Halaas JL, Breslow JL, Sladek FM. Orphan receptor HNF-4 and bZip protein C/EBPα bind to overlapping regions of the apolipoprotein B gene promoter and synergistically activate transcription. *J Biol Chem* 1993; **268:** 16831-16838.

236. Sladek FM, Zhong WM, Lai E, Darnell JE. Liver-enriched transcription factor HNF-4 is a novel member of the steroid hormone receptor superfamily. *Genes Dev* 1990; **4:** 2353-2365.

237. IJpenberg A, Jeannin E, Wahli W, Desvergne B. Polarity and specific sequence requirements of PPAR/RXR heterodimer binding to DNA. A functional analysis of the malic enzyme gene PPAR response element. *J Biol Chem* 1997; **272:** 20108-20117.

238. Robinson CE, Wu X, Morris DC, Grimble JM. DNA bending is induced by binding of the PPARγ2 heterodimer to its response element in the murine lipoprotein lipase promoter. *Biochem Biophys Res Commun* 2002; **244:** 671-677.

239. Forman BM, Umesono K, Chen J, Evans RM. Unique response pathways are established by allosteric interactions among nuclear hormone receptors. *Cell* 1995; **81:** 541-550.

240. Issemann I, Prince RA, Tugwood JD, Green S. The retinoid X receptor enhances the function of the PPAR. *Biochimie* 1993; **75:** 251-256.

241. Tontonoz P, Singer S, Forman BM *et al.* Terminal differentiation of human liposarcoma cells induced by ligands for PPARγ and the retinoid X receptor. *Proc Natl Acad Sci U S A* 1997; **94:** 237-241.

242. Elstner E, Muller C, Koshizuka K *et al.* Ligands for PPARγ and retinoic acid receptor inhibit growth and induce apoptosis of human breast cancer cells *in vitro* and in BNX mice. *Proc Natl Acad Sci U S A* 1998; **95:** 8806-8811.

243. Asou H, Verbeek W, Williamson E *et al.* Growth inhibition of myeloid leukaemia cells by troglitazone, a ligand for PPARγ, and retinoids. *Int J Oncol* 1999; **15:** 1027-1031.

244. Kamei Y, Xu L, Heinzel T *et al.* A CBP integrator complex mediates transcriptional activation and AP-1 inhibition by nuclear receptors. *Cell* 1996; **85:** 403-414.

245. Smith CL, Onate SA, Tsai MJ, Malley BW. CREB binding protein acts synergistically with steroid receptor coactivator-1 to enhance steroid receptor-dependent transcription. *Proc Natl Acad Sci U S A* 1996; **93:** 8884-8888.

246. Ogryzko VV, Schiltz RL, Russanova V, Howard BH, Nakatani Y. The transcriptional co-activators p300 and CBP are histone acetyltransferases. *Cell* 1996; **87:** 953-959.

247. Spencer TE, Jenster G, Burcin MM *et al.* Steroid receptor coactivator-1 is a histone acetyltransferase. *Nature* 1997; **389:** 194-198.

248. Yang W, Rachez C, Freedman LP. Discrete roles for PPARγ and RXR in recruiting nuclear receptor coactivators. *Mol Cell Biol* 2000; **20:** 8008-8017.

249. Onate SA, Tsai SY, Tsai MJ, Malley BW. Sequence and characterisation of a coactivator for the steroid hormone receptor superfamily. *Science* 1995; **270:** 1354-1357.

250. Voegel JJ, Heine MJ, Zechel C, Chambon P, Gronemeyer H. TIF2, a 160 kDa transcriptional mediator for the ligand-dependent activation function AF-2 of nuclear receptors. *EMBO J* 1996; **15:** 3667-3675.

251. Torchia J, Rose DW, Inostroza J *et al.* The transcriptional co-activator p/CIP binds CBP and mediates nuclear-receptor function. *Nature* 1997; **387:** 677-684.

252. Chen H, Lin RJ, Schiltz RL *et al.* Nuclear receptor coactivator ACTR is a novel histone acetyltransferase and forms a multimeric activation complex with p/CAF and CBP/p300. *Cell* 1997; **90:** 569-580.

253. Li H, Gomes PJ, Chen JD. RAC3, a steroid/nuclear receptor-associated coactivator that is related to SRC-1 and TIF2. *Proc Natl Acad Sci U S A* 1997; **94:** 8479-8484.

254. Anzick SL, Kononen J, Walker RL *et al.* AIB1, a steroid receptor coactivator amplified in breast and ovarian cancer. *Science* 1997; **277:** 965-968.

255. Takeshita A, Cardona GR, Koibuchi N, Suen CS, Chin WW. TRAM-1, A novel 160-kDa thyroid hormone receptor activator molecule, exhibits distinct properties from steroid receptor coactivator-1. *J Biol Chem* 1997; **272:** 27629-27634.

256. Zhu Y, Kan L, Qi C *et al.* Isolation and characterisation of PPAR-interacting protein (PRIP) as a coactivator for PPAR. *J Biol Chem* 2000; **275:** 13510-13516.

257. Gelman L, Zhou G, Fajas L, Raspe E, Fruchart JC, Auwerx J. p300 interacts with the N- and C-terminal part of PPARγ2 in a ligand-independent and -dependent manner, respectively. *J Biol Chem* 1999; **274:** 7681-7688.

258. Nakajima T, Uchida C, Anderson SF *et al.* RNA helicase A mediates association of CBP with RNA polymerase II. *Cell* 1997; **90:** 1107-1112.

259. Chakravarti D, LaMorte VJ, Nelson MC *et al.* Role of CBP/p300 in nuclear receptor signalling. *Nature* 1996; **383:** 99-103.

260. Dowell P, Ishmael JE, Avram D, Peterson VJ, Nevrivy DJ, Leid M. p300 functions as a coactivator for the PPARα. *J Biol Chem* 1997; **272:** 33435-33443.

261. Yang XJ, Ogryzko VV, Nishikawa J, Howard BH, Nakatani Y. A p300/CBP-associated factor that competes with the adenoviral oncoprotein E1A. *Nature* 1996; **382:** 319-324.

262. Voegel JJ, Heine MJ, Tini M, Vivat V, Chambon P, Gronemeyer H. The coactivator TIF2 contains three nuclear receptor-binding motifs and mediates transactivation through CBP binding-dependent and -independent pathways. *EMBO J* 1998; **17:** 507-519.

263. Yao TP, Ku G, Zhou N, Scully R, Livingston DM. The nuclear hormone receptor coactivator SRC-1 is a specific target of p300. *Proc Natl Acad Sci U S A* 1996; **93:** 10626-10631.

264. Kurokawa R, Kalafus D, Ogliastro MH *et al.* Differential use of CREB binding protein-coactivator complexes. *Science* 1998; **279:** 700-703.

265. Freedman LP. Increasing the complexity of coactivation in nuclear receptor signalling. *Cell* 1999; **97:** 5-8.

266. Chen S, Johnson BA, Li Y *et al.* Both coactivator LXXLL motif-dependent and -independent interactions are required for PPARγ function. *J Biol Chem* 2000; **275:** 3733-3736.

267. Puigserver P, Adelmant G, Wu Z *et al.* Activation of PPARγ coactivator-1 through transcription factor docking. *Science* 1999; **286:** 1368-1371.

268. Puigserver P, Wu Z, Park CW, Graves R, Wright M, Spiegelman BM. A cold-inducible coactivator of nuclear receptors linked to adaptive thermogenesis. *Cell* 1998; **92:** 829-839.

269. Yuan CX, Ito M, Fondell JD, Fu ZY, Roeder RG. The TRAP220 component of a thyroid hormone receptor- associated protein (TRAP) coactivator complex interacts directly with nuclear receptors in a ligand-dependent fashion. *Proc Natl Acad Sci U S A* 1998; **95:** 7939-7944.

270. Masuda N, Yasumo H, Furusawa T, Tsukamoto T, Sadano H, Osumi T. Nuclear receptor binding factor-1 (NRBF-1), a protein interacting with a wide spectrum of nuclear hormone receptors. *Gene* 1998; **221:** 225-233.

271. Yasumo H, Masuda N, Furusawa T, Tsukamoto T, Sadano H, Osumi T. Nuclear receptor binding factor-2 (NRBF-2), a possible gene activator protein interacting with nuclear hormone receptors. *Biochim Biophys Acta* 2000; **1490:** 189-197.

272. Heinlein CA, Ting HJ, Yeh S, Chang C. Identification of ARA70 as a ligand-enhanced coactivator for the PPARγ. *J Biol Chem* 1999; **274:** 16147-16152.

273. Treuter E, Albrektsen T, Johansson L, Leers J, Gustafsson JA. A regulatory role for RIP140 in nuclear receptor activation. *Mol Endocrinol* 1998; **12:** 864-881.

274. Miyata KS, McCaw SE, Meertens LM, Patel HV, Rachubinski RA, Capone JP. Receptor-interacting protein 140 interacts with and inhibits transactivation by PPARα and liver-X-receptor α. *Mol Cell Endocrinol* 1998; **146:** 69-76.

275. Zhou YC, Waxman DJ. Cross-talk between janus kinase-signal transducer and activator of transcription (JAK-STAT) and PPARα signalling pathways. Growth hormone inhibition of PPARα transcriptional activity mediated by stat5b. *J Biol Chem* 1999; **274:** 2672-2681.

276. Davies GF, McFie PJ, Khandelwal RL, Roesler WJ. Unique ability of troglitazone to up-regulate PPAR expression in hepatocytes. *J Pharmacol Exp Ther* 2002; **300:** 72-77.

277. Takamura T, Nohara E, Nagai Y, Kobayashi K. Stage-specific effects of a thiazolidinedione on proliferation, differentiation and PPARγ mRNA expression in 3T3-L1 adipocytes. *Eur J Pharmacol* 2001; **422:** 23-29.

278. Kopf E, Plassat JL, Vivat V, De The H, Chambon P, Rochette-Egly C. Dimerisation with RXRs and phosphorylation modulate the retinoic acid-induced degradation of retinoic acid receptors α and γ through the ubiquitin-proteasome pathway. *J Biol Chem* 2000; **275:** 33280-33288.

279. Rosenbaum SE, Greenberg AS. The short- and long-term effects of TNFα and BRL 49653 on PPARγ2 gene expression and other adipocyte genes. *Mol Endocrinol* 1998; **12:** 1150-1160.

280. Hauser S, Adelmant G, Sarraf P, Wright HM, Mueller E, Spiegelman BM. Degradation of the PPARγ is linked to ligand-dependent activation. *J Biol Chem* 2000; **275:** 18527-18533.

281. Hershko A, Ciechanover A. The ubiquitin system for protein degradation. *Annu Rev Biochem* 1992; **61:** 761-807.

282. Nawaz Z, Lonard DM, Dennis AP, Smith CL, Malley BW. Proteasome-dependent degradation of the human oestrogen receptor. *Proc Natl Acad Sci U S A* 1999; **96:** 1858-1862.

283. Lange CA, Shen T, Horwitz KB. Phosphorylation of human progesterone receptors at serine^{294} by MAP kinase signals their degradation by the 26S proteasome. *Proc Natl Acad Sci U S A* 2000; **97:** 1032-1037.

284. Shalev A, Siegrist-Kaiser CA, Yen PM *et al.* The PPARα is a phosphoprotein: Regulation by insulin. *Endocrinology* 1996; **137:** 4499-4502.

285. Adams M, Reginato MJ, Shao D, Lazar MA, Chatterjee VK. Transcriptional activation by PPARγ is inhibited by phosphorylation at a consensus mitogen-activated protein kinase site. *J Biol Chem* 1997; **272:** 5128-5132.

286. Hu E, Kim JB, Sarraf P, Spiegelman BM. Inhibition of adipogenesis through MAP kinase-mediated phosphorylation of PPARγ. *Science* 1996; **274:** 2100-2103.

287. Zhang B, Berger J, Zhou G *et al.* Insulin- and mitogen-activated protein kinase-mediated phosphorylation and activation of PPARγ. *J Biol Chem* 1996; **271:** 31771-31774.

288. Camp HS, Tafuri SR. Regulation of PPARγ activity by mitogen-activated protein kinase. *J Biol Chem* 1997; **272:** 10811-10816.

289. Reginato MJ, Krakow SL, Bailey ST, Lazar MA. Prostglandins promote and block adipogenesis through opposite effects on PPAR. *J Biol Chem* 1998; **273:** 1855-1858.

290. Mueller E, Sarraf P, Tontonoz P *et al.* Terminal differentiation of human breast cancer through PPARγ. *Mol Cell* 1998; **1:** 465-470.

291. Huang Q, Alvares K, Chu R, Bradfield CA, Reddy JK. Association of PPAR and Hsp72. *J Biol Chem* 1994; **269:** 8493-8497.

292. Baniahmad A, Tsai MJ. Mechanisms of transcriptional activation by steroid hormone receptors. *J Cell Biochem* 1993; **51:** 151-156.

293. Vanden Heuvel JP. Peroxisome proliferator-activated receptors: A critical link among fatty acids, gene expression and carcinogenesis. *J Nutr Suppl.* 1999; **129:** 575S-580S.

294. Ledwith BJ, Manam S, Troilo P, Joslyn DJ, Galloway SM, Nichols WW. Activation of immediate-early gene expression by peroxisome proliferators *in vitro*. *Mol Carcinog* 1993; **8:** 20-27.

295. Lazarow PB, De Duve C. A fatty acyl-CoA oxidising system in rat liver peroxisomes; enhancement by clofibrate, a hypolipidaemic drug. *Proc Natl Acad Sci U S A* 1976; **73:** 2043-2046.

296. Lazarow PB. Three hypolipidaemic drugs increase hepatic palmitoyl-coenzyme A oxidation in the rat. *Science* 1977; **197:** 580-581.

297. Reddy JK, Goel SK, Nemali MR *et al.* Transcription regulation of peroxisomal fatty acyl-CoA oxidase and enoyl-CoA hydratase/3-hydroxyacyl-CoA dehydrogenase in rat liver by peroxisome proliferators. *Proc Natl Acad Sci U S A* 1986; **83:** 1747-1751.

298. Hardwick JP, Song BJ, Huberman E, Gonzalez FJ. Isolation, complementary DNA sequence, and regulation of rat hepatic lauric acid ω-hydroxylase (cytochrome P-450LA ω). Identification of a new cytochrome P-450 gene family. *J Biol Chem* 1987; **262:** 801-810.

299. Gibson GG, Orton TC, Tamburini PP. Cytochrome P-450 induction by clofibrate. Purification and properties of a hepatic cytochrome P-450 relatively specific for the 12- and 11-hydroxylation of dodecanoic acid (lauric acid). *Biochem J* 1982; **203:** 161-168.

300. Sharma R, Lake BG, Gibson GG. Co-induction of microsomal cytochrome P-452 and the peroxisomal fatty acid β-oxidation pathway in the rat by clofibrate and di-(2-ethylhexyl)phthalate. Dose-response studies. *Biochem Pharmacol* 1988; **37:** 1203-1206.

301. Muerhoff AS, Griffin KJ, Johnson EF. The PPAR mediates the induction of CYP4A6, a cytochrome P450 fatty acid ω-hydroxylase, by clofibric acid. *J Biol Chem* 1992; **267:** 19051-19053.

302. Mannaerts GP, Thomas J, Debeer LJ, McGarry JD, Foster DW. Hepatic fatty acid oxidation and ketogenesis after clofibrate treatment. *Biochim Biophys Acta* 1978; **529:** 201-211.

303. Christiansen RZ, Osmundsen H, Borrebaek B, Bremer J. The effects of clofibrate feeding on the metabolism of palmitate and erucate in isolated hepatocytes. *Lipids* 1978; **13:** 487-491.

304. Rodriguez JC, Gil-Gomez G, Hegardt FG, Haro D. PPAR mediates induction of the mitochondrial 3-hydroxy-3-methylglutaryl-CoA synthase gene by fatty acids. *J Biol Chem* 1994; **269:** 18767-18772.

305. Kaikaus RM, Chan WK, Lysenko N, Ray R, Ortiz de Montellano PR, Bass NM. Induction of peroxisomal fatty acid β-oxidation and liver fatty acid-binding protein by peroxisome proliferators. Mediation via the cytochrome P-450IVA1 omega-hydroxylase pathway. *J Biol Chem* 1993; **268:** 9593-9603.

306. Castelein H, Gulick T, Declercq PE, Mannaerts GP, Moore DD, Baes MI. The PPAR regulates malic enzyme gene expression. *J Biol Chem* 1994; **269:** 26754-26758.

307.Thuillier P, Anchiraico GJ, Nickel KP *et al.* Activators of PPARα partially inhibit mouse skin tumour promotion. *Mol Carcinog* 2000; **29:** 134-142.

308.Jackson LM, Bennett AJ, Watson S, Wahli W, Hawkey CJ. The role of PPARα in colonic malignancy. First International Symposium on PPARs: From Basic Science to Clinical Applications. 20. 2001.

309.Gariot P, Barrat E, Mejean L, Pointel JP, Drouin P, Debry G. Fenofibrate and human liver. Lack of proliferation of peroxisomes. *Arch Toxicol* 1983; **53:** 151-163.

310.Collett GP, Betts AM, Johnson MI *et al.* PPARα is an androgen-responsive gene in human prostate and is highly expressed in prostatic adenocarcinoma. *Clin Cancer Res* 2000; **6:** 3241-3248.

311.He TC, Chan TA, Vogelstein B, Kinzler KW. PPARδ is an APC-regulated target of non-steroidal anti-inflammatory drugs. *Cell* 1999; **99:** 335-345.

312.Kersten S, Desvergne B, Wahli W. Roles of PPARs in health and disease. *Nature* 2000; **405:** 421-424.

313.Park BH, Vogelstein B, Kinzler KW. Genetic disruption of PPARδ decreases the tumourigenicity of human colon cancer cells. *Proc Natl Acad Sci U S A* 2001; **98:** 2598-2603.

314.Gupta RA, Tan J, Krause WF *et al.* Prostacyclin-mediated activation of PPARδ in colorectal cancer. *Proc Natl Acad Sci U S A* 2000; **97:** 13275-13280.

315.Tong BJ, Tan J, Tajeda L *et al.* Heightened expression of cyclooxygenase-2 and PPAR-δ in human endometrial adenocarcinoma. *Neoplasia* 2000; **2:** 483-490.

316.Fielding CJ, Fielding PE. Molecular physiology of reverse cholesterol transport. *J Lipid Res* 1995; **36:** 211-228.

317.Schaffer JE, Lodish HF. Expression cloning and characterisation of a novel adipocyte long chain fatty acid transport protein. *Cell* 1994; **79:** 427-436.

318.Wu Z, Xie Y, Bucher NLR, Farmer SR. Conditional ectopic expression of C/EBPβ in NIH3T3 cells induces PPAR and stimulates adipogenesis. *Genes Dev* 1995; **9:** 2350-2363.

319.Wu Z, Bucher NLR, Farmer SR. Induction of PPARγ during the conversion of 3T3 fibroblasts into adipocytes is mediated by C/EBPβ, C/EBPδ and glucocorticoids. *Mol Cell Biol* 1996; **16:** 4128-4136.

320.Rieusset J, Auwerx J, Vidal H. Regulation of gene expression by activation of the PPAR with rosiglitazone (BRL49653) in human adipocytes. *Biochem Biophys Res Commun* 1999; **265:** 265-271.

321.Moller DE, Flier JS. Insulin-resistance mechanisms, syndromes and implications. *N Engl J Med* 1991; **325:** 938-948.

322.Berger J, Bailey P, Biswas C *et al.* TZDs produce a conformational change in PPARγ: Binding and activation correlate with anti-diabetic actions in db/db mice. *Endocrinology* 1996; **137:** 4189-4195.

323.Ek J, Urhammer SA, Sorensen TI, Andersen T, Auwerx J, Pedersen O. Homozygosity of the Pro12Ala variant of the PPARγ2: divergent modulating effects on body mass index in obese and lean Caucasians men. *Diabetol* 1999; **42:** 892-895.

324.Mancini FP, Vaccaro O, Sabatino L *et al.* Pro12Ala substitution in the PPARγ2 is not associated with type 2 diabetes. *Diabetes* 1999; **48:** 1466-1468.

325.Valve R, Sivenius K, Miettinen R *et al.* Two polymorphisms in the PPAR gene are associated with severe overweight among obese women. *J Clin Endocrinol Metab* 1999; **84:** 3708-3712.

326.Deeb S, Fajas L, Nemoto M, Laakso M, Fujimoto W, Auwerx J. A Pro12Ala substitution in the human PPARγ2 is associated with decreased receptor activity, improved insulin sensitivity and lowered body mass index. *Nat Genet* 1998; **20:** 284-287.

327.Ristow M, Muller-Wieland D, Pfeiffer A, Krone W, Kahn CR. Obesity associated with a mutation in a genetic regulator of adipocyte differentiation. *New Engl J Med* 1998; **339:** 953-959.

328.Masugi J, Tamori Y, Kasuga M. Inhibition of adipogenesis by a COOH-terminally truncated mutant of PPARγ2 in 3T3-L1 cells. *Biochem Biophys Res Commun* 1999; **264:** 93-99.

329.Barroso I, Gurnell M, Crowley VE *et al.* Dominant negative mutations in human PPARγ associated with severe insulin resistance, diabetes mellitus and hypertension. *Nature* 1999; **402:** 880-883.

330.Gurnell M, Wentworth JM, Agostini M *et al.* A dominant-negative PPARγ mutant is a constitutive repressor and inhibits PPARγ-mediated adipogenesis. *J Biol Chem* 2000; **275:** 5754-5759.

331.Ricote M, Li AC, Willson TM, Kelly CJ, Glass CK. The PPARγ is a negative regulator of macrophage activation. *Nature* 1998; **391:** 79-82.

332.Auwerx J. PPARγ, the ultimate thrifty gene. *Diabetol* 1999; **42:** 1049.

333.Tontonoz P, Nagy L, Alvarez JG, Thomazy VA, Evans RM. PPARγ promotes monocyte/macrophage differentiation and uptake of oxidised LDL. *Cell* 1998; **93:** 241-252.

334.Nagy L, Tontonoz P, Alvarez JG, Chen H, Evans RM. Oxidised LDL regulates macrophage gene expression through ligand activation of PPARγ. *Cell* 1998; **93:** 229-240.

335.Chinetti G, Griglio S, Antonucci M *et al.* Activation of PPARs α and γ induces apoptosis of human monocyte-derived macrophages. *J Biol Chem* 1998; **273:** 25573-25580.

336.Yang XY, Wang LH, Chen T *et al.* Activation of human T lymphocytes is inhibited by PPARγ agonists. PPARγ co-association with transcription factor NFAT. *J Biol Chem* 2000; **275:** 4541-4544.

337.Watanabe T, Haraoka S, Shimokama T. Inflammatory and immunological nature of atherosclerosis. *Int J Cardiol* 1996; **54:** S51-S60.

338.Ross R. Atherosclerosis - an inflammatory disease. *New Engl J Med* 1999; **340:** 115-126.

339.Ricote M, Huang JT, Welch JS, Glass CK. The PPARγ as a regulator of monocyte/macrophage function. *J Leukoc Biol* 1999; **66:** 733-739.

340.Takahashi N, Okumura T, Motomura W, Fujimoto Y, Kawabata I, Kohgo Y. Activation of PPARγ inhibits cell growth and induces apoptosis in human gastric cancer cells. *FEBS Lett* 1999; **455:** 135-139.

341.Chang TH, Szabo E. Induction of differentiation and apoptosis by ligands of PPARγ in non-small cell lung cancer. *Cancer Res* 2000; **60:** 1129-1138.

342.Han SW, Greene ME, Pitts J, Wada RK, Sidell N. Novel expression and function of PPARγ in human neuroblastoma cells. *Clin Cancer Res* 2001; **7:** 98-104.

343.Cimini AM, Cristiano L, Colafarino S, Miranda M, Ceru MP. PPARs and RXRs in human neuroblastoma and glioblastoma cell lines. Effects of natural and synthetic ligands. *First International Symposium on PPARs: From Basic Science to Clinical Applications.* 2001; 19.

344.Kroll TG, Sarraf P, Pecciarini L *et al.* PAX8-PPARgamma1 fusion oncogene in human thyroid carcinoma [corrected]. *Science* 2000; **289:** 1357-1360.

345.Smith WM, Zhou XP, Kurose K *et al.* Opposite association of two PPARγ variants with cancer: over-representation of H449H in endometrial carcinoma cases and under-representation of P12A in renal cell carcinoma cases. *Hum Genet* 2001; **109:** 146-151.

346.Butler R, Mitchell SH, Tindall DJ, Young CY. Non-apoptotic cell death associated with S-phase arrest of prostate cancer cells via the PPARγ ligand, 15-deoxy-$\Delta^{12,14}$-prostaglandin J_2. *Cell Growth Differ* 2000; **11:** 49-61.

347.Keelan JA, Sato TA, Marvin KW, Lander J, Gilmour RS, Mitchell MD. 15-deoxy-$\Delta^{12,14}$-prostaglandin J_2, a ligand for PPARγ, induces apoptosis in JEG3 choriocarcinoma cells. *Biochem Biophys Res Commun* 1999; **262:** 579-585.

348.Altiok S, Xu M, Spiegelman BM. PPARγ induces cell cycle withdrawal: inhibition of E2F/DP DNA-binding activity via down-regulation of PP2A. *Genes Dev* 1997; **11:** 1987-1998.

349.DuBois RN, Gupta R, Brockman J, Reddy BS, Krakow SL, Lazar MA. The nuclear eicosanoid receptor, PPARγ, is aberrantly expressed in colonic cancers. *Carcinogenesis* 1998; **19:** 49-53.

350.Lefebvre AM, Chen I, Desreumaux P *et al.* Activation of the PPARγ promotes the development of colon tumours in C57BL/6J-APCMin/+ mice. *Nat Med* 1998; **4:** 1053-1057.

351.Saez E, Tontonoz P, Nelson MC *et al.* Activators of the nuclear receptor PPARγ enhance colon polyp formation. *Nat Med* 1998; **4:** 1058-1061.

352.Sarraf P, Mueller E, Smith WM *et al.* Loss-of-function mutations in PPARγ associated with human colon cancer. *Mol Cell* 1999; **3:** 799-804.

353.Brockman JA, Gupta RA, DuBois RN. Activation of PPARγ leads to inhibition of anchorage-independent growth of human colorectal cancer cells. *Gastroenterology* 1998; **115:** 1049-1055.

354.Webb CP, Van Aelst L, Wigler MH, Woude GF. Signalling pathways in Ras-mediated tumourigenicity and metastasis. *Proc Natl Acad Sci U S A* 1998; **95:** 8773-8778.

355.Demetri GD, Fletcher CD, Mueller E *et al.* Induction of solid tumour differentiation by the PPARγ ligand troglitazone in patients with liposarcoma. *Proc Natl Acad Sci U S A* 1999; **96:** 3951-3956.

356.Thiele CJ, Reynolds CP, Israel MA. Decreased expression of NMYC precedes retinoic acid-induced morphological differentiation of human neuroblastoma. *Nature* 1985; **313:** 404-406.

357.Clay CE, Namen AM, Atsumi G *et al.* Influence of J series prostaglandins on apoptosis and tumourigenesis of breast cancer cells. *Carcinogenesis* 1999; **20:** 1905-1911.

358.Darzynkiewicz Z, Bruno S, Del Bino G *et al.* Features of apoptotic cells measured by flow cytometry. *Cytometry* 1992; **13:** 795-808.

359.Wyllie AH, Kerr JF, Currie AR. Cell death: the significance of apoptosis. *Int Rev Cytol* 1980; **68:** 251-306.

360.Wyllie AH, Morris RG, Smith AL, Dunlop D. Chromatin cleavage in apoptosis: association with condensed chromatin morphology and dependence on macromolecular synthesis. *J Pathol* 1984; **142:** 67-77.

361.Bowen ID, Lockshin RA. *Cell death in biology and pathology.* London: Chapman and Hall 1981.

362.Rohn TT, Wong SM, Cotman CW, Cribbs DH. 15-deoxy-$\Delta^{12,14}$-prostaglandin J_2, a specific ligand for PPARγ, induces neuronal apoptosis. *Neuroreport* 2001; **12:** 839-843.

363.Lawrence BP, Brown WJ. Autophagic vacuoles rapidly fuse with pre-existing lysosomes in cultured hepatocytes. *J Cell Sci* 1992; **102 (Pt 3):** 515-526.

364.Dunn WA. Studies on the mechanisms of autophagy: formation of the autophagic vacuole. *J Cell Biol* 1990; **110:** 1923-1933.

365.Dunn WA. Studies on the mechanisms of autophagy: maturation of the autophagic vacuole. *J Cell Biol* 1990; **110:** 1935-1945.

366.Clarke PGH. Developmental cell death: morphological diversity and multiple mechanisms. *Anal Embryol* 1990; **181:** 195-213.

367.Zakeri Z, Bursch W, Tenniswood M, Lockshin RA. Cell death: programmed, apoptosis, necrosis, or other? *Cell Death Differ* 1995; **2:** 87-96.

368.Jia L, Dourmashkin RR, Allen PD, Gray AB, Newland AC, Kelsey SM. Inhibition of autophagy abrogates TNFα induced apoptosis in human T-lymphoblastic leukaemic cells. *Br J Haematol* 1997; **98:** 673-685.

369.Folkman J. Tumour angiogenesis: therapeutic implications. *N Engl J Med* 1971; **285:** 1182-1186.

370.Folkman J, Klagsbrun M. Angiogenic factors. *Science* 1987; **235:** 442-447.

371.Xin X, Yang S, Kowalski J, Gerritsen ME. PPARγ ligands are potent inhibitors of angiogenesis *in vitro* and *in vivo*. *J Biol Chem* 1999; **274:** 9116-9121.

372.Fong GH, Rossant J, Gertsenstein M, Breitman ML. Role of the Flt-1 receptor tyrosine kinase in regulating the assembly of vascular endothelium. *Nature* 1995; **376:** 66-70.

373.Ferrara N, Davis-Smyth T. The biology of vascular endothelial growth factor. *End Rev* 1997; **18:** 4-25.

374.Ilan N, Mahooti S, Madri JA. Distinct signal transduction pathways are utilised during the tube formation and survival phases of *in vitro* angiogenesis. *J Cell Sci* 1998; **111:** 3621-3631.

375.Chapman HA. Plasminogen activators, integrins, and the co-ordinated regulation of cell adhesion and migration. *Curr Opin Cell Biol* 1997; **9:** 714-724.

376.Ellis CN, Varani J, Fisher GJ *et al.* Troglitazone improves psoriasis and normalises models of proliferative skin disease: ligands for PPAR inhibit keratinocyte proliferation. *Arch Dermatol* 2002; **136:** 609-616.

377.Su CG, Wen X, Bailey ST *et al.* A novel therapy for colitis utilising PPARγ ligands to inhibit the epithelial inflammatory response. *J Clin Invest* 1999; **104:** 383-389.

378.Combs CK, Johnson DE, Karlo JC, Cannady SB, Landreth GE. Inflammatory mechanisms in Alzheimer's disease: inhibition of β-amyloid-stimulated pro-inflammatory responses and neurotoxicity by PPARγ agonists. *J Neurosci* 2000; **20:** 558-567.

379.Kitamura Y, Shimohama S, Koike H *et al.* Increased expression of cyclo-oxygenases and PPARγ in Alzheimer's disease brains. *Biochem Biophys Res Commun* 1999; **254:** 582-586.

380.Westen H, Bainton DF. Association of alkaline phosphatase-positive reticulum cell in bone marrow with granulocyte precursors. *J Exp Med* 1979; **150:** 919-937.

381.Bianco P, Costantini M, Dearden LC, Bonucci E. Alkaline phosphatase positive precursors of adipocytes in the human bone marrow. *Br J Haematol* 1988; **68:** 401-403.

382.Diascro DDJ, Vogel RL, Johnson TE *et al.* High fatty acid content in rabbit serum is responsible for the differentiation of osteoblasts into adipocytes-like cells. *J Bone Miner Res* 1998; **13:** 96-106.

383.Lecka-Czernik B, Gubrij I, Moerman E *et al.* Inhibition of Osf2/Cbfa1 expression and terminal osteoblast differentiation by PPARγ2. *J Cell Biochem* 1999; **74:** 357-371.

384.Jilka RL, Weinstein RS, Takahashi K, Parfitt AM, Manolagas SC. Linkage of decreased bone mass with impaired osteoblastogenesis in a murine model of accelerated senescence. *J Clin Invest* 1996; **97:** 1732-1740.

385.Kajkenova O, Lecka-Czernik B, Gubrij I *et al.* Increased adipogenesis and myelopoiesis in the bone marrow of SAMP6, a murine model of defective osteoblastogenesis and low turnover osteopaenia. *J Bone Miner Res* 1997; **12:** 1772-1779.

386.Huan B, Kosovsky MJ, Siddiqui A. RXRα transactivates the hepatitis B virus enhancer 1 element by forming a heterodimeric complex with the PPAR. *J Virol* 1995; **69:** 547-551.

387.Yu X, Mertz JE. Differential regulation of the pre-C and pre-genomic promoters of human hepatitis B virus by members of the nuclear receptor superfamily. *J Virol* 1997; **71:** 9366-9374.

388.Ladias JA. Convergence of multiple nuclear receptor signalling pathways onto the long terminal repeat of HIV-1. *J Biol Chem* 1994; **269:** 5944-5951.

389.Hayes MM, Lane BR, King SR, Markovitz DM, Coffey MJ. PPARγ agonists inhibit HIV-1 replication in macrophages by transcriptional and post-translational effects. *J Biol Chem* 2002.

390.Hanahan D, Jessee J, Bloom FR. Plasmid transformation of *Escherichia coli* and other bacteria. *Methods Enzymol* 1991; **204:** 63-113.

391.Tumilowicz JJ, Nichols WW, Cholon JJ, Greene AE. Definition of a continuous human cell line derived from neuroblastoma. *Cancer Res* 1970; **30:** 2110-2118.

392.Safaei R, Prochazka V, Detmer K, Boncinelli E, Lawrence HJ, Largman C. Modulation of HOX2 gene expression following differentiation of neuronal cell lines. *Differentiation* 1992; **51:** 39-47.

393.Hall CV, Jacob PE, Ringold GM, Lee F. Expression and regulation of *Escherichia coli* lacZ gene fusions in mammalian cells. *J Mol Appl Genet* 1983; **2:** 101-109.

394.Luckow B, Schutz G. CAT constructions with multiple unique restriction sites for the functional analysis of eukaryotic promoters and regulatory elements. *Nucleic Acids Res* 1987; **15:** 5490.

395.Makela TP, Koskinen PJ, Vastrik I, Alitalo K. Alternative forms of Max as enhancers or suppressors of MYC-ras co-transformation. *Science* 1992; **256:** 373-377.

396.Sellins KS, Cohen JJ. Gene induction by γ-irradiation leads to DNA fragmentation in lymphocytes. *J Immunol* 1987; **139:** 3199-3206.

397.Gunji H, Kharbanda S, Kufe D. Induction of internucleosomal DNA fragmentation in human myeloid leukaemia cells by 1-β-D-arabinofuranosylcytosine. *Cancer Res* 1991; **51:** 741-743.

398.Ritke MK, Rusnak JM, Lazo JS *et al.* Differential induction of etoposide-mediated apoptosis in human leukaemia HL-60 and K562 cells. *Mol Pharmacol* 1994; **46:** 605-611.

399.Krishan A. Rapid flow cytofluorometric analysis of mammalian cell cycle by propidium iodide staining. *J Cell Biol* 1975; **66:** 188-193.

400.Nicoletti I, Migliorati G, Pagliacci MC, Grignani F, Riccardi C. A rapid and simple method for measuring thymocyte apoptosis by propidium iodide staining and flow cytometry. *J Immunol Methods* 1991; **139:** 271-279.

401.Hayat MA. *Basic techniques for electron microscopy.* London: Academic Press 1986.

402.Reynolds ES. The use of lead citrate at high pH as an electron opaque stain in electron microscopy. *J Cell Biol* 1963; **17:** 208-212.

403.Gorman C. High efficiency gene transfer into mammalian cells. Oxford: IRL Press 1985: 143-180.

404.Cham BE, Knowles BR. A solvent system for delipidation of plasma or serum without protein precipitation. *J Lipid Res* 1976; **17:** 176-181.

405.Begin ME, Das UN, Ells G, Horrobin DF. Selective killing of human cancer cells by polyunsaturated fatty acids. *Prostaglandins Leukot Med* 1985; **19:** 177-186.

406.Chen ZY, Istfan NW. Docosahexaenoic acid is a potent inducer of apoptosis in HT-29 colon cancer cells. *Prostaglandins Leukot Essent Fatty Acids* 2000; **63:** 301-308.

407.Siddiqui RA, Jenski LJ, Neff K, Harvey K, Kovacs RJ, Stillwell W. Docosahexaenoic acid induces apoptosis in Jurkat cells by a protein phosphatase-mediated process. *Biochim Biophys Acta* 2001; **1499:** 265-275.

408.Maehle L, Eilertsen E, Mollerup S, Schonberg S, Krokan HE, Haugen A. Effects of n-3 fatty acids during neoplastic progression and comparison of *in vitro* and *in vivo* sensitivity of two human tumour cell lines. *Br J Cancer* 1995; **71:** 691-696.

409.Rizzo MT, Regazzi E, Garau D *et al.* Induction of apoptosis by arachidonic acid in chronic myeloid leukaemia cells. *Cancer Res* 1999; **59:** 5047-5053.

410.Jungling E, Kammermeier H. A one-vial method for routine extraction and quantification of free fatty acids in blood and tissue by HPLC. *Anal Biochem* 1988; **171:** 150-157.

411.Stubbs CD, Smith AD. Physiological concentrations of fatty acids in plasma of more than 30 μM induce formation of lipid droplets in cells. *Biochim Biophys Acta* 1984; **779:** 89-137.

412.Das UN. Arachidonic acid as a mediator of some of the actions of phorboImyristate acetate, a tumour promoter and inducer of differentiation. *Prostaglandins Leukot Essent Fatty Acids* 1991; **42:** 241-244.

413.Leary WP, Robinson KM, Booyens J, Dippenaar N. Some effects of γ-linolenic acid on cultured human oesophageal carcinoma cells. *S Afr Med J* 1982; **62:** 681-683.

414.Albino AP, Juan G, Traganos F *et al.* Cell cycle arrest and apoptosis of melanoma cells by docosahexaenoic acid: association with decreased pRb phosphorylation. *Cancer Res* 2000; **60:** 4139-4145.

415.Deliconstantinos G. Physiological aspects of membrane lipid fluidity in malignancy. *Anticancer Res* **7:** 1011-1021.

416.Kruman II, Kostenko MA, Gordon RY, Popov VI, Umansky SR. Differentiation and apoptosis of murine neuroblastoma cells N1E115. *Biochem Biophys Res Commun* 1993; **191:** 1309-1318.

417.Schmidt ML, Kuzmanoff KL, Ling-Indeck L, Pezzuto JM. Betulinic acid induces apoptosis in human neuroblastoma cell lines. *Eur J Cancer* 1997; **33:** 2007-2010.

418.Yuste VJ, Bayascas JR, Llecha N, Sanchez-Lopez I, Boix J, Comella JX. The absence of oligonucleosomal DNA fragmentation during apoptosis of IMR-5 neuroblastoma cells: disappearance of the caspase-activated DNase. *J Biol Chem* 2001; **276:** 22323-22331.

419.Zou H, Henzel WJ, Liu X, Lutschg A, Wang X. Apaf-1, a human protein homologous to *C. elegans* CED-4, participates in cytochrome c-dependent activation of caspase-3. *Cell* 1997; **90:** 405-413.

420.Alnemri ES. Mammalian cell death proteases: a family of highly conserved aspartate specific cysteine proteases. *J Cell Biochem* 1997; **64:** 33-42.

421.Janicke RU, Sprengart ML, Wati MR, Porter AG. Caspase-3 is required for DNA fragmentation and morphological changes associated with apoptosis. *J Biol Chem* 1998; **273:** 9357-9360.

422.Liang Y, Yan C, Schor NF. Apoptosis in the absence of caspase 3. Oncogene 20[45], 6570-6578. 2001.

423.Kaufmann SH, Desnoyers S, Ottaviano Y, Davidson NE, Poirier GG. Specific proteolytic cleavage of poly(ADP-ribose) polymerase: an early marker of chemotherapy-induced apoptosis. *Cancer Res* 1993; **53:** 3976-3985.

424.Lippke JA, Gu Y, Sarnecki C, Caron PR, Su MS. Identification and characterisation of CPP32/Mch2 homologue 1, a novel cysteine protease similar to CPP32. *J Biol Chem* 1996; **271:** 1825-1828.

425.De Murcia G, Schreiber V, Molinete M *et al.* Structure and function of poly(ADP-ribose) polymerase. *Mol Cell Biochem* 1994; **138:** 15-24.

426.Biederbick A, Kern HF, Elsasser HP. Monodansylcadaverine (MDC) is a specific *in vivo* marker for autophagic vacuoles. *Eur J Cell Biol* 1995; **66:** 3-14.

427.Xue L, Fletcher GC, Tolkovsky AM. Autophagy is activated by apoptotic signalling in sympathetic neurones: an alternative mechanism of death execution. *Mol Cell Neurosci* 1999; **14:** 180-198.

428.Sato H, Ishihara S, Kawashima K *et al.* Expression of PPARγ in gastric cancer and inhibitory effects of PPARγ agonists. *Br J Cancer* 2000; **83:** 1394-1400.

429.De Urquiza AM, Liu S, Sjoberg M *et al.* Docosahexaenoic acid, a ligand for the retinoid X receptor in mouse brain. *Science* 2000; **290:** 2140-2144.

430.Lovat PE, Lowis SP, Pearson AD, Malcolm AJ, Redfern CP. Concentration-dependent effects of 9-*cis* retinoic acid on neuroblastoma differentiation and proliferation *in vitro*. *Neurosci Lett* 1994; **182:** 29-32.

431.Clay CE, Namen AM, Fonteh AN, Atsumi G, High KP, Chilton FH. 15-deoxy-$\Delta^{12,14}$Prostaglandin J_2 induces diverse biological responses via PPARγ activation in cancer cells. *Prostaglandins Other Lipid Mediat* 2000; **62:** 23-32.

432.Clay CE, Namen AM, Atsumi G *et al.* Magnitude of PPARγ activation is associated with important and seemingly opposite biological responses in breast cancer cells. *J Investig Med* 2001; **49:** 413-420.

433.Kim IK, Lee JH, Sohn HW, Kim HS, Kim SH. Prostaglandin A_2 and Δ^{12} - prostaglandin J_2 induce apoptosis in L1210 cells. *FEBS Lett* 1993; **321:** 209-214.

434.Guan YF, Zhang YH, Breyer RM, Davis L, Breyer MD. Expression of PPARγ in human transitional bladder cancer and its role in inducing cell death. *Neoplasia* 1999; **1:** 330-339.

435.Ponzoni M, Bocca P, Chiesa V *et al.* Differential effects of *N*-(4-hydroxyphenyl)retinamide and retinoic acid on neuroblastoma cells: apoptosis versus differentiation. *Cancer Res* 1995; **55:** 853-861.

436.Boix J, Llecha N, Yuste VJ, Comella JX. Characterisation of the cell death process induced by staurosporine in human neuroblastoma cell lines. *Neuropharmacology* 1997; **36:** 811-821.

437.Schleiermacher G, Peter M, Michon J *et al.* Two distinct deleted regions on the short arm of chromosome 1 in neuroblastoma. *Genes Chromosomes Cancer* 1994; **10:** 275-281.

438.Takeda O, Homma C, Maseki N *et al.* There may be two tumour suppressor genes on chromosome arm 1p closely associated with biologically distinct subtypes of neuroblastoma. *Genes Chromosomes Cancer* 1994; **10:** 30-39.

439.Yang HW, Chen YZ, Piao HY, Takita J, Soeda E, Hayashi Y. DNA fragmentation factor 45 (DFF45) gene at 1p36.2 is homozygously deleted and encodes variant transcripts in neuroblastoma cell line. *Neoplasia* 2001; **3:** 165-169.

440.Enari M, Sakahira H, Yokoyama H, Okawa K, Iwamatsu A, Nagata S. A caspase-activated DNase that degrades DNA during apoptosis, and its inhibitor ICAD. *Nature* 1998; **391:** 43-50.

441.Liu X, Zou H, Slaughter C, Wang X. DFF, a heterodimeric protein that functions downstream of caspase-3 to trigger DNA fragmentation during apoptosis. *Cell* 1997; **89:** 175-184.

442.Liu X, Li P, Widlak P *et al.* The 40-kDa subunit of DNA fragmentation factor induces DNA fragmentation and chromatin condensation during apoptosis. *Proc Natl Acad Sci U S A* 1998; **95:** 8461-8466.

443.Teitz T, Wei T, Valentine MB *et al.* Caspase 8 is deleted or silenced preferentially in childhood neuroblastomas with amplification of MYCN. *Nat Med* 2000; **6:** 529-535.

444.Schweichel JU, Merker HJ. The morphology of various types of cell death in pre-natal tissues. *Teratology* 1973; **7:** 253-266.

445.Lemasters JJ, Nieminen AL, Qian T *et al.* The mitochondrial permeability transition in cell death: a common mechanism in necrosis, apoptosis and autophagy. *Biochim Biophys Acta* 1998; **1366:** 177-196.

446.Cataldo AM, Barnett JL, Berman SA *et al.* Gene expression and cellular content of cathepsin D in Alzheimer's disease brain: evidence for early up-regulation of the endosomal-lysosomal system. *Neurone* 1995; **14:** 671-680.

447.Anglade P, Vyas S, Javoy A *et al.* Apoptosis and autophagy in nigral neurones of patients with Parkinson's disease. *Histol Histopathol* 1997; **12:** 25-31.

448.Bursch W, Ellinger A, Kienzl H *et al.* Active cell death induced by the anti-oestrogens tamoxifen and ICI 164 384 in human mammary carcinoma cells (MCF-7) in culture: the role of autophagy. *Carcinogenesis* 1996; **17:** 1595-1607.

449.Chi S, Kitanaka C, Noguchi K *et al.* Oncogenic Ras triggers cell suicide through the activation of a caspase-independent cell death program in human cancer cells. *Oncogene* 1999; **18:** 2281-2290.

450.Hammond EM, Brunet CL, Johnson GD *et al.* Homology between a human apoptosis specific protein and the product of Apg5, a gene involved in autophagy in yeast. *FEBS Lett* 1998; **425:** 391-395.

451.Bursch W, Ellinger A, Gerner C, Frohwein U, Schulte-Hermann R. Programmed cell death (PCD). Apoptosis, autophagic PCD, or others? *Ann N Y Acad Sci* 2000; **926:** 1-12.

452.Bursch W, Hochegger K, Torok L, Marian B, Ellinger A, Hermann RS. Autophagic and apoptotic types of programmed cell death exhibit different fates of cytoskeletal filaments. *J Cell Sci* 2000; **113 (Pt 7):** 1189-1198.

453.Heggeness MH, Simon M, Singer SJ. Association of mitochondria with microtubules in cultured cells. *Proc Natl Acad Sci U S A* 1978; **75:** 3863-3866.

454.Ball EH, Singer SJ. Mitochondria are associated with microtubules and not with intermediate filaments in cultured fibroblasts. *Proc Natl Acad Sci U S A* 1982; **79:** 123-126.

455.Tanaka Y, Kanai Y, Okada Y *et al.* Targeted disruption of mouse conventional kinesin heavy chain, kif5B, results in abnormal peri-nuclear clustering of mitochondria. *Cell* 1998; **93:** 1147-1158.

456.De Vos K, Goossens V, Boone E *et al.* The 55 kDa tumour necrosis factor receptor induces clustering of mitochondria through its membrane-proximal region. *J Biol Chem* 1998; **273:** 9673-9680.

457.Vale RD, Fletterick RJ. The design plan of kinesin motors. *Annu Rev Cell Dev Biol* 1997; **13:** 745-777.

458.Reers M, Smith TW, Chen LB. J-aggregate formation of a carbocyanine as a quantitative fluorescent indicator of membrane potential. *Biochemistry* 1991; **30:** 4480-4486.

459.Smiley ST, Reers M, Mottola-Hartshorn C *et al.* Intracellular heterogeneity in mitochondrial membrane potentials revealed by a J-aggregate-forming lipophilic cation JC-1. *Proc Natl Acad Sci U S A* 1991; **88:** 3671-3675.

460.Biedler JL, Helson L, Spengler BA. Morphology and growth, tumourigenicity, and cytogenetics of human neuroblastoma cells in continuous culture. *Cancer Res* 1973; **33:** 2643-2652.

461.Zaizen Y, Taniguchi S, Suita S. The role of cellular motility in the invasion of human neuroblastoma cells with or without NMYC amplification and expression. *J Pediatr Surg* 1998; **33:** 1765-1770.

462.Selig RA, Madafiglio J, Haber M, Norris MD, White L, Stewart BW. Ferritin production and desferroxamine cytotoxicity in human neuroblastoma cell lines. *Anticancer Res* 1 A.D.; **13:** 721-725.

463.Palakurthi SS, Aktas H, Grubissich LM, Mortensen RM, Halperin JA. Anticancer effects of thiazolidinediones are independent of PPARγ and mediated by inhibition of translation initiation. *Cancer Res* 2001; **61:** 6213-6218.

464.Rossi A, Elia G, Santoro MG. 2-Cyclopenten-1-one, a new inducer of heat shock protein 70 with antiviral activity. *J Biol Chem* 1996; **271:** 32192-32196.

465.Tsubouchi Y, Kawahito Y, Kohno M, Inoue_ K, Hla T, Sano H. Feedback control of the arachidonate cascade in rheumatoid synoviocytes by 15-deoxy-$\Delta^{12,14}$-prostaglandin J_2. *Biochem Biophys Res Commun* 2001; **283:** 750-755.

466.Johnson TE, Vogel R, Rutledge SJ, Rodan G, Schmidt A. Thiazolidinedione effects on glucocorticoid receptor-mediated gene transcription and differentiation in osteoblastic cells. *Endocrinology* 1999; **140:** 3245-3254.

467.Louet JF, Chatelain F, Decaux JF *et al.* Long-chain fatty acids regulate liver carnitine palmitoyltransferase I gene (L-CPT I) expression through a PPARα-independent pathway. *Biochem J* 2001; **354:** 189-197.

468.DeLuca JG, Doebber TW, Kelly LJ *et al.* Evidence for PPARα-independent peroxisome proliferation: effects of PPARγ/δ-specific agonists in PPARα-null mice. *Mol Pharmacol* 2000; **58:** 470-476.

469.Karakida N, Sugita K, Inukai T *et al.* The PPARγ induces apoptosis of HL-60 cells: Implication of down-regulation of cMYC transcript via the TCF-4 pathway. Yatomi, Y. Haematopoiesis - Apoptosis and cell cycle regulation. Blood 84(S). 1994.

470.Blanquart C, Barbier O, Fruchart JC, Staels B, Glineur C. The nuclear receptor PPARα is degraded by proteasome in a ligand manner. First International Symposium on PPARs: From Basic Science to Clinical Applications. 44. 2001.

471.Ghosh S, May MJ, Kopp EB. NF-κB and Rel proteins: evolutionarily conserved mediators of immune responses. *Annu Rev Immunol* 1998; **16:** 225-260.

472.Lipton SA. Janus faces of NF-κB: neurodestruction versus neuroprotection. *Nat Med* 1997; **3:** 20-22.

473.Feng Z, Porter AG. NFκB/Rel proteins are required for neuronal differentiation of SH-SY5Y neuroblastoma cells. *J Biol Chem* 1999; **274:** 30341-30344.

474.Kurata S, Wakabayashi T, Ito Y *et al.* Human neuroblastoma cells produce the NF-κB-like HIV-1 transcription activator during differentiation. *FEBS Lett* 1993; **321:** 201-204.

475.Murre C, McCaw PS, Baltimore D. A new DNA binding and dimerisation motif in immunoglobulin enhancer binding, daughterless, MyoD, and myc proteins. *Cell* 1989; **56:** 777-783.

476.Landschulz WH, Johnson PF, McKnight SL. The leucine zipper: a hypothetical structure common to a new class of DNA binding proteins. *Science* 1988; **240:** 1759-1764.

477.Gu W, Cechova K, Tassi V, Dalla Favera R. Opposite regulation of gene transcription and cell proliferation by cMYC and Max. *Proc Natl Acad Sci U S A* 1993; **90:** 2935-2939.

478.Bello-Fernandez C, Packham G, Cleveland JL. The ornithine decarboxylase gene is a transcriptional target of cMYC. *Proc Natl Acad Sci U S A* 1993; **90:** 7804-7808.

479.Ayer DE, Lawrence QA, Eisenman RN. Mad-Max transcriptional repression is mediated by ternary complex formation with mammalian homologues of yeast repressor Sin3. *Cell* 1995; **80:** 767-776.

480.Packham G, Cleveland JL. cMYC and apoptosis. *Biochim Biophys Acta* 1995; **1242:** 11-28.

481.Schwab M, Amler LC. Amplification of cellular oncogenes: a predictor of clinical outcome in human cancer. *Genes Chromosomes Cancer* 1990; **1:** 181-193.

482.Kohl NE, Kanda N, Schreck RR *et al.* Transposition and amplification of oncogene-related sequences in human neuroblastomas. *Cell* 1983; **35:** 359-367.

483.Van der Kok K, Van der Osinga J, de Leij Buys CH. Localisation of amplified cMYC and NMYC in small cell lung cancer cell lines. *Cancer Genet Cytogenet* 1989; **38:** 1-8.

484.Breitman TR, Selonick SE, Collins SJ. Induction of differentiation of the human promyelocytic leukaemia cell line (HL-60) by retinoic acid. *Proc Natl Acad Sci U S A* 1980; **77:** 2936-2940.

485.Campisi J, Gray HE, Pardee AB, Dean M, Sonenshein GE. Cell cycle control of cMYC but not c-ras expression is lost following chemical transformation. *Cell* 1984; **36:** 241-247.

486.Hann SR, Eisenman RN. Proteins encoded by the human cMYC oncogene: differential expression in neoplastic cells. *Mol Cell Biol* 1984; **4:** 2486-2497.

487.Ramsay G, Evan GI, Bishop JM. The protein encoded by the human proto-oncogene cMYC. *Proc Natl Acad Sci U S A* 1984; **81:** 7742-7746.

488.Cultraro CM, Bino T, Segal S. Regulated expression and function of the cMYC antagonist, Mad1, during a molecular switch from proliferation to differentiation. *Curr Top Microbiol Immunol* 1997; **224:** 149-158.

489.Goulding MD, Chalepakis G, Deutsch U, Erselius JR, Gruss P. Pax-3, a novel murine DNA binding protein expressed during early neurogenesis. *EMBO J* 1991; **10:** 1135-1147.

490.Chalepakis G, Stoykova A, Wijnholds J, Tremblay P, Gruss P. Pax: gene regulators in the developing nervous system. *J Neurobiol* 1993; **24:** 1367-1384.

491.Epstein DJ, Vekemans M, Gros P. Splotch (Sp2H), a mutation affecting development of the mouse neural tube, shows a deletion within the paired homeodomain of Pax-3. *Cell* 1991; **67:** 767-774.

492.Tassabehji M, Read AP, Newton VE *et al.* Mutations in the PAX3 gene causing Waardenburg syndrome type 1 and type 2. *Nat Genet* 1993; **3:** 26-30.

493.Barr FG, Galili N, Holick J, Biegel JA, Rovera G, Emanuel BS. Rearrangement of the PAX3 paired box gene in the paediatric solid tumour alveolar rhabdomyosarcoma. *Nat Genet* 1993; **3:** 113-117.

494.Fredericks WJ, Galili N, Mukhopadhyay S *et al.* The PAX3-FKHR fusion protein created by the t(2;13) translocation in alveolar rhabdomyosarcomas is a more potent transcriptional activator than PAX3. *Mol Cell Biol* 1995; **15:** 1522-1535.

495.Reeves FC, Fredericks WJ, Rauscher FJ, Lillycrop KA. The DNA binding activity of the paired box transcription factor Pax-3 is rapidly down regulated during neuronal cell differentiation. *FEBS Lett* 1998; **422:** 118-122.

496.Reeves FC, Burdge GC, Fredericks WJ, Rauscher FJ, Lillycrop KA. Induction of antisense Pax-3 expression leads to the rapid morphological differentiation of neuronal cells and an altered response to the mitogenic growth factor bFGF. *J Cell Sci* 1999; **112 (Pt 2):** 253-261.

497.Boulaire J, Fotedar A, Fotedar R. The functions of the cdk-cyclin kinase inhibitor $p21^{WAF1}$. *Pathol Biol (Paris)* 2000; **48:** 190-202.

498.Poluha W, Poluha DK, Chang B *et al.* The cyclin-dependent kinase inhibitor $p21^{WAF1}$ is required for survival of differentiating neuroblastoma cells. *Mol Cell Biol* 1996; **16:** 1335-1341.

499.Taylor WR, Stark GR. Regulation of the G_2/M transition by p53. *Oncogene* 2001; **20:** 1803-1815.

500.Hosoi G, Hara J, Okamura T *et al.* Low frequency of the p53 gene mutations in neuroblastoma. *Cancer* 1994; **73:** 3087-3093.

501.Keshelava N, Zuo JJ, Waidyaratne NS, Triche TJ, Reynolds CP. p53 mutations and loss of p53 function confer multidrug resistance in neuroblastoma. *Med Pediatr Oncol* 2000; **35:** 563-568.

502.Moll UM, LaQuaglia M, Benard J, Riou G. Wild-type p53 protein undergoes cytoplasmic sequestration in undifferentiated neuroblastomas but not in differentiated tumours. *Proc Natl Acad Sci U S A* 1995; **92:** 4407-4411.

503.Wolff A, Technau A, Ihling C *et al.* Evidence that wild-type p53 in neuroblastoma cells is in a conformation refractory to integration into the transcriptional complex. *Oncogene* 2001; **20:** 1307-1317.

504.Sidell N, Koeffler HP. Modulation of Mr 53,000 protein with induction of differentiation of human neuroblastoma cells. *Cancer Res* 1988; **48:** 2226-2230.

505.Patel L, Pass I, Coxon P, Downes CP, Smith SA, Macphee CH. Tumour suppressor and anti-inflammatory actions of PPARγ agonists are mediated via up regulation of PTEN. *Curr Biol* 2001; **11:** 764-768.

506.Di Cristofano A, Pandolfi PP. The multiple roles of PTEN in tumour suppression. *Cell* 2000; **100:** 387-390.

507.Myers MP, Pass I, Batty IH *et al.* The lipid phosphatase activity of PTEN is critical for its tumour suppressor function. *Proc Natl Acad Sci U S A* 1998; **95:** 13513-13518.

508.Liaw D, Marsh DJ, Li J *et al.* Germline mutations of the PTEN gene in Cowden disease, an inherited breast and thyroid cancer syndrome. *Nat Genet* 1997; **16:** 64-67.

509.Franke TF, Yang SI, Chan TO *et al.* The protein kinase encoded by the Akt proto-oncogene is a target of the PDGF-activated phosphatidylinositol 3-kinase. *Cell* 1995; **81:** 727-736.

510.Dace A, Zhao L, Park KS *et al.* Hormone binding induces rapid proteasome-mediated degradation of thyroid hormone receptors. *Proc Natl Acad Sci U S A* 2000; **97:** 8985-8990.

511.Osburn DL, Shao G, Seidel HM, Schulman IG. Ligand-dependent degradation of retinoid X receptors does not require transcriptional activity or coactivator interactions. *Mol Cell Biol* 2001; **21:** 4909-4918.

512.Li XY, Boudjelal M, Xiao JH *et al.* 1,25-Dihydroxyvitamin D_3 increases nuclear vitamin D_3 receptors by blocking ubiquitin/proteasome-mediated degradation in human skin. *Mol Endocrinol* 1999; **13:** 1686-1694.

513.Vedeckis WV, Ali M, Allen HR. Regulation of glucocorticoid receptor protein and mRNA levels. *Cancer Res* 1989; **49:** 2295s-2302s.

514.Camp HS, Tafuri SR, Leff T. c-Jun N-terminal kinase phosphorylates PPARγ1 and negatively regulates its transcriptional activity. *Endocrinology* 1999; **140:** 392-397.

515.Mueller E, Smith M, Sarraf P *et al.* Effects of ligand activation of PPARγ in human prostate cancer. *Proc Natl Acad Sci U S A* 2000; **97:** 10990-10995.

516.Wright HM, Clish CB, Mikami T *et al.* A synthetic antagonist for the PPARγ inhibits adipocyte differentiation. *J Biol Chem* 2000; **275:** 1873-1877.

517.Fehlberg S, Trautwein S, Goke A, Goke R. Bisphenol A diglycidyl ether (BADGE) induces apoptosis in tumour cells independently of PPAR, in caspase-dependent and -independent manners. *Biochem J* 2002; **362:** 573-578.

518.Helene C, Toulme JJ. Specific regulation of gene expression by antisense, sense and antigene nucleic acids. *Biochim Biophys Acta* 1990; **1049:** 99-125.

519.Plachov D, Chowdhury K, Walther C, Simon D, Guenet JL, Gruss P. *Pax8*, a murine paired box gene expressed in the developing excretory system and thyroid gland. *Development* 1990; **110:** 643-651.

520.Poleev A, Fickenscher H, Mundlos S *et al.* PAX8, a human paired box gene: isolation and expression in developing thyroid, kidney and Wilms' tumours. *Development* 1992; **116:** 611-623.

521.De The H, Chomienne C, Lanotte M, Degos L, Dejean A. The t(15;17) translocation of acute promyelocytic leukaemia fuses the retinoic acid receptor α gene to a novel transcribed locus. *Nature* 1990; **347:** 558-561.

522.Dong S, Zhu J, Reid A *et al.* Amino-terminal protein-protein interaction motif (POZ-domain) is responsible for activities of the promyelocytic leukaemia zinc finger-RAR-α fusion protein. *Proc Natl Acad Sci U S A* 1996; **93:** 3624-3629.

523.Chen Z, Guidez F, Rousselot P *et al.* PLZF-RARα fusion proteins generated from the variant t(11;17)(q23;q21) translocation in acute promyelocytic leukaemia inhibit ligand-dependent transactivation of wild-type RARs. *Proc Natl Acad Sci U S A* 1994; **91:** 1178-1182.

524.Rossi DL, Acebron A, Santisteban P. Function of the homeo and paired domain proteins TTF-1 and Pax-8 in thyroid cell proliferation. *J Biol Chem* 1995; **270:** 23139-23142.

525.Dehbi M, Pelletier J. PAX8-mediated activation of the wt1 tumour suppressor gene. *EMBO J* 1996; **15:** 4297-4306.

526.Fraizer GC, Shimamura R, Zhang X, Saunders GF. PAX 8 regulates human WT1 transcription through a novel DNA binding site. *J Biol Chem* 1997; **272:** 30678-30687.

527.Hann SR, Sloan-Brown K, Spotts GD. Translational activation of the non-AUG-initiated cMYC 1 protein at high cell densities due to methionine deprivation. *Genes Dev* 1992; **6:** 1229-1240.

528.Hann SR. Methionine deprivation regulates the translation of functionally-distinct cMYC proteins. *Adv Exp Med Biol* 1995; **375:** 107-116.

529.Wood JN, Bevan SJ, Coote PR *et al.* Novel cell lines display properties of nociceptive sensory neurones. *Proc R Soc Lond B Biol Sci* 1990; **241:** 187-194.

530.Schinner S, Dellas C, Schröder M *et al.* Repression of glucagon gene transcription by PPARγ through inhibition of PAX6 transcriptional activity. *J Biol Chem* 2002; **277:** 1941-1948.

531.Moritake H, Horii Y, Kuroda H, Sugimoto T. Analysis of PTEN/MMAC1 alteration in neuroblastoma. *Cancer Genet Cytogenet* 2001; **125:** 151-155.

532.Editor. PPAR - The good news and the bad. *Nat Med* 1998; **4:** 981.

533.Jalink K, Hordijk PL, Moolenaar WH. Growth factor-like effects of lysophosphatidic acid, a novel lipid mediator. *Biochim Biophys Acta* 1994; **1198:** 185-196.

534.Spiegel S, Milstien S. Sphingolipid metabolites: members of a new class of lipid second messengers. *J Membr Biol* 1995; **146:** 225-237.

535.Volpe JJ, Limori Y, Haven GG, Goldberg RI. Relation of cellular phospholipid composition to oligodendroglial differentiation in C-6 glial cells. *J Neurochem* 1986; **46:** 475-482.

536.Moolenaar WH. Lysophosphatidic acid, a multifunctional phospholipid messenger. *J Biol Chem* 1995; **270:** 12949-12952.

537.Jalink K, Eichholtz T, Postma FR, van Corven EJ, Moolenaar WH. Lysophosphatidic acid induces neuronal shape changes via a novel, receptor-mediated signalling pathway: similarity to thrombin action. *Cell Growth Differ* 1993; **4:** 247-255.

538.Jalink K, van Corven EJ, Hengeveld T, Morii N, Narumiya S, Moolenaar WH. Inhibition of lysophosphatidate- and thrombin-induced neurite retraction and neuronal cell rounding by ADP ribosylation of the small GTP-binding protein Rho. *J Cell Biol* 1994; **126:** 801-810.

539.Hecht JH, Weiner JA, Post SR, Chun J. Ventricular zone gene-1 (vzg-1) encodes a lysophosphatidic acid receptor expressed in neurogenic regions of the developing cerebral cortex. *J Cell Biol* 1996; **135:** 1071-1083.

540.An S, Bleu T, Hallmark OG, Goetzl EJ. Characterisation of a novel subtype of human G protein-coupled receptor for lysophosphatidic acid. *J Biol Chem* 1998; **273:** 7906-7910.

541.Postma FR, Jalink K, Hengeveld T, Moolenaar WH. Sphingosine-1-phosphate rapidly induces Rho-dependent neurite retraction: action through a specific cell surface receptor. *EMBO J* 1996; **15:** 2388-2392.

542.Van Brocklyn JR, Tu Z, Edsall LC, Schmidt RR, Spiegel S. Sphingosine 1-phosphate-induced cell rounding and neurite retraction are mediated by the G protein-coupled receptor H218. *J Biol Chem* 1999; **274:** 4626-4632.

543.Sato K, Tomura H, Igarashi Y, Ui M, Okajima F. Exogenous sphingosine 1-phosphate induces neurite retraction possibly through a cell surface receptor in PC12 cells. *Biochem Biophys Res Commun* 1997; **240:** 329-334.

544.Lee MJ, Van Brocklyn JR, Thangada S *et al.* Sphingosine-1-phosphate as a ligand for the G protein-coupled receptor EDG-1. *Science* 1998; **279:** 1552-1555.

545.Cuvillier O, Pirianov G, Kleuser B *et al.* Suppression of ceramide-mediated programmed cell death by sphingosine-1-phosphate. *Nature* 1996; **381:** 800-803.

546.Arends MJ, Morris RG, Wyllie AH. Apoptosis. The role of the endonuclease. *Am J Pathol* 1990; **136:** 593-608.

547.Baker DL, Desiderio DM, Miller DD, Tolley B, Tigyi G. Direct quantitative analysis of lysophosphatidic acid molecular species by stable isotope dilution electrospray ionisation liquid chromatography mass spectrometry. *Anal Biochem* 2001; **292:** 287-295.

548.Tigyi G, Miledi R. Lysophosphatidates bound to serum albumin activate membrane currents in *Xenopus* oocytes and neurite retraction in PC12 pheochromocytoma cells. *J Biol Chem* 1992; **267:** 21360-21367.

549.Eichholtz T, Jalink K, Fahrenfort I, Moolenaar WH. The bioactive phospholipid lysophosphatidic acid is released from activated platelets. *Biochem J* 1993; **291 (Pt 3):** 677-680.

550.Weiner JA, Chun J. Schwann cell survival mediated by the signalling phospholipid lysophosphatidic acid. *Proc Natl Acad Sci U S A* 1999; **96:** 5233-5238.

551.Raff MC, Miller RH, Noble M. A glial progenitor cell that develops in vitro into an astrocyte or an oligodendrocyte depending on culture medium. *Nature* **303:** 390-396.

552.Van Brocklyn JR, Lee MJ, Menzeleev R *et al.* Dual actions of sphingosine-1-phosphate: extracellular through the Gi-coupled receptor Edg-1 and intracellular to regulate proliferation and survival. *J Cell Biol* 1998; **142:** 229-240.

553.Pyne S, Chapman J, Steele L, Pyne NJ. Sphingomyelin-derived lipids differentially regulate the extracellular signal-regulated kinase 2 (ERK-2) and c-Jun N-terminal kinase (JNK) signal cascades in airway smooth muscle. *Eur J Biochem* 1996; **237:** 819-826.

554.Meyer Z, Lass H, Alemany R *et al.* Sphingosine kinase-mediated Ca^{2+} signalling by G-protein-coupled receptors. *EMBO J* 1998; **17:** 2830-2837.

555.Hall A. Ras-related GTPases and the cytoskeleton. *Mol Biol Cell* 1992; **3:** 475-479.

556.Fukushima N, Kimura Y, Chun J. A single receptor encoded by vzg-1/lpA1/edg-2 couples to G proteins and mediates multiple cellular responses to lysophosphatidic acid. *Proc Natl Acad Sci U S A* 1998; **95:** 6151-6156.

557.Monard D, Rentsch M, Schuerch-Rathgeb Y, Lindsay RM. Morphological differentiation of neuroblastoma cells in medium supplemented with delipidated serum. *Proc Natl Acad Sci U S A* 1977; **74:** 3893-3897.

558.Chawla A, Lazar MA. Peroxisome proliferator and retinoid signalling pathways co-regulate preadipocyte phenotype and survival. *Proc Natl Acad Sci U S A* 1994; **91:** 1786-1790.

559.Al-Makdissy N, Bianchi A, Younsi M *et al.* Down-regulation of PPARγ gene expression by sphingomyelins. *FEBS Lett* 2001; **493:** 75-79.

560.Frisch SM, Francis H. Disruption of epithelial cell-matrix interactions induces apoptosis. *J Cell Biol* 1994; **124:** 619-626.

561.Danen EH, Yamada KM. Fibronectin, integrins, and growth control. *J Cell Physiol* 2001; **189:** 1-13.

562.Jones JL, Walker RA. Integrins: a role as cell signalling molecules. *Mol Pathol* 1999; **52:** 208-213.

563.MacPherson I, Montagnier L. Agar suspension culture for the selective assay of cells transformed by polyoma virus. *Virology* 1964; **23:** 291-294.

564.Stoker M, Neill C, Berryman S, Waxman V. Anchorage and growth regulation in normal and virus-transformed cells. *Int J Cancer* 1968; **3:** 683-693.

565.Wiegmann K, Schutze S, Machleidt T, Witte D, Kronke M. Functional dichotomy of neutral and acidic sphingomyelinases in tumour necrosis factor signalling. *Cell* 1994; **78:** 1005-1015.

566.Zhou XP, Smith WM, Gimm O *et al.* Over-representation of PPARγ sequence variants in sporadic cases of glioblastoma multiforme: preliminary evidence for common low penetrance modifiers for brain tumour risk in the general population. *J Med Genet* 2000; **37:** 410-414.

567.Liang XH, Kleeman LK, Jiang HH *et al.* Protection against fatal Sindbis virus encephalitis by beclin, a novel Bcl-2-interacting protein. *J Virol* 1998; **72:** 8586-8596.

568.Liang XH, Jackson S, Seaman M *et al.* Induction of autophagy and inhibition of tumourigenesis by beclin 1. *Nature* 1999; **402:** 672-676.

569.Liang XH, Yu J, Brown K, Levine B. Beclin 1 contains a leucine-rich nuclear export signal that is required for its autophagy and tumour suppressor function. *Cancer Res* 2001; **61:** 3443-3449.

570.Kabeya Y, Mizushima N, Ueno T *et al.* LC3, a mammalian homologue of the yeast Apg8p, is localised in autophagosome membranes after processing. *EMBO J* 2000; **19:** 5720-5728.

571.Mizushima N, Sugita H, Yoshimori T, Ohsumi Y. A new protein conjugation system in human. The counterpart of the yeast Apg12p conjugation system essential for autophagy. *J Biol Chem* 1998; **273:** 33889-33892.

572.Tanida I, Tanida-Miyake E, Komatsu M, Ueno R, Kominami E. Human Apg3p/Aut1p homologue is an E2 enzyme for multiple substrates,GATE-16, GABARAP and MAP-LC3, and facilitates the conjugation of hApg12p to hApg5p. *J Biol Chem* 2002; **277:** 13739-13744.

573.Wu J, Spiegel S, Sturgill TW. Sphingosine-1-phosphate activates the mitogen-activated protein kinase pathway by a G protein-dependent manner. *J Biol Chem* 1995; **270:** 11484-11488.

574.Johnston PV. *Encyclopaedia of Human Biology.* San Diego: Academic Press 1991.

575.Datta SR, Banach D, Kojuma H *et al.* Activation of the CPP32 protease in apoptosis induced 1-β-D-arabinofuranosylcytosine and other DNA-damaging agents. *Blood* 1996; **88:** 1936-1943.